Characterisation of histone modifications at insulator elements

Meiji Kit-Wan Ma

B. Sc (Hons), MPhil

Submitted in fulfilment of the requirements for

the Degree of PhD

Institute of Cancer Sciences

College of Medical, Veterinary and Life Sciences

University of Glasgow

May 2011

ABSTRACT

The genomes of higher eukaryotes are marked by distinct chromatin domains, which allow for the control of different gene expression states. It is thought that the boundaries of chromatin domains could be formed by DNA sequence elements called insulators. The paradigm HS4 insulator element is located at a boundary between the *β-globin* gene cluster and an adjacent condensed chromatin domain. Proteins that bind to the HS4 sequence recruit enzymes that mediate a number of histone modifications generally associated with chromatin accessibility. Inspired by yeast genetic studies, we hypothesised that H2B ubiquitination might be a key regulator of these 'active' marks. It was found that HS4 and another chromatin boundary at the neighbouring *FOLR1* gene locus, HSA/HSB, are sites of H2B ubiquitination. The ubiquitination E3 ligase RNF20 was found to be necessary for global H2B ubiquitination and for methylation of H3K4, in a *trans*-histone modification pathway that is conserved from yeast to man. RNAi-mediated knockdown of RNF20 not only resulting in the depletion of H2B ubiquitination normally found at chromatin boundaries, but also disrupted their H3K4 methylation and acetylation at multiple histones. H2B ubiquitination is a master controller of the active chromatin state at the HS4 and HSA/HSB chromatin boundaries. Long term depletion of RNF20 expression leads to a compromise of the boundaries, allowing the spreading of heterochromatin into the *FOLR1* and *β-globin* gene loci, resulting in gene silencing. This study also looked at the recruitment of factors that mediate the incorporation of the histone variant H2A.Z at chromatin boundary elements in vertebrates. It was found that insulator binding proteins control H2A.Z incorporation and acetylation.

TABLE OF CONTENTS

LIST OF TABLES

LIST OF FIGURES

ACKNOWLEDGEMENTS

I would like to thank my principal supervisor Dr Adam West for giving me a chance to work in his lab; it is definitely a critical step in my science career path. Also thanks for his guidance and support in the last three years. Many thanks go to my co-supervisor Prof Barry Gusterson and advisor Dr David Vetrie for their suggestions on my research project and keeping me on track. I would also like to thank Dr Katherine West for her support, guidance and reading my thesis. A special thanks goes to Prof. Gavin Sandilands for his technical support of FACS analysis. I would like to express my gratitude to the examination board, Prof. Kevin Hiom and Prof. Peter Adams, for reading my thesis and their constructive comments.

I would like to express my gratitude to our previous colleagues, Dr Carol Heath, Dr Alan Hair and Dr Dan Li. Thanks Carol for helping along when I was new to the lab. Thank you so much Alan for establishing the knockdown lines, which contributed most findings in my project. Thanks Dan for her initiation of the VEZF1-H2A.Z project and technical support for coimmunoprecipitation assays. I would like to thank all present and past members in the lab for their help and support, especially Dr Grainne Barkness for her encouragement and guidance and Dr Ruslan Strogantsev for inspiring discussions.

Many thanks go to the Overseas Research Students Awards Scheme and the Medicine Faculty Scholarship for their financial support for my PhD study. I am grateful to have the Scientific Networking award financially support me to attend the 9th EMBL Conference: Transcription and Chromatin in Germany. It was a great experience of presenting and discussing my research findings and thoughts with experts in the chromatin field.

Last but not least, I would like to express my deep gratitude to my family and friends. Thanks my parents for always supporting my decisions even though they may not agree with me sometimes. Thank my brother so much for being my IT consultant and saving my computers/laptops so many times. I am grateful to have all my friends share laughter with me and encourage me as always even though we are geographically far apart. Thanks for organising so many gatherings every time I went home, all of you did remind me I am so beloved.

AUTHOR DECLARATION

I declare that, except where explicit reference is made to the contribution of others, that this dissertation is the result of my own work and has not been submitted for any other degree at the University of Glasgow or any other institution.

Signature _____

Printed name Meiji Kit-Wan Ma

CHAPTER 1

Introduction

DNA (deoxyribonucleic acid), the genetic material passed to the next generation in every cell division, is packaged into nucleosomes to form chromatin. The DNA information shapes all the cellular phenotypes that form multicellular organisms. However, the study of DNA sequence alone has not fully explained why and how cells differentiate into different cell types. While every cell of a multicellular organism contains the same genetic material in the form of DNA, the cell phenotypes are a result of gene expression that is tightly regulated. It has become clear over the last two decades that epigenetic information stored in chromatin contributes to the regulation of gene expression without altering DNA sequence. Epigenetic information is contained in chemical modifications of DNA or histone proteins, another major component of chromatin. It has been proposed that genes are located in chromatin domains that can have different chromatin states to allow or repress gene expression. Chromatin boundaries are required to separate these domains to allow regulation of gene expression independent of the genomic neighbourhood. It is predictable that loss of chromatin boundaries would lead to disease, cancer or even lethality resulting from aberrant gene expression. Here, I will present a study of chromatin boundary establishment and maintenance. Results suggest a novel histone modification cascade occurring at chromatin boundaries to antagonise nearby intrusive silencing effects.

1.1 DNA packaging and chromatin structure

1.1.1 Hierarchical structure of chromatin

In most eukaryotic cell nuclei, DNA is tightly packaged into chromatin. A nucleosome, the basic unit of chromatin, consists of ~146 base pairs (bp) of DNA wrapped around a histone octamer of two copies of histone H2A-H2B dimers and H3-H4 dimers (Figure 1.1) [Campos & Reinberg, 2009]. A linker histone binds the DNA coming in and out of the nucleosome to stabilise the structure. Nucleosomes are linked by linker DNA that ranges in size from 10 – 80 bp to form a "10 nm beads-on-a-string" structure. It is thought that the strings of nucleosomes are folded into a 30 nm chromatin fibre, resulting in approximately 50-fold compaction (Figure 1.2). The folding process is suggested to be driven by interaction between individual nucleosomes. There are two proposed models, the solenoid and zigzag models, describing the structure of a 30 nm chromatin fibre [Tremethick, 2007]. In the solenoid model, consecutive nucleosomes are next to each other in the fibre, forming a simple one-start helix (Figure 1.3, left panel). In the zigzag model, nucleosomes are arranged as a zigzag such that two rows of nucleosomes form, and the straight linker DNA crisscrosses each stack of nucleosomes leading to a two-start helix (Figure 1.3, right panel). The 30 nm chromatin fibre is subject to further levels of compaction to form interphase chromatin [Németh & Länst, 2003]. Mitotic chromosomes are in the highest order of structures which formation is suggested to be a result of hierarchical folding facilitated by condensin proteins [Woodcock & Ghosh, 2010]. Except in mitosis when the chromosome is entirely tightly folded, chromatin in interphase is not uniformly folded. Regions consisting of actively transcribed genes are generally more permissive while heterochromatin is usually more compact and resistant to protein access. Such specialised chromatin organisation is regulated by chromatin remodelling complexes accompanied with histone modifications.

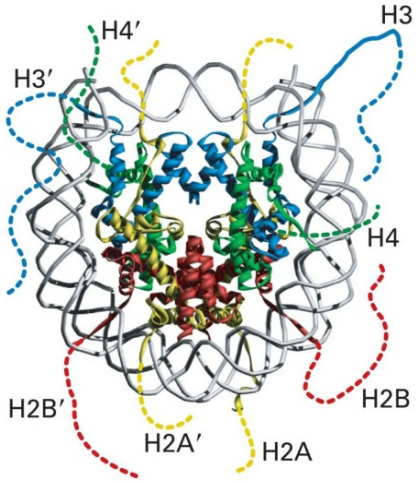

Figure 1.1 Structure of a nucleosome. A histone octamer constituted of two copies of each of the four histone core proteins is wrapped by double-stranded DNA (white helices) with around 146 bp. Adapted from Lodish *et al*, 2004.

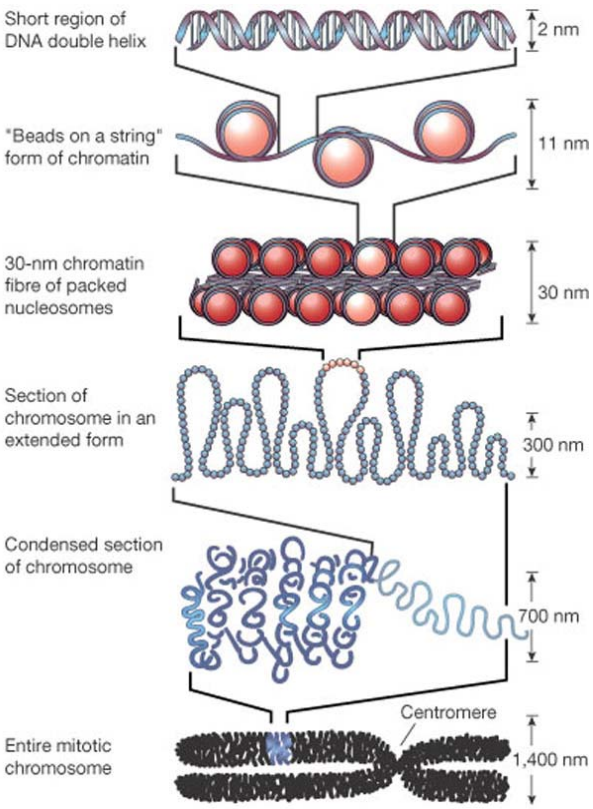

Figure 1.2 The DNA folding within a chromatin structure. Adapted from Felsenfeld and Groudine, 2003.

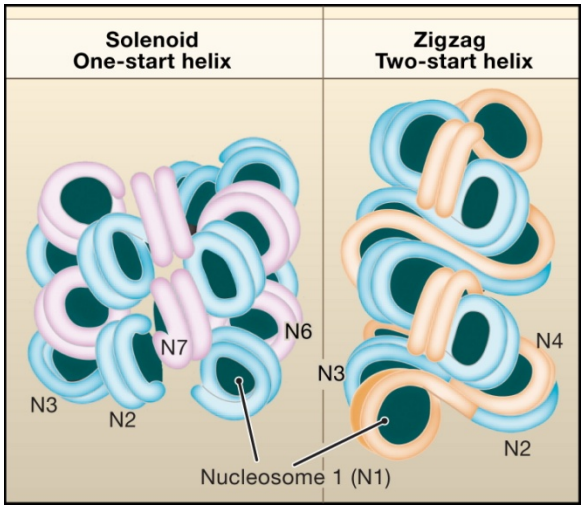

Figure 1.3 Proposed models for the 30 nm chromatin fibre. A simple one-start helix is proposed in the solenoid model, in which nucleosomes are arranged next to each other along the same helical path. Alternative helical gyres are shown in blue and magenta. A two-start helix is proposed in the zigzag model, in which nucleosomes are arranged as a zigzag and the linker DNA crisscrossing between the adjacent rows of nucleosomes. Alternative helical gyres are shown in blue and orange. Adapted from Tremethick, 2007.

1.1.2 Hierarchical structure of genes

In eukaryotic genomes, genes are usually comprised of a promoter, transcribed region and a transcription termination site (Figure 1.4). The transcribed region consist of segments of coding sequences (exons) which are intervened by non-coding sequences (introns) that are excised from

the primary transcript after transcription. Regulatory elements for gene expression are not necessary to be adjacent to their target genes. Many of them are indeed distal regulatory elements that could be located as far as a million base pairs apart from the target gene [Noonan & McCallion, 2010] (Figure 1.5).

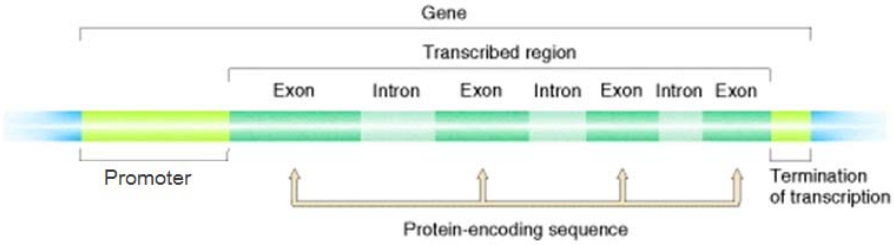

Figure 1.4 Schematic representation of an eukaryotic gene. Modified from Griffiths *et al*, 2000.

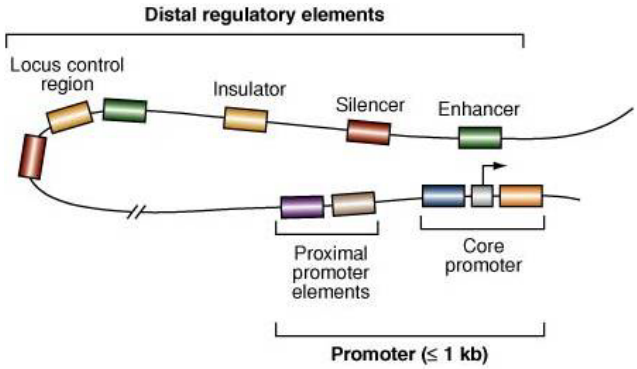

Figure 1.5 Genome organisation of transcription regulatory elements. A promoter is typically composed of a core promoter element and few proximal promoter elements. Enhancers, silencers, insulators and locus control regions are regarded as distal regulatory elements because of their distal action on promoters. Adapted from Maston *et al*, 2006.

1.1.2.1 Promoters

Promoters are the sites for the assembly of transcription machinery that is required to initiate transcription. A promoter determines the orientation and origin of transcription, and is usually composed of a core promoter element and several proximal promoter elements (Figure 1.5). The core promoter element serves as a docking site for the assembly of the transcription preinitiation complex (PIC), which directs RNA polymerase II to TSS [Matson *et al*, 2006]. TATA box within the core promoter element was initially thought to be indispensable for the PIC assembly

because of the binding of transcription factor II D (TFIID) that is essential to initiate the assembly but bioinformatincs analysis revealed that there may be undefined elements to serve as a nucleation point for the PIC assembly [Gershenzon & Ioshikhes, 2005]. Nevertheless, the low transcription activity of the assembled PIC, only referred as basal transcription level, requires proximal promoter elements for efficient transcription. Proximal promoter elements typically located upstream of the core promoter element are binding sites for transcription activators (Figure 1.5). The binding of transcription activators in turn facilitates the recruitment of transcription machinery components and chromatin modifying factors that are essential for the PIC to overcome barriers to transcription initiation and elongation [Orphanides *et al*, 1996]. Transcription efficiency is further regulated by distal regulatory elements such as enhancer and silencers as discussed below (Figure 1.6).

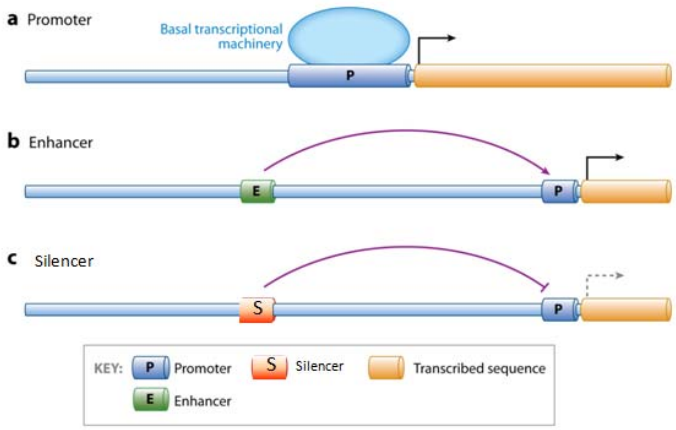

Figure 1.6 Functions of various regulatory elements. **a**. Promoter is the nucleation site for the assembly of transcription machinery, but the assembled complex only confers basal transcriptional activity. Transcription activity can be further activated or repressed by a distal enhancer **(b)** or silencer **(c)**, respectively. Modified from Noonan & McCallion, 2010.

1.1.2.2 Enhancers

Enhancers are distal regulatory elements that activate transcription (Figure 1.6b). Enhancers can function on a promoter that is up to a million base pairs apart [Noonan & McCallion, 2010]. They can be located either 5' or 3' end of the gene promoter. Moreover, the action of enhancers on promoters is usually temporal and modular, so they can activate transcription in different cells

at different times. The function of enhancers is similar to that of the promoter. Enhancers contain binding sites of transcription activator proteins, which in turn, recruit histone modifying and chromatin remodelling enzymes to facilitate the chromatin opening and transcription activity [Noonan & McCallion, 2010].

1.1.2.3 Silencers

In contrast to enhancers, silencers are DNA sequence elements that repress gene transcription (Figure 1.6c). Like enhancers, silencers can be resided on either 5' or 3' of the gene promoter and they can work on target promoters that are up to one million base pair apart. The orientation and distance between a promoter and silencer generally do not affect the function of silencers, although some position- and orientation-dependent silencers also have been identified [Ogbourne & Antails, 1998]. Transcription repressor proteins interact with specific DNA elements within silencers for recruiting histone modification enzymes and chromatin remodelers to generate a compact chromatin structure that is unfavourable for transcription [Maston *et al*, 2010]. Repressor proteins bind to a silencer could in turn compete with an enhancer for the same promoter, or block the binding of activators indirectly. Alternatively, the effect of silencers could even more directly act on the promoter by inhibiting the PIC assembly. Polycomb response elements (PRE) are well known silencers that negatively regulate homeotic genes in ES cells. Protein factors such as GAGA have been found to bind to both PRE and promoters of PRE target genes, suggesting that PRE and target promoters are brought together in close proximity [Levine *et al*, 2004].

1.1.3 Histone proteins

Histone proteins are constituents of chromatin, accounting for up to 45% of total nuclear proteins [Frederik *et al*, 1980]. Presumably because of their structural role and functional role that regulates gene expression, they are well conserved from yeast to man [Thatcher & Gorovsky, 1994]. In order to bind to negatively charged DNA, they are evolved as highly basic proteins.

There are three major classes of histone proteins: core histones, histone variants and linker histones. All of them are responsible for both the basic structural and functional roles in regulating the chromatin accessibility.

1.1.3.1 Core histones

The canonical core histones H3, H4, H2A and H2B are generally expressed during S phase so their incorporation into chromatin is mostly replication-dependent [Osley, 1991]. The crystal structure of a nucleosome revealed that the histone dimer and octamer formation, as well as the interaction between histones and DNA, are *via* their conserved histone fold domains [Arents & Moudrianakis, 1995; Luger *et al*, 1997]. The histone fold domain is a well conserved, ordered structure whereas the N-terminal tail of histone is poorly structured and varies between histones [Davey *et al*, 2002; Luger *et al*, 1997] (Figure 1.7). These random-coil structures of the N-terminal regions as well as the short protease-accessible C-terminal domains protruding the nucleosome are highly accessible for post-translational modifications and protein binding.

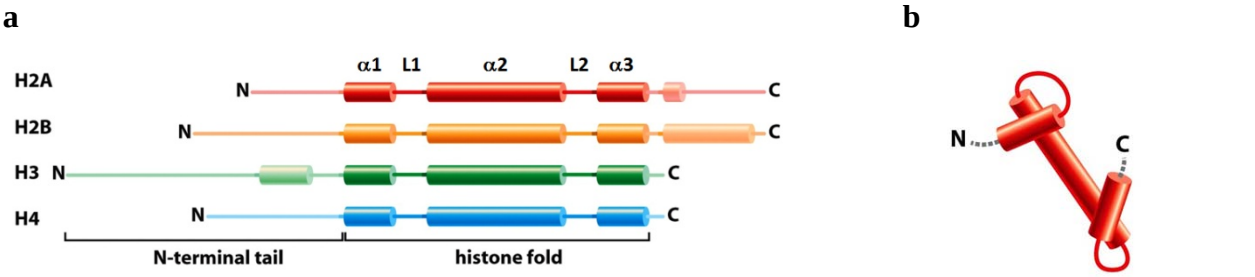

Figure 1.7 The overall organisation of core histone proteins. **a**. Conservation of histone fold domain between core histones. **b**. A tertiary structure of histone fold domain. Modified from Alberts *et al*, 2008.

The conserved histone fold domain is comprised of three α-helices (α1, α2 and α3) separated by two loops (L1 and L2) [Arents *et al*, 1991] (Figure 1.7a). These helices provide an interface for interaction between histone proteins to form H3-H4 and H2A-H2B dimers, an $(H3\text{-}H4)_2$ tetramer and eventually a histone $(H3\text{-}H4)_2$ – $(H2A\text{-}H2B)_2$ octamer [Arents *et al*, 1991; Arents & Moudrianakis, 1995; Luger *et al*, 1997] (Figure 1.8). The histone fold domains and regions

extended from them confer a docking site for DNA that is wrapped the histone octamer with 1.7 turns with ~146 bp to form a nucleosome [Luger *et al*, 1997]. The extensive binding of the histone octamer to DNA with 142 hydrogen bonds directs the DNA double helix twisting to form superhelix, resulting in DNA compaction [Richmond & Davey, 2003].

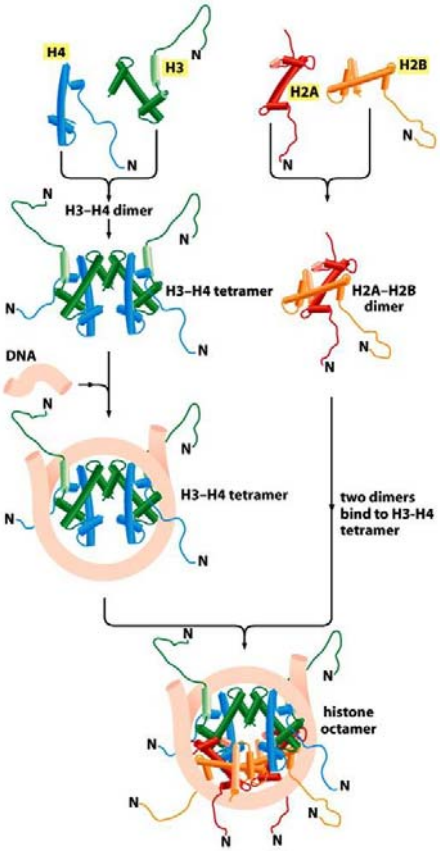

Figure 1.8 Schematic representation of nucleosome assembly. Histone dimers of H4-H3 and H2A-H2B are formed by interaction between their histone domain interfaces. The histone domain interactions further direct the association of histone dimers to form a H4-H3 tetramer that binds to DNA. Two H2A-H2B dimers eventually bind to the DNA wrapping H3-H4 tetramer to form a nucleosome. Adapted from Alberts *et al*, 2008.

1.1.3.2 Histone variants

Histone variants describe core and linker histone genes with amino acid sequence difference compared with their canonical counterparts, which are also incorporated into chromatin. These variants, unlike canonical histones, are expressed throughout the cell cycle, and their deposition does not rely on replication; they could be incorporated into chromatin in any phases of the cell cycle [Hardy & Robert, 2010]. Variants of histones H3 and H2A have been the most studied to date, while those of H4 and H2B have only been recently identified [Hardy & Robert, 2010]. Although the structures of histone variants are very similar to their canonical counterparts, they are incorporated into specific chromosomal locations to carry out distinct functions.

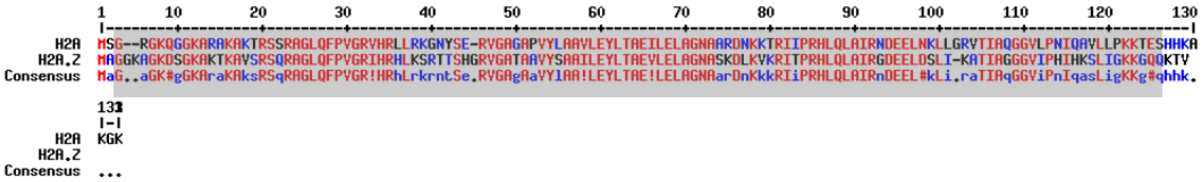

Figure 1.9 Sequence alignment of H2A (NP_066390) and H2A.Z (NP_002097). The histone fold domain is shaded in gray.

Histone H2A has the most number of variants among the four core histones to date; they are H2A.Z, H2A.X, H2A.Bbd (H2A Barr body-deficient) and macroH2A. They have different molecular sizes and are localised at specific loci within the genome. H2A.Z, sharing 58% identity with the canonical H2A (Figure 1.9), is the variant with most complicated roles in chromatin structure maintenance. Unlike canonical H2A, H2A.Z is actively deposited into chromatin in interphase in a replication-independent manner by chromatin remodelling complexes, the SWR1 complex in yeast and the SRCAP/TIP60 complexes in human [Mizuguchi *et al*, 2004; Wong *et al*, 2007].

H2A.Z has been reported to negatively and positively regulate chromatin accessibility; both of the regulatory roles might be explained by the structural differences between H2A.Z and H2A. The difference in amino acid sequences between H2A.Z and H2A was found to be responsible for weakening the interaction between the (H2A.Z-H2B) dimer and the $(H3\text{-}H4)_2$ tetramer [Suto *et al*, 2000]. Nucleosomes containing H2A.Z are more susceptible to salt-induced dissociation compared with H2A nucleosomes [Abbott *et al*, 2001; Zhang *et al*, 2005]. A recent study has found that nucleosomes containing both H2A.Z and H3.3 are the least stable among nucleosome with different combinations of canonical histones and histone variants [Jin *et al*, 2009]. However, contrasting reports showing H2A.Z nucleosomes are more stable in high salt condition compared with their canonical H2A counterparts were also documented [Park *et al*, 2004; Thambirajah *et al*, 2006]. Note that these studies were performed on nucleosomes reconstituted from recombinant H2A.Z, which lacks post-translational modifications that may significantly influence nucleosomal properties, so the true scenario in genomes and specific loci might be

missed. Moreover, H2A.Z may regulate chromatin accessibility by recruiting linker proteins, assembly factors and chromatin remodelling complexes *via* its additional metal binding site and an extended acidic patch [Suto *et al*, 2000].

A distinct feature of H2A.Z within eukaryotic genomes is that it is present in nucleosomes that are highly positioned around the transcription start sites (TSS), +1 nucleosomes in particular, of both active and inactive genes [Albert *et al*, 2007; Barski *et al*, 2007; Mavrich *et al*, 2008; Raisner *et al*, 2005] (Figure 1.10). Even so, a certain positive correlation between the gene expression level and H2A.Z occupancy is observed in human [Barski *et al*, 2007; Conerly *et al*, 2010]. The role of H2A.Z in transcription is complicated as it is responsible for the recruitment of RNA polymerase II and RNA polymerase pausing [Adam *et al*, 2001; Hardy *et al*, 2009; Mavrich *et al*, 2008]. Apart from transcription, H2A.Z is also enriched at other regulatory elements including enhancers in human and chromatin barriers in yeast [Barski *et al*, 2007; Jin *et al*, 2009; Meneghini *et al*, 2003]. H2A.Z at yeast barriers was clearly shown to block the binding of Sir (silent information regulator) proteins, thus preventing the spreading of heterochromatin [Babiarz *et al*, 2006; Meneghini *et al*, 2003; Venkatasubrahmanyam *et al*, 2007]. The acetylation state of H2A.Z is the key to yeast barrier activity. Yeast mutants bearing no Htz1 or unacetylable Htz1 (yeast ortholog of H2A.Z) exhibit similar phenotypes of boundary defects [Babiarz *et al*, 2006]. Whether H2A.Z plays a role at vertebrate insulators is undefined although genome-wide studies have found that H2A.Z occupancy is commonly elevated at sites of CTCF binding, suggesting a role in enhancer blocking [Barski *et al*, 2007; Jin *et al*, 2009].

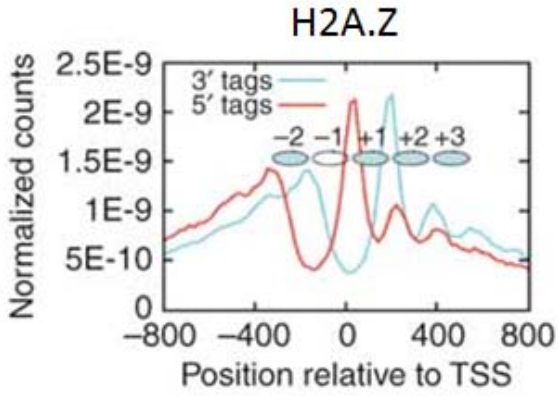

Figure 1.10 H2A.Z distribution around TSS. The genome-wide distribution of H2A.Z was examined with chromatin immunoprecipitation (ChIP) coupled with DNA sequencing (ChIP-seq). The red and blue lines represent forward and reverse reads of sequencing data, respectively. The ovals indicate the nucleosome position. Modified from Jin *et al*, 2009.

A study in *Arabidopsis thaliana* found that H2A.Z occupancy is refractory to DNA methylation in the genome. DNA methylation is considered to be a repressive epigenetic mark that is occurred at CpG (cytosine-guanosine) dinucleotides in vertebrates, of which the 5th carbon of cytosine is covalently linked to a methyl group to form a 5'-methylcytosine. The process is catalysed by DNA methyltransferases (DNMT) using *S*-adenosylmethionine (SAM) as substrate. DNA methylation is also found in other eukaryotes including plants except yeast, fruit flies and roundworms [Lee *et al*, 2010]. DNA methylation is considered as an epigenetic mark associated with gene silencing. The binding of transcription factors could be blocked by the extra methyl group on DNA. CTCF is an example that its binding to DNA is abolished by DNA methylation [Bell & Felsenfeld, 2000; Hart *et al*, 2000]. Apart from that, many methylated DNA binding proteins are associated with chromatin repressive complexes so their binding would in turn lead to transcription repression and inhibition of chromatin accessibilities [Jones *et al*, 1998; Le Guezennec *et al*, 2006; Nan *et al*, 1998; Prokhortchouk & Hendrich, 2002; Prokhortchouk *et al*, 2001; Yoon *et al*, 2003]. Therefore, preventing DNA methylation is a way of protecting genes from silencing. The mutually exclusive occupancy of DNA methylation and H2A.Z in the genomes of *Arabidopsis thaliana* and other eukaryotes including human suggests that H2A.Z is a potential mechanism of preventing DNA methylation [Conerly *et al*, 2010; Zemach *et al*, 2010; Zilberman *et al*, 2008]. Knockout of the *Arabidopsis* homolog of the histone replacement factor *Swr1*, *PIE1* (photoperiod-independently early flowering 1), results in a loss of H2A.Z incorporation and leads to an increase in DNA methylation at previous sites of H2A.Z

incorporation. However, knockout of *MET1* (methyltransferase 1) not only reduces DNA methylation but also results in an elevation of H2A.Z at previously methylated sites, implicating H2A.Z deposition could be both a cause and consequence of retaining DNA unmethylated or active DNA demethylation. The counteracting mechanism between H2A.Z deposition and DNA methylation remains undetermined.

1.1.4 Chromatin remodelling complexes

Chromatin state is very dynamic as DNA has to be exposed in a regulated manner for many DNA activities, such as transcription, repair, recombination and replication. Chromatin remodelling complexes are involved in nucleosome eviction, repositioning or deposition.

1.1.4.1 ATPase family types

Chromatin remodelling complexes utilise ATP hydrolysis to generate energy for chromatin remodelling; therefore, all of them consist of at least one ATPase subunit. Two well conserved domains DExx and HELICc are found in the ATPase subunit of chromatin remodelling complexes (Figure 1.11). There are at least four families of chromatin remodelling complexes: SWI/SNF (switching defective/sucrose nonfermenting), ISWI (Imitation switch), CHD (chromodomain, helicase, DNA binding) and INO80 (Inositol requiring 80) (Table 1.1). They are classified based on the differences of regions flanking the two ATPase domain parts. These regions vary in size and domain components, allowing binding of different non-catalytic complex subunits and histone proteins. The two ATPase parts of SWI/SNF, ISWI and CHD are separated by a short insertion and INO80 by a long insertion (Figure 1.11). Apart from the ATPase domain, the catalytic subunit also contains other domains for the binding of non-catalytic subunits and histone proteins to regulate the ATPase activity and direct the remodelers to suitable locations (Table 1.2). For instance, the HSA domain in both SWI/SNF and INO80 have been reported to allow the binding of several actin-related proteins (ARP) while the bromodomains and chromodomains are for recognition of acetylated and methylated histone tails,

respectively [Brehm *et al*, 2004; Hassan *et al*, 2002; Szerlong *et al*, 2008; Winston & Allis, 1999]. ARPs are suggested to regulate the ATPase activity [Szerlong *et al*, 2003; Szerlong *et al*, 2008]. The binding to histone proteins, on the other hand, targets the remodelers to specific loci, such as the chromodomain of CHD1, which selectively tethers the remodelling complex to methylated lysine 4 on histone H3 (H3K4me) [Flanagan *et al*, 2005]. Although the ATPase subunit of ISWI does not contain either bromo- or chromo-domain, it is also able to bind to histones or DNA *via* its SANT or SLIDE domains, respectively, tethering the remodelling complex on the chromatin substrate [Boyer *et al*, 2004; Grüne *et al*, 2003].

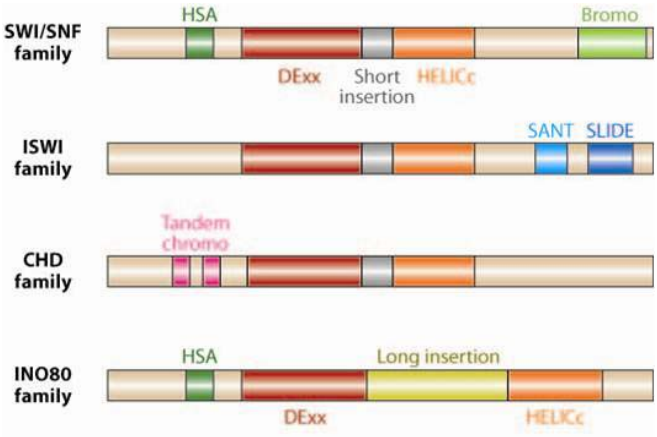

Figure 1.11 Structures of ATPase subunits of different families of chromatin remodelling complexes. Adapted from Clapier & Cairns, 2009.

Remodelling complex family	Yeast			Human		
	Complex	ATPase	Function on chromatin	Complex	ATPase	Function on chromatin
SWI/SNF	SWI/SNF	Swi2/Snf2	- Transcription activation, elongation and repression - Replication - DSB repair - Targeting by activators or corepressors	BAF	hBRM/BRG1 (SMARCA2/ SMARCA4)	- Targeting by activators - Transcription elongation
	RSC	Sth1	- Pol II/III regulation - Spindle-assembly checkpoint - Chromosome segregation and cohesion - Targeting by activators - DSB repair	PBAF (Polycomb-associated BAF)	BRG1 (SMARCA4)	- Function at kinetochore during mitosis - Ligand-dependent transcriptional activation
				ATRX	ATRX	- H3.3 incorporation with Daxx - Transcription repression - Heterochromatin formation and maintenance of chromatin stability
ISWI	ISW1	Isw1	- Transcription activation, elongation and termination	NURF	SNF2L (SMARCA1)	- Transcription activation
	ISW2	Isw2	- Replication - Transcription repression - Repression of antisense transcription	CHRAC	SNF2H (SMARCA5)	- Chromatin assembly
				ACF	SNF2H (SMARCA5)	- Replication - Chromatin assembly
CHD	CHD1	Chd1	- Replication regulation - Transcription regulation, elongation and termination	CHD1	CHD1	- Maintain open chromatin structure for pluripotency of ES cells - Transcription activation - H3.3 incorporation with histone chaperone HIRA
				NURD	CHD3, CHD4	- Transcriptional repression and silencing with deacetylation
INO80	INO80	Ino80	- DNA repair - Pol II activation - Replication - Core histone removal	INO80	hINO80	- DNA repair - Transcription activation
	SWR1	Swr1	- Htz1 (H2A.Z) deposition - DNA repair coupled with phoso-H2A recruitment	SRCAP	SRCAP	- H2A.Z incorporation
				TIP60	p400	- H2A.Z deposition and acetylation - Transcription activation and repression - DNA repair - Mitotic checkpoint

Table 1.1 Summary of chromatin remodelling enzymes in yeast and human. Derived from Barak *et al*, 2003; Batsche *et al*, 2006; Baumann *et al*, 2010; Clapier *et al*, 2009; Gaspar-Maia *et al*, 2009; Hall & Georgel, 2007; Ho & Crabtree, 2010; Konev *et al*, 2007; Lewis *et al*, 2010; Mohrmann & Verrijzer, 2004; Picketts *et al*, 1996; Saha *et al*, 2006; Sapountzi *et al*, 2006; Tang *et al*, 2004; Xue *et al*, 2000. A nomenclature system has been introduced for ATPases of the human SWI/SNF and ISWI complexes [Ring *et al*, 1998], referring to SMARC (SWI/SNF-related, Matrix-associated, Actin-dependent Regulator Chromatin). The new names under the SMARC nomenclature system of the human ATPase subunits are shown in brackets. While the new names are still not commonly employed in publications to date, the old naming system will be still used in this thesis hereafter.

Remodelling complex family	Remodelling complex	ATPase subunit	Non-catalytic subunits
SWI/SNF	BAF	hBRM/BRG1	- BAF155 - BAF170 - BAF60a/b/c - hSNF5 - BAF57 - BAF53A/B - β-ACTIN
ISWI	NURF	SNF2L	- BPTF - RbAp46, 48
CHD	NURD	CHD3, CHD4 (also known as Mi-2α, Mi-2β)	- MBD3 - MTA1, 2, 3 - HDAC1, 2 - RbAp46/48 - p66α,β
INO80	SRCAP	SRCAP	- REPTIN52 - PONTIN52 - BAF53A - ARP6 - GAS41 - DMAP1 - YL-1 - H2A.Z, H2B - ZnF-HIT1
	TIP60	p400	- REPTIN52 - PONTIN52 - BAF53A - ACTIN - GAS41 - DMAP1 - YL-1 - BRD8 - TRRAP - TIP60 - MRG15, MRGX - FLJ11730 - MRGBP - EPC1, EPC-like - ING3

Table 1.2 Components of some human chromatin remodelling complexes. Derived from Bao & Shen, 2007; Clapier & Cairns, 2009.

1.1.4.2 Mechanisms of action

Nucleosome sliding is a proposed mechanism of chromatin remodelling complexes' action [Clapier and Cairns, 2009; Saha *et al*, 2006]. The DNA binding domain binds linker DNA so that the remodelling complex is tethered on chromatin. The ATPase subunit interacting with a nucleosome is thought to use ATP hydrolysis as a source of energy to push the DNA towards the nucleosome dyad and a DNA loop is generated. The DNA loop may propagate along the nucleosome following breaking some histone-DNA contacts, when the loop propagation resolves

into the linker DNA where the DNA binding domain binds to, nucleosome repositioning occurs. The remodelling complex releases from the nucleosome and reloads on the chromatin again for another round of action (Figure 1.12). After several cycles of ATP hydrolysis required nucleosome repositioning, nucleosome sliding occurs.

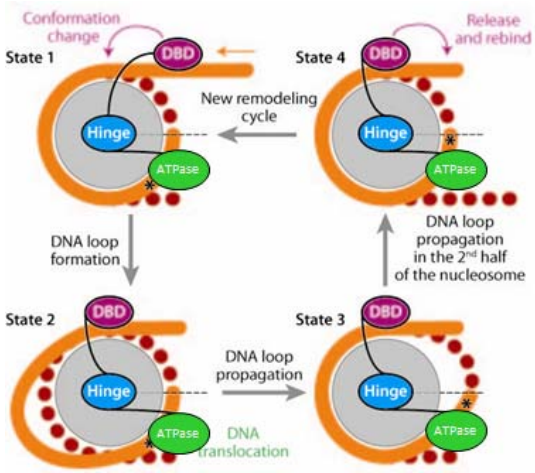

Figure 1.12 Schematic diagram showing the action mechanism of chromatin remodelling complex. Modified from Clapier and Cairns, 2009.

Chromatin remodelling complexes not only repositions nucleosome, but also facilitates histone variant exchange. It is thought that following DNA loop formation, histone chaperones may be able to remove histone dimers, which in turn allows incorporation of histone dimers with histone variants. Chz1, for instance, it is a histone chaperone specific to H2A.Z-H2B dimer and was found to work cooperatively with the Swr1 complex in yeast to catalyse H2A-H2A.Z exchange [Luk *et al*, 2007]. However, it is not known whether DNA loop formation is a prerequisite for the Chz1 binding to nucleosomes, if so, how the loop is formed precisely on the nucleosome where H2A-H2B resides is not understood.

1.1.4.3 Targeting and specific roles in transcription

Although these chromatin remodelers share some similarities, they do not function redundantly; rather, they have diverse functions and are recruited to specific chromatin regions (Table 1.1). Almost all of them have been reported to have both positive and negative effects on the chromatin structure. The ISWI family, for instance, it is primarily suggested to be responsible for

chromatin assembly [Ito *et al*, 1997], maintenance of the high-order of chromatin structure [Deuring *et al*, 2000] and transcription repression [Goldmark *et al*, 2000]. However, one of its family members, NURF (nucleosome remodelling factor), can positively regulate transcription possibly because of its nucleosome sliding activity [Hamiche *et al*, 1999; Mizuguchi *et al*, 1997].

Similarly, SWI/SNF can promote transcription activation as well as repression. The SWI/SNF family is known to promote transcription by remodelling the chromatin structure for binding of transcription activators or even recruiting activators itself [Burns & Peterson, 1997; Hirschhorn *et al*, 1992; Neely *et al*, 2002]. However, a genome-wide study showed that transcription activation is not a universal function of SWI/SNF remodelers. Deletion of both Swi and Snf in yeast leads to elevated expression of some genes, suggesting they could also play a repressive role in transcription [Sudarsanam *et al*, 2000].

A dual role in regulation of chromatin structure is also observed in the CHD family. The NURD (nucleosome remodelling and deacetylation) complex containing histone deacetylation activity can be detected at both active and inactive genes, suggesting that it can both activate and repress transcription [Miccio *et al*, 2010]. The CHD family is classified by the presence of a chromodomain-containing ATPase subunit, which appears to target the remodelers to specific genetic loci. The specificity of CHD1 to histone tails of H3 with trimethylation on lysine 4 (H3K4me3) directs the complex to active chromatin but excludes it from H3K4me3 depleted heterochromatin [Flanagan *et al*, 2005; Kelley *et al*, 1999; Strokes *et al*, 1995; Strokes *et al*, 1996].

1.1.4.4 Histone replacement

The INO80 family is well known to be associated with histone variants. The INO80 complex interacts with H2A.X for DNA repair, whereas the closely related family member, SWR1 in yeast is responsible for H2A.Z deposition into chromatin *via* facilitating the exchange of

H2A-H2B for H2A.Z-H2B dimers [Kobor *et al*, 2004; Mizuguchi *et al*, 2004; Morrison *et al*, 2004]. INO80 is suggested to mediate remodelling at DSB by generating single-stranded DNA, exposing the lesion for repairing factors [van Attikum *et al*, 2004]. In contrast, SWR1 incorporates H2A.Z mostly at promoters and other regulatory elements. The non-redundant roles of chromatin remodelers and their specific occupancy across the genome contribute the complex regulation of chromatin organisation.

1.2 Histone Modifications

The core histone proteins are subject to many post-translational modifications including methylation, acetylation, phosphorylation, poly(ADP-ribosyl)ation (PARylation), proline isomerisation, sumoylation and ubiquitination (Figure 1.13). These mostly occur on the protruding, unstructured N-terminal histone tails and the short but accessible C-termini. Histone modifications are a major component of epigenetic information and can regulate the binding of other factors, and in some cases, can alter the chromatin stability by changing the interaction between histones and DNA. The functions of histone modifications are diverse, depending on which amino acid of histone is modified and what the modification status is.

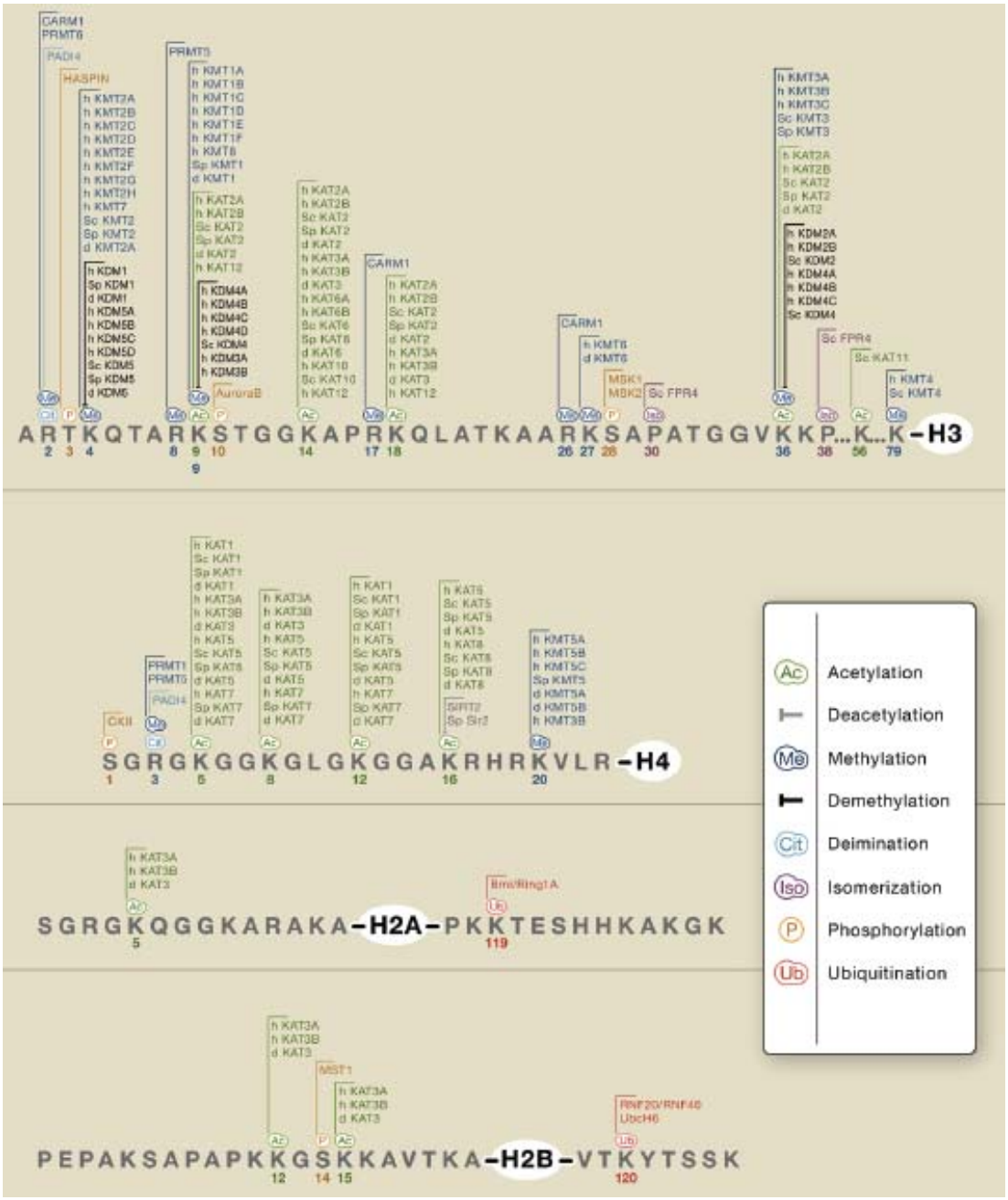

Figure 1.13 Commonly found histone modifications on core histones and the responsible enzymes. The numbering of amino acid residues are according to the human histone sequences. Note that CARM1 is PRMT4 under the new nomenclature system for arginine methyltransferases. Adapted from Kouzarides, 2007.

1.2.1 Histone methylation

There are several methylation states of both lysine and arginine, and each can have differing effects on chromatin structure and function (Figure 1.14). Lysine can be mono- (me1), di- (me2) or even tri-methylated (me3), whereas arginine can only be mono- or di-methylated but dimethylation can be symmetrical (me2s) or asymmetrical (me2as) (Figure 1.15). Methylation on

lysines 4, 9, 27 and 36 of histone H3, on lysine 20 of H4, on arginine 8 of H3 and on arginine 3 of H4, has gained the most attention in the past years.

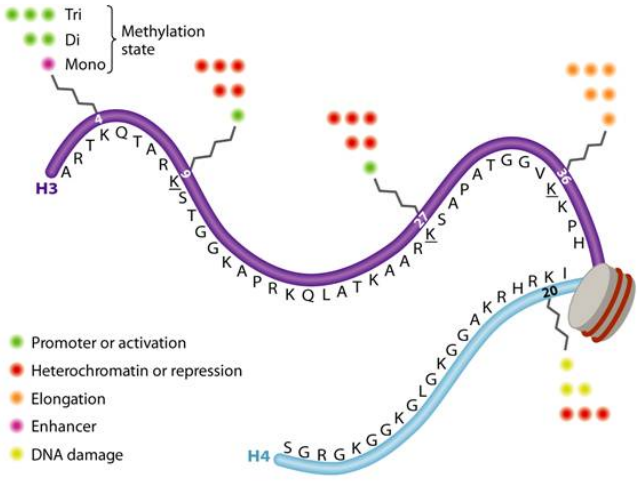

Figure 1.14 Schematic diagram showing major methylation on histones H3 and H4 and their related functions. Methylation states are indicated as number of dots and their associated functions are depicted as distinct colours in the figure key. Adapted from Mosammaparast and Shi, 2010.

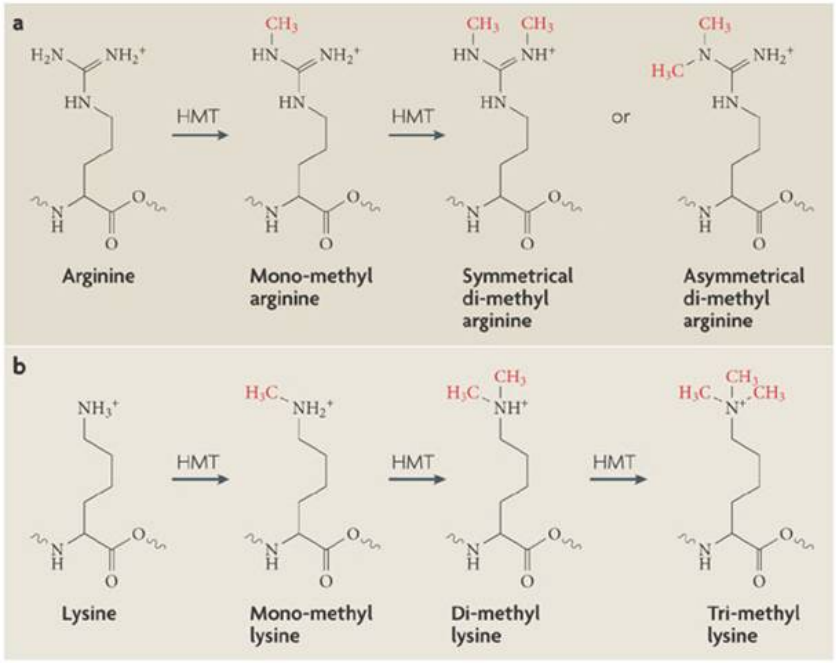

Figure 1.15 Methylation states of arginine and lysine. **a**. Arginine can be mono- or di-methylated, and the latter can be symmetrical and asymmetrical. Symmetrical dimethylation refers to one methyl group added to each nitrogen of the guanidinium group, whereas two methyl groups are added to the same nitrogen of the guanidinium group in asymmetrical dimethylation. **b**. Lysine can be mono-, di- or tri-methylated, depending on the number of methyl groups added to one lysine. Adapted from Klose and Zhang, 2007.

1.2.1.1 Lysine methylation

Lysine methylation on histones is catalysed by lysine methyltransferases (KMT) that are specific for both the methylation states and sequence context of lysine residues (Table 1.3). Methylation of histone H3 on lysine 4 (H3K4me) is catalysed by the Set1 protein in yeast and the SET1 complexes or the SET domain-containing MLL (mixed-lineage leukemia) complexes in human [Briggs *et al*, 2001; Santo-Rosa *et al*, 2002; Yokoyama *et al*, 2004]. H3K4 methylation is linked to active gene transcription. Genome-wide studies have shown that promoters and transcription start sites are enriched in H3K4me3, and the levels are positively correlated to gene expression [Barski *et al*, 2007; Bernstein *et al*, 2005; Wang *et al*, 2008]. This scenario appears to be conserved from yeast to higher eukaryotes [Liang *et al*, 2004; Santo-Rosa *et al*, 2002; Schneider *et al*, 2004]. Deletion of the *Set1* gene in *S. cerevisiae* leads to repression of most genes [Boa *et al*, 2003], further confirming the essential role of H3K4 methylation in transcription. The distribution of dimethylated H3K4 (H3K4me2) is broader and differs between yeast and other eukaryotes. H3K4me2 spans gene coding regions in yeast but the distribution of H3K4me2 is more likely to overlap the H3K4me3 enriched sites around TSSs in higher eukaryotes [Barski *et al*, 2007; Bernstein *et al*, 2002; Schneider *et al*, 2004; Liang *et al*, 2004]. H3K4me can act as a signal for the binding of chromodomain containing proteins of various chromatin remodelling enzymes, and can promote both the binding as well as the activity of the transcription machinery (Table 1.4). For example, it has been shown that H3K4me3 is crucial for the binding of the NURF complex to the promoter and loss of such binding results in impaired expression of the *HOX* gene in *Xenopus* during development [Wysocka *et al*, 2006]. Moreover, genome-wide patterns of H3K4me3 and RNA polymerase II significantly overlap [Barski *et al*, 2007] and the binding of TFIID to promoters is dependent on H3K4me3 [Vermeulen *et al*, 2007]. Apart from transcription activation, H3K4 methylation is also involved in V(D)J recombination during lymphocyte development and repression of RNA polymerase II mediated cryptic transcription [Liu *et al*, 2007; Matthews *et al*, 2007; Pinskaya *et al*, 2009], suggesting plasticity of H3K4 methylation in chromatin activity regulation.

Histone residue	New name	Old name	Methylation state		Function
H3K4	KMT2A	MLL1	mono/di		
	KMT2B	MLL2	mono/di/tri		
	KMT2C	MLL3	mono/di/tri		
	KMT2D	MLL4	mono/di/tri	-	Transcription activation
	KMT2E	MLL5	di/tri	-	Chromatin remodelling
	KMT2F	hSET1A	mono/di/tri		
	KMT2G	hSET1B	mono/di/tri		
	KMT2H	ASH1	di/tri		
	KMT7	SET7/9	mono/di/tri		
H3K9	KMT1A	SUV39H1	di/tri	-	Heterochromatin formation/silencing
	KMT1B	SUV39H2	di/tri	-	Heterochromatin formation/silencing
	KMT1C	G9a	mono/di	-	Euchromatic H3K9 methylation
	KMT1D	EuHMTase/GLP	mono/di	-	Heterochromatin formation/silencing
	KMT1E	ESET/SETDB1	di/tri	-	Transcription repression
	KMT1F	CLL8	Unknown	-	Unknown
	KMT8	RIZ1	mono/di	-	Transcription repression
H3K27	KMT6	EZH2	mono/di/tri	-	Transcription repression
H3K36	KMT3A	SET2	mono/di/tri	-	Transcription activation
				-	Transcription repression
	KMT3B	NSD1	mono/di/tri	-	Transcription activation
	KMT3C	SYMD2	mono/di/tri	-	Transcription activation
H3K79	KMT4	DOT1L	mono/di/tri	-	Transcription activation
				-	Checkpoint activation
				-	DNA repair
H4K20	KMT5A	Pr-SET7/8	mono	-	Transcription repression
	KMT5B	SUV4-20H1	mono/di/tri	-	DNA damage response
				-	Heterochromatin formation/silencing
	KMT5C	SUV4-20H2	mono/di/tri	-	Heterochromatin formation/silencing

Table 1.3 Summary of human KMTs. Derived from Allis *et al*, 2007; Hublitz *et al*, 2009; Li *et al*, 2008; Lucio-Eterovic *et al*, 2010; Schotta *et al*, 2004; Sebastian *et al*, 2009; Shilatifard, 2008; Shukla *et al*, 2009; Wang *et al*, 2007; Yuan *et al*, 2009.

H3K4me binding protein	Methylation state recognition	Function
BPTF	H3K4me3	Chromatin remodelling
CHD1	H3K4me2/3	Chromatin remodelling, splicing
ING2	H3K4me3	Gene silencing
ING1	H3K4me3	DNA repair
TAF3	H3K4me3	Gene activation

Table 1.4 Table showing protein factors recognising methylated H3K4 and their functions in chromatin activities. Modified from Shukla *et al*, 2009.

Besides H3K4 methylation, H3K36 and H3K79 methylation are also associated with transcription regulation. Unlike H3K4me2 and H3K4me3 that are commonly found at promoters, levels of H3K36 and H3K79 methylation, especially those with higher methylation states (me2 or me3), are usually enriched at gene bodies [Guenther *et al*, 2007; Pokholok *et al*, 2005; Shanbazian *et al*, 2005; Vakoc *et al*, 2006]. H3K36me3 and K79me2/3 positively correlate with transcription activity [Guenther *et al*, 2007]. However, similar to H3K4 methylation, H3K36 methylation also appears to be responsible for gene repression in certain scenarios. Deletion of *Set2*, which is responsible for H3K36 methylation in yeast leads to dramatic induction of GAL4 [Landry *et al*, 2003]. Moreover, artificial tethering of Set2 to the promoter in a *lacZ* reporter assay also results in reduced expression of *lacZ* [Strahl *et al*, 2002], suggesting a dual role of H3K36 methylation in transcription. The repressive role of H3K36 methylation in transcription appears to prevent cryptic transcription initiation by cooperation with histone deacetylases (HDAC) [Lee & Shilatifard, 2007]. H3K79 methylation, in addition, has been shown to be required for preventing the spread of heterochromatin. Lysine 79 on H3 is not on the exposed N-tail; rather, it is located close to the core histone domain (Figure 1.13), and where is suggested to be an interface for binding of silencing factors that are essential for transcriptional silencing in yeast [Park *et al*, 2002]. Therefore, methylation on this residue catalysed by DOT1, an unusual KMT without a SET domain, might lead to changes of the nucleosome structure or, simply block the binding of Sir proteins. The affinity of Sir proteins towards the H3K79 unmethylated tail is shown to be higher than to the methylated one [van Welsem *et al*, 2008].

By contrast, methylation of H3K9, H3K27 and H4K20 are generally associated with transcription repression, conferring a negative effect on chromatin accessibility. Like other lysine methylation, their functions are also dependent on methylation state. The trimethylation states of H3K9 (H3K9me3) and H4K20 (H4K20me3) are usually associated with chromatin repression and commonly found in heterochromatin and transcriptionally silenced loci, whereas mono- and di-methylation are more widely spread, and also present in euchromatin [Rice *et al*, 2003; Schotta *et al*, 2004; Zhou *et al*, 2010]. H3K9me3 and H4K20me3 are responsible for position effect variegation (PEV) resulting in variegated expression of transgenes commonly observed in *Drosophila* [Reuter & Spierer, 1992; Schotta *et al*, 2004]. The causes of PEV will be discussed in Section 1.3.2.4. In vertebrates, SUV39H1 and SUV39H2 trimethylate H3K9, G9a and G9a-related protein (GLP) dimethylate the same residue but mostly in euchromatin [Aagaard *et al*, 1999; O' Carroll *et al*, 2000; Rea *et al*, 2000; Tachibana *et al*, 2001; Tachibana *et al*, 2005]. Interestingly, although SUV39H1 is only able to methylate H3K9, double null *Suv39h* mouse embryonic fibroblasts (MEF) exhibit a loss not only of H3K9me3 at pericentric heterochromatin, but also of H4K20me3, which is established by Suv4-20h1 and Suv4-20h2 [Schotta *et al*, 2004]. It suggests that there is interplay between these two modifications, in which H3K9me3 appears to precede H4K20me3 during heterochromatin establishment. Chromodomain-containing HP1 proteins are suggested to bridge these two histone modifications together. Methylated H3K9 provides an epitope for HP1 binding, which in turn recruits Suv4-20h1 and Suv4-20h2 to methylate H4K20me3 at heterochromatin [Lachner *et al*, 2001; Schotta *et al*, 2004]. Apart from H4K20me3, H3K9me3 also works cooperatively with H3K27 methylation. It was showed in mice that H3K9me3 and H3K27me1 are enriched at pericentric heterochromatin. However, in the H3K9me3 depleted condition resulting from *Suv39h* knockout, H3K27me3 appears to take up the leading role in heterochromatin to compensate the loss of H3K9me3 [Peters *et al*, 2003].

Active and repressive methylation marks do not always oppose each other. There are chromatin domains, called bivalent domains, which are enriched in both H3K27me3 and H3K4me3. Genes

residing in these domains are silent but poised for activation [Bernstein *et al*, 2006]. This bivalent feature is believed to be especially crucial in development as well as differentiation as shown in ES cells [Bernstein *et al*, 2006; Mikkelsen *et al*, 2007; Pan *et al*, 2007]. Among various developmental-related loci, *HOX* genes are mostly repressed by the H3K27me3 mark in stem cells [Cao *et al*, 2002; Müller *et al*, 2002]. Several groups have shown that EZH2 (enhancer of zeste homologue 2), a SET domain containing of polycomb group (PcG) protein, is responsible for the trimethylation of H3K27 [Cao *et al*, 2002; Czermin *et al*, 2002; Kuzmichev *et al*, 2002; Müller *et al*, 2002]. Deletion of this KMT does lead to derepression of *Hox* genes in *Drosophila* [Cao *et al*, 2002]. The H3K27me3 mark contributes gene silencing by acting as a recognition mark on the polycomb response elements (PRE) of *HOX* genes for binding of the chromodomain protein Pc (Polycomb) of repressive complex PRC1 (polycomb repressive complex 1). Such binding in turn facilitates a series of gene silencing effects accompanied with monoubiquitination of H2A [Cao *et al*, 2005; Fischle *et al*, 2003; Min *et al,* 2003; Wang *et al*, 2004]. Even so, recent genomic studies of histone methylation profiles in differentiated cells showed that bivalent domains are not restricted to undifferentiated ES cells but also present in differentiated cells, suggesting a crucial role of H3K27me3 in gene silencing in diverse cell types [Barski *et al*, 2007; Mikkelsen *et al*, 2007].

1.2.1.2 Arginine methylation

Arginine is another residue that can be methylated on histones. Arginines 2, 8, 17 and 26 of histone H3 and arginine 3 of histone H4 were shown to be methylated in mammals (Figure 1.13) [Klose & Zhang, 2007]. There are up to 11 protein arginine methyltransferases (PRMT) (PRMT 1 – 11) have been identified in human so far even though not all of them are able to methylate histone proteins. Of the identified PRMTs, only PRMT1, PRMT4, PRMT5 – 9 are found to be responsible for arginine methylation on histone proteins to date (Table 1.5) [Chen *et al*, 1999; Cook *et al*, 2006; Guccione *et al*, 2007; Lee *et al*, 2005a; Lee *et al*, 2005b; Schurter *et al*, 2001; Strahl *et al*, 2001]. Functions and impacts on chromatin activities of arginine methylation have

not been examined in depth but similar to lysine methylation, the effects on chromatin are also dependent on the methylation site and state. Even dimethylation, whether the arginine is asymmetrically or symmetrically methylated can impose opposite effects on chromatin activities [Lee *et al*, 2005c]. Such discrepancy in the symmetry of dimethylation may result in recruiting different binding proteins to the chromatin for regulation of transcription or other activities.

PRMT	Type	Substrate specificity	Function
PRMT1	I	H4R3	Transcriptional activation
PRMT4	I	H3R2, 17, 26, 128, 129, 131, 134	Transcriptional activation
PRMT5	II	H3R8, H4R3	Transcriptional repression
PRMT6	I	H2A, H3R2, H4	Inhibit H3K4 trimethylation
PRMT7	II	H2A, H4R3	Imprinting in male germ cells
PRMT8	I	H4	Unknown
PRMT9	II	H2A, H4	Unknown

Table 1.5 Table showing substrate specificity of PRMTs and impacts of the arginine methylation on chromatin activities. Derived from Hyllus *et al*, 2007; Pal & Sif, 2007; Guccione *et al*, 2007. Only PRMTs can methylate histone proteins are shown here.

1.2.1.3 Histone demethylation

Histone methylation was considered for some time as a stable mark that was not subject to turnover. However, the discovery of a large number of histone lysine demethylases (KDM) reveals a more dynamic nature to these modifications. KDMs have specificity against histone residue and even methylation state (Table 1.6). LSD1 (lysine specific demethylase 1) was the first KDM to be identified, which removes the methyl group on lysine 4 monomethylated histone H3 [Shi *et al*, 2004]. Although the crystal structure of LSD1 revealed the capability to demethylate all the three methylation states of H3K4, LSD1 has no demethylase activity towards trimethylated H3K4 [Shi *et al*, 2004; Stavropoulos *et al*, 2006].

New name	Old name	Specificity	Function
KDM1	LSD1/BHC110	- H3K4me1/2 - H3K9me1/2	- Transcription activation - Transcription repression - Heterochromatin formation
KDM2A	JHDM1a/FBXL11	- H3K36me1/2	- Transcription elongation
KDM2B	JHDM1b/FBXL10	- H3K36me1/2	- Transcription elongation
KDM3A	JHDM2a	- H3K9me1/2	- Androgen receptor gene activation - Spermatogenesis
KDM3B	JHDM2b	- H3K9me	- Unknown
KDM4A	JMJD2A/JHDM3A	- H3K9me2/3 - H3K36me2/3	- Transcription repression - Genome integrity - Activation of androgen receptor dependent transcription
KDM4B	JMJD2B	- H3K9me2/3 - H3K36me2/3	- Heterochromatin formation
KDM4C	JMJD2C/GASC1	- H3K9me2/3 - H3K36me2/3	- Transcription activation - Transcription repression
KDM4D	JMJD2D	- H3K9me2/3	- Activation of androgen receptor dependent transcription - Transcription activation - Transcription repression
KDM5A	JARID1A/RBP2	- H3K4me2/3	- Retinoblastoma-interacting protein
KDM5B	JARID1B/PLU-1	- H3K4me1/2/3	- Transcription repression
KDM5C	JARID1C/SMCX	- H3K4me2/3	- X-linked mental retardation
KDM5D	JARID1D/SMCY	- H3K4me2/3	- Male-specific antigen
KDM6A	UTX	- H3K27me2/3	- Transcription activation
KDM6B	JMJD3	- H3K27me2/3	- Transcription activation

Table 1.6 Summary of human KDMs. Derived from Allis *et al*, 2007; Shin & Janknecht, 2007a; Shin & Janknecht, 2007b. As these KDMs are better known with their old names, the old naming system will be used in this thesis.

JmjC (Jumonji-C)-containing enzymes define the largest class of KDMs that are capable to demethylate trimethylated lysines. There are at least 27 JmjC-containing proteins identified in recent years. 15 of them have been shown to demethylate lysines on the H3 tails and one to demethylate arginines on H3 and H4 [Agger *et al*, 2008]. Like KMTs, JmjC-containing KDMs are specific to both the sequence context and methylation state for demethylation (Table 1.6).

The mechanism of arginine demethylation is not fully understood. It has been suggested that histone demethylimination is involved in the process in which peptidylarginine deiminase (PADI) enzymes can convert unmodified or methylated arginine residues to citrulline (Figure 1.16). PADI4 is suggested to be responsible for the conversion of methylated histone arginine to citrulline, such that the level of histone arginine methylation is reduced [Cuthbert *et al*, 2004; Wang *et al*, 2004]. However, it is not known whether the citrullinated arginine can be fully reversed to an unmodified arginine, other enzymatic pathways might be required or alternatively, the citrullinated histone is simply replaced by an unmodified one by chromatin remodelling complexes.

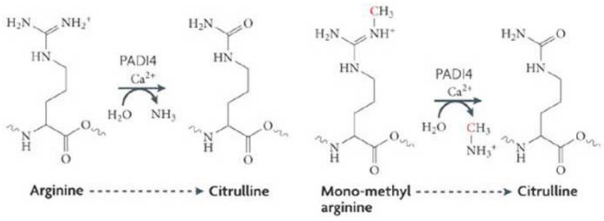

Figure 1.16 Deimination of arginine (left) and demethylimination of methylated arginine (right) using PADI4 as an example. After the conversion, methylated arginine becomes citrulline. Adapted from Klose and Zhang, 2007.

1.2.2 Histone acetylation

While histone methylation plays a dual role in transcription and regulation of chromatin structure, histone acetylation is mostly responsible for maintaining a transcriptionally permissive chromatin structure. All four core histones can be acetylated (Figure 1.13). Histone acetyltransferases (KAT) catalyse the addition of an acetyl group to a lysine residue using acetyl Co-A as substrate (Figure 1.17). Like KMTs, KATs have substrate specificity, targeting specific histones and lysine residues for modification (Table 1.7).

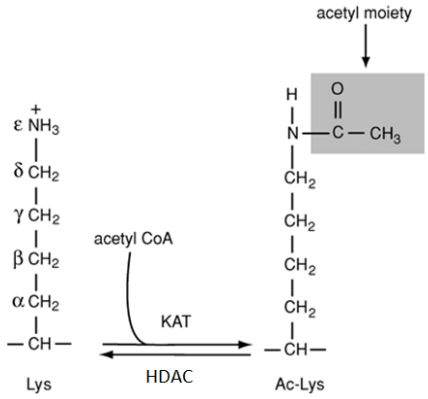

Figure 1.17 Lysine acetylation and deacetylation. Modified from Pelletier *et al*, 2008.

As the addition of an acetyl group neutralises the positive charge of the lysine side chain, it is hypothesised that histone acetylation weakens the interaction between negatively charged DNA and basic histone tails. Some previous studies showed that there are indeed some perturbations to histone-DNA contacts by histone acetylation [Ausió & van Holde, 1986; Simpson, 1978]. However, contrasting results question whether neutralisation of histone charges is sufficient to alter chromatin structure. Even in the same study performed by Ausió and van Holde, they found that in physiological ionic strength, nucleosomes containing hyperacetylated or minimally acetylated histones are persistently folded [Ausió & van Holde, 1986]. It was also observed that hyperacetylated and hypoacetylated histones exhibit similar binding affinities for nucleosomal DNA [Mutskov *et al*, 1998]. Furthermore, mutating the acetylable lysines of histone H3 to same charged arginine or uncharged glycine residues also display similar phenotypes in yeast [Mann and Grunstein, 1992], altogether arguing against the essential role of the lysine positive charge in chromatin folding. Taken together, these results suggest that factors other than charge neutralisation contribute to the role of histone acetylation in alteration of chromatin structure.

New name	Old name	Specificity	Function
KAT1	HAT1	- H4K5/K12	- Histone deposition - DNA repair
KAT2A	hGCN5	- H3K9/K14/K18 - H2B	- Transcription activation
KAT2B	PCAF	- H3K9/K14/K18 - H2B	- Transcription activation
KAT3A	CBP	- H2AK5 - H2BK12/K15	- Transcription activation
KAT3B	p300	- H2AK5 - H2BK12/K15	- Transcription activation
KAT4	TAF1	- H3 - H4	- Transcription activation
KAT5	TIP60/PLIP	- H4K5/K8/K12/K16 - H2A - H2A.Z	- Transcription activation - DNA repair
KAT6A	MOZ/MYST3	- H3K14	- Transcription activation
KAT6B	MORF/MYST4	- H3K14	- Transcription activation
KAT7	HBO1/MYST2	- H4K5/K8/K12 - H3	- Transcription - DNA replication
KAT8	HMOF/MYST1	- H4K16	- Chromatin boundaries - Dosage compensation - DNA repair
KAT9	ELP3	- H3 - H4	- Transcription elongation
KAT12	TFIIIC90	- H3K9/K14/K18	- Polymerase III transcription
KAT13A	SRC1	- H3 - H4	- Transcription activation
KAT13B	ACTR	- H3 - H4	- Transcription activation
KAT13C	P160	- H3 - H4	- Transcription activation
KAT13D	CLOCK	- H3 - H4	- Transcription activation

Table 1.7 List of human KATs and their substrate specificities and related functions in chromatin activities. Derived from Allis *et al*, 2007; Han *et al*, 2008; Winkler *et al*, 2002. Old names of KATs will still be used throughout this thesis because they are better known with these names.

In addition to the potential effects on histone charge, histone acetylation also acts as a recognition mark for the transcription factors and chromatin remodelling complexes. Like histone methylation, there is a recognition domain specific to histone acetylation, called the bromodomain, commonly found in transcription coactivators and chromatin remodelling complexes [Hassan *et al*, 2002; Hassan *et al* 2007; Sanchez & Zhou, 2009; Winston & Allis, 1999] (Table 1.8). It has been shown that H3 lysine 14 acetylation (H3K14ac) can enhance binding affinity of the RSC (remodels the structure of chromatin) complex to the nucleosomes and acetylated H4 can increase catalytic activity of the complex [Ferreira *et al*, 2007]. Furthermore, the SWI/SNF complex preferentially displaces acetylated histones *in vitro* [Chandy *et al*, 2006], demonstrating the necessity of histone acetylation in chromatin remodelling activity. Moreover, a bromodomain protein Bdf1 (bromodomain-containing protein 1) recognising acetylated H4 is a subunit of the TFIID complex that initiates transcription [Durrant & Pugh, 2007], suggesting that histone acetylation is required for transcription.

Protein category	Bromodomain protein	Function
Histone acetyltransferase	p300	Transcription coactivation
	PCAF	
	CBP	
	$TAF_{II}250$	
	GCN5	
Histone methyltransferase	MLL	Transcription coactivation
Chromatin remodelling	BRM	Transcription coactivation/corepression
	BRG1	

Table 1.8 Table showing bromodomain containing proteins in human and their functions. Modified from de la Cruz *et al*, 2005.

There is also a relationship between gene body acetylation and transcription elongation. Several KATs such as CBP (CREB binding protein) and PCAF (p300/CBP-associated factor) have been shown to physically interact with complexes involved in transcription elongation [Cho *et al*, 1998; Wery *et al*, 2004; Wittschieben *et al*, 1999]. Therefore, the trailing patterns of H3 and H4 acetylation along active transcribed regions may be a result of the passage of RNA polymerase II

and may set as epigenetic memory to facilitate subsequent rounds of transcription [Wang *et al*, 2008]. On the other hand, the presence of bromodomains in KATs associated with RNA polymerase II suggests the possibility that the transcription machinery is directed to sites for transcription *via* binding to acetylated histones [Kanno *et al*, 2004; Jacobson *et al*, 2000; Obrdlik *et al*, 2008].

Due to the intrinsic potential of histone acetylation to initiate transcription, it needs to be tightly regulated to prevent aberrant transcription activation and cryptic transcription within gene bodies [Carrozza *et al*, 2005; Joshi & Struhl, 2005]. At least 18 histone deacetylases (HDAC) have been identified thus far in mammals and up to 11 (HDAC 1 – 11) in human [Hildmann *et al*, 2007; Ropero & Esteller, 2007]. The substrate specificity of HDACs is still poorly understood. HDACs are generally considered to be transcription corepressors due to the interaction with several repressive complexes, including mSin3A (mammalian Sin3 homolog A), NuRD and CoREST [Dannenberg *et al*, 2005; You *et al*, 2001; Zhang *et al*, 1999]. The Rpd3 (reduced potassium dependency 3, the yeast homolog of mammlian HDAC1/2) complex, for instance, possesses histone deacetylation activity and can prevent transcription initiation. The bromodomain-containing subunits Eaf3 (Esa1p-associated factor 3) and Rco1 appear to target the entire complex towards transcribed regions to carry out deacetylation in order to prevent transcription initiation within the coding regions [Carrozza *et al*, 2005; Joshi & Struhl, 2005; Keogh *et al*, 2005; Li *et al*, 2007]. Repression of gene expression mediated by histone deacetylation is also observed in higher eukaryotes [Brehm *et al*, 1998; Evert *et al*, 2006]. Nevertheless, histone deacetylation is not restricted to gene repression; it is also involved in other chromatin activities, such as DNA repair or even transcription activation in some cases, apparently depending on what protein complexes the HDAC associates with [Hildmann *et al*, 2007].

1.2.3 Histone ubiquitination

Unlike other post-translational modifications, ubiquitination involves the conjugation of a ~8.5 kDa ubiquitin protein to a lysine residue of the target substrate covalently. The ubiquitination pathway typically involves E1 (ubiquitin-activating enzyme), E2 (ubiquitin-conjugating enzyme) and E3 (ubiquitin ligase), where the E3 typically determines the substrate specificity (Figure 1.18). Substrates can be mono- or poly-ubiquitinated; the ubiquitination state determines the fate of proteins. In general, polyubiquitinated proteins are targets of the 26S proteasome for degradation. In contrast, monoubiquitination does not usually result in degradation, and it is more likely to act as a signal for diverse cellular functions. Histone ubiquitination discussed hereafter mostly focuses on histone monoubiquitination. Histone ubiquitination is reversible through the action of deubiquitination enzymes.

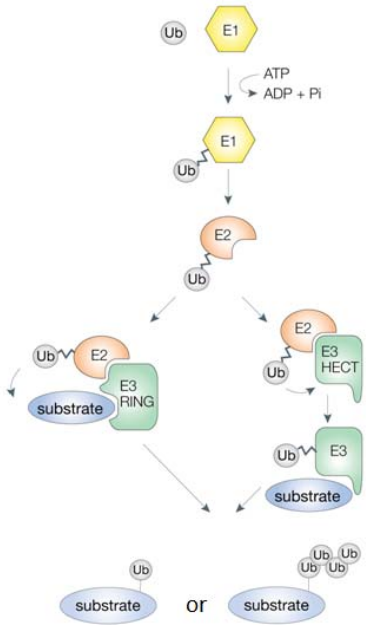

Figure 1.18 The ubiquitination pathway. Ubiquitin is firstly activated by E1 in an ATP-dependent manner. The activated ubiquitin is then transferred to E2 and ultimately conjugated to a target substrate in the presence of E3. The substrate can be either mono- or poly-ubiquitinated. There are two classes of E3 ligases, RING (really interesting new gene) and HECT (homologus to the E6-AP carboxyl terminus). Ubiquitin usually does not form covalent bond with a RING E3 while it does with a HECT E3. The figure is modified from Woelk *et al*, 2007.

All four core histones can be ubiquitinated but the functions of H3 and H4 ubiquitination are not very clear [Goldknopf & Busch, 1975; Osley, 2006; Wang *et al*, 2006; West & Bonner, 1980]. A ubiquitin moiety is conjugated to lysine 119 of H2A (H2AK119ub1) and to lysine 120 (equivalent to lysine 123 in *S. cerevisiae*) of H2B (H2BK120ub1) in mammals [Böhm *et al*, 1980; Thorne *et al*, 1987]. One might expect that the attachment of such a large molecule to

histones would induce massive structural changes on histones, nucleosomes or even chromatin, given that the sizes of histones (14 – 17 kDa) and ubiquitin (8.5 kDa) are quite comparable. However, evidence supporting this structural disturbance is scarce, and also replacement of ubiquitin by a bulkier SUMO (small ubiquitin-like modifier) protein does not even destabilise the chromatin [Chandrasekharan *et al*, 2009]. Interestingly, a recent report demonstrated that ubiquitinated H2B can enhance nucleosome stability [Chandrasekharan *et al*, 2009; Jason *et al*, 2002]. Even so, ubiquitination of H2A and H2B is involved in the regulation of various chromatin activities, such as transcription activation, repression, elongation, heterochromatin establishment and DNA repair. There is growing consensus that the regulation of chromatin processes by this histone ubiquitination is more likely to be mediated *via* recruitment of other protein complexes, rather than altering the chromatin structure directly.

1.2.3.1 H2A ubiquitination

H2A and H2B ubiquitination appear to play opposite roles in transcriptional regulation. Ubiquitination of H2A correlates with gene silencing whereas that of H2B correlates with transcription activity. H2AK119ub1 is localised to heterochromatin and the inactivated X chromosome [Baarends *et al*, 1999; Baarends *et al*, 2005; Smith *et al*, 2004]. There are several E3 ligases specific to H2A in which RING1B and 2A-HUB are the two prevalent ones associated with repressive chromatin complexes (Figure 1.19). RING1B is a well characterised example that associates with at least three repressive complexes: the PRC1, E2F-6.com-1 (E2F transcription factor 6 complex 1) and FBXL10-BcoR corepressors complexes [Cao *et al*, 2005; Ogawa *et al*, 2002; Sánchez *et al*, 2007; Wang *et al*, 2004]. These repressive complexes are responsible for generating repressive histone marks, H3K9 and H3K27 methylation, as well as H3K4 demethylation, linking H2AK119ub1 to gene silencing [Cao *et al*, 2002; Muller *et al*, 2002; Ogawa *et al*, 2002; Sanchez *et al*, 2007; Wang *et al*, 2004]. Conversely deubiquitination of H2AK119ub1 is correlated with transcription activity. At least four histone deubiquitination enzymes have been identified to be able to deubiquitinate H2A (Figure 1.19), they are associated

with complexes required for transcription and gene activation [Joo *et al*, 2007; Nakagawa *et al*, 2008; Zhao *et al*, 2008].

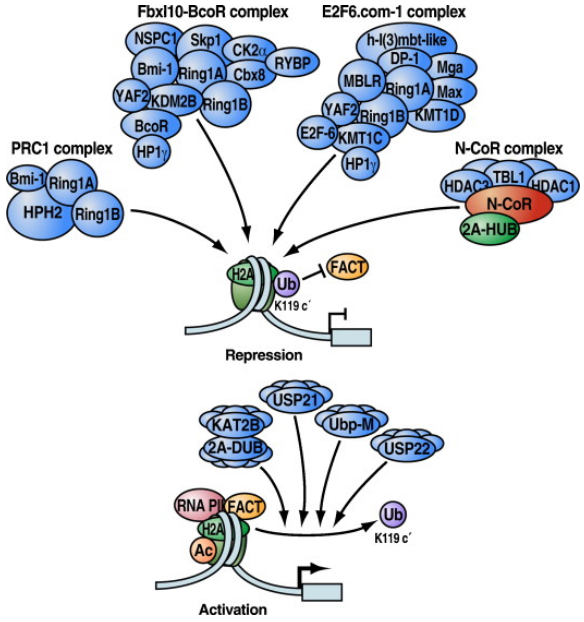

Figure 1.19 Examples of effects of H2A ubiquitination on gene expression. RING1B and 2A-HUB are E3 ligases specific to H2A. RING1B is a component of several repressive complexes including PRC1, FBXL10-BcoR and E2F-6.com.1 whereas 2A-HUB associates with the N-CoR complex. These complexes are involved in gene expression repression through catalysing H2A ubiquitination. On the contrary, H2A deubiquitination enzymes promote gene activation by removing ubiquitin from H2Aub. Adapted from Zhou *et al*, 2009.

1.2.3.2 H2B ubiquitination

1.2.3.2.1 Factors required for H2B ubiquitination

The first H2B ubiquitination ligase was firstly identified in *S. cerevisiae* as a cell size control factor Bre1 [Hwang *et al*, 2003]. It interacts with the E2 conjugating enzyme Rad6 [Wood *et al*, 2003]. Both Bre1 and Rad6 are essential for monoubiquitination of H2B on lysine 123 (H2BK123ub1) in yeast [Hwang *et al*, 2003; Robzyk *et al*, 2000]. The same H2B ubiquitination appears to be conserved from yeast to higher eukaryotes. Human Rad6 homologs, HR6A and HR6B, also serve as E2 conjugating enzymes [Kim *et al*, 2009]. By using sequence alignment, yeast Bre1 homologs were also found in other species including human [Hwang *et al*, 2003]. There are two Bre1 homologs in human, RNF20 and RNF40, forming a complex for the ubiquitination activity. siRNA induced knockdown of RNF20 or RNF40 results in a decreased level of H2B ubiquitination (H2BK120ub1) [Kim *et al*, 2005; Zhu *et al*, 2005]. In addition to RNF20/40, more other E3 ligases for H2B ubiquitination have been identified in humans. MDM2 (mouse double minute 2) and BRCA1/BARD1 (breast cancer susceptibility gene

1/BRCA1 associated RINF domain 1) have been shown to be able to ubiquitinate H2B *in vitro* [Minsky & Oren, 2004; Thakar *et al*, 2010]. A chromatin remodelling complex factor BAF250/ARID1 (BRG1-assoicated factor 250/AT rich interactive domain 1) was also recently shown to ubiquitinate H2B *in vitro* and siRNA induced knockdown of this E3 ligase leads to a reduction of H2BK120ub1 globally [Li *et al*, 2010]. Nevertheless, except RNF20/40, the other human E3 ligases have not been studied in depth and it remains elusive whether they target the same or different genomic loci of H2B for ubiquitination.

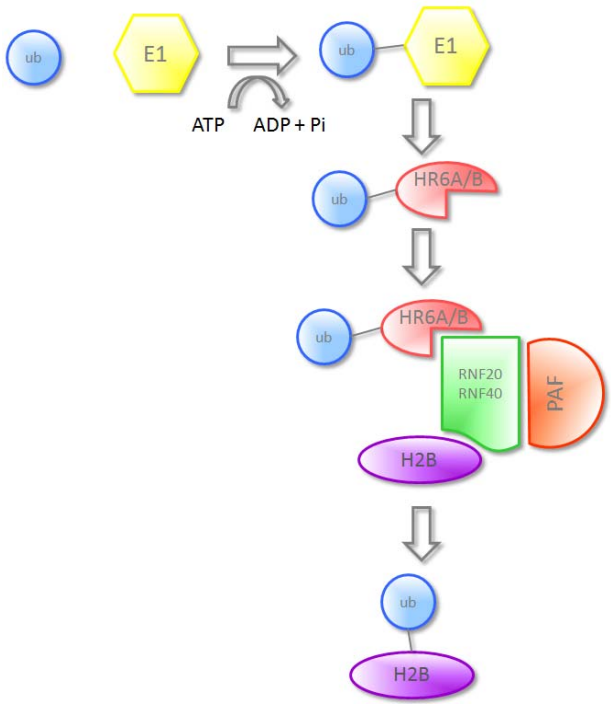

Figure 1.20 The H2B ubiquitination pathway in humans. Ubiquitin (ub) is firstly activated by E1 with ATP hydrolysis. The activated ubiquitin attached to E1 is then passed to E2, HR6A or HR6B. The ubiquitin is finally transferred from E2 to H2B in the presence of RNF20/40 and PAF1 complexes where only RNF20/40 determines the substrate specificity.

Unlike the conventional ubiquitination pathway, E1, E2 and E3 are not sufficient to drive efficient H2B ubiquitination on gene loci (Figure 1.20). The PAF1 (RNA polymerase II associated factor) complex is also required for H2B ubiquitination in yeast and humans, and deletion of any of the complex subunits results in loss of H2BK123ub1 in yeast [Ng *et al*, 2003; Xiao *et al*, 2005]. It is suggested that the intact PAF1 complex is required to bridge the E3 and E2 enzymes together [Zhu *et al*, 2005]. Other factors, such as kinases responsible for phosphorylation of RNA polymerase II for instance, are required for efficient ubiquitination of nucleosomal H2B at gene loci. Deletion of Kin28 (CDK7 in humans) in *S. cerevisiae* abolishes

phosphorylation of serine 5 at the RNA polymerase II CTD (C-terminal heptapeptide repeat sequences), and also the global level of H2BK123ub1 is seriously diminished [Xiao *et al*, 2005]. It suggests that Kin28 plays a role in facilitating H2B ubiquitination but the mechanism is not known (Figure 1.21b). It is not clear whether the phosphorylation on RNA polymerase II is essential for subsequent steps of the ubiquitination pathway or if Kin28 works on the pathway directly by stimulating or recruiting the H2B ubiquitination machinery. The Bur kinases responsible for phosphorylation of serine 2 at the RNA polymerase II CTD during transcription elongation are also required for H2B ubiquitination in yeast. It was shown that the Bur kinases are able to phosphorylate not only the RNA polymerse II but also the E2 conjugating enzyme of H2B ubiquitination Rad6 such that the conjugase activity is augmented (Figure 1.21b) [Laribee *et al*, 2005; Wood *et al*, 2005]. The conjugase activity of the human Rad6 ortholog HR6A is also augmented by CDK2 phosphorylation, suggesting conservation of this regulatory pathway [Sarcevic *et al*, 2002]. Another protein factor, Lge1 (large 1), one of the cell size control factors identified together Bre1 in yeast, was recently shown to be required for the recruitment of Bre1 to actively transcribed genes [Hwang *et al*, 2003; Song & Ahn, 2010]. The involvement of more auxiliary protein factors in the H2B ubiquitination pathway compared with the conventional protein ubiquitination suggests that H2B ubiquitination is tightly regulated by different means in order to achieve different functions in the genome.

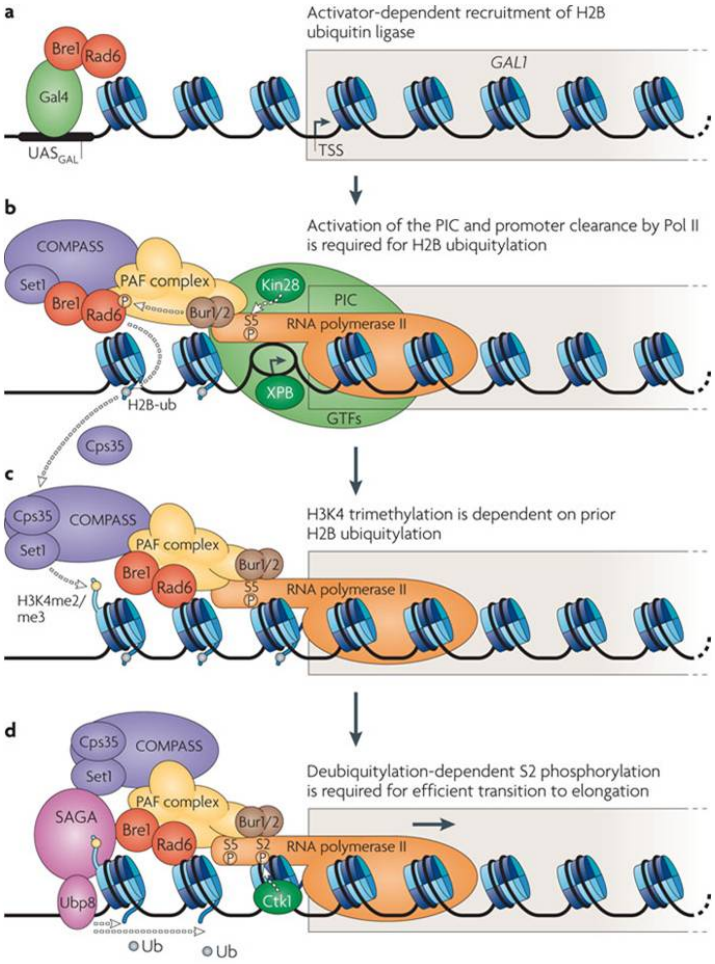

Figure 1.21 Sequential events on chromatin leading to H2B ubiquitination-coupled transcription upon gene activation in yeast. Adapted from Weake and Workman, 2010.

1.2.3.2.2 Relationship between H2B ubiquitination and transcription

H2B ubiquitination and gene transcription are interdependent. Ubiquitinated H2B is enriched at the gene bodies in the yeast genome and at both the gene bodies and promoter in the human genome (Figure 1.22), suggesting a link between gene transcription and H2B ubiquitination [Minsky *et al*, 2008; Schulze *et al*, 2009]. The necessity of transcription for efficient H2B ubiquitination is supported by findings that an addition of NTPs for proper transcription is required to detect H2BK120ub1 and conversely, blocking transcription with drug inhibitors leads to a global loss of H2B ubiquitination [Kim *et al*, 2009; Minsky *et al*, 2008; Pavri *et al*, 2006]. A recent study found that the binding of RNF20 to chromatin is *via* the elongating form of RNA polymerase II, explaining the requirement of transcription for H2B ubiquitination at gene loci [Zhang & Yu, 2011]. Conversely, proper transcription also depends on H2B ubiquitination.

Knockdown of RNF20 represses the *HOX* and *p53* gene expression in humans and deletion of *Rad6* or *Bre1* in yeast results in increased sensitivity to 5-fluorouracil, a drug inhibitor of transcription elongation [Shema *et al*, 2009; Xiao *et al*, 2005; Zhu *et al*, 2005].

a **b**

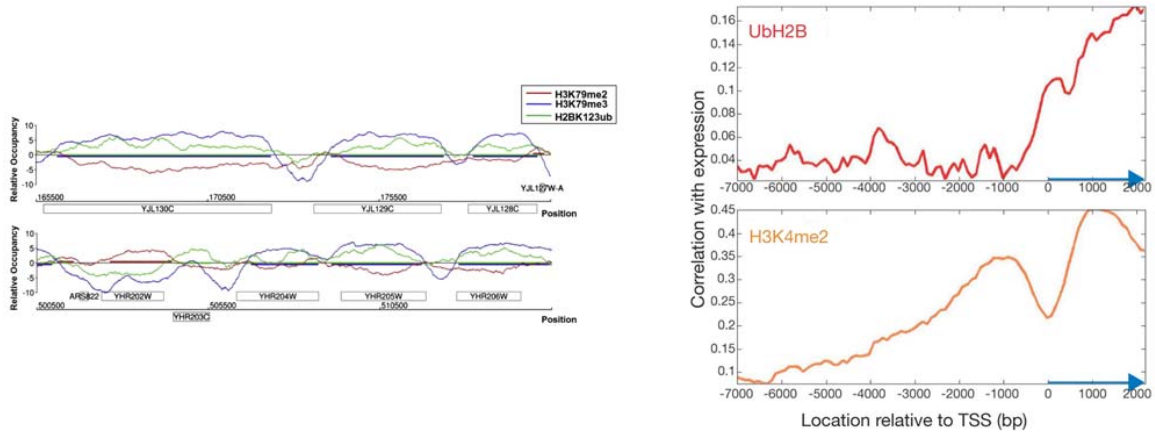

Figure 1.22 Occupancy of ubiquitinated H2B in the yeast **(a)** and human genomes **(b)**. Adapted from Minsky *et al*, 2008 and Schulze *et al*, 2009.

The role of H2B ubiquitination in transcription is suggested to be chromatin structure regulation, possibly through the regulation of the FACT (facilitates chromatin transcription) activity. FACT is a histone chaperone binding to H2A-H2B dimer so it plays a crucial role in both destabilisation of chromatin structure for transcription and chromatin structure restoration following the passage of RNA polymerase II [Orphanides *et al*, 1999]. The FACT activity stimulated by H2BK120ub1 helps destabilising chromatin structure to overcome the nucleosomal barrier to the passage of RNA polymerase II [Belotserkovskaya *et al*, 2003; Pavri *et al*, 2006]. Following the wake of elongating RNA polymerase II, histone redeposition is required to restore the chromatin structure for binding of transcription factors for next round of transcription. The accumulation of Spt16, the largest subunit of FACT, at the *GAL1* gene is found to require ubiquitinated H2B in yeast, suggesting a chromatin stabilisation role of H2B ubiquitination during transcription [Fleming *et al*, 2008]. Although these studies suggest a requirement of H2B ubiquitination in transcription elongation, an *in vitro* transcription assay using H2BK120R, H2B mutant that cannot be ubiquitinated, argues against the hypothesis. It

was showed that the transcription activity on H2B- or H2BK120R-containing nucleosomes is more or less the same [Kim *et al*, 2009]. However, the transcription assay was performed with recombinant chromatin template, effects of genomic contexts and other histone modifications on gene transcription are completely ignored. Moreover, as H2B ubiquitination could be required for transcription in a gene-specific manner according to an observation that RNF20 knockdown does not lead to a global gene repression [Shema *et al*, 2009], the generalisation of using recombinant chromatin template to represent the chromatin *in vivo* for the transcription assay may not reflect the real scenario at the specific gene loci in the genome.

Although H2B ubiquitination is required for transcription in certain scenarios, the level of ubiquitinated H2B is not and cannot be persistently maintained high during transcription. Yeast Ubp8 (USP22 in human), a component of the SAGA (Spt-Ada-Gcn5-Acetyltransferase) complex facilitating the assembly of PIC, is able to deubiquitinate H2BK123ub1 and such activity is needed for efficient transcription (Figure 1.21d) [Bhaumik & Green, 2001; Henry *et al*, 2003; Zhang *et al*, 2008; Zhao *et al*, 2008]. Deletion of *ubp8* results in an elevated global level of H2BK123ub1 and repression of SAGA-regulated genes [Daniel *et al*, 2004; Henry *et al*, 2003]. A time course experiment on the induced *GAL1* gene in yeast demonstrated that H2BK123ub1 increases with increasing *GAL1* mRNA at the early stages upon induction but the level of H2BK123ub1 decreases and finally reaches the background level again following the accumulation of mRNA, [Henry *et al*, 2003]. This result suggests that H2B ubiquitination is required for transcription activation and probably also for the early stage of elongation but deubiquitination is also required. Deubiquitination of H2B is shown to be essential for the binding of the Ctk1 phosphorylase that is responsible for the transition of the RNA polymerase II from the activated form to the elongating form [Wyce *et al*, 2007].

1.2.3.2.3 Other roles of H2B ubiquitination in the genome

H2B ubiquitination has been found to be a master regulator of H3K4 and H3K79 methylation but such regulation is not linked to transcription. It was shown that deletion of *rad6* or *bre1* in yeast results in lowered levels of di- and tri-methylation of H3K4 and K79 [Briggs *et al*, 2002; Dover *et al*, 2002; Shahbazian *et al*, 2005; Sun & Allis, 2002; Wood *et al*, 2003]. The crosstalk between H2B ubiquitination and this H3 methylation is conserved in mammals [Zhu *et al*, 2005; Kim *et al*, 2005; Kim *et al*, 2009]. However, the link is unidirectional because abolishment of this H3 methylation by deletion of KMT genes *dot1* and *set1* does not alter the global level of H2BK123ub1 in yeast [Ng *et al*, 2002; Sun & Allis, 2002]. The crosstalk mechanism will be discussed in detail in Section 1.2.4. Despite the active role of ubiquitinated H2B in transcription and that H3K4 methylation is a mark of active transcription; H2B ubiquitination does not appear to facilitate transcription *via* H3K4 methylation. By comparing the gene expression profiles of fission yeast mutants exhibiting defects in H3K4 methylation and H2B ubiquitination, it showed that changes of expression profiles in the two mutants do not overlap [Tanny *et al*, 2007]. Furthermore, while H2BK123ub1 spans the entire gene bodies in yeast, H3K4me3 only peaks at gene promoters and declines along the coding regions [Pokholok *et al*, 2005; Schulze *et al*, 2009]. The results suggest that the functions of these two histone modifications in transcription are different and H2B ubiquitination-mediated H3K4 methylation seems to have another role in the genome. Moreover, the effect of mutation H3K4A, which cannot be methylated, on the inducible *GAL* gene expression differs from that of H2BK123R, which cannot be ubiquitinated, further implying non-overlapping roles of H3K4 and H2BK123 modifications in transcription [Fleming *et al*, 2008].

Another role for H2B ubiquitination in chromatin is that of counteracting heterochromatin silencing in yeast. Expression of the *URA3* gene located near the telomere of chromosome VII is silenced in yeast strains without ubiquitinated H2B [Sun & Allis, 2002]. Ubp10 is another yeast deubiquitination enzyme, and its deletion of *Ubp10* results in a global increase in H2BK123ub1

[Gardner *et al*, 2005]. Ubp10 appears not to be associated with the transcriptional machinery; it is more likely to be associated with heterochromatin silencing. Several studies in yeast have found that Ubp10 is preferentially localised at silent domains and telomeres [Gardner *et al*, 2005; Emre *et al*, 2005]. While H3K79 methylation is mediated by H2B ubiquitination and is unfavourable for the Sir protein binding that is required for heterochromatin formation, Upb10 is suggested to actively deubiquitinate H2B at silent loci to facilitate heterochromatin silencing [Emre *et al*, 2005]. The physical interaction between Ubp10 and Sir proteins further indicates that deubiquitination is essential for heterochromatin formation [Kahana & Gottschling, 1999]. H2B ubiquitination seems to be required for anti-silencing in *Drosophila* and *Arabidopsis*. Knockdown of *Drosophila USP22* (homolog of yeast Ubp8) results in an increase in H2B ubiquitination as expected but represses PEV induced transgene silencing [Zhao *et al*, 2008]. Similarly, mutation of SUP32/UBP26, which deubiquitinates H2B in *Arabidopsis*, results in an increase in H2B ubiquitination and the release of heterochromatic silencing of transgenes, accompanied by lower levels of H3K9me2 and DNA methylation [Sridar *et al*, 2007]. However, a similar scenario of antagonising heterochromatin formation by H2BK120ub1 has not been observed in vertebrates. It still remains unclear whether vertebrates adopt the same mechanism to maintain the chromatin organisation.

1.2.4 Crosstalk between histone modifications

Histone modifications are deciphered by specific "reader modules" that are present in histone modifiers, transcription factors or chromatin binding proteins (Table 1.9). They may be responsible for directing chromatin binding proteins/complexes to target sites or providing a platform for the anchoring. These reader modules sometimes work in conjunction with others in the same protein or in a multi-protein complex such that high specificity or affinity is achieved. Accumulating evidence emerges that this multivalent property could facilitate a more dynamic control of the binding of various proteins/complexes. By altering one histone modification, the binding affinity of the current resident protein is modified, in turn allows or inhibits competition

for other protein complexes [Ruthenburg *et al*, 2007].

Reader module		Histone mark
Bromodomain		Acetylated histone tails
Chromodomain or chromodomain-like	Chromodomain	H3K9me2/3, H3K27me2/3
	Double chromodomain	H3K4me1/2/3
	Chromo barrel	H3K36me2/3
	Double/tandem tudor	H3K4me3, H4K20me1/2/3
	MBT (malignant brain tumour) repeats	H4K20me1/2, H1K26me1/2 H3K4me1, H3K9me1/2
PHD (plant homeodomain) finger		H3K4me3, unmethylated H3K4 H3K9me3, H3K36me3
WD40 repeat		Unmodified H3R2, H3K4me2
14-3-3		H3S10ph, H3S28ph
BRCT (breast cancer carboxyl-terminal)		H2A.XS139ph

Table 1.9 Table showing histone modifications recognised by reader modules. Modified from Taverna *et al*, 2007.

As shown in many earlier mentioned histone modification examples, an addition or a removal of histone mark can influence others, these phenomena collectively known as histone crosstalk. Crosstalk of histone modifications can be in a *cis* or *trans* manner, depending on whether the two interacting or counteracting histone modifications are on the same histone (*cis*) or different histones (*trans*) (Figure 1.23).

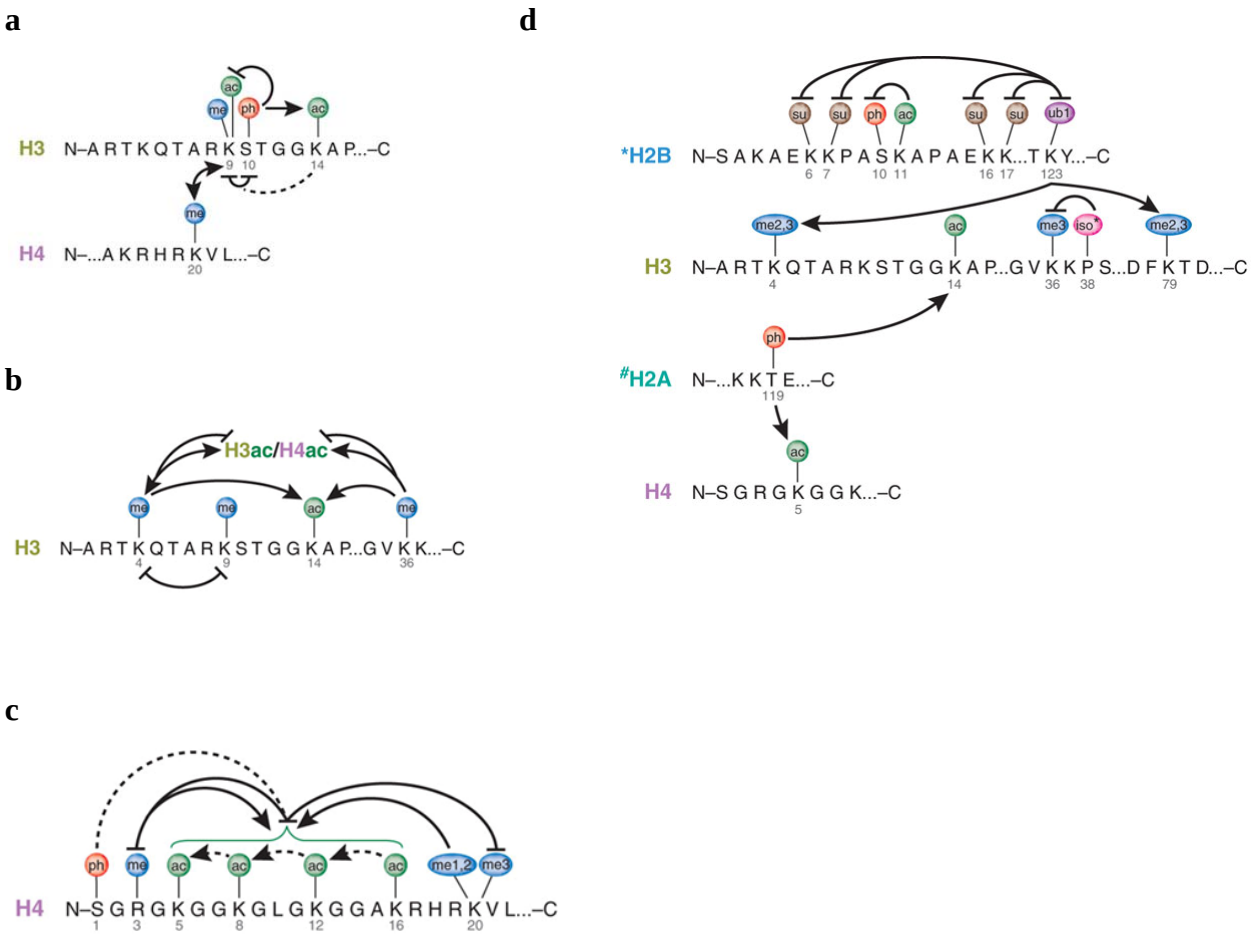

Figure 1.23 Examples of histone crosstalk pathways. **a**. Crosstalk between H3K9, H3S10 and H3K14. **b**. Crosstalk between H3 methylation and H3/H4 acetylation. **c**. Crosstalk between major H4 histone modifications. **d**. *Trans*- and *cis*-histone crosstalk between H2A/H2B and H3/H4. "#" indicates it is only an observation in *Drosophila* to date. Adapted from Latham and Dent, 2007.

While it might not be surprising that the modifications of histone residues in close proximity can influence each other, histone crosstalk can also occur in a *trans* manner. The crosstalk between H2B ubiquitination and H3K4/K79 methylation is the best studied example. The linkage between H3K4 methylation and H2B ubiquitination is mediated by the COMPASS (Complex proteins associated with Set1) complex in yeast [Lee *et al*, 2007]. In the absence of H2B ubiquitination, the H3K4-specific KMT Set1 can bind to target sites and is able to mono, but not di- or tri-methylate H3K4 [Lee *et al*, 2007]. The crystal structure of yeast Set1 catalytic domain showed that Set1 is indeed similar to monomethyltransferases that harbour a tyrosine within the catalytic pocket, while this residue is usually substituted as phenylalanine in di- and

tri-methyltransferases [Takahashi *et al*, 2009]. While Set1 is a component of the COMPASS complex that consists of other non-catalytic subunits (Figure 1.24), interaction of Set1 with these subunits is found to act as the phenylalanine/tyrosine switch to regulate the di- and tri-methylation activity of Set1. It was found that binding of Cps40, Cps60 and Cps35 is required to switch on the di- and tri-methylation activity of Set1. Their binding is suggested to modify the catalytic pocket for the accommodation of trimethylated lysine [Lee *et al*, 2007; Schneider *et al*, 2005; Takahashi *et al*, 2009]. Of these three COMPASS subunits, only the binding of Cps35 requires prior H2B ubiquitination, demonstrating the crosstalk mechanism between H3K4 di-/tri-methylation and H2B ubiquitination [Lee *et al*, 2007]. The sequence orthologs of Cps35 in humans are WDR82 and WDR5, but note that WDR5 is also suggested to be the human ortholog of yeast Cps30 [Shilatifard, 2008]. WDR82 has also been shown to be recruited to SET1 complexes in an H2BK120ub1-dependent manner, and is able to stimulate the SET1 KMT activity to result in higher methylation states [Lee *et al*, 2008; Vitaliano-Prunier *et al*, 2008; Wu *et al*, 2008]. The SET1 protein in the human MLL complexes (COMPASS-like complexes) also consists of tyrosine within the active site and SET1 alone is only able to monomethylate H3K4 *in vitro* [Southall *et al*, 2009]. Although the binding of the MLL complex subunits RbBP5, Ash2 and WDR5 can stimulate the KMT activity of MLL1 *in vitro*, it is not known whether higher methylation states of H3K4 result and whether the binding of these subunits is H2BK120ub1-dependent [Dou *et al*, 2006; Southall *et al*, 2009].

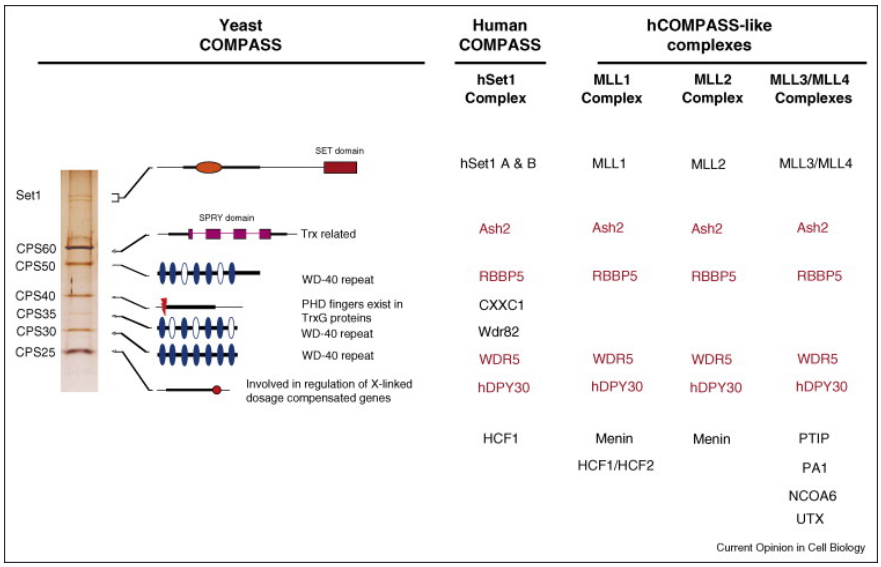

Figure 1.24 Complex components of the yeast and human COMPASS and COMPASS-like complexes. The components of the human SET1 and MLL (COMPASS-like) complexes similar to yeast counterparts are shown in red. Adapted from Shilatifard, 2008.

Compared with the crosstalk mechanism between H2B ubiquitination and H3K4 methylation, the mechanism of H2B ubiquitination facilitating H3K79 methylation is less defined. Nevertheless, it was shown that the recruitment of Cps35 to chromatin is also able to augment the di- and tri-methylation activity of H3K79 KMT DOT1 to nucleosomes although DOT1 is not present in the yeast COMPASS and human SET1 complexes, but how the DOT1 activity is stimulated by Cps35 is not known [Lee *et al*, 2007]. It is also suggested that ubiquitinated H2B itself can directly activate DOT1 as shown in an *in vitro* system using reconstituted nucleosomes [McGinty *et al*, 2008]. However, how and whether the *in vitro* stimulation of DOT1 by ubiquitinated H2B is occurred on native nucleosomes *in vivo* is undetermined.

More evidence of the *trans*-histone crosstalk is emerging, such as crosstalk between H3 methylation and histone acetylation (Figure 1.23b). It was found that chromodomains recognising methylated H3K4 are present in many KAT complexes such as TIP60 and SAGA [Doyon *et al*, 2004; Peña *et al*, 2006; Pray-Grant *et al*, 2005], which are responsible for both H3 and H4 acetylation. The methylated H3K36 recognising protein Eaf3 in the Rpd3 complex with HDAC activity links H3K36 methylation and histone deacetylation together [Li *et al*, 2007].

Collectively, histone modifications not only act a signal for protein binding, rather, they work in a cooperative manner possibly to regulate the chromatin states precisely.

1.2.5 Histone modifications at gene regulatory elements

Promoters and enhancers are generally enriched in active histone modification but their histone modification profiles are not same. Another distinct feature of promoters is their specialised histone modification profile. As mentioned earlier, promoters are generally enriched in H3K4me3 with the highest levels at transcriptionally active promoters (Figure 1.25) [Barski *et al*, 2007; Guether *et al*, 2007; Wang *et al*, 2007]. Histone acetylation, especially H3K9 and K14 acetylation, is essential for the TFIID binding to initiate transcription [Agalioti *et al*, 2002]. H3 acetylation is enriched at nearly 70% of gene promoters, not all of which are active [Guenther *et al*, 2007]. The most highly active promoters are enriched in H3K4me3, H3K9ac and H3K14ac together with other histone acetylation on H4, H2A and H2B (Figure 1.25) [Barski *et al*, 2007; Wang *et al*, 2007]. Early studies using DNaseI or micrococcal nuclease digestion found that transcription start sites (TSS) are more prone to be digested compared with other chromatin regions [Keene & Elgin, 1981; Wu, 1980], implicating a high accessible chromatin structure for binding of transcription factors and coactivators. This nucleosome depleted signature appears to correlate with gene expression that it is absent in silent gene promoters in human [Heintzman *et al*, 2007]. It is thought that the highly accessible structure is due to nucleosome depletion. However, recent findings of studying nucleosome stability found that TSSs consist of unstable nucleosomes containing histone variants H3.3 and H2A.Z [Jin & Felsenfeld, 2007; Jin *et al*, 2009]. Therefore, instead of complete depletion of nucleosomes, TSS nucleosomes are more likely to be turned over very rapidly. In human, two prominent peaks of H2A.Z flanking TSS (at -2 and +1 nucleosomes) are detected (Figure 1.10) [Barski *et al*, 2007; Jin *et al*, 2009; Schones *et al*, 2008]. They are referred to highly positioned nucleosomes. These well positioned nucleosomes especially the +1 nucleosome, which is conserved in many eukaryotes, are suggested to be important to pause RNA polymerase II for preparation of the transition from

initiation to elongation or to prevent anti-sense initiation [Cairns, 2009; Mavrich *et al*, 2008]. However, such well positioned nucleosomes are barriers to the RNA polymerase II passage, chromatin remodelling complexes are needed to overcome this barrier for proper transcription.

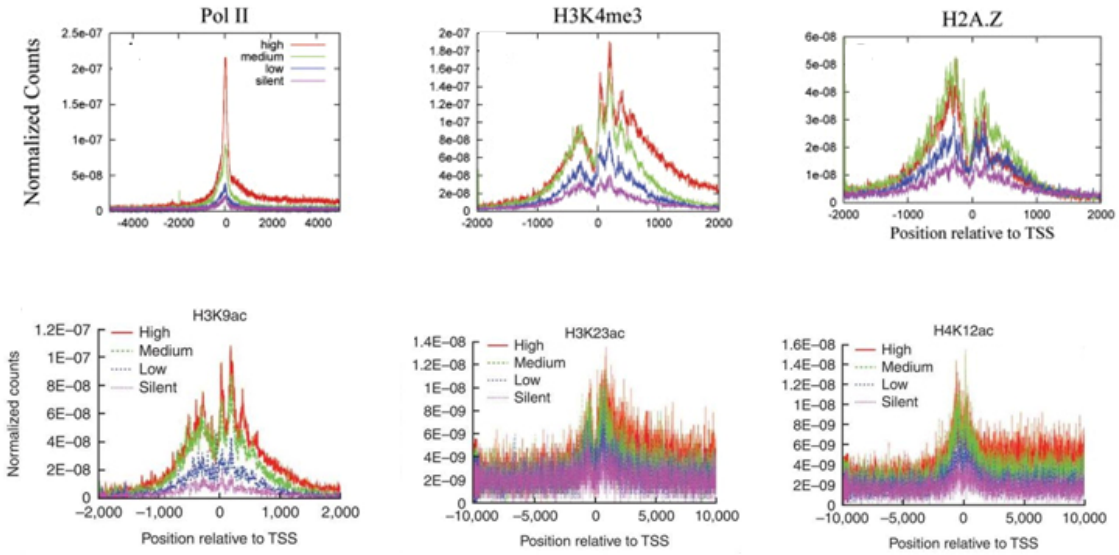

Figure 1.25 Overview of histone modifications at promoters. The expression levels of the categories genes are depicted as colours in the key of each graph. Modified from Barski *et al*, 2007 and Wang *et al*, 2007.

Enhancers and promoters also share similar histone modification patterns; although genome-wide studies also demonstrated that there are some distinct differences between the two classes of regulatory elements [Heintzman *et al*, 2007; Wang *et al*, 2007]. Three H3K4 methylation states are detected at enhancers but H3K4me1 is particularly enriched [Heintzman *et al*, 2007; Heintzman *et al*, 2009; Wang *et al*, 2007]. Histone acetylation and H2A.Z are detected at enhancers, but their levels of enrichment are relative to the expression levels of their target genes [Barski *et al*, 2007; Wang *et al*, 2007]. Enhancers are also DNase hypersensitive; almost all of them consist of at least one hypersensitive site [Wang *et al*, 2007].

1.3 Chromosomal Organisation of Gene Expression

While chromatin states determine gene expression, actively transcribed genes are required to be resided in chromatin domains that are permissive for protein access and so for transcription. Chromatin with permissive chromatin structure is called euchromatin. The chromatin structure of chromatin domains comprised of silent genes and genome structural components, such as telomeres and centromeres is usually more repressive, these regions are known as heterochromatin regions.

1.3.1 Chromosomal domains

Studies of the *β-globin* loci in vertebrates revealed that transcriptionally active and inactive chromatin domains differ not only in protein accessibility, but also histone modification patterns [Bresnick *et al*, 2006]. There are extensive studies on the mammalian and chicken *β-globin* loci revealing how chromatin domains are established and regulated by alteration of histone modifications and binding of chromatin remodelling complexes. The chromatin domain features and their establishment within the chicken *β-globin* locus will be discussed in depth in Section 1.5.

Endonuclease enzymes cleave the phosphodiester bond within DNA; compact chromatin structures with inaccessible DNA are more resistant to digestion. In contrast, chromatin regions with more open chromatin structures are more sensitive to digestion; the digestion patterns therefore reflect the chromatin structure. By using endonuclease digestion, such as DNaseI and micrococcal nuclease, it was found that transcriptionally active chromatin domains possess more open chromatin structure. Regulatory elements such as promoters and enhancers are the most hypersensitive to digestion. Binding of transcription factors and coactivators appear to maintain the open chromatin structures [Kukreti *et al*, 2010].

As discussed earlier (Section 1.2), active histone marks such as H3K4me3 and histone acetylation are usually enriched in active chromatin domains with high transcription activity [Barski *et al*, 2007; Wang *et al*, 2008]. Mapping of histone modifications across the human *β-globin* locus revealed that the correlation of active histone mark density and transcription activity also exists within local chromatin domains. It was found that H3K4me3 and H3ac are enriched at the actively transcribed Gγ and Aγ in fetal stages [Hsu *et al*, 2009; Kim *et al*, 2007]. In contrast, inactive chromatin domains, including silent gene loci, telomeres and centromeres are usually enriched in repressive histone marks such H3K9, H3K27 and H4K20 methylation and lack active histone marks [Barski *et al*, 2007; Rice *et al*, 2003; Schotta *et al*, 2004; Zhou *et al*, 2010].

1.3.2 Heterochromatin domains

Heterochromatin regions are typically gene poor and generally transcriptionally inactive. The levels of transcription from genes within heterochromatin are low and many studies demonstrated that integration of a transgene into heterochromatin regions result in silencing, suggesting that the chromatin environment of heterochromatin is unfavourable for transcription [Grewal & Elgin, 2002; Huisinga *et al*, 2006; Wallrath, 2002].

1.3.2.1 Significance of heterochromatin

Heterochromatin is enriched in repressive histone marks, H3K27me3, H4K20me3 and H3K9me3 in particular, and lacks active histone marks such as H3K4me2, H3K4me3 and acetylation [Barski *et al*, 2007; Rice *et al*, 2003; Schotta *et al*, 2004; Zhou *et al*, 2010]. Heterochromatin also contains SUV39H1/2 and SUV4-20H1/2, which are the KMTs responsible for the establishment of H3K9 and H4K20 methylation and repressive protein complexes containing HP1, which binds H3K9me3 [Kwon & Workman, 2008; Lachner *et al*, 2001; Nakayama *et al*, 2001; O' Carroll *et al*, 2000; Rea *et al*, 2000; Schotta *et al*, 2004].

The relatively stable heterochromatin structure of is crucial for maintaining the genome stability. Repetitive DNA sequences are potential sites for homologous recombination, and repressive heterochromatin appears to inhibit this event [Ellermeier *et al*, 2010; Peng & Karpen, 2008]. Expression of potentially harmful transposable elements is also suppressed by heterochromatin [Lippman & Martienssen, 2004; Peng & Karpen, 2008; Slotkin & Martienssen, 2007]. The rigid structures of constitutive heterochromatin, such as centromeres, not only act as docking sites for cohesin binding to facilitate sister-chromatin cohesion but also needs to be strong enough to withstand the forces exerted by mitotic spindles during chromosome segregation [Bernard, 2001; Nonaka e*t al*, 2001; Oliveira *et al*, 2005]. In contrast to constitutive heterochromatin, facultative heterochromatin is regulated and varies between cell types. A well studied example of facultative heterochromatic silencing is X chromosome inactivation in female mammals. Female mammals have two X chromosomes whereas there is only one in males. In order to balance X-linked gene expression between sexes, one of the two X chromosomes has to be silenced. Heterochromatinization to inactivate one X chromosome is one of the means for dosage compensation [Plath *et al*, 2002].

1.3.2.2 Heterochromatin establishment

The molecular mechanism of heterochromatin formation is best studied in *S. pombe*. Given the transcriptionally repressive nature of heterochromatin, it has come as some surprise that transcription is required for heterochromatin establishment. It has been shown that RNA polymerase II is associated with heterochromatin machinery and transcribes non-coding RNA transcripts of centromeric-like sequences of the *S. pombe MAT* locus [Djupedal *et al*, 2005; Kato *et al*, 2005]. The single-stranded RNA (ssRNA) is reverse transcribed by RNA-dependent RNA polymerase (RdRP) to synthesise double-stranded RNA (dsRNA) [Motamedi *et al*, 2004; Sugiyama *et al*, 2005]. The dsRNA is cleaved by a RNA endonuclease Dicer to form small interfering RNA (siRNA) [Hannon, 2002; Kanellopoulou *et al*, 2005; Kawamura *et al*, 2008], which in turn is loaded onto the small RNA binding protein Argonaute (Ago) [Hutvagner &

Simard, 2008]. The Ago protein present in the RNA-induced transcription gene-silencing (RITS) complex "slices" the siRNA to become single-stranded by its endogenous ribonuclease activity and directs the entire complex to the heterochromatin site where the sequence is complementary to the siRNA [Irvine *et al*, 2006; Verdel *et al*, 2004] (Figure 1.26). Such process is essential for heterochromatin formation that deletion of the RNAi machinery factors *Dicer* or *Ago* results in reduced H3K9 methylation, a histone mark associated with heterochromatin, at pericentric regions and represses anti-silencing effects on reporter genes integrated into centrometric repeats [Buker *et al*, 2007; Volpe *et al*, 2002].

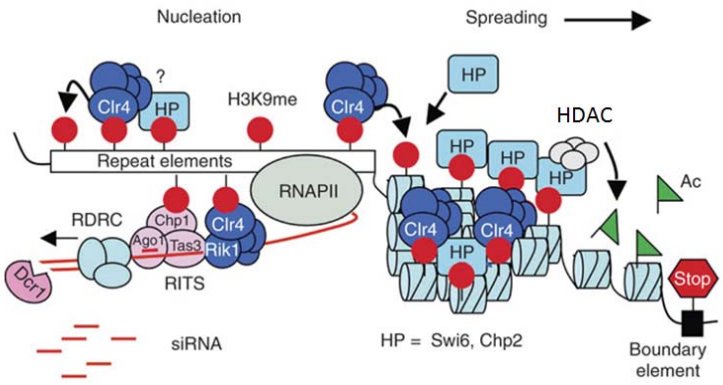

Figure 1.26 Schematic representation of heterochromatin formation. This is a pathway representing the process occurred in yeast so proteins denoted are yeast homologs. Note that RdRC responsible for reverse transcription to generate dsRNA has not been identified in mammals. Red lollipops represent methylated H3K9 whereas green flags represent histone acetylation. Modified from Zhang *et al*, 2008.

The link between RNAi and heterochromatin histone modification establishment was recently suggested to be mediated by a LIM domain protein, Stc1, which is present in the CLRC (Clr4-Rik1-Cul4) complex that has H3K9 lysine methyltransferase activity [Bayne *et al*, 2010; Nakayama *et a*l, 2001]. Stc1 also associates with RITS *via* Ago1 and this interaction is proposed to be responsible for bringing Clr4 to sites of RITS binding to promote H3K9 methylation. Methylation of H3K9 therefore not only facilitates the spreading of heterochromatin (Section 1.3.2.3), but also appears to start the heterochromatin propagation (Figure 1.26).

Although no RdRP has yet been identified in *Drosophila* and mammals, the heterochromatinestablishment pathway does still seem to be conserved from *S. pombe* to higher eukaryotes. Both forward and reverse strands of heterochromatin transcripts and protein components required for the further processing of dsRNA have been identified in both yeast and vertebrates [Irvine *et al*, 2006; Kanellopoulou *et al*, 2005]. dsRNA in mammals might be generated by other mechanisms such as bidirectional transcription of the repeated heterochromatin sequences or self-pairing of the ssRNA. Similar to yeast, heterochromatin formation is defective in *Drosophila* and vertebrates if the RNAi machinery is abolished by depletion of DICER or AGO proteins [Deshpande *et al*, 2005; Fagegaltier *et al*, 2008; Fukagawa *et al*, 2004; Giles *et al*, 2010]. The RNAi machinery might be envisioned to nucleate heterochromatin formation; however, its alone does not seem to be able to initiate *de novo* heterochromatin formation because H3K9 methylation is required for the binding of RITS [Sadaie *et al*, 2004]. Deletion of *Dicer* leads to accumulation of heterochromatin transcripts but cannot completely abolish heterochromatin in murine ES cells [Murchison *et al*, 2005]. These implicate that siRNA is required for heterochromatin formation but its alone is not sufficient to initiate the process, how it is initiated in the first place remains enigmatic.

1.3.2.3 Heterochromatin spreading

H3K9 methylation plays the central role in heterochromatin spreading. The SUV39 family of H3K9 KMTs (SUV39H1 and SUV39H2 in humans) possess a SET domain for the KMT activity, and also a chromodomain that recognises methylated H3K9 [Kouzarides, 2002; Zhang *et al*, 2008]. These “read” and “write” abilities are believed to self-reinforce H3K9 KMTs binding, and thus propagate the heterochromatin-associated histone mark H3K9me3 along the chromatin. As prior H3K9 deacetylation is required for the methylation on the same residue, the interaction between H3K9 KMT and HDAC appears not only to ensure the histone H3 being methylated is deacetylated, but also to prepare the adjacent nucleosomes to be ready for H3K9 methylation such that heterochromatin propagation could be carried out more efficiently [Czermin *et al*,

2001].

Heterochromatin propagation is also facilitated by binding of HP1 in mammals (yeast homolog of Swi6) [Grewal & Jia, 2007]. HP1 consists of a chromodomain that is also specific H3K9me2/3 [Bannister *et al*, 2001; Lachner *et al*, 2001]. Loss of HP1 binding at heterochromatin is observed as a result of deletion of H3K9 KMTs *Clr4* or *Suv39h* in yeast or mouse, respectively [Nakayama *et al*, 2001; Lachner *et al*, 2001]. The binding of HP1 to H3K9me2/3 in turn recruits more H3K9 KMTs due to the multifunctional chromoshadow domain (CSD) of HP1. The CSD is able to interact with SU(VAR)3-9, the *Drosophila* homolog of SUV39H, and this interaction is suggested to help H3K9 methylation propagation along the chromatin [Bannister *et al*, 2001; Schotta *et al*, 2002]. CSD of HP1 also allows HP1 self-dimerisation, which in turn may help chromatin compaction [Brasher *et al*, 2000; Cowieson *et al*, 2000]. Furthermore, similar to SUV39H, HP1 also associates with HDACs, possibly deacetylating the neighbouring histone proteins for H3K9 KMTs to act on [Kim *et al*, 2004; Yamada *et al*, 2005]. Besides promoting repressive marks in histone level, HP1 also facilitates DNA methylation by recruiting DNMTs [Fuks *et al*, 2003; Lehnertz *et al*, 2003; Smallwood *et al*, 2007]. DNA methylation is a repressive mark commonly found in heterochromatin or silenced region. The recruitment of DNMTs by HP1 and the interaction between MBDs and H3K9 KMTs helps H3K9me3 spreading by self-reinforcing themselves [Delpus *et al*, 2002; Fuks, 2005; Lande-Diner *et al*, 2007; Rountree *et al*, 2000].

1.3.2.4 Position effects on gene expression

While chromatin environment can determine gene expression, positions of gene integration can lead to activation or repression. There are two position effects leading to altered gene expression, known as position effect variegation (PEV) and chromosomal position effect (CPE) [Recillas-Targa *et al*, 2004]. It was shown in *Drosophila* that a transgene can be activated and repressed depending on the site of integration; such phenomena are collectively known as

chromosomal position effects (CPE). Repression of the transgene is observed if it is integrated into heterochromatin. Transgene activation would result if it is integrated into active chromatin regions with nearby enhancers [Roseman *et al*, 1993].

PEV is defined as variegated gene expression from cell to cell when a gene is translocated into the proximity of heterochromatin. PEV caused by heterochromatin was first described in *Drosophila*. It has been found that a transgene integrated into the genome near heterochromatin has varied expression levels among a population of cells. The level of repression is inversely proportional to the distance from the transgene to heterochromatin, implicating an occurrence of heterochromatin spreading [Girton & Johansen, 2008]. Similar observations were also widely reported in yeast and vertebrates [Bühler *et al*, 2007; Hiragami-Hamada *et al*, 2009]. The repression can be rescued by the deletion of proteins involved in the formation of heterochromatin, further confirming that the reduced transgene expression observed is due to heterochromatin spreading [Bühler *et al*, 2007; Volpe *et al*, 2002].

1.4 Insulators protect genes from aberrant expression

The organisation of chromosomal domains and the restriction of promiscuous enhancers require the setting of boundaries. As genes could be non-specifically activated by nearby enhancers or silenced by heterochromatin encroachment, the genome appears to have evolved some DNA elements to counteract these effects, these elements are collectively known as insulators.

1.4.1 Insulator activities: barrier and enhancer-blocking activities

An insulator is defined as a DNA sequence element that has the ability to shield a gene from its chromosomal environment. There are two insulator activities heterochromatin barrier and enhancer-blocking activities. Two reporter assays have been used to identify insulators.

Heterochromatin barrier activity is commonly defined by analysing the ability of putative insulator barriers to shield a reporter transgene from chromosomal position effect silencing [Gaszner & Felsenfeld, 2006]. Transgenes without insulator protection would exhibit variable expression when randomly integrated into a genome. The expression level of a transgene depends on its chromosomal location; one integrated into or close to heterochromatin is silenced while one located in euchromatin remains expressed. However, due to the abundance of self-propagation property of heterochromatin, most transgene integrants succumb to silencing in long-term culture (Figure 1.27b). Contrastingly, if the reporter construct is flanked by insulators with heterochromatin barrier activity, expression of the transgene can persist for a long time (Figure 1.27a).

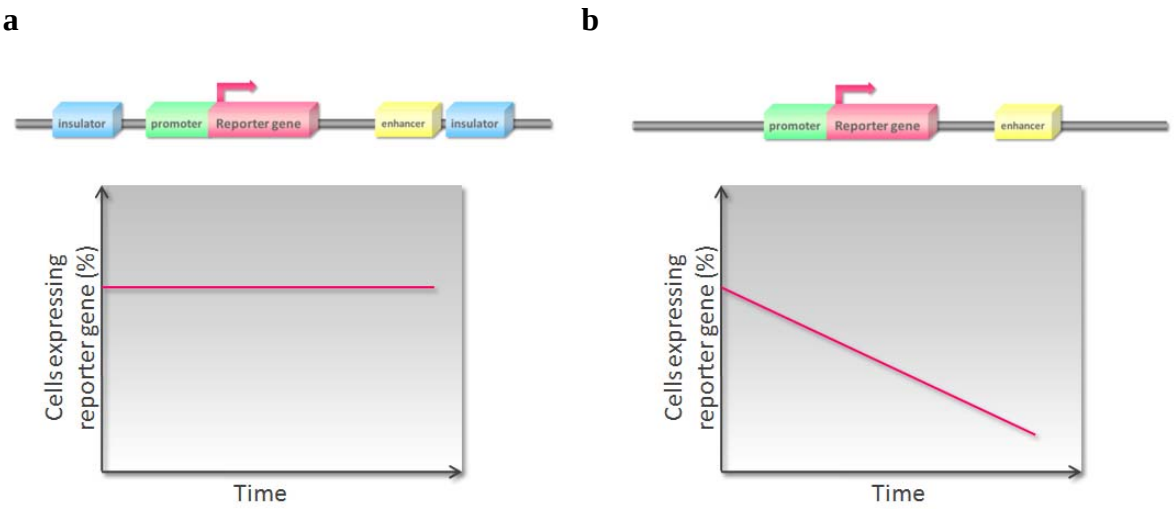

Figure 1.27 Schematic representation of insulator barrier assays. **a**. The reporter gene construct including the promoter and enhancer is flanked by putative insulators at both the 5' and 3' ends. Functional insulator barriers are able to maintain the transgene expression along the time course. **b**. In the absence of insulators, expression of the transgene decreases with time.

A second activity that defines an insulator is enhancer blocking, where the insulator activity interrupts the communication between a linked promoter and enhancer specifically when positioned between the two. In contrast to silencing events, an enhancer blocker does not interfere with the interaction between the promoter and enhancer when located at either side of the promoter-enhancer pair (Figure 1.28).

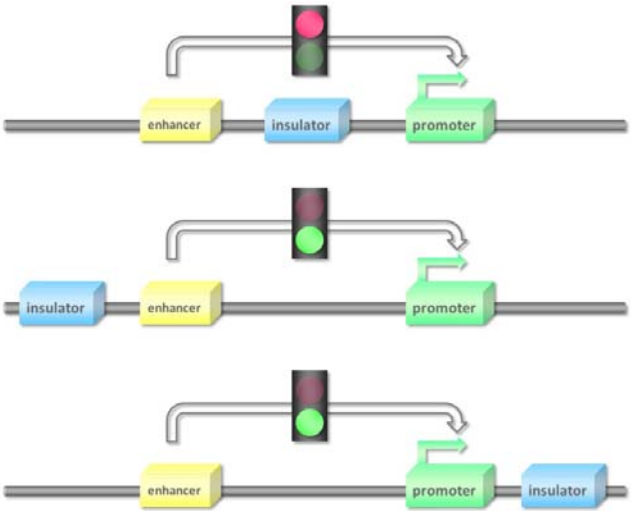

Figure 1.28 Schematic diagram of enhancer blocking assay design. The interaction between an enhancer and a promoter is blocked by an insulator (red sign) if the insulator is positioned between the two, no transcription is then allowed. The insulator cannot impose any effects on the communication between the promoter and enhancer (green sign) if it is located at either side of the promoter-enhancer pair.

1.4.2 The discovery of insulators

Insulator elements have been identified of genomes from yeast to human. Insulators were firstly identified in *Drosophila*. Two insulator elements, scs (specialised chromosome structures) and scs', were identified at the borders of the open chromatin domain of the *heat short protein 70* (*hsp70*) locus [Kellum & Schedl, 1991; Kellum & Schedl, 1992]. Heterochromatin barriers are also found in yeast. Many *tRNA* genes located near heterochromatic centromeres and telomeres in yeast have been identified to be insulator barriers that restrict spreading of silenced heterochromatin [Haldar & Kamakaka, 2006]. It has been found in *S. cerevisiae* that the $tRNA^{Thr}$ gene located adjacent to the silenced *HMR* (hidden MAT right) locus can halt spreading of heterochromatin silencing [Donze *et al*, 1999; Donze & Kamakaka, 2001]. More recently, multiple *tRNA* genes have been found within centromeres, separating the inner repeats with more open chromatin structure from the heterochromatic outer repeats in *S. pombe*. These genes act as barriers to delimit the spread of heterochromatin from the outer repeats to the inner repeats. Deletion of the $tRNA^{Ala}$ gene results in repression of the reporter gene *ura4+* inserted into the inner repeats, and the repression is accompanied by a gain of H3K9me2, suggesting that $tRNA^{Ala}$ has barrier activity [Scott *et al*, 2006]. In vertebrates, the chicken HS4 element is a well studied insulator. It lies within the chicken *β-globin* locus separating the *globin* gene clusters from the nearby condensed heterochromatin region. Its barrier activity has been characterised by using insulator barrier assays. It was found that a transgene flanked with HS4 at both sides can remain expressed after long-term culture [Dickson *et al*, 2010; Pikaart *et al*, 1998; Recillas-Targa *et al*, 2002; Rincón-Arano *et al*, 2007]. The HS4 insulator element will be discussed in detail in Section 1.5.2.

Enhancer blockers are common in *Drosophila*. The *gypsy* element is a well characterised insulator with both heterochromatin barrier and enhancer blocker activity [Gdula *et al*, 1996]. *gypsy* is a retrotransposon element that contains binding sites for a zinc finger nuclear factor Su(Hw) (suppressor of Hairy-wing). Insertion of this element can block all effects from distal

enhancers while communication between the promoter and proximal enhancers is unaffected [Geyer & Corces, 1992]. In vertebrates, it was recently found that CTCF (CCCTC-binding factor) functions cooperatively with Cohesin proteins for enhancer-blocking activity. Cohesin is first found to be required for proper cohesion of sister chromatids following replication in S phase. The interaction of cohesin complexes with chromatin is in a CTCF-dependent manner [Ohlsson *et al*, 2010]. Genome wide mapping of CTCF and Cohesin binding sites found that they colocalise in the human genome [Wendt *et al*, 2008]. In addition to the essential role in cell division, the CTCF-cohesin complex is also required for insulator enhancer-blocker activity. An imprinting control region (ICR) located within the *Igf2/H19* locus is a well known CTCF-dependent insulator present in humans and mice (Figure 1.29) [Bell & Felsenfeld, 2000; Hark *et al*, 2000]. The ICR element is responsible for the monoallelically expression of the *Igf2* (*insulin-like growth factor 2*) and *H19* genes. These two genes are imprinted genes in *Igf2* is only expressed from the paternal allele and *H19* only from the maternal one [Bartolomei *et al*, 1991; DeChiara *et al*, 1991]. They are located on the same chromosome and potentially activated by the same sets of enhancers. The ICR positioned between the two genes is a key factor to accomplish the monoallelic expression through mediating the CTCF binding. Recently, it was found that the Cohesin complex is also required for the enhancer blocking activity of ICR. The altered expression profiles of *IGF2* and *H19* in CTCF and Cohesin depleted cells are similar [Wendt *et al*, 2008]. CTCF is also required for the enhancer blocking activity of the chicken HS4 insulator element. Although several insulator proteins bind to HS4, only the CTCF binding site is indispensable for enhancer blocking activity [Bell *et al*, 1999]. There are at least 30 CTCF binding sites in the human genome [Takai *et al*, 2001]; however, it is unclear if they are enhancer blockers in their endogenous context.

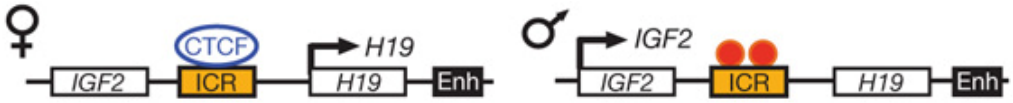

Figure 1.29 Schematic representation of the *IGF2/H19* locus. CTCF is only able to bind to ICR of the maternal allele. DNA methylation (red dots) of the ICR on the paternal allele abolishes the CTCF binding. While DNA methylation inhibits the binding of CTCF, the methylated paternal copy of ICR allows the expression of *IGF2* [Holmgren *et al*, 2001; Kanduri *et al*, 2000; Szabo *et al*, 2000]. Adapted from Wendt *et al*, 2008.

1.4.3 Proposed mechanisms of barrier activity

Experimental evidence indicates that barrier elements employ a variety of mechanisms to counter propagation of heterochromatin (Figure 1.30) [West & Fraser, 2005]. As heterochromatin propagation is a processive process that induces continuous histone modifications and binding of repressive protein complexes, blocking access to nucleosome substrates is the common feature of all these mechanisms.

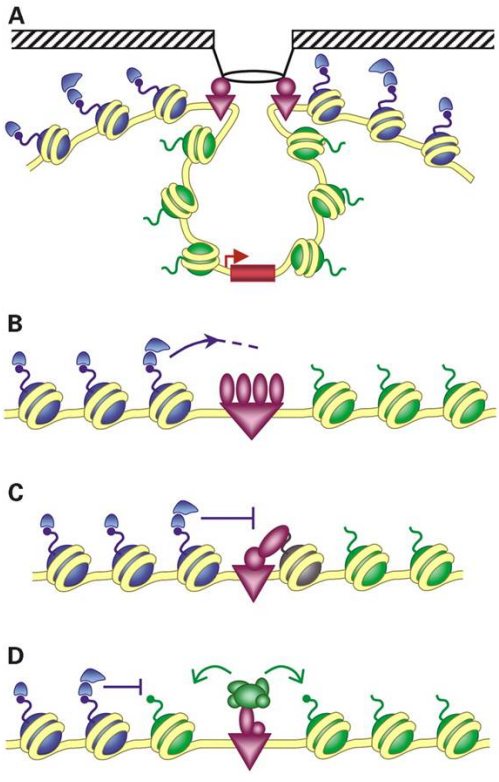

Figure 1.30 Proposed mechanisms of barrier activity. **A**. Nuclear structure tethering. Barriers (purple) tethered to nuclear structural component (black) may block the spread of histone modifications (blue dots) and heterochromatin factors (blue) from heterochromatin to euchromatin such that a flanked gene can maintain its transcription permissive structure. **B**. Nucleosome gap. A nucleosome gap can be formed by inhibition of nucleosome placement by barrier-binding proteins. Nucleosomes thereby are not available for binding of heterochromatin factors. **C**. Nucleosome masking. Barrier-binding proteins interacting with histones directly may mask binding sites for heterochromatin factors. **D**. Histone code manipulation. Recruitment of histone modification enzymes (green) at barriers establishes active histone modifications (green dots), which can compete with the propagation of heterochromatin factor binding. Adapted from West & Fraser, 2005.

1.4.3.1 Nuclear structure tethering

Tethering to a fixed nuclear structure may hinder the nucleosome access for heterochromatin formation complexes by stereo topological hindrance (Figure 1.30A). It has been shown in *S. cerevisiae* that artificial tethering of the *HML* locus to the nuclear pore complex (NPC) can form a barrier to silencing of the locus [Ishii *et al*, 2002]. While yeast active genes are found to be clustered at nuclear pores [Casolari *et al*, 2004], such tethering may direct the silenced locus to a transcriptionally active compartment for gene reactivation instead of simply protect the locus from heterochromatin silencing. This tethering model also does not explain why the barrier activity is position dependent and why the reporter gene is required to be flanked by barriers on both sides. Although the *HML* locus can be prevented from silencing by artificial tethering, the same tethering approach cannot block silencing at the *HMR* locus [Oki *et al*, 2004]. It suggests that the nuclear structure tethering strategy could be applied on certain gene loci but does not act as a universal approach to form a barrier to silencing. Nuclear structure tethering is observed on *Drosophila* and vertebrate barriers [Capelson & Corces, 2005; Yusufzai *et al*, 2004]. The *Drosophila* gypsy insulator element has been found to be preferentially located at the nuclear periphery [Gerasimova *et al*, 2000]. Although the Su(Hw) protein is essential for the gypsy barrier activity [Roseman *et al*, 1993], the Su(Hw) binding site alone is not able to direct the flanked transgene to the nuclear periphery [Xu *et al*, 2004], suggesting that Su(Hw) contributes the barrier activity by mechanism other than nuclear structure tethering. The well characterised vertebrate insulator element HS4 has been also shown to be tethering to nuclear matrix. The binding of CTCF was found to be essential for the tethering probably due to the interaction of CTCF and nucleophosmin [Yusufzai *et al*, 2004]. Given that the binding of CTCF is neither sufficient nor required for the HS4 barrier activity, HS4 does not seem to employ nuclear structure tethering as a mechanism for its barrier activity [Recillas-Targa *et al*, 2002].

1.4.3.2 Nucleosome gap

A more extreme approach to interrupt heterochromatin spreading is generation of a nucleosome gap (Figure 1.30B). DNA sequences unfavourable for nucleosome formation have been shown to form boundaries against silent chromatin [Bi *et al*, 2004]. Moreover, several chromatin barriers have been found to be hypersensitive to DNase I digestion [Chung *et al*, 1997; Cuvier *et al*, 1998; Li *et al*, 2002]. A genomic tethering experiment in yeast has shown that tethering a subunit (Snf6p) of the chromatin remodelling complex SWI/SNF to the silenced *HMR* locus generates a putative chromatin barrier that is able to protect the integrated reporter gene from heterochromatin silencing accompanied by a localised elevation of chromatin accessibility [Oki *et al*, 2004]. It suggests that generation of nucleosome gap by chromatin remodelling complexes may be able to halt heterochromatin silencing. However, tethering of other subunits of the SWI/SNF complex does not result in the same effect. Integration of the chicken HS4 insulator element into the human *ε-globin* locus also results in a localised elevation of chromatin accessibility [Zhao *et al*, 2006]. However, the nucleosome gap formation is dependent on the HS4 barrier activity dispensable factor CTCF so the necessity of nucleosome gap for barrier activity has not been proved. Given that chromatin is usually folded in a high-order structure (Section 1.1.1), nucleosome gap with a few nucleosome depletion may not be sufficient to counteract heterochromatin spreading.

1.4.3.3 Nucleosome masking

Instead of removing nucleosomes completely, nucleosomes at chromatin barriers can be masked by barrier-binding proteins (Figure 1.30C). For example, the transcription factor CTF1 binds directly to the histone H3 tail and is proposed to prevent the binding of repressive Sir proteins in *S. cerevisiae* [Ferrari *et al*, 2004]. Mammalian CTF1 can protect transgenes from silencing by adjacent telomeric chromatin but it remains elusive as to whether the mechanism in yeast is conserved in mammals [Esnault *et al*, 2009]. However, it is often not easy to distinguish whether the barrier activity conferred by insulator proteins is due to a simple nucleosome masking or

recruitment of other protein factors to achieve other barrier activity mechanisms [Huang *et al*, 2007; West *et al*, 2004; Zlatanova & Caiafa, 2009].

1.4.3.4 Histone code manipulation

A more active approach to set up a barrier to heterochromatin propagation is by manipulating histone modifications. In this model, histone modifying enzymes are recruited to establish chromatin states unfavourable for heterochromatin propagation (Figure 1.30D) [Donze & Kamakaka, 2002; West & Fraser, 2005]. Histone acetylation can act as a chain terminator to heterochromatin spreading as histone deacetylation is a critical step in heterochromatin formation. It was demonstrated that artificial tethering of KATs to sites next to heterochromatin can protect a reporter gene from silencing in *S. cerevisiae* and the anti-silencing activity is positively correlated with the number of the artificial KAT tethering sites [Chiu *et al*, 2003]. Moreover, the hyperacetylated domain resulted from the KAT tethering is sizable that a significant level of histone acetylation encompasses 2 kb from the tethering site. It suggests that a relatively small chromatin barrier (< 100 bp) with histone acetylation is sufficient to protect a substantial chromatin region from heterochromatin silencing. The anti-silencing effect from histone acetylation may be explained by the fact that the binding of Sir proteins to histones can be abolished by histone acetylation. Higher the degree of acetylation, lower the Sir protein binding affinity is [Carmen *et al*, 2002]. In the vertebrate genome, active histone modifications including histone acetylation have been observed at constitutive peaks at chromatin boundaries with a sharp transition from heterochromatin associated histone marks and DNA methylation [Brinkman *et al*, 2007; Huang *et al*, 2005; Litt *et al*, 2001a; Litt *et al*, 2001b; Morshead *et al*, 2003]. It agrees to the yeast model that a small region with active histone modifications is sufficient to act as a barrier to heterochromatin propagation. Although the role of SIR proteins in heterochromatin spreading in vertebrates is not as clearly shown as in yeast, binding of repressive complexes associated with heterochromatin spreading may be also blocked by active histone modifications. The role of histone modifications has been studied most intensively at the

chicken *β-globin* HS4 insulator, and is discussed in detail in Section 1.6. Although this model seems to explain how an insulator barrier is established, the passive mechanisms of insulator barriers discussed above can still not be ruled out. The barrier activity mechanisms are not mutually exclusive, and could be found on a single insulator element. The binding of insulator proteins could mask or compete for nucleosomes to prevent binding of heterochromatin factors, and could also recruit histone modifying enzymes to maintain the open chromatin structure.

1.5 The chicken *β-globin* gene cluster

The chicken *β-globin* locus is a well characterised model for studying developmentally regulated gene expression. The locus consists of four *β-globin* genes ρ, β^H, β^A and ε (Figure 1.31) that are expressed in erythroid cells in a developmental stage-specific manner [Felsenfeld, 1993]. Following fertilisation, the embryonic ρ and ε globin genes are expressed in the primitive lineage cells until day 4 – 5. Upon day 4 – 5, the adult globin genes β^A and β^H are expressed in the definitive lineage cells. Using DNase I mapping analysis, it was found that there are 12 hypersensitive sites and most of them are tissue- or developmental stage-specific. Of the 12 hypersensitive sites, hypersensitive sites 1 – 4 (HS1 – 4) and the $\beta^{A/\varepsilon}$ enhancer located at a hypersensitive site are present in all developmental stages of erythroid cells [Reitman & Felsenfeld, 1990]. HS1 – 3 in addition to the $\beta^{A/\varepsilon}$ enhancer are responsible for the regulation of *β-globin* gene expression [Mason *et al*, 1995]. 16 kb upstream of the *β-globin* locus is the *FOLR1* gene (Figure 1.31), which encodes a folate receptor that is only expressed in erythroid progenitors prior to the expression of the *globin* genes [Prioleau *et al*, 1999]. HSA is thought to regulate *FOLR1* expression, and is DNase I hypersensitive in erythroid progenitors that express *FOLR1*, but is absent in terminally differentiated adult erythrocytes. In between the *β-globin* gene clusters and *FOLR1*, there is a chromatin region that is fully DNA methylated and resistant to DNaseI digestion throughout all developmental stages. There are three DNaseI hypersensitive sites upstream of the 16 kb condensed region, including HSA.

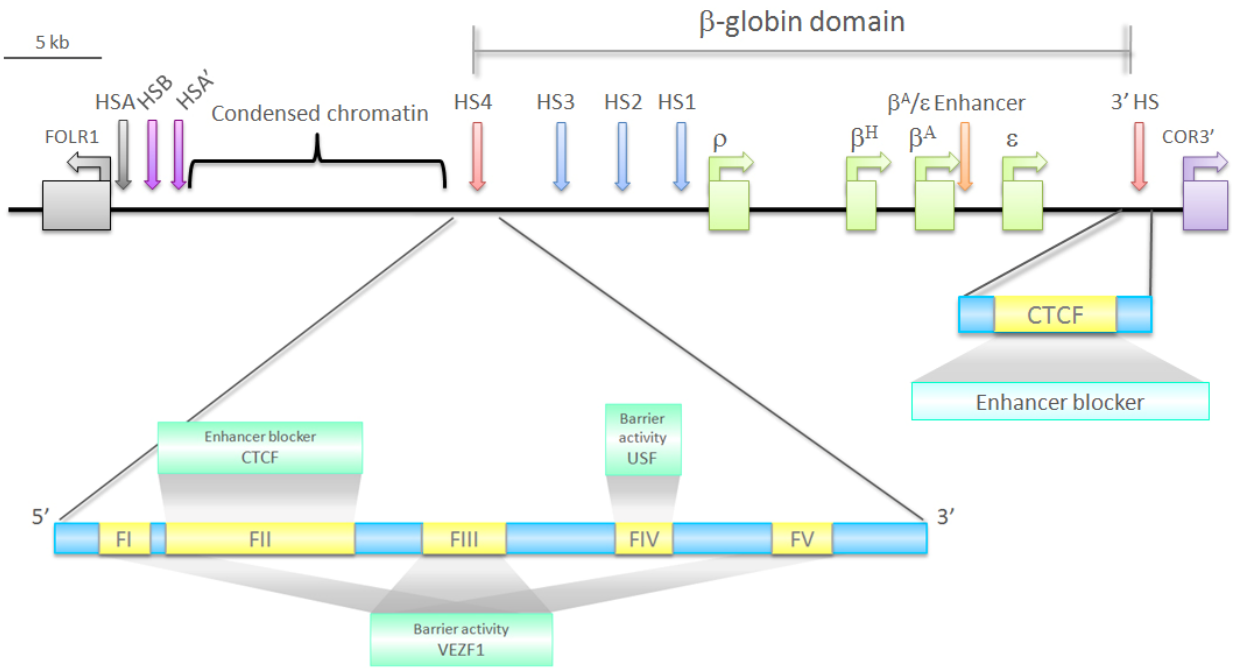

Figure 1.31 Schematic diagram of the chicken *β-globin* locus. Green boxes on the locus depict the position of the globin genes. DNaseI hypersensitive sites are indicated by arrows. The *FOLR1* gene is shown as a gray box. Following the hypersensitive site 3' HS, there are clusters of olfactory genes (COR). There are two identified insulators within the locus. One is the HS4 element and the other one is near the 3' end of the locus, 3' HS. HS4 consists of both enhancer-blocking and barrier activities but the CTCF bound 3' HS element only has enhancer-blocking activity.

1.5.1 Histone modifications at the chicken *FOLR1* and *β-globin* gene loci

The high resolution maps of histone modifications across gene loci during vertebrate development were completed at the chicken *β-globin* locus [Litt *et al*, 2001a; Litt *et al*, 2001b]. It was shown that on Day 10 and 15, a developmental stage when only β^A and β^H are expressed, the entire *β-globin* domain is enriched in H3K4me2, H3ac and H2A.Zac [Bruce *et al*, 2005; Litt *et al*, 2001a; Litt *et al*, 2001b] (Figure 1.32c & Figure 1.33a). DNase I mapping also showed that the whole *β-globin* domain is accessible in these cells, contrasting with the constitutively condensed, inaccessible 16 kb region. It is unlike other mammalian gene loci that usually show a sharp transition of active histone marks, the active histone modification patterns suggest an open chromatin structure of the *β-globin* domain. Contrastingly, H3K4me2, H3ac and H2A.Zac are not enriched at the *β-globin* domain in cells that do not express any of the *globin* genes (Figure 1.32a, Figure 1.32b, Figure 1.33b & Figure 1.33c). Similar to the *β-globin* gene locus, the active

histone modification patterns of the *FOLR1* locus is also correlated with the gene expression state. Active modifications H3K4me2, H3ac and H2A.Zac are found at the chicken *FOLR1* locus in erythroid progenitor cells that express *FOLR1*.

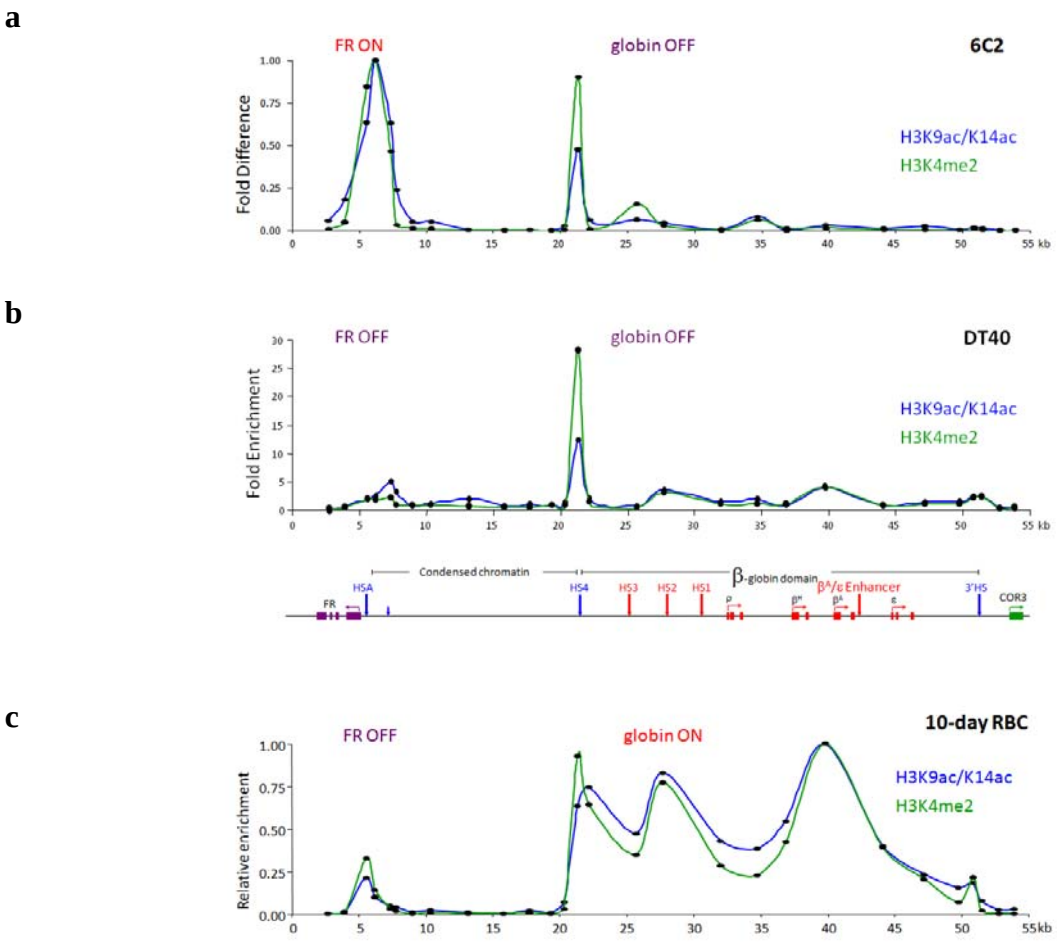

Figure 1.32 H3 histone modification profiles across the chicken *FOLR1* and *β-globin* locus in chicken cells with different expression levels of the *FOLR1* and *β-globin* genes. ChIP analyses of H3K4me2 and H3K9ac14ac in chicken 10-day red blood cells (RBC) **(a)**, chicken 6C2 erythroleukaemia cells **(b)** and chicken B cells DT40 **(c)**. Adapted from Litt *et al*, 2001a and Litt *et al*, 2001b. All these cells have different expression profiles of the *FOLR1* and *β-globin* genes that 10-day RBC express the *β-globin* genes but not *FOLR1*, 6C2 cells express *FOLR1* only whereas none of these genes are expressed in DT40.

In contrast, the 16 kb condensed chromatin region is depleted of active histone marks in all developmental stages (Figure 1.32 & Figure 1.33). Rather, it is uniformly enriched in the repressive histone mark H3K9me2 and the DNA remains inaccessible [Prioleau *et al*, 1999; Litt *et al*, 2001a; Litt *et al*, 2001b] (Figure 1.34). Across the *FOLR1* and *β-globin* loci, H3K9me2 is

also widely distributed except the two hypersensitive sites HSA and HS4, suggesting a protective mechanism at these sites against repressive histone mark propagation (Figure 1.34). Interestingly, these two sites are enriched in H3K4me2, H3ac and H2A.Zac although the enrichment at HSA is relatively correlated with the *FOLR1* expression state, probably associated with its regulatory role on the *FOLR1* expression [Prioleau *et al*, 1999]. However, the enrichment of active histone modifications at HS4 is not affected by the expression states of the neighbouring *FOLR1* and globin genes, and DNase I mapping showed that HS4 remains hypersensitive in various cell types and all the developmental stages of erythroid cells [Bruce *et al*, 2005; Litt *et al*, 2001a; Litt *et al*, 2001b; Reitman & Felsenfeld, 1990] (Figure 1.32 & Figure 1.33). These results suggest the chromatin structure of HS4 is persistently active.

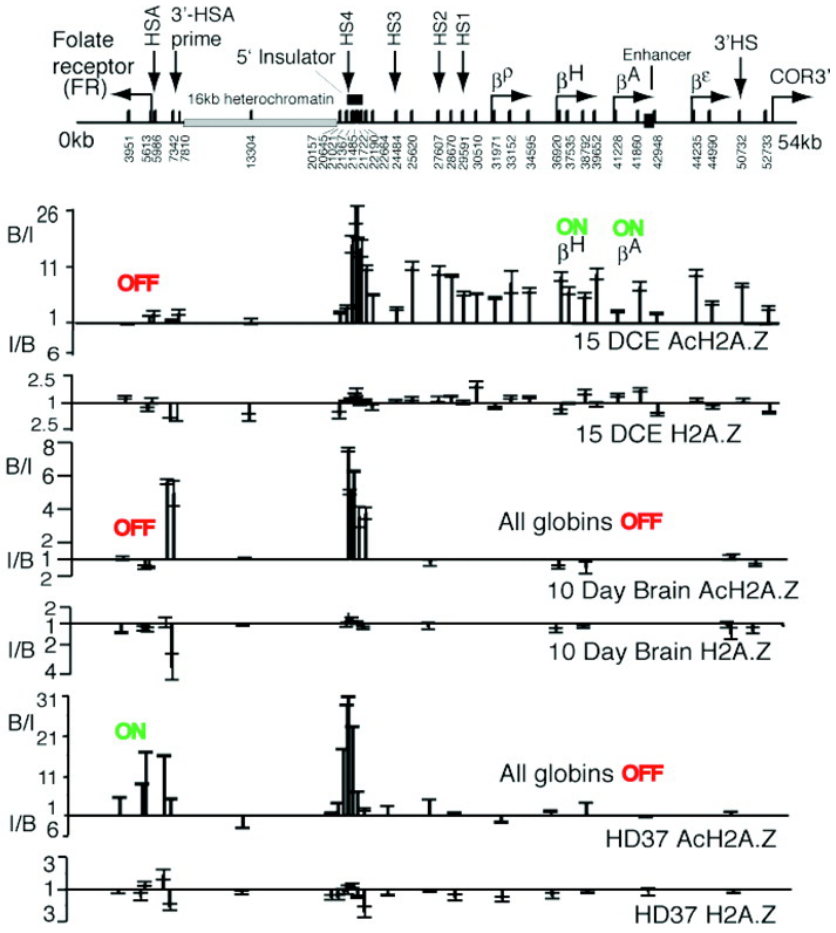

Figure 1.33 Profiles of H2A.Z and H2A.Zac across the chicken *FOLR1* and *β-globin* locus in 15-day chicken erythrocytes (15DCE), 10-day chicken brain tissue and HD37 chicken erythroblasts with different expression levels of the *FOLR1* and *β-globin* genes. Adapted from Bruce *et al*, 2005.

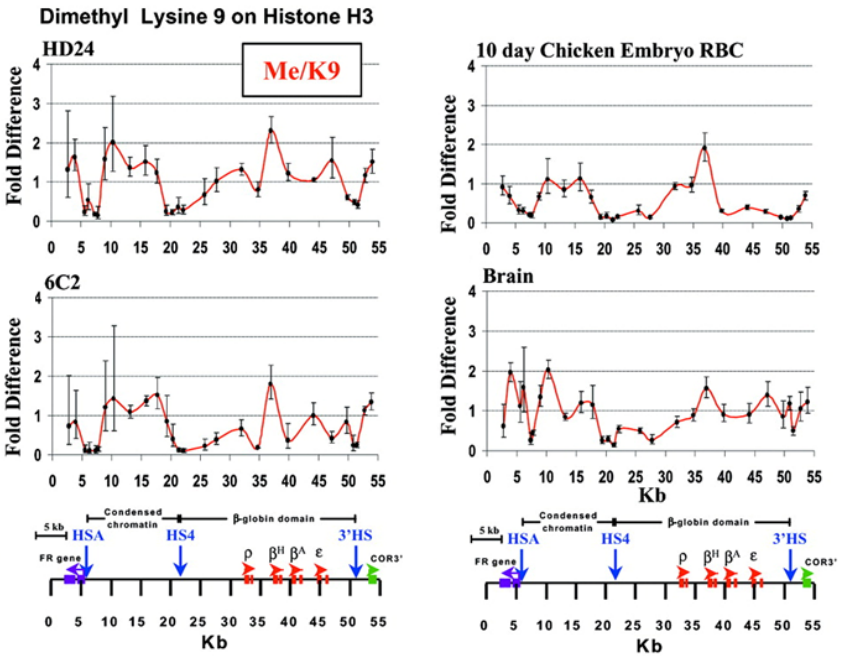

Figure 1.34 Profile of H3K9me2 across the chicken *FOLR1* and *β-globin* locus in HD24 chicken erythroleukemia cells arrested at the erythroid burst-forming unit stage (BFU-E), 6C2 cells, 10-day RBC and brain tissues. Adapted from Litt *et al*, 2001a.

1.5.2 The chicken *β-globin* insulator

HS4 is the only constitutive DNaseI hypersensitive sites of the locus [Reitman & Felsenfeld, 1990]. The 275 bp core HS4 element has been identified to be a boundary separating the 16 kb condensed chromatin region and the *β-globin* gene domain. It is enriched in active histone modifications H3K4me2 and H3ac in different developmental stages of erythroid cells and in other brain cells that do not express *β-globin* genes and *FOLR1* [Prioleau *et al*, 1999; Litt *et al*, 2001a; Litt *et al*, 2001b]. Although HS4 is CpG rich and possesses promoter-like chromatin state, it does not function as a promoter. No mRNA transcript and promoter activity of HS4 can be detected, in addition to the undetectable binding of RNA polymerase II [Chung *et al*, 1997; Giles *et al*, 2010; Huang *et al*, 2007].

By using DNaseI digestion mapping, it was found that there are five footprints on HS4 and they were subsequently identified to be binding sites for CTCF, USF1/2 and VEZF1 [Bell *et al*, 1999; Chung *et al*, 1997; Dickson *et al*, 2010; West *et al*, 2004]. These binding proteins are responsible for the HS4 insulator activity. CTCF binding to footprint II (FII) is indispensible for the

enhancer-blocking activity while the USF1/2 binding sites (FIV) and VEZF1 binding sites (FI, FIII and FV) are all required for the barrier activity (Figure 1.35) [Bell *et al*, 1999; Dickson *et al*, 2010; Recillas-Targa *et al*, 2002; West *et al*, 2004]. Although HS4 possesses two insulator activities, the two activities do not rely on each other and are separable. The CTCF binding site required for the enhancer-blocking activity can be removed without compromising the barrier activity [Recillas-Targa *et al*, 2002; Yao *et al*, 2003].

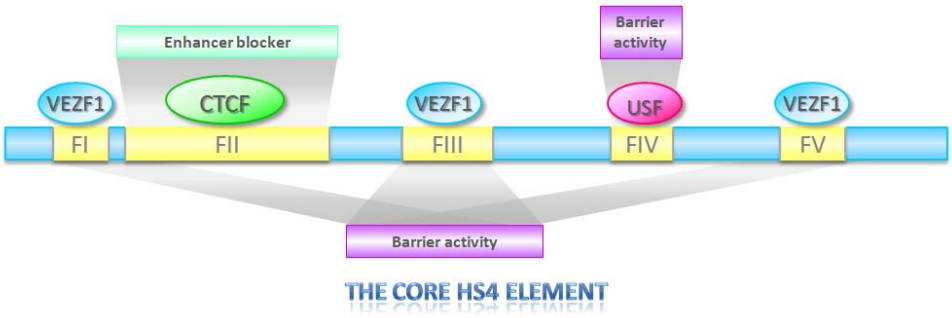

Figure 1.35 Schematic representation of factor binding at the HS4 element.

1.5.3 CTCF-mediated enhancer-blocking activity of the HS4 insulator

It was originally demonstrated that HS4 possesses enhancer-blocking activity using gene reporter assays in erythroid cell lines [Bell *et al*, 1999; Chung *et al*, 1993; Chung *et al*, 1997]. HS4 can be distinguished from a conventional silencer because it blocks enhancer action only when positioned between a promoter and an enhancer [Recillas-Targa *et al*, 1999]. A 90 bp HS4 fragment containing the CTCF (FII) and one of the VEZF1 (FIII) binding sites was found to be required and sufficient for performing enhancer blocking activity in erythroid cells. By studying the enhancer blocking activity with HS4 footprint deletion mutants, only the CTCF-binding site was shown to be indispensible for the enhancer blocking activity of HS4 [Recillas-Targa *et al*, 1999].

One possible role of CTCF in the enhancer-blocking activity of HS4 is to tether the insulator element to nucleolar surface. It was shown that transgenic HS4 in human cells is located at mostly nucleolar periphery or nucleolar boundaries. Mutation of the CTCF site disrupts this

localisation. The self assembly property of CTCF and its interaction with nuclear structural proteins, lamin proteins and nucleophosmin, appear to be responsible for the tethering [Yusufzai *et al*, 2004a; Yusufzai *et al*, 2004b]. The CTCF mediated tethering is proposed to form chromatin loop such that interaction between an enhancer and a promoter is prevented [Yusufzai *et al*, 2004b]. It remains to be determined whether the endogenous HS4 insulator forms loops or mediates tethering in chicken cells.

1.5.4 USF1/2 and VEZF1 mediate the barrier activity of the HS4 insulator

The HS4 barrier activity was identified using barrier assays. A reporter transgene integrated into the genome of erythroid cells showed that HS4 can prevent silencing of the transgene by chromosomal position effect after long-term culture [Dickson *et al*, 2010; Pikaart *et al*, 1998; Recillas-Targa *et al*, 2002; Rincón-Arano *et al*, 2007]. HS4 can act as a barrier regardless of the genomic environment. It was shown that flanking the *ankyrin* gene locus, whose barrier element had been previously removed, with the chicken HS4 in transgenic mice can restore the expression of the *ankyrin* gene [Gallagher *et al*, 2010]. The barrier activity of HS4 is also of practical use, and has benefitted experiments involving transgene integration [Frazar *et al*, 2003; Guglielmi *et al*, 2003]. Similar to the enhancer activity, the barrier activity of HS4 does not require the entire insulator element. A HS4 mutant without the CTCF binding site is still able to protect a transgene from silencing in barrier assays. However, all the USF and VEZF1 binding sites are required for the barrier activity [Recillas-Targa *et al*, 2002].

1.5.5 The HS4 element protects flanked regions from DNA methylation

An important role for vertebrate barriers appears to be protection from silencing mediated by DNA methylation. HS4 has been shown to protect a transgene and itself from DNA methylation [Dickson *et al*, 2010; Mutskov *et al*, 2002]. It was suggested histone acetylation can prevent DNA methylation. Studies of DNA methylation on a HS4 flanked transgene reveal that the transgene and HS4 remain unmethylated while the noninsulated transgene is silenced and

accompanied by DNA methylation [Mutskov *et al*, 2002]. Comparison of histone acetylation on the noninsulated transgene before and after gene silencing reveals that silencing is accompanied by the loss of histone acetylation and a gain of DNA methylation across the entire transgene [Mutskov *et al*, 2002; Mutskov *et al*, 2004]. Moreover, the silenced transgene is bound by MBD3, a methyl DNA binding protein, and Mi2, a repressive complex containing HDAC activity. However, the possibility that histone acetylation and DNA hypomethylation at the transgene are simply a result of active transcription cannot be ruled out. In the study of Mutskov *et al* (2002), it was shown that deletion of the transgene enhancer leads to a loss of histone acetylation and expression of the transgene, and results in a hypermethylated promoter even though the transgene is insulated by HS4. It might not be surprising that transcription can help establishment of histone acetylation as many KATs bind to enhancers to activate transcription and that they are brought along by RNA polymerase II during transcription [Travers, 1999]. Moreover, transcription associated complexes may compete the binding of gene promoters with DNMTs [Bird, 2002]. The mechanism of histone acetylation in preventing DNA methylation is yet to be defined. Another possible approach of HS4 to block DNA methylation may be through H2A.Z incorporation as HS4 is enriched in H2A.Z and, which seems to be able to exclude DNA methylation [Bruce *et al*, 2005; Conerly *et al*, 2010; Zemach *et al*, 2010; Zilberman *et al*, 2008]. However, there is no such evidence thus far.

Recently, our lab has found that VEZF1 plays a role in protecting a transgene from *de novo* DNA methylation. It has been shown that deletion of VEZF1 binding sites at HS4 results in DNA methylation across the transgene promoter after long-term culture. This report also clearly demonstrated that the increase in DNA methylation is not simply a consequence of reduced transcription activity because the transgene flanked by the HS4 mutant without USF binding sites is silenced but the DNA remains unmethylated (Figure 1.36) [Dickson *et al*, 2010]. In addition to HS4, VEZF1 appears to be capable of protecting endogenous CpG islands from *de novo* methylation. A CpG island containing *APRT* gene promoter has been found to be protected

from DNA methylation by VEZF1 [Dickson *et al*, 2010]. These results suggest that VEZF1 can protect transgene from DNA methylation. However, the mechanisms and factors involved are not understood.

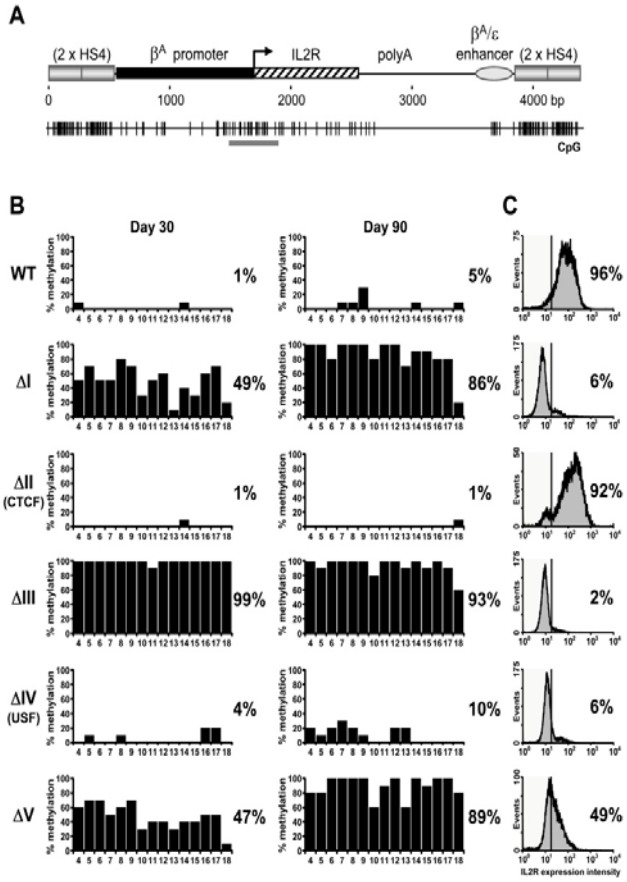

Figure 1.36 Deletion of VEZF1 binding sites of HS4 leads to DNA methylation on the reporter gene promoter. **A**. Schematic representation of the *IL2R* reporter transgene construct. The gray bar underlines the distribution of CpG dinucleotides where DNA methylation states were examined by bisulfite sequencing. **B**. CpG methylation was studied after 30 and 90 days of culture. Histograms represent percentage of DNA methylation on each CpG sites across the examined region, the overall percentage of DNA methylation is indicated besides each histogram. **C**. Expression of *IL2R* in each footprint deleted construct. The percentage of cells expressing the *IL2R* reporter gene is indicated. Adapted from Dickson *et al*, 2010.

1.6 A link between active histone modifications and the barrier activity of the HS4 insulator element

1.6.1 The HS4 insulator element is enriched in active histone modifications

HS4 is an example of explaining how an insulator manipulates histone modifications to achieve insulator barrier activity. As mentioned earlier, it is persistently enriched in active histone modifications, demarcating a sharp transition from the neighbouring silencing histone patterns to an active one. ChIP analyses on the chicken *β-globin* locus showed that HS4 is rich in H3K4me2, acetylation of histones H3, H4 and H2A.Z as well as asymmetric dimethylation of H4R3 (H4R3me2as) [Bruce *et al*, 2005; Huang *et al*, 2005; Litt *et al*, 2001a; Litt *et al*, 2001b] (Figure 1.37).

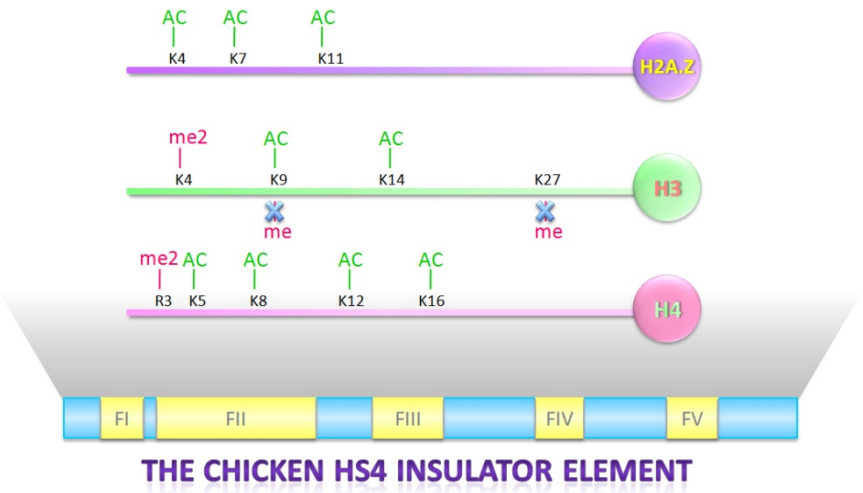

Figure 1.37 Summary of histone modifications at HS4. The HS4 element is constitutively enriched in H2A.Z acetylation (H2A.ZK4acK7acK11ac), H3K4me2, H3 acetylation (H3K9acK14ac), H4 acetylation (H4K5acK8acK12acK16ac) and asymmetric H4R3 dimethylation (H4R3me2as). Heterochromatin-associated histone marks H3K9me2/3 and H3K27me3 are depleted at HS4.

Mapping of histone modifications on HS4 deletion mutants has identified FIV, the USF binding site, is as being responsible for the recruitment of active histone marks [West *et al*, 2004]. Several histone modification enzymes have been shown to interact with USF1, including the H3K4-specific KMTs SET1 and SET7/9, H3-specific KAT PCAF as well as H4R3-specific KMT PRMT1 [Huang *et al*, 2005; West *et al*, 2004]. siRNA mediated knockdown of USF1 results in a

loss of all these histone marks with a concomitant increase in heterochromatin-associated H3K9me2 [Huang *et al*, 2007; West *et al*, 2004]. Expression of a dominant negative USF1 mutant that has no DNA binding ability but is still capable of forming heterodimers with USF2 abolishes the HS4 barrier activity [Huang *et al*, 2007]. These results suggest that active modifications at HS4 are directed by the binding of USF proteins, and that these marks are crucial for the anti-silencing effect of HS4.

Interestingly, H4R3me2as seems to promote H3 and H4 acetylation. PRMT1, which is responsible for asymmetric dimethylation of H4R3, binds at HS4. siRNA mediated knockdown of PRMT1 causes a loss of H3 and H4 acetylation [Huang *et al*, 2005], implicating a histone cascade occurring at HS4. The role of H2A.Zac at HS4 is not known. Although it is relatively clear in yeast barrier elements that H2A.Z can counteract the binding of the Sir silencing proteins [Babiarz *et al*, 2006; Meneghini *et al*, 2003; Venkatasubrahmanyam *et al*, 2007], it is not understood whether it plays the same role at HS4. More importantly, how these active marks are regulated and counteract heterochromatin spreading are yet to be studied. It is thought that the recruitment of several active marks to HS4 prevents the propagation of repressive marks and associated heterochromatin proteins. However, the precise details of these mechanisms are yet to be shown.

1.6.2 A potential role for histone ubiquitination at the HS4 insulator element

It has been found that the HS4 insulator barrier is enriched in H3K4me2 and that is essential for the barrier activity [West *et al*, 2004]. Histone methylation was considered as a stable mark that can persist for a very long time. However, the discovery of histone demethylases suggests a dynamic nature of histone methylation (Section 1.2.1.3). Demethylation of H3K4me2 is no exception. There are several H3K4-specific demethylases and some of them are associated with heterochromatin propagation complexes [Christensen *et al*, 2007; Iwase *et al*, 2007; Klose *et al*, 2007; Lee *et al*, 2005; Rudolph *et al*, 2007]. Although active promoters are generally enriched in

H3K4me2 and even H3K4me3 (Section 1.2.5), active transgenes integrated into heterochromatin have been reported to be shut down in long term culture [Pikaart *et al*, 1998; Recillas-Targa *et al*, 2004]. It suggests that demethylation is actively occurred at many gene loci and it could lead to chromosomal silencing. To maintain the high level of H3K4me2 for the barrier activity, HS4 needs to counteract the binding of demethylase complexes and/or employ a pathway to persistently methylate H3K4. Inspired by previous studies in yeast and mammals that H3K4 di- and tri-methylation is triggered by H2B ubiquitination (Section 1.2.3.2.3 & 1.2.4), it might be possible that HS4 recruits the H2B ubiquitination-H3K4 methylation *trans*-histone pathway to drive constant H3K4 dimethylation for the barrier activity.

1.6.3 Preliminary evidence for histone ubiquitination at the HS4 insulator element

Due to the lack of anti-ubiquitinated H2B antibody at the beginning of the study, the distribution of ubiquitinated histones across the chicken *β-globin* locus was mapped by using native chromatin immunoprecipitation (ChIP) with anti-ubiquitin antibody. The native ChIP approach could prevent the detection of ubiquitinated non-histone proteins. Preliminary data showed that ubiquitinated histones are enriched at HS4, the peak overlays with that of H3K4me2 (compare Figure 1.38 & Figure 1.32). Similar to H3K4 dimethylation, the significant level of ubiquitination histones at HS4 does not appear to be correlated with the *FOLR1* and *β-globin* gene expression.

a

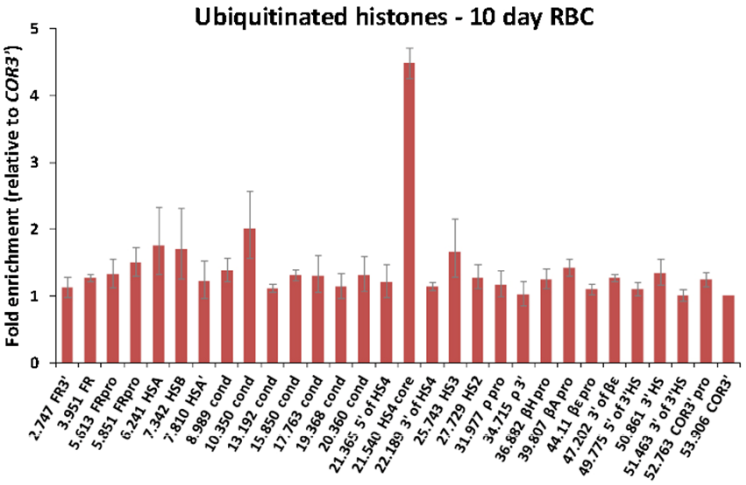

b

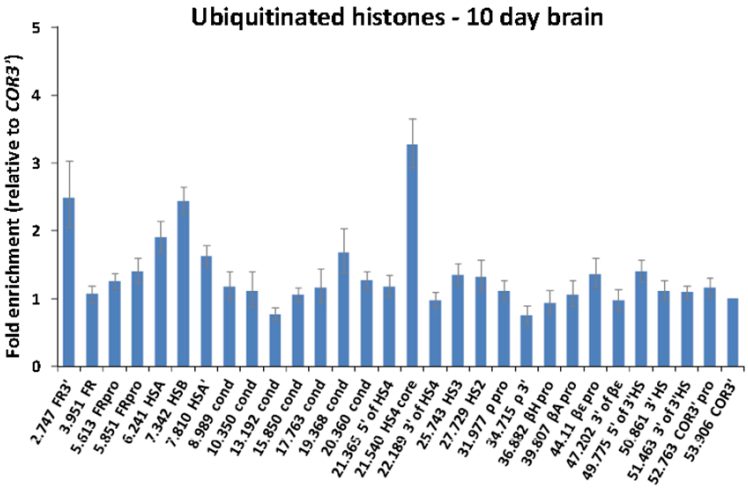

c

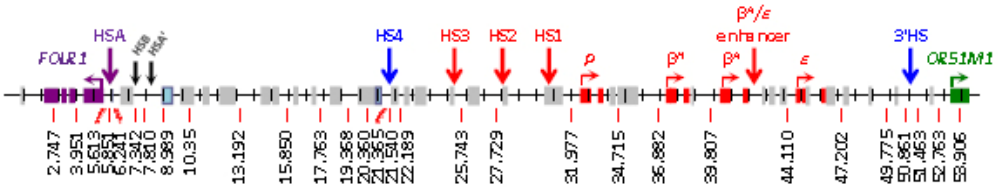

Figure 1.38 HS4 is enriched in ubiquitinated histones. The level of ubiquitinated histones across the chicken *β-globin* locus was analysed with native ChIP. Chromatin was prepared from 10-day RBC **(a)** and 10-day brain **(b)** separately for ChIP with ubiquitin-specific antibodies [Ma *et al*, 2011]. The *globin* genes are expressed in chicken 10-Day RBC but not in 10-Day brain. *FOLR1* is not expressed in both 10-Day RBC and brain. **c**. Primer sets used in the quantitative analyses.

H3K4me2 at HS4 is dependent upon the binding site for USF proteins that deletion of the USF binding site from HS4 or knockdown of USF1 results in a dramatic loss of H3K4me2 as well as other active histone marks [Huang *et al*, 2007; West *et al*, 2004]. To determine whether USF was

also required for the histone ubiquitination at HS4, Dr. Carol Heath performed native ChIP in 6C2 cells harbouring transgenic HS4 elements. It was found that only deletion of the USF binding site, footprint IV, results in a loss of histone ubiquitination. HS4 elements missing either CTCF or VEZF1 binding sites retain the levels of histone ubiquitination (Figure 1.39). However, these results could not prove whether the ubiquitinated histone at HS4 is H2B and whether the ubiquitination is required for the establishment of H3K4me2 at HS4, perhaps other active histone modifications, and for the barrier activity.

a

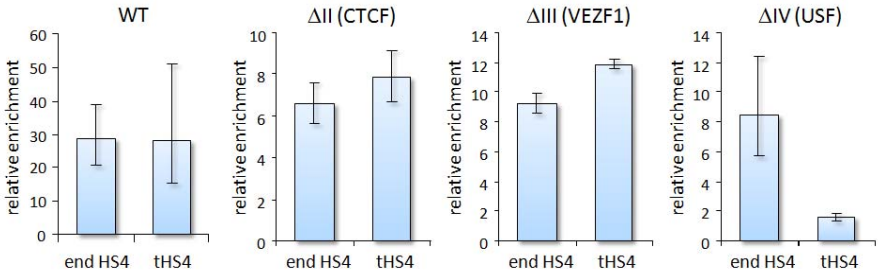

b

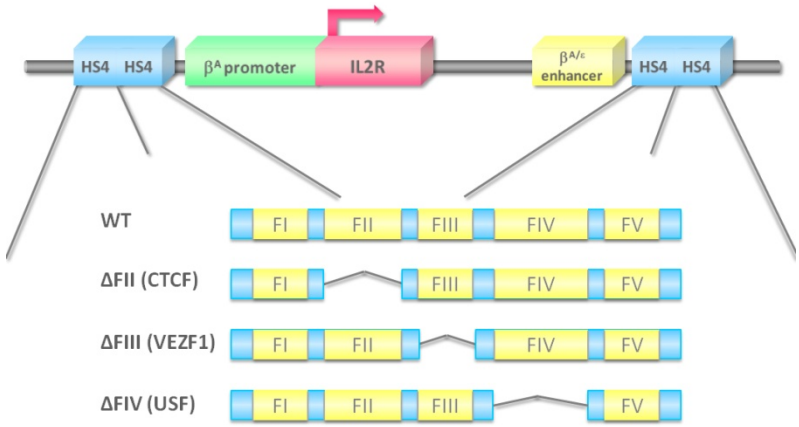

Figure 1.39 Native ChIP analyses of ubiquitinated histones at the transgenic HS4 elements. **a**. The ChIP assay was carried out in 6C2 cells carrying transgenic HS4 elements (tHS4) with deletion of different protein binding sites. The levels of ubiquitinated histones at the transgenic elements were compared with the cell lines' corresponding endogenous HS4 elements (end HS4). Apart from the USF binding site (ΔIV) deletion mutant, CTCF (ΔII) and VEZF1 (ΔIII) binding site deletion mutants were also examined [Ma *et al*, 2011]. **b**. Schematic diagram of the transgenic constructs.

CHAPTER 2

Methods and Materials

2.1 Materials

Antibody	Company	Catalogue number
H3K4me2	Millipore	07-030
H3K4me3	Millipore	05-745R
H3K9me2	Abcam	ab1220
H3K9me3	Millipore	07-523
H3K27me3	Millipore	07-449
H3K79me2	Abcam	ab3594
H3K79me3	Abcam	ab2621
H3	Millipore	07-690
H3ac	Millipore	06-599
H4ac	Millipore	06-598
H4K20me3	A kind gift from Prof. Judd Rice [Sims *et al*, 2006]	
H2Aub	Millipore	05-678
H2A.Z	Millipore	07-594
H2A.Zac	Abcam	ab18262
H2BK120ub1	A kind gift from Prof. Moshe Oren [Minsky *et la*, 2008]	
	Médimabs	MM-0029
CD25-PE	Dako/	R0811/
	Miltenyi Biotec	130-091-024
ARP6	Sigma-Aldrich	A1857
BAF53A	Abcam	Ab3882
CTCF	Millipore	06-917
PAF1	Abcam	ab20662
PONTIN52	Santa Cruz	sc-15259
RbBP5	Bethyl Lab	A300-109A
REPTIN52	Abcam	ab36569
RNF20	Bethyl Lab	A300-715A
TBP	Abcam	ab51841
TIP60	Santa Cruz	sc-5725
VEZF1	In-house raised [Gowher *et al*, 2008]	
Ubiquitin	Santa Cruz	sc-8017
Ubiquitinated conjugates	Enzo Life Sciences	BML-PW8810-0500
USF1	Abnova	H00007391-A01
Anti-goat IgG-HRP	Dako	P0160

Anti-mouse IgG-HRP	Pierce	1858413
Anti-rabbit IgG-HRP	Pierce	1858415
Anti-sheep IgG-HRP	Santa Cruz	sc-2473
Normal goat IgG	Santa Cruz	Sc-2028
Normal mouse IgG	Santa Cruz	Sc-2025
Normal rabbit IgG	Santa Cruz	Sc-2025

Table 2.1 List of antibodies used.

Enzyme	Company	Catalogue number
Micrococcal nuclease (MNase)	Sigma-Aldrich	N-5386
Protease K	Sigma-Aldrich	P5568
RNase H	Promega	M428A
SuperScript® III Reverse Transcriptase	Invitrogen	18080-044

Table 2.2 List of enzymes used.

Chemical	Company	Catalogue
4-(2-aminoethyl) benzenesulfonyl fluoride hydrochloride (AEBSF)	Sigma-Aldrich	A8456
1-bromo-3-chloropropane (BCP)	Sigma-Aldrich	B9673
37% Formaldehyde	Amresco	0493
Bovine serum albumin (BSA)	Fisher	BPE1605-100
Doxycycline	Sigma-Aldrich	D9891
Glycogen	Roche	10 901 393 001
Hank's buffered saline	Sigma-Aldrich	H6648
Leupeptin	Sigma-Aldrich	L2884
Nickel acetate	Sigma-Aldrich	244066
N-ethylmaleimide	Sigma-Aldrich	E3876
Phenol/Chloroform:isoamyl alcohol 25:24:1	Sigma-Aldrich	P3803
Pepstatin	Sigma-Aldrich	P5318
Sodium azide	Sigma-Aldrich	S8032
Sodium butyrate	Sigma-Aldrich	B5887
TRI Reagent®	Sigma-Aldrich	T9424

Table 2.3 List of chemicals used.

Tissue culture reagent	Company	Catalogue number
Chicken serum	SLI	S-606-HI
Dimethyl sulfoxide (DMSO)	Sigma	P8418
Foetal bovine serum	Autogen Bioclear	7.01
Foetal bovine serum (tetracycline-free)	Autogen Bioclear	7.01T
HEPES buffer solution	Gibco®	15630-056
Geneticin (G418)	Invitrogen	11811031
Minimum essential medium α (α-MEM)	Gibco®/Lonza	32571-028/BE02-002F
Penicillin/Streptomycin mixture	Lonza	DE17-602E
RPMI 1640 medium	Lonza	BE12-702F/U1
2-mercaptoethanol	Gibco®	31350-100

Table 2.4 List of tissue culture reagents used.

Reagent	Company	Catalogue number
Anti-FLAG® M2 affinity gel	Sigma	A2220
Bio-Gel® P-6DG Gel	Bio-Rad	150-0738
FastStart SYBR green Master (ROX)	Roche	04 673 514 001
Prestained protein ladder	Fermentas	SM0671
Protein A agarose	Millipore	16-125
Protein G agarose	Millipore	16-266
Quant-iT™ PicoGreen® dsDNA reagent	Invitrogen	P7589
Quick Start Bradford 1X Dye reagent	Bio-Rad	500-0205
SafeView stain	NBS	NBS-SV1
SuperSignal West Dura extended duration substrate	Thermo Scientific	34076
TaqMan® Universal PCR master mix, No AmpErase® UNG	Applied Biosystems	4324018
100 bp DNA ladder	NEB	N3231L
1kb bp DNA ladder	Invitrogen	15615-024

Table 2.5 List of other molecular biology reagents used.

2.2 Cell lines

2.2.1 6C2 cells and derivatives

6C2 is a chicken erythroid cell line arrested at the colony forming unit erythrocyte (CFU-E) stage [Beug *et al*, 1982]. 6C2 cells and their derivatives including transgenic HS4 footprint deletion mutants (8103 WT, 10401 ΔI, 10506 ΔII, 10615 ΔIII, 10901 ΔIV and 8d5 ΔV) [Recillas-Targa *et al*, 2002; West *et al*, 2004] were grown in the same formula of media (α-MEM supplemented with 10% Foetal bovine serum, 2% heat inactivated chicken serum, 1 mM HEPES, 25 μM 2-mercaptoethanol, 1% Penicillin/Streptomycin) and maintained in a similar way. Cells thawed from a frozen stock were added into 5 ml of 6C2 growth medium and then spun down at 1,000 g for 5 minutes to remove DMSO. Cell pellet was resuspended in 10 ml of medium and grown in a T25 flask at 37 ^{o}C with 5% of CO_2. They were split typically twice a week when reaching ~80% confluence by adding 1/10 of cells into fresh medium. Cell lines incorporated with the transgenic HS4 footprint deletion mutants and lentiviral RNF20 knockdown cells were also split twice a week but in a ratio 1 to 5. Frozen stocks were made as freezing $1x10^7$ of cells in 1 ml of freezing medium (foetal bovine serum supplemented with 10% DMSO) per stock at -80^{o}C, stored in liquid nitrogen for long term storage. Lentiviral RNF20 knockdown cells were maintained similarly except that serum used in the growth and freezing media was tetracycline-free. RNF20 knockdown was induced by adding DOX to the growth medium to a final concentration 1 μg/ml.

2.2.2 K562 cells and derivatives

K562 is a well established immortalised myelogenous leukaemia line derived from human leukemia cells [Klein *et al*, 1976; Lozzio & Lozzio, 1975]. Wild type K562 cells, and cell lines containing the stably integrated HS4 flanked VEZF1-CaM-FLAG construct (D3/6 line) as well as an empty vector control line integrated with the HS4 flanked CaM-FLAG coding sequence (S3F1 line) were grown with the same procedures. Cells were grown in K562 growth medium (RPMI 1640 medium supplemented with 10% foetal bovine serum, 1% Penicillin/Streptomycin)

at 37 ^{o}C with 5% CO_2. DMSO was removed from newly thawed cells by spinning down and then resuspending in fresh medium. They were split twice a week in a ratio one volume of cells to 10 volumes of medium. For D3/6 and S3F1 lines, 75 μg/ml of geneticin was added in the medium. Lentiviral VEZF1 knockdown cells were also maintained in a similar way except tetracycline-free serum was used in all steps to minimise knockdown leakage. VEZF1 knockdown was induced by adding DOX to the growth medium to a final concentration 1 μg/ml. Frozen stocks were prepared by freezing 10^7 cells in foetal bovine serum supplemented with 10% DMSO.

2.3 Protein immunoprecipitation and western blotting analysis

2.3.1 Preparation of protein nuclear extracts

All buffers were supplemented with protease inhibitors 25 μg/ml AEBSF, 0.5 μg/ml Leupeptin and 0.7 μg/ml Pepstatin prior to use. Two 140 mm dishes of cells were harvested by centrifugation at 1,000 g for 5 minutes. The cell pellet was washed with PBS (10 mM Na_2HPO_4, pH 7.4, 1.76 mM KH_2PO_4, 2.7 mM KCl, 137 mM NaCl) twice and then lysed with 2 ml of hypotonic buffer (20 mM HEPES, pH 8, 0.2% NP-40, 0.1 mM EDTA). Nuclei were collected by centrifugation at 2,500 g for 5 minutes at 4 ^{o}C. Cell nucleic were solubilised in 300 μl of high salt buffer (20 mM HEPES, pH 8, 0.2% NP-40, 0.4 M NaCl, 13.3% glycerol) at 4 ^{o}C for at least 30 minutes. Insoluble cell debris was removed by spinning at 16,000 g for 5 minutes. Protein concentrations of nuclear proteins were measured with Bradford assay. The extraction was proportionally scaled up for immunoprecipitation against FLAG tagged VEZF1.

2.3.2 Bradford assay

Bradford assay was performed with a 96-well microplate. 5 μl of protein sample was added into 250 μl of Bradford assay solution and gently mixed. Absorbance at 595 nm was then measured. A standard curve of bovine serum albumin (BSA) concentrations 1 mg/ml to 0.0625 mg/ml were established (Figure 2.1). Protein concentration of samples was calculated from the equation (y=mx+c) of the standard curve.

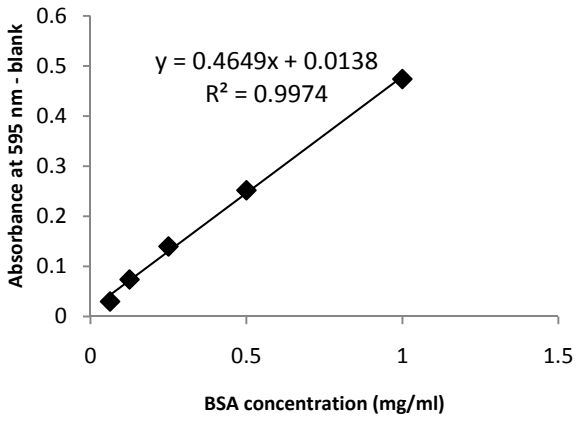

Figure 2.1 An example of BSA standard curve. BSA was diluted by water for the standard curve establishment. Absorbance readings at 595 nm of BSA samples were subtracted to that of a blank control consisting Bradford assay solution only. A straight trend line was drawn by Microsoft Excel and an equation was obtained from the line for calculation of sample protein concentration.

2.3.3 Immunoprecipitation of FLAG tagged proteins

Calcium chloride was added into nuclear proteins samples with final concentration 1 mM for micrococcal nuclease (MNase) digestion to reduce nuclear aggregates which could lead to non-specific binding during immunoprecipitation. 1.5 mg of nuclear proteins were incubated with 2 units of MNase at 4 ^{o}C for 1 hour. The digestion was quenched with 5 mM EGTA. Insoluble nuclear debris was removed by spinning at 16,000 g for 10 minutes. The protein samples were then diluted in no salt FLAG binding buffer (10 mM Tris, pH 8, 0.1% Triton X-100, 10% glycerol) to achieve a final NaCl concentration of 120 mM. EGTA was then supplemented to a final concentration of 5 mM. For 1.5 mg of nuclear proteins, 100 µl (50% slurry in FLAG binding buffer) of anti-FLAG M2 affinity agarose was used. Binding was carried out at 4^{o}C overnight with gentle rotation. Unbound proteins were washed away by 5 times of rotational mixing in 1 ml of FLAG binding buffer (no salt FLAG binding buffer supplemented with 100 mM NaCl) for 2 minutes followed by centrifugation at 3000 g for 1 minute. After the last wash, 50 µl of 2X SDS loading dye (100 mM Tris, pH 6.8, 4% SDS, 0.2% w/v bromophenol blue, 200 mM dithiothreitol (DTT), 20% v/v glycerol) was added and then boiled at 100 ^{o}C for 10 minutes to elute bound proteins. The presence of target proteins was detected using western blotting analysis.

2.3.4 Detection of target proteins using western blotting analysis

In general, 25 µg of nuclear protein, 20 µl of immunoprecipitated protein or 7 µg of nucleosomes was loaded. Different percentages of Tris-glycine separating gels were set according to the sizes of target proteins (Table 2.6). Stacking gel (Table 2.7) was set on top of the separating gel and wells were made by insertion of comb. Electrophoresis was carried out under constant current 30 mA per gel with SDS electrophoresis buffer (25 mM Tris, 250 mM glycine, 0.1% SDS).

Separation of protein sizes	**12 – 45 kDa**	**10 – 70 kDa**	**15 – 100 kDa**	**25 – 200 kDa**
Percentage of separating gel	**15%**	**12.5%**	**10%**	**8%**
40% acrylamide (ml)	2.25	1.875	1.5	1.185
4X separation buffer (ml) (1.5 M Tris, pH 8.8, 0.4% SDS)	1.5	1.5	1.5	1.5
Distilled water (ml)	2.175	2.55	2.925	3.24
10% APS (µl)	75	75	75	75
TEMED (µl)	3	3	3	3

Table 2.6 Recipes of separating gels with various percentages.

40% acrylamide (ml)	0.328
4X stacking buffer (ml) (0.5 M Tris, pH 6.8, 0.4% SDS)	0.656
Distilled water (ml)	1.6
10% APS (µl)	37.5
TEMED (µl)	3

Table 2.7 Recipe of stacking gel preparation.

Proteins separated by electrophoresis were transferred to a methanol activated PVDF membrane under constant voltage 35 V for 1.5 hours in transfer buffer (25 mM Tris, 192 mM Glycine, 10% methanol v/v, 0.01% SDS). Membrane with transferred proteins was blocked by TBST (25 mM Tris, pH 8, 150 mM NaCl, 2.7 mM KCl, 0.2% Tween-20) with 5% milk or BSA, depending on the protein of interest (Table 2.8). Binding of primary antibody in blocking agent (TBST with milk or BSA) was performed at 4 ^{o}C overnight in a Kapak pouch with gentle shaking. Excess primary antibody was washed away by shaking with TBST for 3 times with 10 minutes each. The washed membrane was then incubated with secondary antibody diluted in TBST in the presence of 5% milk or BSA for 2 hours at room temperature. Dilutions of primary and secondary antibodies were used according to manufactures' suggestions (Table 2.8). Excess secondary antibody was removed by shaking with TBST for 3 times with 10 minutes each. Bands were visualised by a CCD camera (Fujifilm) with SuperSignal West Dura extended duration substrate.

Protein of interest	Blocking reagent	Primary antibody dilution	Secondary antibody & dilution
H3K4me2	BSA	1:1000	Anti-rabbit IgG-HRP 1:15000
H3K4me3	BSA	1:1000	Anti-rabbit IgG-HRP 1:15000
H3K9me2	BSA	1:1000	Anti-mouse IgG-HRP 1:10000
H3K9me3	BSA	1:1000	Anti-rabbit IgG-HRP 1:15000
H3K27me3	BSA	1:1000	Anti-rabbit IgG-HRP 1:15000
H3K79me2	BSA	1:1000	Anti-rabbit IgG-HRP 1:15000
H3K79me3	BSA	1:1000	Anti-rabbit IgG HRP 1:15000
H3	BSA	1:10000	Anti-rabbit IgG-HRP 1:15000
H3ac	BSA	1:1000	Anti-rabbit IgG-HRP 1:15000
H4ac	BSA	1:1000	Anti-rabbit IgG-HRP 1:15000
H4K20me3	BSA	1:15000	Anti-rabbit IgG-HRP 1:15000
H2Aub	BSA	1:2000	Anti-mouse IgG-HRP 1:10000
H2A.Z	BSA	1:1000	Anti-rabbit IgG-HRP 1:15000
H2A.Zac	BSA	1:1000	Anti-sheep IgG-HRP 1:7500
H2BK120ub1	BSA	1:2000	Anti-mouse IgG-HRP 1:10000
ARP6	Milk	1:1000	Anti-rabbit IgG HRP 1:15000
BAF53A	Milk	1:1000	Anti-rabbit IgG HRP 1:15000
CTCF	Milk	1:1000	Anti-rabbit IgG-HRP 1:15000
PAF1	Milk	1:500	Anti-rabbit IgG-HRP 1:15000
PONTIN52	Milk	1:500	Anti-goat IgG-HRP 1:10000
RbBP5	Milk	1:1000	Anti-rabbit IgG-HRP 1:15000
REPTIN52	Milk	1:500	Anti-rabbit IgG-HRP 1:15000
RNF20	Milk	1:1000	Anti-rabbit IgG-HRP 1:15000
TBP	Milk	1:2000	Anti-mouse IgG-HRP 1:10000
TIP60	Milk	1:500	Anti-goat IgG-HRP 1:10000
VEZF1	Milk	1:2000	Anti-rabbit IgG-HRP 1:15000
USF1	Milk	1:1000	Anti-mouse IgG-HRP 1:10000

Table 2.8 Table showing binding conditions of primary and secondary antibodies for western blotting analyses.

2.4 Crosslinking chromatin immunoprecipitation

2.4.1 Crosslinked chromatin preparation

All buffers were supplemented with protease inhibitors prior to use as in Section 2.3.1. 10 mM of N-ethylmaleimide was added to inhibit deubiquitination if histone ubiquitination was investigated. Crosslinking chromatin immunoprecipitation was performed as described previously [Litt *et al*, 2001b]. Crosslinked chromatin was usually prepared in a large scale for cells up to 2 x 10^8. Chromatin prepared was proceeded to immunoprecipitation immediately or stored at -80 ^oC for future use.

Briefly, 6C2 or K562 cells were resuspended in fresh growth medium to achieve cell concentration 2 x 10^7 cells per ml. Crosslinking buffer (7% formaldehyde, 0.1 M NaCl, 1 mM EDTA, 0.5 mM EGTA, 50 mM HEPES, pH 8) was added to bring the formaldehyde final concentration to 1%. Incubation at room temperature for 2 – 30 minutes followed, depending on which protein was studied (Table 2.9). Crosslinking reactions were quenched for 5 minutes with glycine in a final concentration of 125 mM. The crosslinked cells were pelleted at 1000 g for 5 minutes and then lysed with 15 ml of cell lysis buffer 1 (0.25% Triton X-100, 10 mM EDTA, 0.5 mM EGTA, 10 mM Tris, pH 8). Cell nuclei were obtained by centrifugation at 800 g for 5 minutes at 4 ^oC. The pellet was washed with 15 ml of cell lysis buffer 2 (0.2 M NaCl, 1 mM EDTA, 0.5 mM EGTA, 10 mM Tris, pH 8). Nuclei were solubilised in nuclear lysis buffer (50 mM Tris, pH 8, 10 mM EDTA, 0.5% SDS) on ice for 30 minutes. The chromatin volume was brought to 2 ml with X-ChIP buffer (1.1% Triton X-100, 1.2 mM EDTA, 16.7 mM Tris, pH 8, 167 mM NaCl, 0.01% SDS) for sonication. Chromatin was fragmented by sonication (Misonix) for a total time of 10 minutes in regular 10 second pulses, separated by resting for 30 seconds to obtain 500 bp fragments. Insoluble materials were removed by centrifugation at 15,000 g for 10 minutes at 4 ^oC. Chromatin from this point was either used for immunoprecipitation or stored at -80 ^oC.

Cells	X-linking duration	Antibodies	Amount of antibodies
6C2	10 minutes	Anti-CTCF	10 µl
	20 minutes	Anti-RbBP5	10 µg
	20 minutes	Anti-RNF20	10 µg
	20 minutes	Anti-PAF1	10 µg
	10 minutes	Anti-VEZF1	15 µg
	10 minutes	Anti-USF1	10 µl
	2 minutes	Anti-H2BK120ub1	5 µg
	4 minutes	Anti-H3K4me2	20 µl
	4 minutes	Anti-H3K4me3	15 µg
K562	30 minutes	Anti-ARP6	10 µl
	30 minutes	Anti-BAF53A	5 µg
	30 minutes	Anti-PONTIN52	10 µg
	30 minutes	Anti-REPTIN52	10 µg
	30 minutes	Anti-SRCAP	10 µg
	30 minutes	Anti-TIP60	10 µg
	30 minutes	Anti-TRRAP	5 µg
	10 minutes	Anti-VEZF1	15 µg

Table 2.9 Table showing crosslinking conditions and antibodies used in crosslinking ChIP analyses.

2.4.2 Chromatin immunoprecipitation

Sonicated chromatin was diluted with X-ChIP buffer to obtain cell chromatin from 1 x 10^7 per ml. 100 µl of chromatin was saved as input material for quantitative PCR. 1 ml of chromatin for immunoprecipitation was pre-cleared using 5 µg of non-immunised normal IgG and 100 µl (50% slurry in X-ChIP buffer) of protein A/G agarose at 4 ^oC for 2 hours. Specific antibodies (Table 2.9) were added and then incubated at 4 ^oC overnight with rotation. Addition of 100 µl (50% slurry in X-ChIP buffer) of protein A/G agarose was then followed. Binding was carried out at 4 ^oC for 3 hours with rotation. The agarose was washed extensively with washing buffers 1(0.1% SDS, 1% Triton X-100, 2 mM EDTA, 20 mM Tris, pH 8, 150 mM NaCl), 2 (0.1% SDS, 1% Triton X-100, 2 mM EDTA, 20 mM Tris, pH 8, 500 mM NaCl) and 3 (0.25 M LiCl, 1% NP-40, 0.5% sodium deoxycholate, 1 mM EDTA, 10 mM Tris, pH 8), and twice with TE washing buffer (10 mM Tris, pH 8, 1 mM EDTA) by rotational mixing in 1 ml of washing buffer for 2 minutes

each. Bound chromatin was eluted twice with 350 µl of elution buffer (1% SDS, 0.1 M $NaHCO_3$) for quantitative PCR analysis or boiled with 50 µl of 2X SDS loading dye for 20 minutes for western blotting analysis. Eluates intended for quantitative PCR analysis were prepared reversal of crosslinks by incubation at 65 ^oC overnight in the presence of 225 mM NaCl. Proteins were subsequently digested using 20 µg of proteinase K at 45 ^oC for two hours. DNA released was purified using conventional phenol/chloroform method for quantitative PCR.

2.4.3 DNA extraction

700 µl of phenol/chloroform isoamyl mixture was added into 700 µl of ChIP eluates. The two-phase mixture was vortexed for 1 minute following centrifugation at 10,000 g for 5 minutes. The upper aqueous layer was transferred in another microfuge tube. 700 µl of chloroform was added and vortexed for 1 minute. Separation was again carried out by centrifugation at 10,000 g for 5 minutes. DNA in the upper aqueous layer was precipitated following the addition of 1.3 ml of 100% ethanol and 10 µg of glycogen and incubation at room temperature for 30 minutes. DNA was pelleted by centrifugation at 16,000 g for 25 minutes and washed twice with 300 µl of 70% ethanol with centrifugation at 16,000 g for 5 minutes. The pellet was dried briefly at 50 ^oC for about 5 minutes and then resuspended in 120 µl of 10 mM Tris. DNA from input material was extracted alongside and sizes of chromatin fragments were analysed with 1.25% TBE (89 mM Tris, 89 mM Boric acid, 2 mM EDTA) agarose gel.

2.5 Native chromatin immunoprecipitation

2.5.1 Low salt native chromatin preparation

All buffers for nucleosome preparation and immunoprecipitation were supplemented with protease inhibitors (Section 2.3.1), 10 mM of sodium butyrate and 10 mM of N-ethylmaleimide was added if histone ubiquitination was investigated. 10 x 140 mm dishes of cells were harvested by centrifugation at 1,000 g for 5 minutes and cell pellets were washed with PBS followed by centrifugation twice. Cells were lysed following resuspension in 6 ml of lysis buffer (10 mM Tris, pH 7.5, 10 mM NaCl, 3 mM $MgCl_2$, 0.4% NP-40). Cell nuclei were pelleted by centrifugation at 2,500 g for 5 minutes and then resuspended in 2 ml of Calcium plus lysis buffer (lysis buffer plus 1 mM $CaCl_2$). 1 µl of cell nuclei suspension was added into 199 µl of urea/NaCl buffer (5 M Urea, 2 M NaCl) for DNA concentration measurement with optical absorbance at 260 nm (DNA concentration in µg/ml = absorbance x 50 x dilution factor). Nuclei were pelleted again and resuspended in Calcium plus lysis buffer as necessary, in order to bring the DNA concentration to 5 mg/ml. The cell nuclei suspension was separated into three equal aliquots for digestion with serially diluted micrococcal nuclease (MNase) with MNase digestion buffer (20 mM Tris, pH 8, 0.25 µM $CaCl_2$, 20% glycerol). The concentration of MNase (X) for digestion was determined by prior small scale digestions to identify the MNase concentration that yielded the most amount of di- and tri-nucleosomes. "X" determined for 6C2 cells was 2 units of MNase per 1 mg of chromatin, and 1.5 units for K562 cells. The pre-warmed three aliquots of cell nuclei were digested with 0.5X, X and 2X of MNase separately. Digestion was carried out at 37 ^{o}C for 17 minutes. Digestion reactions were quenched with 10 mM EDTA and soluble chromatin supernatant (S1) was collected following centrifugation at 2,500 g for 5 minutes. Three digests were combined (S1). The remaining pellet was resuspended with EDTA plus lysis buffer (lysis buffer plus 0.25 mM EDTA) and then left on ice for 15 minutes. Chromatin was released by passing through 20 then 25 gauge needles for 4 times each. Cell debris was removed by centrifugation at 10,000 g for 10 minutes at 4 ^{o}C and the soluble fraction (S2) was saved and pooled together with S1. Nucleosomes were separated according to sizes with sucrose density

gradient centrifugation or saved for western blotting analyses of total chromatin.

2.5.2 Sucrose density gradient centrifugation

Linear 5 to 25% sucrose gradients were generated with buffered sucrose (sucrose (5% or 25% w/v), 10 mM Tris, pH 7.5, 10 mM NaCl, 3 mM EDTA) by using a Gradient Master 107 gradient forming instrument (Biocomp). Program settings for generation of 5 – 25% linear sucrose gradient were 81.5^{o} inclination, 15 rpm and duration 1 minute and 52 seconds. 1.5 mg or 500 µl of S1S2 chromatin was placed on top of a 14 ml gradient and then separated by ultracentrifugation with SW 40 Ti rotor at 31,000 rpm (equivalent to 170614 g at maximum radius) for 14 hours at 4 ^{o}C. 1 ml fractions were collected from top of the gradient. 10 µl of each fraction was digested with 1 µg of Protease K at 37 ^{o}C for 30 minutes in the presence of 0.03% of SDS. Chromatin sizes were analysed with 1.5% of SafeView stained TBE agarose gel. Fractions containing di- and tri-nucleosomes were pooled for 0.1% formaldehyde crosslinking in order to fix unstable nucleosomes. Crosslinking was carried out at room temperature for 13 minutes and then quenched with 125 mM glycine for 5 minutes. Excess crosslinkers, glycine and sucrose exchanged with N-ChIP buffer (10 mM Tris, pH 7.5, 50 mM NaCl, 5 mM EDTA) using an equilibrated 10 ml Bio-gel desalting column (Biorad). The column was packed with P-6DG gel (Biorad) prepared by swelling P-6DG gel powder with N-ChIP buffer overnight at 4 ^{o}C. The concentrations of chromatin preparations were measured with Bradford assay (Section 2.3.2).

2.5.3 Immunoprecipitation of native chromatin

50 µg of nucleosomes were pre-cleared using 100 µl (50% of slurry in N-ChIP buffer) of protein A or G agarose for one immunoprecipitation reaction. The agarose suspension was mixed at 4 ^{o}C for 2 hours with gentle rotation and the agarose was removed by centrifugation at 3000 g for 1 minute. Specific antibody was added to the pre-cleared chromatin (Table 2.10). Nucleosomes were incubated with antibody at 4 ^{o}C for overnight with gentle rotation. 100 µl (50% of slurry in N-ChIP buffer) of protein A or G agarose was added and incubated at 4 ^{o}C for 2 hours. Unbound

proteins were washed away with 1 ml of wash buffer (20 mM Tris, pH 7.4, 150 mM NaCl, 0.2 mM EDTA, 0.1% Tween-20) followed by centrifugation at 3000 g for 1 minute for 5 times. Immunoprecipitated chromatin was eluted with 350 µl of 1.5% SDS elution buffer (N-ChIP buffer supplemented with 1.5% SDS) and then 0.5% SDS (N-ChIP buffer supplemented with 0.5% SDS) elution buffer at room temperature for 15 minutes each. The elution from the two elution steps was pooled and subjected to DNA extraction (Section 2.4.3).

Antibodies	Amount
H3K4me2	10 µl
H3K4me3	10 µl
H3K9me2	10 µg
H3K9me3	10 µl
H3K27me3	10 µl
H3ac	10 µl
H4ac	10 µl
H2A.Z	10 µl
H2A.Zac	10 µg
H2BK120ub1	10 µl
Ubiquitin	20 µg

Table 2.10 Antibodies used in native ChIP analyses for histone modification detection

2.5.4 DNA quantification using PicoGreen® reagent

The procedures were generally followed as the manufacture's recommendation (Invitrogen). All reagents except DNA samples were provided from the kit. Briefly, standard DNA was prepared in two-fold serial dilution with 1X TE buffer for standard curve establishment. The range of standard was from 3.125 ng/µl to 0.00305 ng/µl. DNA from each ChIP experiment was diluted 10-fold while input DNA was diluted 100-fold for measurement. PicoGreen® working solution was prepared by diluting the PicoGreen® stock 400-fold with 1X TE buffer. 10 µl of diluted samples or standard DNA was added into 190 µl of working PicoGreen® solution in duplicates for each samples. Fluorescent signal was measured using a "plate read" function of real-time PCR machine (Stratagene Mx3000P) with excitation at 480 nm and emission intensity collected at 520 nm. Emission readings from the standard DNA were plotted versus DNA concentrations

(Figure 2.2) and an equation (y=mx+c) obtained from the straight line was used for calculation of the sample DNA concentration.

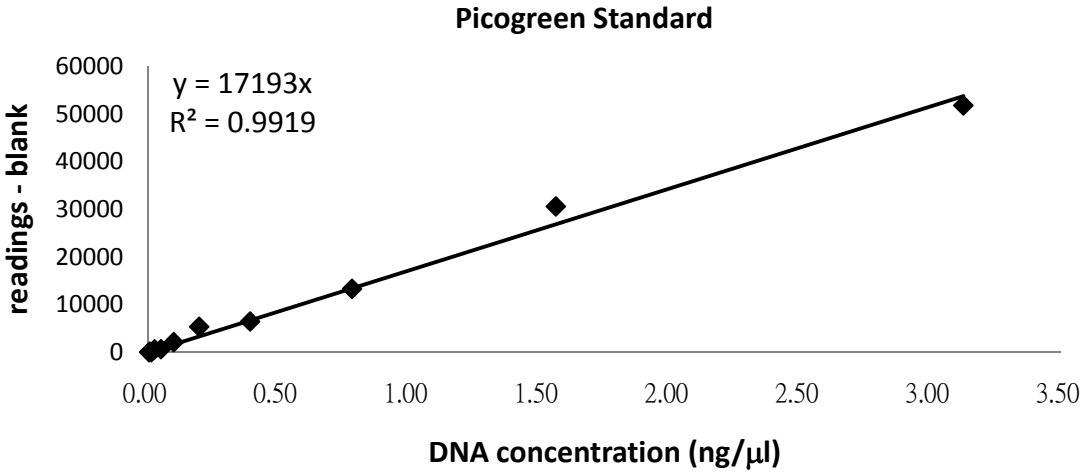

Figure 2.2 An example of PicoGreen® standard curve. The standard curve was established using the lamda standard DNA provided from the invitrogen PicoGreen® kit. Readings of emission at 520 nm of standard samples were subtracted to that of blank and plotted against DNA concentrations.

2.6 Reverse Transcriptase PCR

2.6.1 RNA extraction

5 x 10^6 of 6C2 cells were harvested and lysed in 1 ml of TRI Reagent® (Sigma). 100 µl of 1-bromo-3-chloropropane (BCP) was added and then mixed vigorously. Samples were left at room temperature for 5 minutes. The aqueous upper layer containing extracted RNA was collected following centrifugation at 12,000 g for 15 minutes at 4 ^oC. RNA was precipitated with 500 µl of isopropanol incubation at -20 ^oC for 20 minutes. RNA was pelleted by centrifugation at 12,000 g at 4 ^oC for 15 minutes. The RNA pellet was washed with 500 µl of 70% ethanol followed with centrifugation at 12, 000 at 4 ^oC for 5 minutes twice and then air-dried at room temperature. RNA was resuspended in 50 µl of RNAase-free water.

2.6.2 cDNA synthesis

RNA was quantified by measurement of absorbance at 260 nm with a NanoDrop® ND1000 spectrophotometer (Thermo). 400 ng of RNA was mixed with 0.5 µl of 10 µM of dNTP (mixture of dATP, dCTP, dGTP and dTTP), 1 µl of random hexamer (50 ng/µl) and the final volume was brought to 6.5 µl with RNase-free water. The mixture was denatured at 65 ^oC for 5 minutes, and then left on ice for 1 minute. 2 µl of 5X first strand synthesis buffer, 0.5 µl of RNase OUT, 0.5 µl of 0.1 M DTT and 0.5 µl of SuperScript III reverse transcriptase (Invitrogen) were added to the mixture. cDNA was synthesised by incubation on a thermocycler at 25 ^oC for 10 minutes, 50 ^oC for 50 minutes, 85 ^oC for 5 minutes. A reaction without reverse transcriptase was prepared in parallel to act as a control of genomic DNA contamination in subsequent PCR assays. RNA template was removed by RNAase (2 units) digestion at 37 ^oC for 20 minutes. cDNA was diluted 10 folds with RNase- and DNase-free water for quantitative PCR analysis.

2.7 Real-time quantitative PCR analysis

2.7.1 Real-time PCR reaction setup

2.7.1.1 TaqMan assay

TaqMan chemistry makes use of the principle of fluorescence resonance energy transfer (FRET) to confer a high specificity in quantitative PCR. In addition to conventional forward and reverse primers flanking the target site, a TaqMan probe is also designed which is specific to the target sequence. A TaqMan probe is conjugated with a fluorophore and a quencher at the 5' and 3' ends, respectively. Emission energy of fluorophore followed by excitation is absorbed by the quencher if the two are in close proximity so that the fluorescent signal cannot be detected. While extension of the forward primer occurs and reaches the TaqMan probe that has primed on the same DNA template, degradation of the probe occurs due to the 5' to 3' exonuclease activity of *Taq* polymerase. Therefore, the fluorophore and quencher are no longer in proximity; the fluorescent signal can be detected and is proportional to the amount of specific PCR products (Figure 2.3) [Knemeyer & Marmé, 2007]. Non-specific PCR products without priming of either the forward or TaqMan probe are not detected.

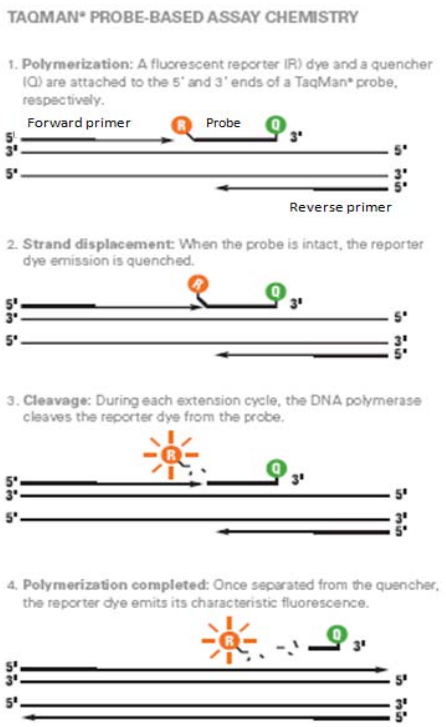

Figure 2.3 Overview of Taqman probe-based assay chemistry. "R" and "Q" indicate the fluorescent reporter dye and quencher, respectively. Modified from the website of Applied Biosystems (www.appliedbiosystems.com).

As the PCR primers and TaqMan probes that are specific to the chicken *β-globin* locus had been widely used in the lab, the TaqMan chemistry was employed in all quantitative PCR analyses following ChIP assays for studying the locus. TaqMan assays were also used for some quantitative PCR analyses for studying human putative insulator elements or other regulatory elements, depending on the availability of TaqMan probes (Appendix I).

DNA of input samples and from native ChIP was usually diluted to 0.2 ng/µl for real-time PCR while no dilution was made for DNA from crosslinking ChIP. Reaction was set up as following:

2X TaqMan PCR reaction mix	10 µl
Forward and reverse primer mix (4.5 nM of each primer)	4 µl
TaqMan probe (working concentration differed between probes)	2µl
DNA template	4 µl
Total volume	20 µl

PCR reactions were performed on a thermal cycler (Roche, LC480) with thermal profiles: denaturing at 95 ^{o}C for 10 minutes, followed by 50 cycles of denaturation at 95 ^{o}C for 10 seconds and annealing/extension at 60 ^{o}C for 45 seconds. Values of cycle threshold (Ct) were obtained using the software LightCycler® 480 platform as shown in Figure 3.5.

2.7.1.2 SYBR® Green

The SYBR® Green chemistry is a relatively cost-effective quantitative PCR assay because the costly TaqMan probe is not involved. This assay is developed based on a fluorescent property of the SYBR Green I dye following the binding to double-stranded DNA [Arya *et al*, 2005]. Therefore, fluorescent signal increases after every amplification cycle with the amount of PCR products (Figure 2.4).

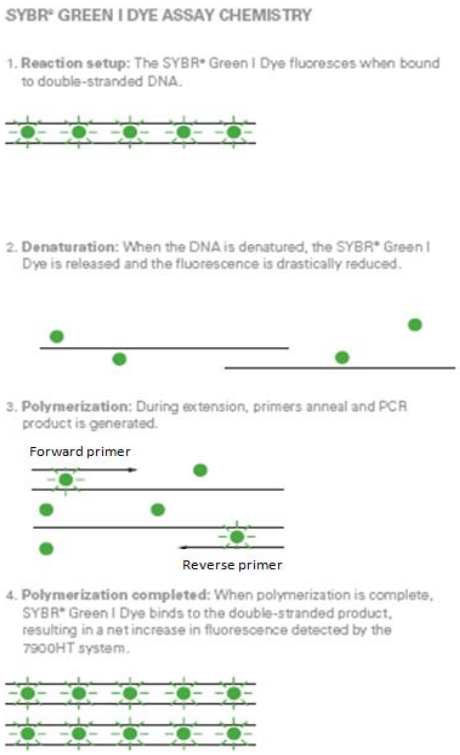

Figure 2.4 Overview of SYBR® Green chemistry. Modified from the website of Applied Biosystems (http://www.appliedbiosystems.com).

Quantitative analyses of RT-PCR and ChIP assays of human regulatory elements without available TaqMan probes were performed with SYBR® Green assays (Appendix I). Concentration of DNA template for SYBR® Green was the same as that was used for TaqMan assay. PCR reaction was set up as followings

2X SYBR® Green mix	4 µl
Forward and reverse primer mix (4.5 nM of each primer)	4 µl
DNA template	4 µl
Water	2 µl
Total volume	20 µl

PCR reactions were carried out on a thermal cycler from Stratagene (Mx3000P) with thermal profiles: denaturating at 95 ^{o}C for 10 minutes, followed by 40 cycles of denaturation at 95 ^{o}C for 15 seconds and annealing/extension at 60 ^{o}C for 30 seconds. Dissociation temperature of PCR products was measured with increasing temperature from 55 ^{o}C to 95 ^{o}C. Ct values were obtained from the software MxPro v.4.01 for data analysis as shown in Figure 3.5.

2.7.2 Data analysis

The relative enrichment of specific sequences in ChIP assays was determined using the comparative Ct method, also known as the $2^{-\Delta\Delta Ct}$ method [Litt *et al*, 2001a; Livak *et al*, 2001; Schmittgen & Livak, 2008]. The method firstly determined the amount of target DNA present in immunoprecipitates relative to that in the input material, that was ΔCt ($\Delta Ct = Ct_{input} - Ct_{ChIP}$). It was then normalised to the enrichment of a negative or positive control region in order to obtain ΔΔCt ($\Delta\Delta Ct = \Delta Ct_{interest} - \Delta Ct_{control}$).

The relative enrichment of target DNA from ChIP versus control sequence is expressed as $2^{\Delta Ct}$. This assumes maximal primer efficiencies, where the amount of PCR products doubles after each cycle of amplification. In practice, however, discrepancies between primer efficiencies can skew data analyses as discussed in Section 3.2.1.3. Fold enrichment calculations therefore incorporated the values of primer efficiencies (E) obtained from the slope of primer standard curve ($E = 10^{-1/slope}$), Ct values resulting from the PCR of a series of genomic DNA of standards for each primer. The relative enrichments of a target site normalised to a control site were calculated from the primer efficiencies of each site, E_t and E_c, respectively. The formula for calculating the fold enrichment of a target site after normalisation to the enrichment of a control site is $E_t^{\Delta Ct}/E_c^{\Delta Ct}$.

Relative mRNA expression levels in RT-PCR analyses were also calculated using the comparative Ct method. The expression of target gene was firstly normalised to a loading control, normally a housekeeping gene, to obtain ΔCt ($\Delta Ct = Ct_{target} - Ct_{loading\ control}$). Change of expression was then compared with an untreated control or wild type to obtain ΔΔCt ($\Delta\Delta Ct = \Delta Ct_{treated} - \Delta Ct_{untreated\ or\ wild\ type}$).

Two sample equal variance Student's t-tests using a two-tailed distribution were applied to obtain p-values from ChIP enrichment values with the t-test function in Microsoft Excel to access the

significance of fold enrichments over controls, or changes of histone modifications upon RNF20 knockdown.

2.8 Flow cytometry analysis

2.8.1 Sample preparation

10^6 6C2 cells were harvested by centrifugation at 1,000 g for 5 minutes. Cells were washed twice with 1 ml of HBSS+ (Hank's buffered saline solution supplemented with 0.1% BSA, 0.1% Sodium azide) following centrifugation. Cells were resuspended in 100 µl of HBSS+ and then 10 µl of anti-IL2R-PE antibody was added. Antibody binding occurred at 4 ^{o}C for 30 minutes in the dark. Excess antibody was removed by washing twice of HBSS+ in 1ml each following centrifugation. Cells obtained from the last wash were resuspended in 500 µl of HBSS+ for flow cytometry analysis.

2.8.2 Data collection and analysis

Flow cytometry analysis was carried out with a FACSCalibur flow cytometer (BD Biosciences) and data was collected using the software CELLQuest. Parameters for data collection were optimised for detection of chicken 6C2 cells, for PE as well as GFP fluorescent signals. Fluorochromes were excited by laser at 488 nm. Emission was collected with the FL1 detector at 530 nm for GFP and the FL2 detector at 585 nm for PE. Voltages were set at 460 V for detectors FL1 and 465 V for FL2. Colour compensation was made correct for the emission of GFP in FL2 (20% FL1) and PE in FL1 (1% FL2). While viewing a forward scatter (FSC, for cell sizes) versus side scatter (SSC, for cellular granularity) plot, viable single cells were gated for analysis. Data from 10,000 viable or GFP expressing cells (knockdown cells) were collected for analysis. Mean or median of fluorescence intensity was an indicator of GFP or IL2R expression. The relative expression level of *IL2R* in knockdown cells was compared to that of wild type or untreated cells by setting expression of control cells to one using FlowJo software (Tree Star, Inc).

CHAPTER 3

Identification of H2B ubiquitination at chromatin boundary elements

3.1 Objectives

In this chapter, the hypothesis that chromatin boundary elements, such as the HS4 insulator, may recruit H2B ubiquitination as part of their chromatin barrier activity will be addressed in the following three objectives.

Objective 1. Confirm that boundary elements are enriched with ubiquitinated histones

a) Establishment and optimisation of native ChIP assays, including
   i. Check the representation of histone modifications and genomic DNA sequences in native chromatin fractions
   ii. Check the immunoprecipitation of H3K4me2/3 from native chromatin
   iii. Determine the efficiency of PCR primer sets in quantitative real-time PCR
   iv. Perform the native ChIP assay for H3K4me2/3
   v. Examine the performance of native chromatin fractions prepared in low salt conditions
b) Native ChIP analysis of histone ubiquitination and H2BK120ub1 across the *FOLR1* and *β-globin* gene loci in erythroid cells
   i. Check the immunoprecipitation of histone ubiquitination and H2BK120ub1 from native chromatin
   ii. Perform the native ChIP assay for histone ubiquitination and H2BK120ub1

Objective 2. Determine whether the H2B-specific ubiquitination ligase RNF20 is recruited to chromatin boundary elements

a) Identify the sequence of the candidate H2B-specific E3 ligase RNF20 in chicken

b) Analyse the specificity of anti-RNF20 antibodies

c) Determine whether RNF20 is bound at chromatin boundary elements

Objective 3. Establish clonal cell lines that permit prolonged knockdown of RNF20 expression

a) Design short hairpin RNA sequences that target chicken RNF20

b) Design of the lentiviral shRNA expression vector system

c) Establishment of clonal cell lines with inducible knockdown of RNF20

d) Western blotting analysis of RNF20 and H2BK120ub1 in knockdown lines

3.2 Confirm that boundary elements are enriched with ubiquitinated histones

3.2.1 Establishment and optimisation of native ChIP assays

The first objective is to confirm that boundary elements are enriched with ubiquitinated histones, H2B monoubiquitination in particular, using ChIP assays. Anti-H2Bub1 antibodies had not been developed when this project began. The only strategy for the ChIP analysis of H2B ubiquitination included tagging the H2B and ubiquitin genes in budding yeast with the FLAG and HA epitope tags, and two-step crosslinking ChIP with anti-FLAG followed by FLAG peptide elution then ChIP with anti-HA antibodies [Henry *et al*, 2003; Kao *et al*, 2004]. This approach was considered to be too problematic for use in this study due to the technical challenge of genetically modifying chicken erythroid cells. Moreover, this two-step ChIP approach may result in false positive results given that a wide variety of non-histone chromatin binding proteins are subject to ubiquitination and that tagged H2B is present in almost all nucleosomes. This approach is likely to yield all ubiquitinated nucleosomes, whether the modification occurs on H2B, other histones or non-histone proteins.

ChIP assays using anti-ubiquitin antibodies and native chromatin preparations offers a more specific approach to studying histone ubiquitination without the need for genetic modification of the tissues under study. My supervisor Dr. Adam West first used this approach to study histone ubiquitination in 10 day chick embryo red blood cells (Section 1.6.3). The native ChIP procedure involves the isolation of nucleosomal fragments following the digestion of nuclei with micrococcal nuclease (MNase) (Figure 3.1). Digested chromatin is then subject to sucrose density gradient fractionation, with mono-, di- and tri-nucleosomes being retained for ChIP assays. Chromatin fragments are immunoprecipitated with specific antibodies and the precipitated genomic DNA is then purified by phenol/chloroform extraction for quantitative PCR analysis of specific sequence enrichments.

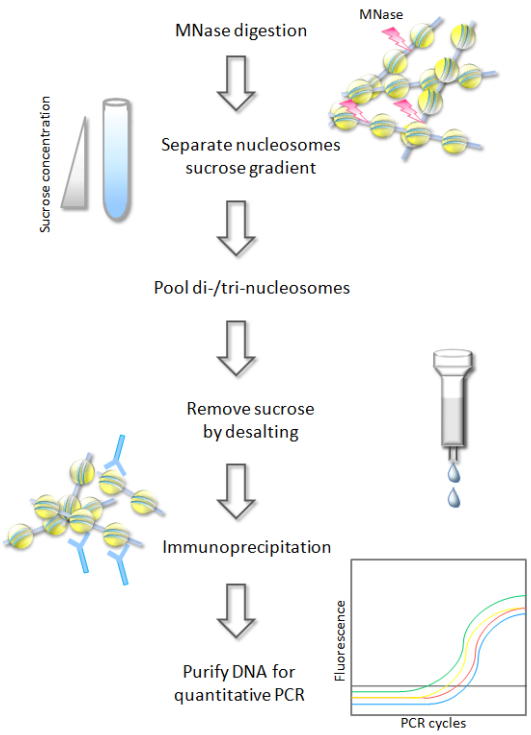

Figure 3.1 Schematic diagram showing the native ChIP procedures.

The necessity of sucrose density fractionation and the inability to store native chromatin for long periods, make this approach more time consuming than conventional crosslinking ChIP analysis. However, there are key advantages of native ChIP over crosslinking ChIP for the analysis of histone modifications [Das *et al*, 2004]. The crosslinking of histone-binding proteins and compact chromatin structures can mask the epitopes recognised by specific anti-histone antibodies, thus lowering ChIP efficiency and potentially skewing ChIP enrichment values for specific sequences. Furthermore, native chromatin preparations can be free of non-histone proteins (Figure 3.2), allowing the study of histone ubiquitination with anti-ubiquitin antibodies.

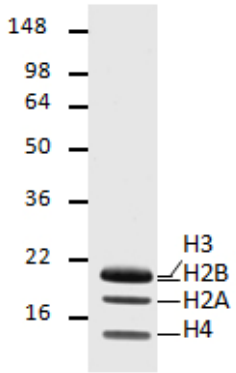

Figure 3.2 Protein content of di-/tri- nucleosomes prepared from 10 day RBC for use in native ChIP assays analysed by Coomassie blue stained polyacrylamide gel [Ma *et al*, 2011].

3.2.1.1 The preparation of native chromatin fractions for high resolution ChIP analyses of active and repressive histone modifications across the *FOLR1* and *β-globin* gene loci

Small chromatin fragments are preferred in ChIP assays to allow maximal resolution and potential enrichment. Mononucleosome fractions offer the highest resolution but the potential for nucleosome sliding and instability in native preparations can present a problem [Meersseman *et al*, 1992]. Another problem is that positioned mononucleosomes may be missed in quantitative PCR as the amplicon sizes in this study range from 60 – 130 bp. Fractions containing di- and tri-nucleosomes are therefore selected in a balance between resolution and chromatin stability. A further concern is the genomic representation of native chromatin preparations, as nuclease accessibility differs across the genome. It was shown by the Felsenfeld group that the combination of three digests with a range of MNase concentrations allows the preparation of di- and tri-nucleosomes from both relaxed and compact structures [Litt *et al*, 2001b].

Native chromatin was prepared from the chicken early erythroid CFU-E stage cell line 6C2, which express the *FOLR1* gene, but are yet to express the *β-globin* genes. Following the Felsenfeld native ChIP approach, nuclei were digested with 0.5X, 1X and 2X concentrations of MNase where "X" was the single concentration that gives the greatest yield of di- and tri-nucleosomes. Digested chromatin was fractionated on 5-25% sucrose density gradients. DNA was extracted from an aliquot of each fraction to determine the nucleosome sizes by agarose gel electrophoresis (Figure 3.3a). Fractions were pooled according to their nucleosome sizes, resulting in five pooled categories, overdigested nucleosomes, mononucleosomes, di-/tri-nucleosomes, polynucleosomes and high molecular weight nucleosomes. These chromatin pools were analysed by western blotting and quantitative PCR assays to determine the representation of active and repressive histone modifications and genomic DNA sequences in each fraction.

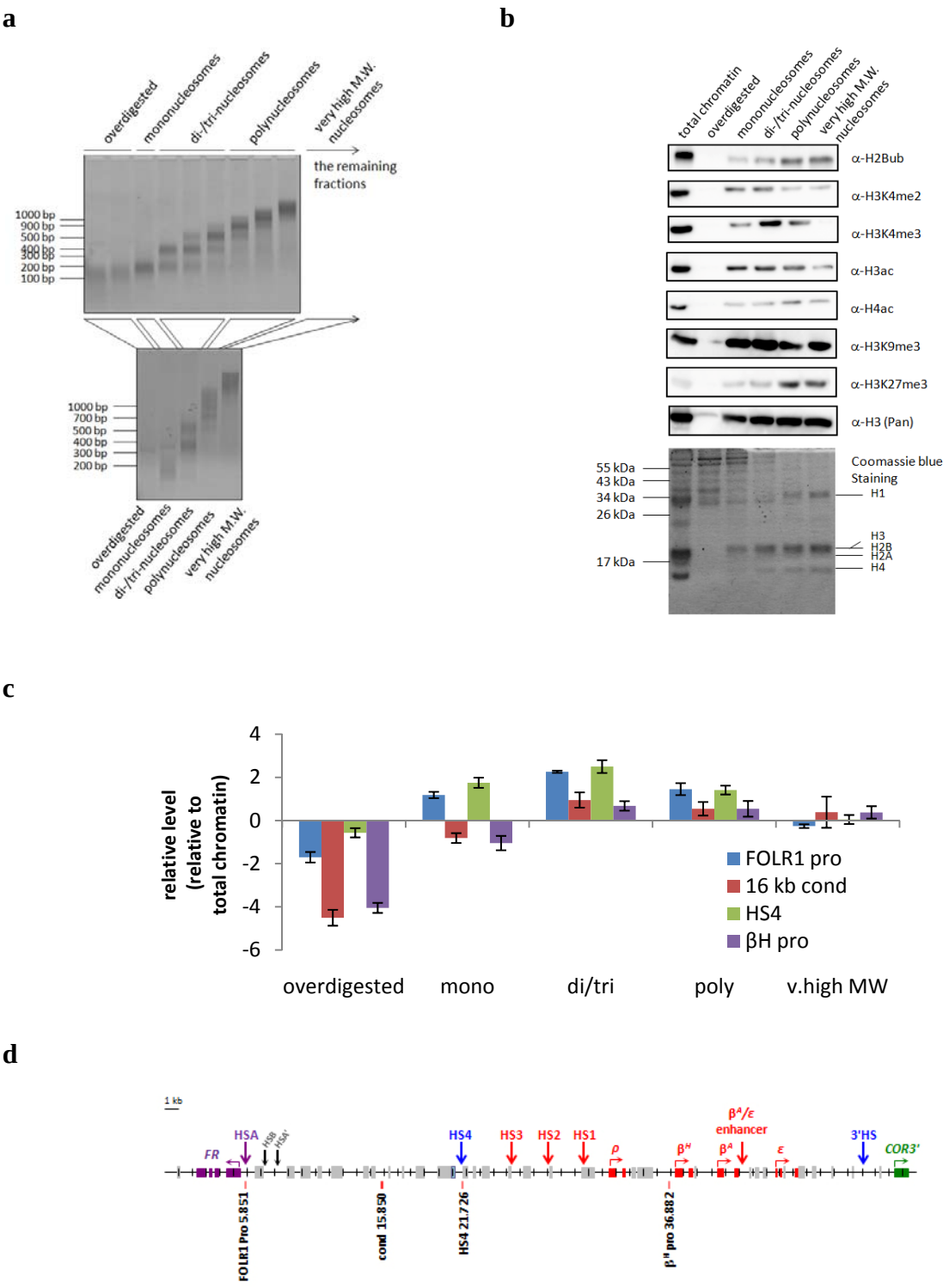

Figure 3.3 Relaxed and condensed chromatin regions are represented in di-/tri-nucleosome fractions. **a**. Upper panel: Agarose gel electrophoresis analysis of the sizes of chromatin in different sucrose fractions. Lower panel: chromatin fractions were pooled according to their sizes and analysed again by agarose gel electrophoresis. **b**. Histone modifications in each chromatin fraction were examined by western blotting. **c**. DNA isolated from each chromatin fractions were determined by quantitative PCR. The relative level was calculated from the differences of Ct values (dCt), dCt = $Ct_{\text{total chromatin}}$ - $Ct_{\text{examined chromatin fraction}}$, where Ct values were obtained as shown in Section 2.7.2. **d**. Primer sets used in this experiment.

Chromatin with high nuclease accessibility present in the mononucleosome fraction was found to have higher levels of H3ac, H3K4me2 and H3K4me3, compared with chromatin with low accessibility in the polynucleosomes and very high molecular weight fractions (Figure 3.3b). H4ac and H3K9me3 levels were equally distributed between chromatin fractions of different sizes. In contrast, the levels of the heterochromatin-associated mark H3K27me3 were highest in fractions with the largest chromatin fragments. H3K9me3, unlike H3K27me3, was not enriched in any particular chromatin fractions. The bulk of H2BK120ub1 is found in less accessible polynucleosome fractions. The di-/tri-nucleosome fraction contained a mixture of each chromatin mark.

Quantitative PCR was used to determine the presence of genomic sequences known to reside in open and condensed chromatin structures in each nucleosomal fraction. The *FOLR1* promoter and HS4 insulator are both DNaseI hypersensitive sites in 6C2 cells [Prioleau *et al*, 1999] and are enriched in both the mononucleosome and di-/tri-nucleosome fractions (Figure 3.3c). Conversely, the transcriptionally inactive 16 kb condensed region and β^H*-globin* promoter, were depleted from mononucleosomes and present in di-/tri-nucleosomes up to higher molecular weight nucleosomes. Therefore, the di-/tri-nucleosome fraction contains a mixture of open and condensed chromatin sequences.

By balancing considerations of nucleosome stability, ChIP resolution and the representation of a variety of histone modifications and genomic regions, the fractions that contain di-/tri-nucleosomes were selected in subsequent ChIP experiments. These fractions contain predominantly core histone proteins, with minimal non-histone protein carryover (Figure 3.2 & Figure 3.3b).

3.2.1.2 Analysis of immunoprecipitates from native chromatin

To validate the performance of native ChIP from fractionated 6C2 chromatin, immunoprecipitations were carried out with anti-H3K4me2 and anti-H3K4me3 antibodies as a trial run. These modifications are particularly well studied in crosslinking ChIP and native ChIP for H3K4me2 in 6C2 cells has been reported previously [Litt *et al*, 2001a]. The two antibodies could immunoprecipitate the corresponding H3K4 methylation from total chromatin prepared following MNase digestion (Figure 3.4a) as well as from di-/tri-nucleosomes purified using sucrose gradients (Figure 3.4b). The method of nucleosome preparation and the buffer conditions for immunoprecipitation are therefore suitable for the detection of these modifications using native ChIP assays.

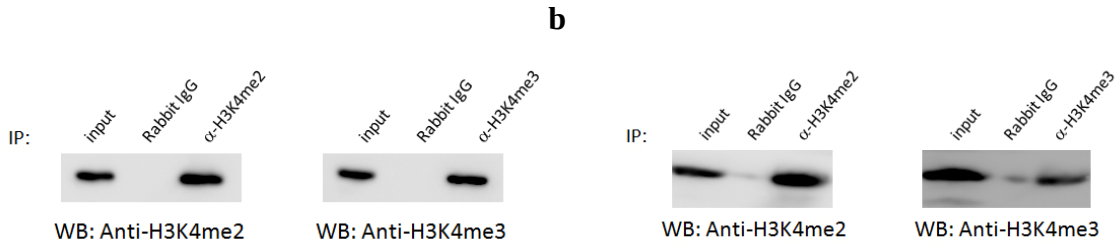

Figure 3.4 Immunoprecipitation of methylated H3K4 from 6C2 cell native chromatin. Chromatin was prepared from 6C2 cells with MNase digestion in native condition. Immunoprecipitation with anti-H3K4me2 and anti-H3K4me3 antibodies was performed on total chromatin resulting from MNase digestion **(a)** and di- and tri-nucleosomes resulting from sucrose gradient fractionation **(b)**. The presence of H3K4me2/3 in immunoprecipitates was examined with the same antibodies used in immunoprecipitation.

3.2.1.3 Determining the efficiency of PCR primer sets for use in quantitative real-time PCR

Genomic DNA sequence enrichments following chromatin immunoprecipitation are quantified by real-time PCR in this study. Real-time PCR machine software is used to determine cycle threshold (Ct) values for each reaction as a direct measure of DNA quantity (Figure 3.5). The enrichments of genomic sequences of interest following ChIP are calculated using the comparative Ct method ($2^{-\Delta\Delta Ct}$) as discussed in Section 2.7.2. This calculates the fold enrichment

of a sequence in immunoprecipitates compared to input DNA (starting chromatin). In order to make comparisons between ChIP experiments, normalisation to a negative or positive control sequence is required ($2^{-\Delta\Delta Ct}$).

a

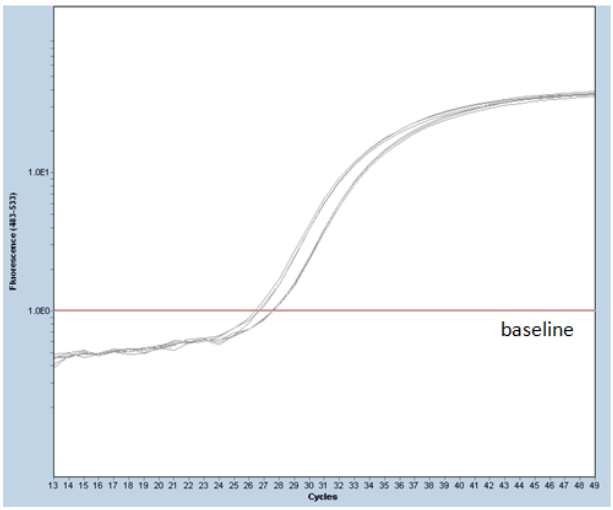

b

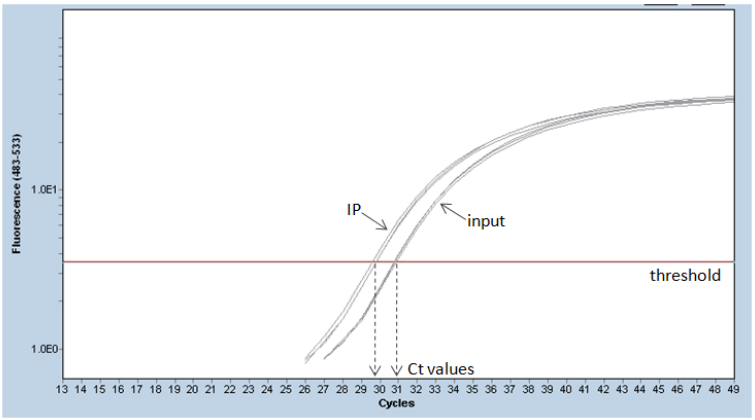

Figure 3.5 Determination of cycle threshold (Ct) values in real-time PCR. Log [fluorescent intensity] is plotted against number of cycles in the log amplification plot. **a**. A baseline (red line) is aimed to remove background noise which is shown in the initial PCR cycles with little change in fluorescent intensities. **b**. A cycle threshold (red line), which is always higher than the baseline, was set at the level where all examined samples are within the linear phase of the log amplification plot. The Ct value is the point where the amplification curve crosses the threshold. "IP" indicates the amplification curves of immunoprecipitated DNA and "input" represents that of DNA from starting chromatin. PCR reactions were performed in triplicate for each DNA sample and the Ct values averaged for the calculation of fold enrichment. Averaged Ct values of IP and input samples in this example were 29.73 and 30.86, respectively. PCR with DNA from input material and immunoprecipitation was always performed on the same PCR plate to maintain the consistency of $dCt = Ct_{input} - Ct_{IP}$.

The comparative Ct equation holds true if the amplification efficiencies of the both the experimental and control primer sets are maximal. Ideally, primer sets have an efficiency (E) equal to two as the amount of DNA doubles after every amplification cycle during the early logarithmic phase of the PCR reaction. However, this is not always possible due to the different annealing temperature of primers, different melting temperatures of substrates, and primer dimer formation, which lower the amplification efficiency. Primer efficiencies not only affect comparison between different primers in the same sample but also potentially affect the quantification of different samples with the same primers. With respect to the $2^{-\Delta\Delta Ct}$ method, when efficiencies of the two primers are not equal to 2, the calculated fold enrichment at a target site relative to a control site is only accurate if the two primers have similar efficiencies. Overestimation would occur if the efficiency of target primer is larger than that of control primer and underestimation would occur in the opposite situation (Table 3.1).

Situation	**Target primer**		**Control primer**		**Fold enrichment**
	E_t	ΔCt	E_c	ΔCt	
Ideal ($E_t = E_c$)	2	-6	2	-2	8
$E_t > E_c$	1.8	-6	1.5	-2	15.11
$E_t < E_c$	1.5	-6	1.8	-2	3.52

Table 3.1 Examples fold enrichment calculation with different primer efficiencies. "E_t" refers to the efficiency of target primer, "E_c" for efficiency of control primer while ΔCt is a Ct difference of ChIP DNA and input sample ($\Delta Ct = Ct_{input} - Ct_{ChIP}$).

The efficiency of each primer set used in this study was therefore determined for incorporation in comparative Ct calculations. Primer efficiency is determined from the observed Ct over a range of genomic DNA standards. The primer efficiency (E) is calculated from the slope of the standard curve, where $E = 10^{-1/slope}$ (Figure 3.6).

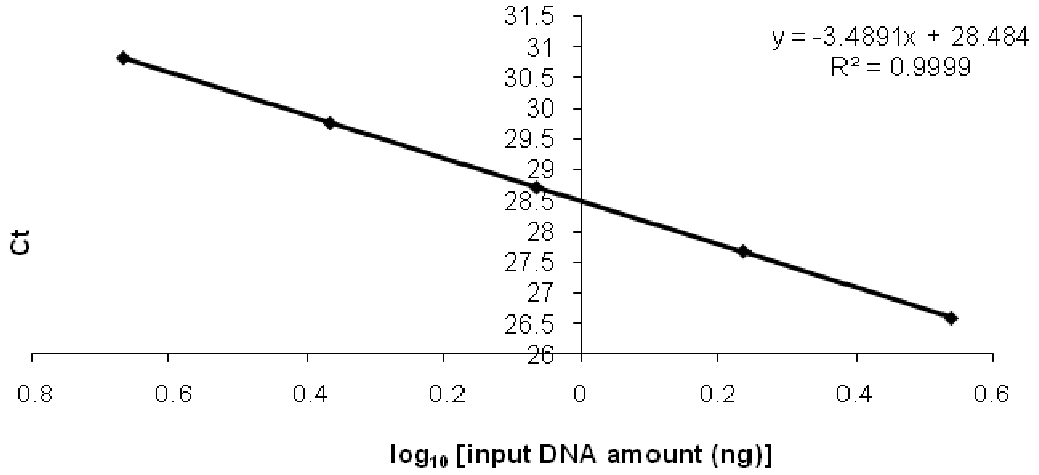

Figure 3.6 Determination of primer efficiency. An example of standard curve establishment for the HS4 insulator sequence primer set 21.726. Native di-/tri-nucleosomes from chicken 6C2 cells were prepared as previously described in Section 3.2.1.1. DNA was purified and diluted in a 2-fold serial dilution such that the amount of DNA template added to each quantitative PCR reaction ranged from 0.2 ng to 3.5 ng. Triplicates of PCR reactions were set up for each DNA template amount. The average Ct values are entered into a scatter plot and a linear trendline was added. The equation representing the line was used to determine the DNA amount of DNA from ChIP. The primer efficiency in this case was 1.93.

3.2.1.4 Native ChIP analysis of H3K4 methylation across the *FOLR1* and *β-globin* gene loci

Native ChIP has previously been used to map H3K4me2 across the *FOLR1* and *β-globin* gene loci in 6C2 cells [Litt *et al*, 2001a]. A pilot native ChIP assay with anti-H3K4me2 antibodies was completed to validate the native ChIP assay system. Enrichments were normalised to a site within the condensed chromatin region located between the *FOLR1* and *β-globin* gene loci at the *globin* locus as this site was adopted as a negative control site in previous studies [Litt *et al*, 2001a; West *et al*, 2004].

In agreement with the previous results, H3K4me2 was detected at the HS4 insulator and the *FOLR1* promoter (Figure 3.7), suggesting that the experimental conditions for the native ChIP assay are suitable for the quantitative analysis of histone modifications. As there is emerging evidence showing that H3K4me3 is a pivotal mark for regulation and binding of histone modifiers and chromatin modelling enzymes [Flanagan *et al*, 2005; Pray-Grant *et al*, 2005; Shi *et al*, 2006; Smith *et al*, 2004], H3K4me3 at the HS4 insulator is also of interest. Similar to

H3K4me2, H3K4me3 was also enriched at HS4 and the *FOLR1* promoter (Figure 3.7). It was not surprising that H3K4me3 was found at the transcriptionally active *FOLR1* promoter as this histone mark is commonly found at promoters especially those of active genes [Barski *et al*, 2007; Guether *et al*, 2007; Wang *et al*, 2007]. Given the colocalisation of H2BK120ub1, H3K4me2 and H3K4me3 at HS4, H2BK120ub1 might be a master regulator of these two states of H3K4 methylation.

a

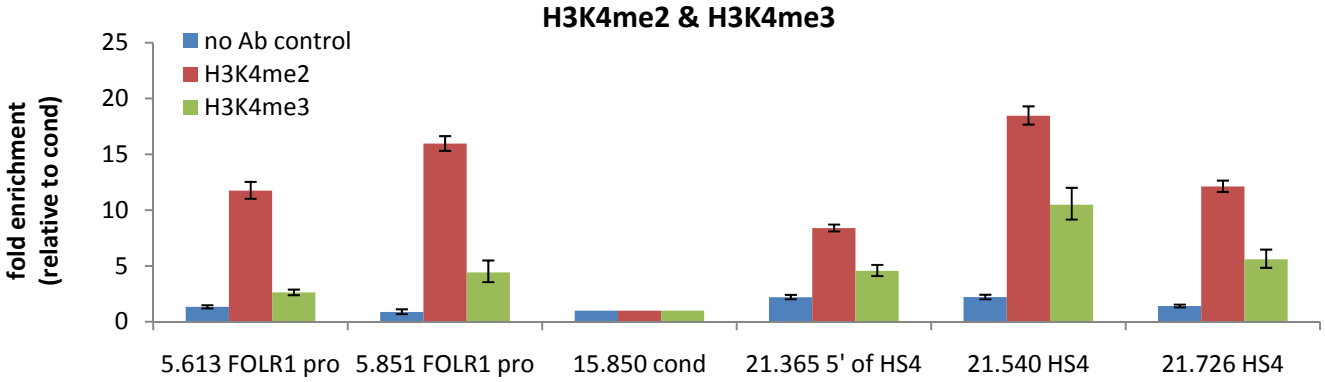

b

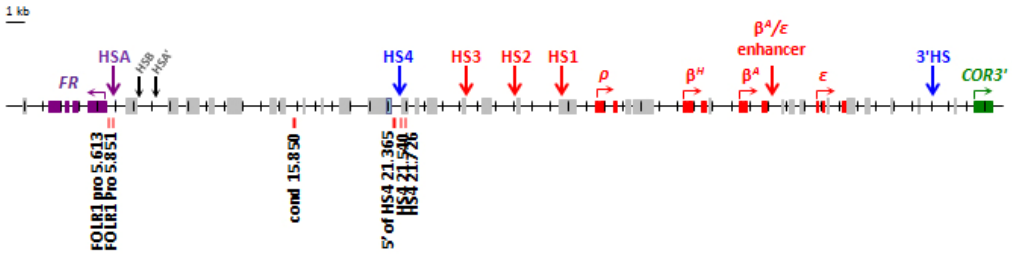

Figure 3.7 The *FOLR1* regulatory elements and the HS4 insulator are enriched in methylated H3K4. **a.** Cell chromatin from 6C2 cells was prepared in native condition by MNase digestion. Di- and tri-nucleosomes fractionated after sucrose gradient separation were pooled and desalted for immunoprecipitation. Enrichment of H3K4me2 and H3K4me3 was examined by quantitative PCR and normalised to the condensed chromatin region (15.850) as background. Student t-tests were applied to examine whether the enrichments of H3K4me2/3 are statistically significant when compared with no antibody control. All H3K4me2 and H3K4me3 enrichments are significant with p-values smaller than 0.001. **b**. Primer used for quantitative PCR.

3.2.1.5 The performance of native chromatin fractions prepared in low salt conditions

It has been reported that nucleosomes containing both the histone variants H2A.Z and H3.3 are unstable so they are easily disrupted by moderate salt concentration *in vitro* [Jin & Felsenfeld, 2007]. Such unstable nucleosomes are commonly found at gene regulatory elements such as promoters [Jin *et al*, 2009]. Although HS4 does not function as a promoter, it does share a very similar histone modification signature with promoters. Indeed, the HS4 nucleosomes have been shown to be enriched in H2A.Z [Bruce *et al*, 2005], it might not be surprising if H3.3 is also present according to the similarity of nucleosomes between the HS4 insulator and promoters. The conventional native ChIP method, includes a step where salt concentration is elevated to remove H1 and its binding proteins. It is possible that this step might destabilise the preparation of nucleosomes at elements such as the HS4 insulator in addition to promoters.

A "low salt" ChIP method was employed according to the reference protocol from Gary Felsenfeld's group [Jin & Felsenfeld, 2007]. This method is the same as the standard native ChIP assay except that the salt elevation step to remove H1 is omitted, and prepared nucleosomes are crosslinked with formaldehyde to fix any unstable nucleosomes (Figure 3.8c). The analysis of H3K4me2 in 6C2 chromatin was repeated using low salt native ChIP. Three concentrations of formaldehyde were tested (0.1%, 0.25% and 0.5%), aiming at avoiding epitope masking by the formaldehyde crosslinking. The crosslinked nucleosomes were passed through a desalting column to remove residual crosslinkers and glycine, the latter was used to stop the crosslinking reaction. It was found that 0.1% formaldehyde was sufficient to fix nucleosomes and gave the lowest background in the non-immune IgG control (Figure 3.8a). Notably, the low salt ChIP appeared to be more sensitive than the conventional "high salt" ChIP. The relative enrichment of H3K4me2 at HS4 detected with "high salt" ChIP was 12-fold (maximum ~20-fold routinely) while that with low-salt ChIP dramatically increased to 50-fold (Figure 3.8b). The optimised low salt ChIP procedures for the subsequent ChIP analyses summarised in Figure 3.8c were adopted for all histone modification studies in this thesis.

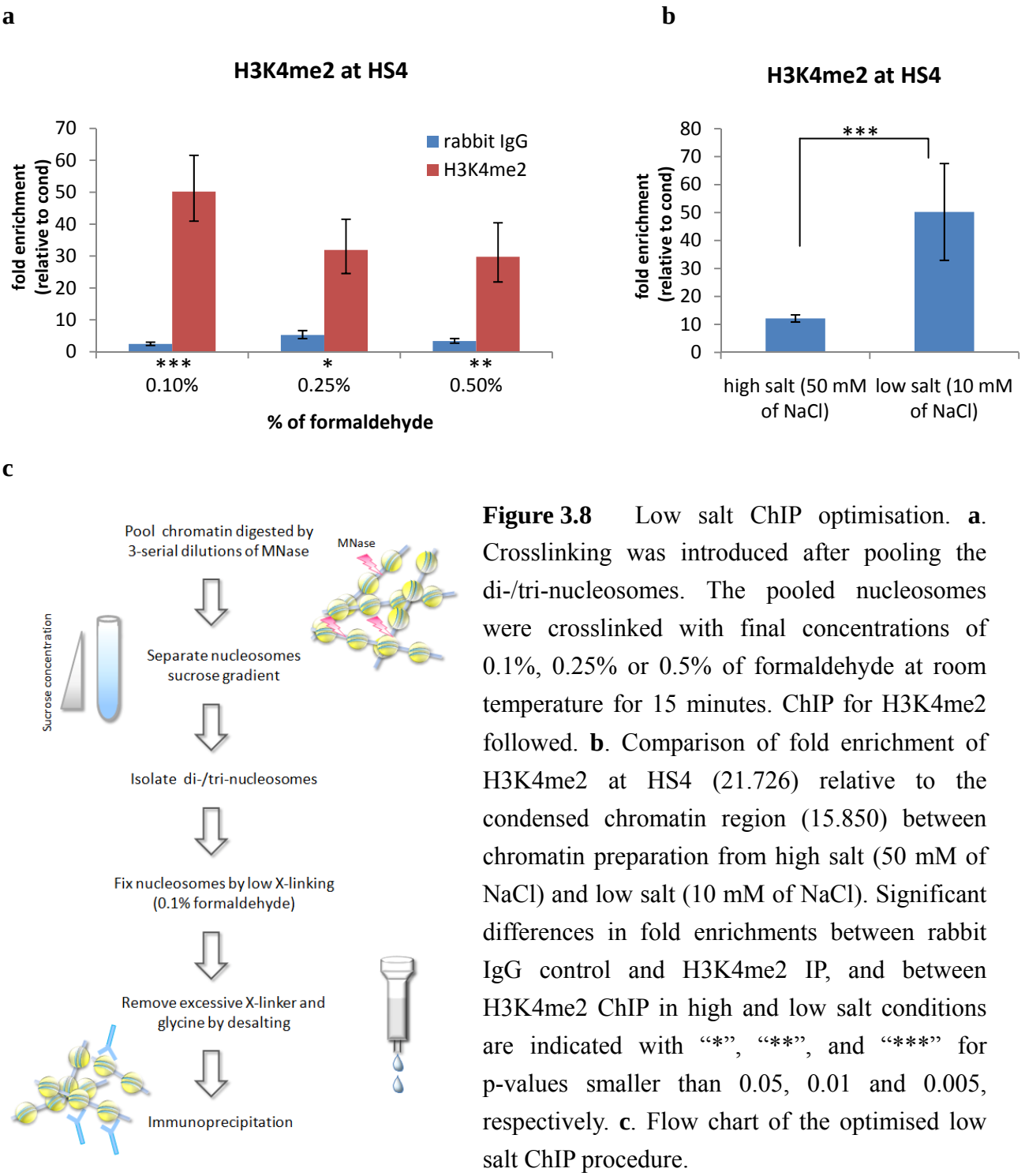

Figure 3.8 Low salt ChIP optimisation. **a**. Crosslinking was introduced after pooling the di-/tri-nucleosomes. The pooled nucleosomes were crosslinked with final concentrations of 0.1%, 0.25% or 0.5% of formaldehyde at room temperature for 15 minutes. ChIP for H3K4me2 followed. **b**. Comparison of fold enrichment of H3K4me2 at HS4 (21.726) relative to the condensed chromatin region (15.850) between chromatin preparation from high salt (50 mM of NaCl) and low salt (10 mM of NaCl). Significant differences in fold enrichments between rabbit IgG control and H3K4me2 IP, and between H3K4me2 ChIP in high and low salt conditions are indicated with "*", "**", and "***" for p-values smaller than 0.05, 0.01 and 0.005, respectively. **c**. Flow chart of the optimised low salt ChIP procedure.

3.2.2 ChIP analysis of histone ubiquitination across the *FOLR1* and *β-globin* gene loci

3.2.2.1 Analysis of histone ubiquitination and H2BK120ub1 immunoprecipitates from native chromatin

To ensure the antibody could recognise chicken ubiquitinated histones on native chromatin prior to ChIP assays, immunoprecipitation followed by western blotting analysis with H2B- and ubiquitin-specific antibodies were carried out. Results showed that the ubiquitin-specific antibody was able to pull down ubiquitinated H2B from native chromatin. The presence of ubiquitinated H2B in the immunoprecipitates was confirmed by H2B-specific antibody and the later developed H2BK120ub1-specific antibody with expected size ~25 kDa (Figure 3.9).

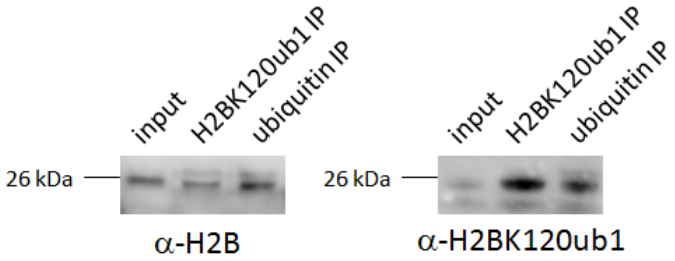

Figure 3.9 Immunoprecipitation with H2BK120ub1- and ubiquitin-specific antibodies on chicken chromatin. Native chromatin from chicken 6C2 cells was prepared with MNase digestion for immunoprecipitation with H2BK120ub1- and ubiquitin-specific antibodies. The presence of H2BK120ub1 in the immunoprecipitates was confirmed with western blotting analyses with H2B- (left panel) and the same H2BK120ub1-specific (right panel) antibodies. The expected size of monoubiquitinated H2B is ~25 kDa.

3.2.2.2 Chromatin boundaries at the *FOLR1* and *β-globin* gene loci are marked by histone ubiquitination

To determine whether the HS4 insulator and other regulatory elements at the *FOLR1* and *β-globin* gene loci are sites of histone ubiquitination, native ChIP of 6C2 cell chromatin was performed using anti-ubiquitin antibodies, which recognised full-length ubiquitin (Figure 3.10a) and ubiquitinated conjugates but not free form of ubiquitin (Figure 3.10b). It was found that the HS4 insulator was significantly enriched in histone ubiquitination using either antibody (p-value=1.6E-04 in Figure 3.10a & p-value=6.1E-07 in Figure 3.10b). Interestingly, the HSA and HSB regulatory elements located between the *FOLR1* gene and the condensed region are

also enriched in histone ubiquitination, but this is only observed using the anti-ubiquitinated conjugate antibody (Figure 3.10b), suggesting that the avoidance of epitope masking is not entirely guaranteed even with the native ChIP approach. HSA/HSB are located at the 5' boundary of the H3K9me2-enriched condensed region [Prioleau *et al*, 1999; Litt *et al*, 2001a]. The HSA/HSB elements may harbour chromatin boundary/insulator activity given their boundary location, their ability to drive position-independent expression of a transgene [Prioleau *et al*, 1999] and the similarity of their histone modifications with the HS4 element.

While the enrichment of histone ubiquitination observed at the HSA/HSB and HS4 chromatin boundary elements is consistent with the proposed role for H2B monoubiquitination, the ChIP enrichments may reflect the ubiquitination of other core histones [West & Bonner, 1980a; West & Bonner, 1980b]. H2BK120ub1-specific antibodies became available during this study [Minsky *et al*, 2008]. The antibody had been shown to be able to recognise human and yeast ubiquitinated H2B but had not been tested in chickens. Native chromatin from chicken 6C2 cells was prepared for immunoprecipitation followed by western blotting to examine if the antibody could recognise H2BK120ub1 in chickens. Results showed that the H2BK120ub1-specific antibody could detect H2BK120ub1 in both native form in immunoprecipitation and denatured form in western blotting as the ubiquitin-specific antibody did (Figure 3.9). The H2BK120ub1 profile across the *β-globin* and *FOLR1* loci was very similar to that of ubiquitinated conjugates. The HS4 insulator and HSA/HSB are also enriched in H2BK120ub1 (Figure 3.11). The result provides direct evidence to confirm the presence of monoubiquitinated H2B at the boundary elements at the *β-globin* and *FOLR1* foci. Moreover, significant enrichment of H2BK120ub1 was also detected at the *FOLR1* promoter and gene body, in agreement to the linkage between H2B ubiquitination and transcription activity [Shema *et al*, 2009; Xiao *et al*, 2005; Zhu *et al*, 2005].

a

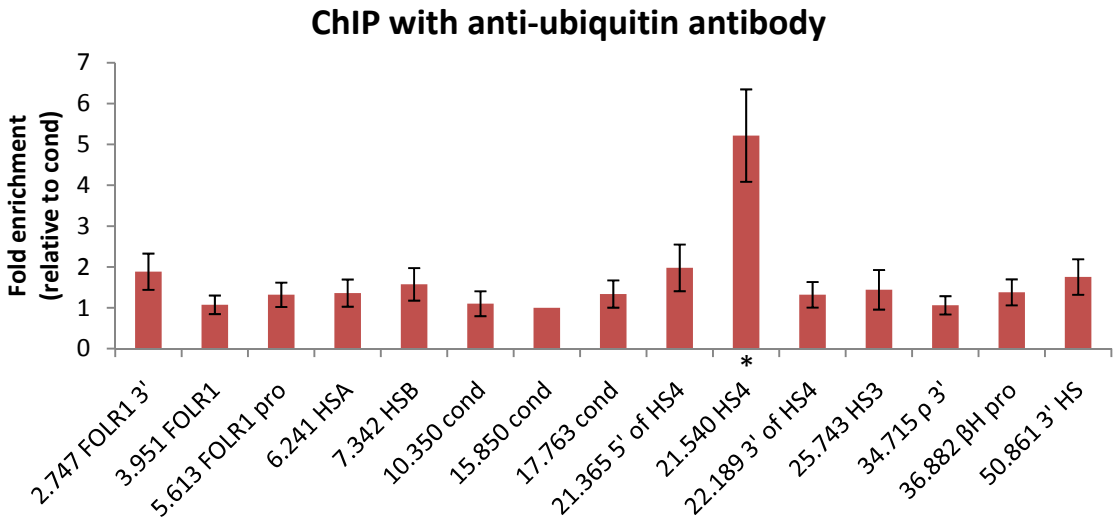

b

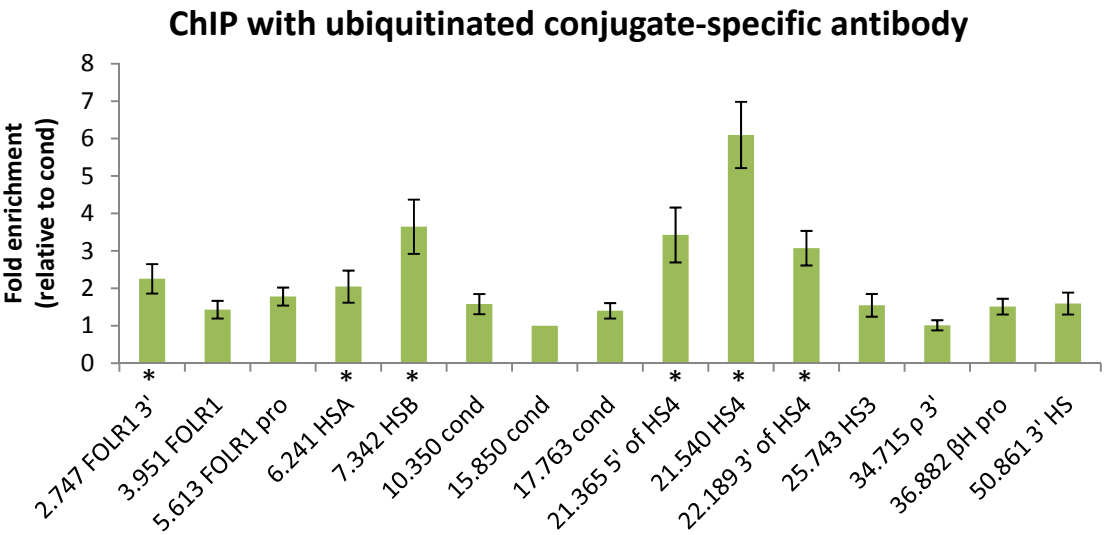

c

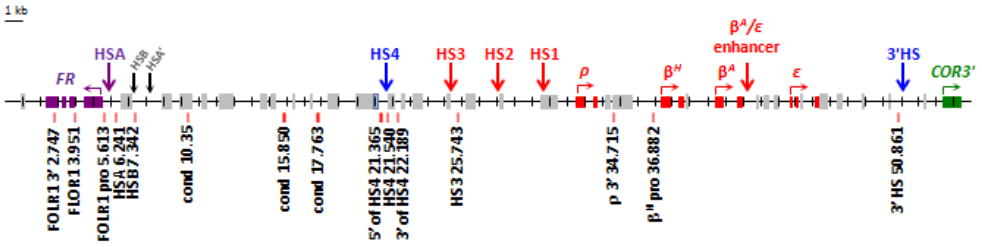

Figure 3.10 Profiles of ubiquitinated histones with different anti-ubiquitin antibodies across the chicken *β-globin* and *FOLR1* loci. Low-salt native ChIP was performed with ubiquitin- **(a)** and ubiquitinated-conjugates-specific **(b)** antibodies in chicken 6C2 cells. Fold enrichments of ubiquitinated histones at examined sited were relative to the condensed chromatin region (15.850) and their levels higher than two and p values smaller than 0.0001 are asterisked. **c**. Primers used for quantitative PCR.

a

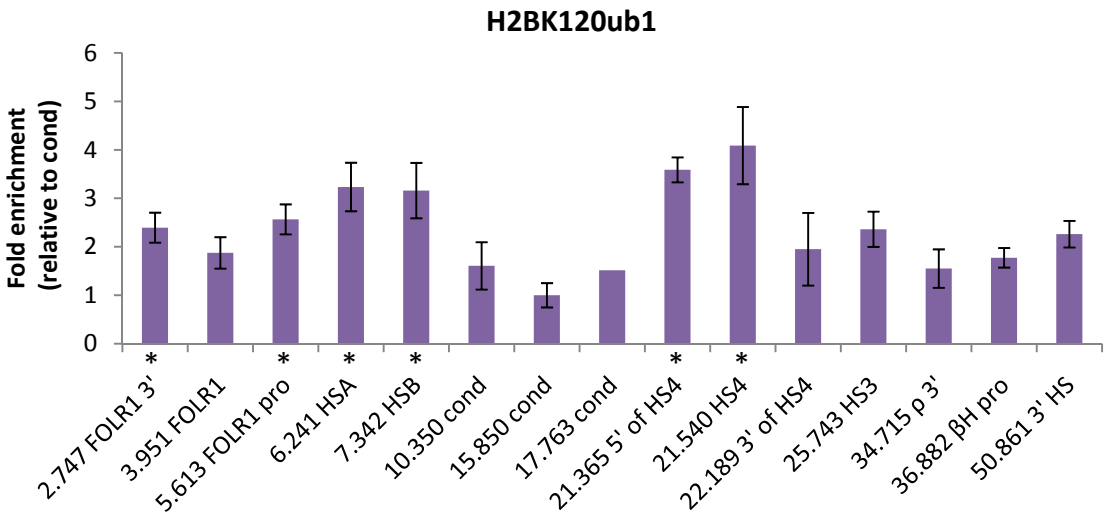

b

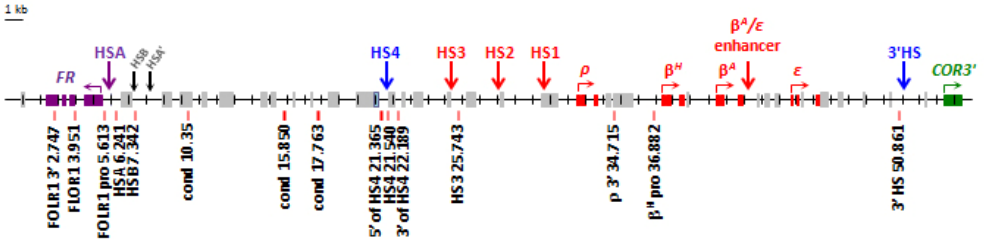

Figure 3.11 Profile of H2BK120ub1 across the chicken *β-globin* and *FOLR1* loci. **a.** Native ChIP with low salt preparation was performed in 6C2 cells with the H2BK120ub1-specific antibody. Fold enrichments of ubiquitinated histones at examined sited were relative to the condensed chromatin region (15.850) and their levels higher than two and p values smaller than 0.0001 are asterisked. **b**. Primers used for quantitative PCR.

3.3 Determining whether the candidate H2B-specific ubiquitination ligase RNF20 is recruited to chromatin boundary elements

The second objective of this chapter is to determine whether RNF20, whose paralogs are known to direct H2B ubiquitination in mammals (Section 1.2.3.2.1), is recruited to chromatin boundary elements in chicken cells. Crosslinking ChIP analysis was used to investigate whether this factor is recruited to the HSA/HSB and HS4 chromatin boundary elements. Crosslinking ChIP involves the fixation of cells with formaldehyde to preserve the interactions of *trans* factors on chromatin. Crosslinked chromatin fragments with sizes averaging ~500 bp are prepared following shearing by sonication. The chromatin fragments bound by the protein of interest are immunoprecipitated with a specific antibody to that protein. DNA from the immunoprecipitated complexes is then released by the reversal crosslinks and purified for quantitative PCR analysis (Figure 3.12).

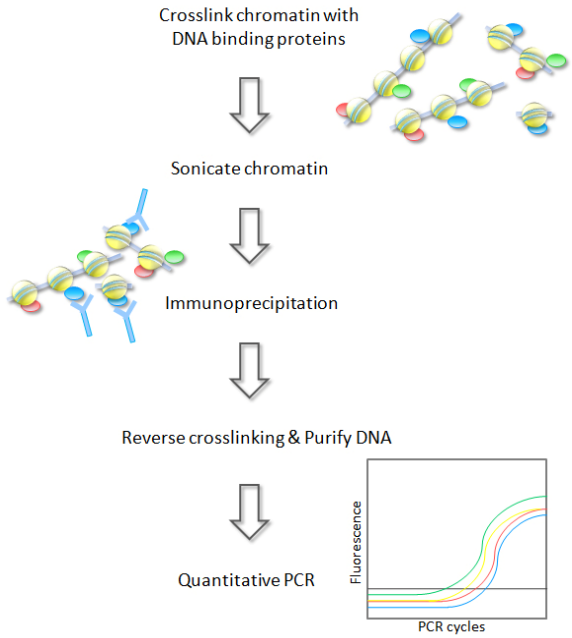

Figure 3.12 Schematic representation of the crosslinking ChIP procedure.

3.3.1 Identification of the sequence for chicken RNF20

The first assembly of the chicken genome was published in 2002 [Boardman *et al*, 2002], but the build remains incomplete and it lacks the annotation of other model organism genomes. There were no annotated genes for chicken RNF20 or RNF40 at the time of this study. To identify

whether RNF20 and RNF40 are present in the chicken genome, a protein BLAST search was carried out with the sequences of the human orthologs as baits and the chicken RNF20 homolog was found. The human and chicken RNF20 proteins share 89% identity in overall protein sequences and 100% identity in the catalytic RING domain (Figure 3.13). Although RNF40 is also essential for the H2B ubiquitination in mammals, no RNF40 homolog could be found by BLAST searching the chicken protein database. A BLAST search of human RNF40 against the BBSRC chicken EST (expressed sequence tag) database, revealed a putative chicken RNF40 homolog that is 85% identical and 92% of similar to human RNF40 (not shown).

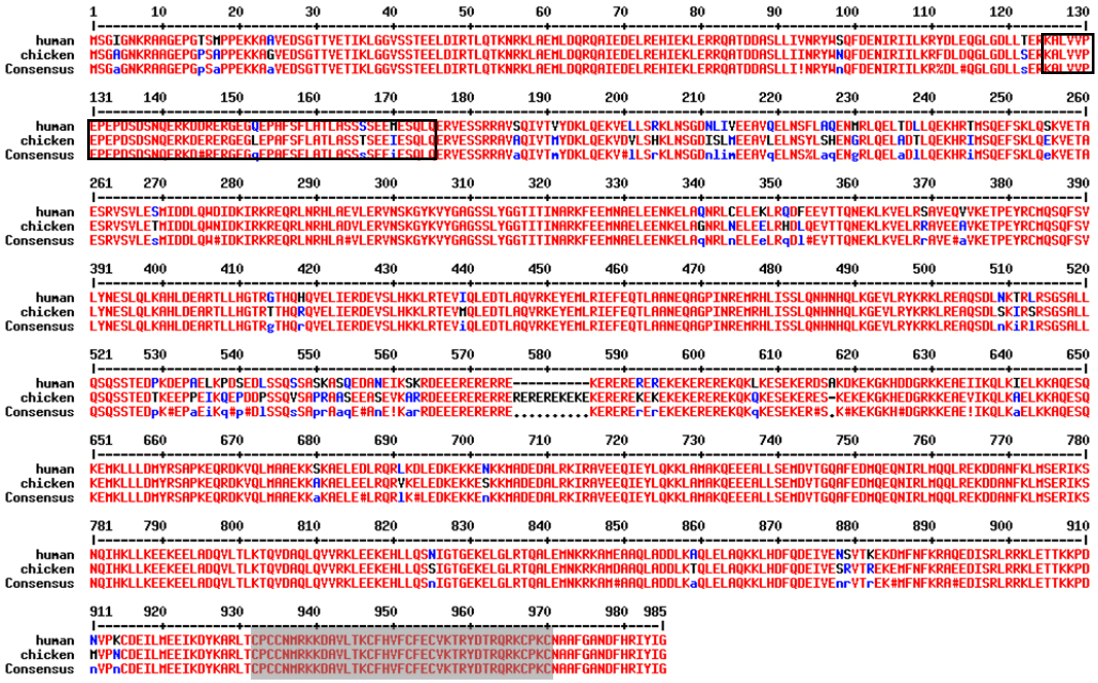

Figure 3.13 Alignment of human and chicken RNF20 protein sequences. Human protein sequence (NP_062538) was aligned with that of chicken (NP_001026605) using web software MultAlin (http://multalin.toulouse.inra.fr/multalin/) [Corpet, 1988]. High consensus amino acids (> 90%) between the two are shown in red, low consensus (< 50%) in blue and intermediate (50 – 90%) in black. Similar residues are indicated with the symbols "!" or "#". A missing corresponding amino acid is indicated by "." in the consensus sequence. The catalytic RING domain is shaded by a gray box. The epitope of the RNF20 antibody used in the study is boxed.

The next objective is to determine whether RNF20 is recruited to chromatin boundary elements by crosslinking ChIP analysis of 6C2 cell chromatin using commercially available antibodies. The available α-RNF20 antibody (Bethyl lab) has not been validated for use in chicken, so it is

important to analyse its specificity and its ability to immunoprecipitate native proteins from chicken cell extracts. The α-RNF20 antibody was raised against a human RNF20 peptide mapped to a region between residue 125 and 175 and has been shown to be specific to the human RNF20 protein [Wu *et al*, 2009]. This region shares 92% identity (47 out of 51 amino acids are identical) with the chicken RNF20 homolog, and chicken RNF20 is the only protein having this amino acid sequence in the chicken protein database (Figure 3.13). The predicted size (estimated by the Compute pI/Mw tool of expasy.org) of chicken RNF20 is 115 kDa. Western blotting analysis showed that the anti-RNF20 antibody predominantly recognised ~120 kDa polypeptide (Figure 3.14). There was also some much weaker recognition of ~60 kDa and ~80 kDa polypeptides. Only the ~120 kDa polypeptide was detected following immunoprecipitation, consistent with a specificity towards native chicken RNF20. Furthermore, only this ~120 kDa polypeptide was depleted following the knockdown of chicken RNF20 by RNA interference with two different short RNA sequences (data follows in Section 3.4.3). It is therefore reasonable to conclude that the commercially available anti-RNF20 antibody specifically recognises full length chicken RNF20 and can immunoprecipitate this protein from cell extracts. The validation that the ~120 kDa band is RNF20 by independent RNA interference experiments negates the need to further identify the ~120 kDa polypeptide by mass spectrometry. This antibody is therefore used in subsequent studies.

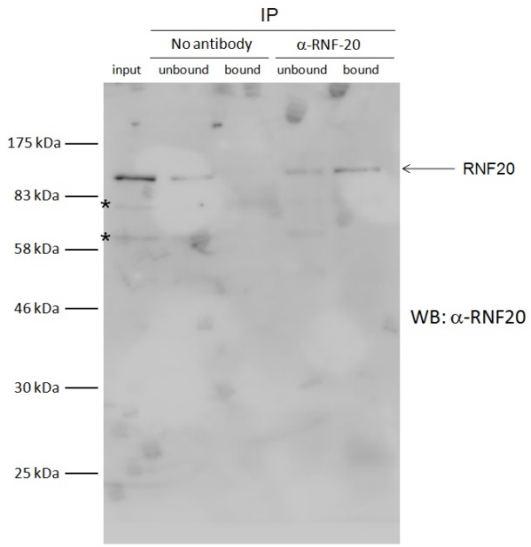

Figure 3.14 Immunoprecipitation of RNF20 from 6C2 nuclear extracts. Western blotting analysis of α-RNF20 recognition of peptides present in 6C2 nuclear extract (input) and immunoprecipitates (IP). The bound and unbound fractions from immunoprecipitations with no antibody or α-RNF20 are shown. The ~120kDa polypeptide that matches the predicted size of chicken RNF20 is indicated by an arrow. Non-specific detection is asterisked.

3.3.2 RNF20 is recruited to chromatin boundary elements

The α-RNF20 antibody described above was used in crosslinking ChIP assays to determine whether RNF20 interacts with chromatin boundary elements in 6C2 cells. The chromatin fragments following the sonication of crosslinked 6C2 cell chromatin were determined to average 400 bp in size (Figure 3.15). ChIP analysis showed statistically significant enrichment of both the *FOLR1* HSA the *β-globin* HS4 chromatin boundary element sequences in the RNF20 chromatin immunoprecipitates (Figure 3.16). This result is consistent with the earlier finding that these elements are also sites of H2B monoubiquitination (Section 3.2.2) and that mammalian RNF20 is only able to monoubiquitinate H2B and not other histones [Kim *et al*, 2005].

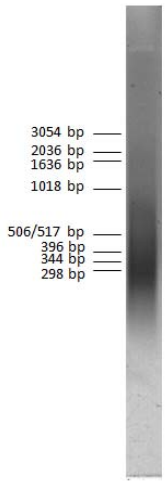

Figure 3.15 Agarose gel electrophoresis analysis of DNA fragments isolated from crosslinked 6C2 cell chromatin after sonication. Chicken 6C2 cells were crosslinked by 1% formaldehyde at room temperature for 20 minutes. Chromatin was sonicated in order to obtain ~ 300 – 500 bp fragments. The sizes of chromatin fragments were analysed by 1.25% TBE agarose gel.

a

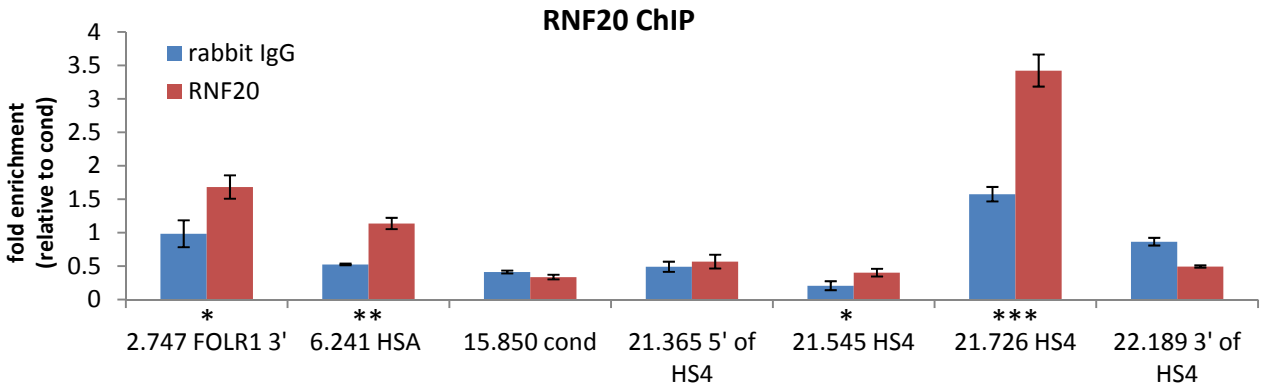

b

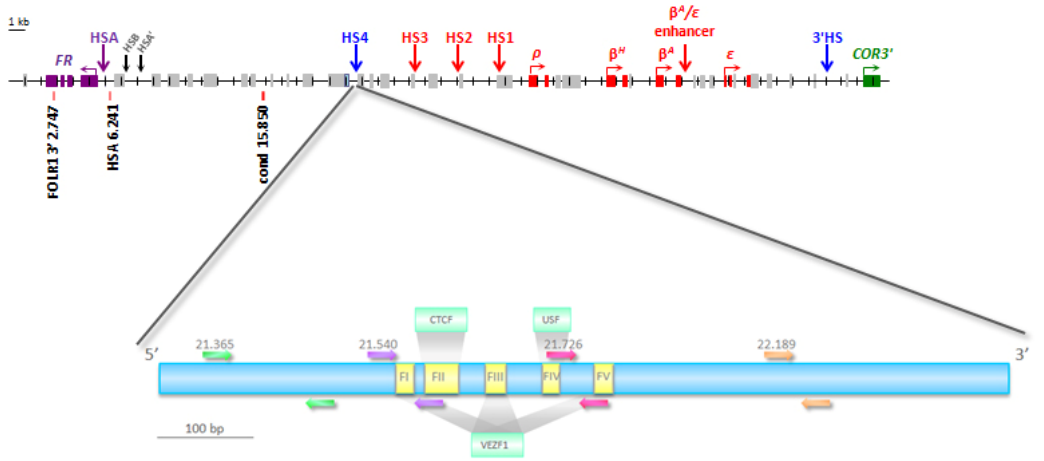

Figure 3.16 RNF20 interacts with chromatin boundary elements in 6C2 cells. **(a)** ChIP analysis with α-RNF20 antibodies. Quantitative PCR was performed with primers flanking the core HS4 and other regions of the chicken *β-globin* locus. Fold enrichments were obtained from $2^{-\Delta Ct}$, which is relative to input. P-values were employed to examine whether differences of fold enrichments between the ChIPs with α-RNF20 and non-immune rabbit IgG antibodies were statistically significant. Significant differences with p-values smaller than 0.05, 0.01 and 0.001 are indicated with one, two and three asterisks, respectively. **(b)** Schematic diagram of locations of quantitative PCR primers used. HS4 and the periphery regions are expanded to show details of the primers priming around HS4.

3.4 Establishment of clonal cell lines that permit long term knockdown of RNF20

3.4.1 Design of short hairpin RNA sequences that target chicken RNF20

It has been demonstrated that the HSA/HSB and HS4 chromatin boundary elements are sites of H2B ubiquitination and are bound by the candidate H2B ubiquitin ligase RNF20. In order to determine whether RNF20 is responsible for H2B monoubiquitination in chicken and to study the effects of depleting this mark on chromatin boundary integrity, RNF20 expression was knocked down by using RNA interference. It has been shown that while mammalian RNF20 and RNF40 function as a heterodimer to mediate H2B ubiquitination in mammals, they do not function redundantly as the depletion of RNF20 alone results in a dramatic reduction of H2BK120ub1 [Zhu *et al*, 2005].

To design effective short interfering RNA (siRNA) triggers for RNF20 knockdown, potential target sequences with 19 nucleotides matching chicken *RNF20* were designed using the RNAi central webtool (http://katahdin.cshl.org:9331/RNAi_web/scripts/main2.pl) and then filtered by several criteria known to improve shRNA efficiency [Mittal, 2004]. As only the antisense strand of the siRNA can direct the RNA-induced silencing complex (RISC) to cleave the sense target mRNA, the incorporation of the antisense strand into the RISC needs to be facilitated. It has been found that the 5' end of the antisense strand has less stable pairing with its complementary, i.e. A-U pairing, is incorporated in the RISC more efficiently. Therefore, potential sequences with A or U at the 5' end of the antisense strand and G or C at the 5' end of the sense strand are chosen. Following the incorporation of the antisense strand into the RISC and pairing to the target mRNA, RISC possessing endonuclease activity cleaves at the central site of the siRNA-mRNA pair. A less stable paring (A-U) at the central site promotes the cleavage so potential siRNA sequences with a U at position 10 were picked. Other criteria such as absence of internal repeats or palindromes and having 30 – 50% of GC content were also considered in order to yield a higher concentration of functional hairpins and to facilitate interaction with the RISC and unwinding. To avoid predictable off-target effects, potential chicken *RNF20* siRNA

sequences that fulfilled the above criteria were BLAST searched against the chicken genome (www.ensembl.org). Two RNF20-specific siRNA triggers were obtained (Figure 3.17).

R1380 5' – GACTCTTGCTGCCAATGAA – 3'

R2628 5' – CAGAGTAACTAGAGAGAAA – 3'

Figure 3.17 Potential siRNA sequences against chicken *RNF20*. The sequences correspond to the sense strands of the chicken *RNF20* mRNA sequences where U is substituted by T.

3.4.2 Design of the lentiviral shRNA expression vector system

The primary aim of the next chapter is to determine the role of H2B monoubiquitination in chromatin boundary integrity. It has previously been shown that the chromosomal silencing of transgenes in chicken 6C2 cells can be a gradual process where silencing occurs over 20-40 days of cell culture [Mutskov & Felsenfeld, 2004; Pikaart *et al*, 1998]. If the depletion of H2B monoubiquitination disrupts the function of the HSA/HSB or HS4 chromatin boundaries, it is unknown whether the heterochromatin could spread from the condensed region into the *FOLR1* or *β-globin* gene loci or at what speed. It is therefore desirable to employ an RNAi system that allows stable RNF20 knockdown for long culture periods. Ideally, the RNAi would also be inducible so we could resolve the initial effects of RNF20 knockdown from longer term adaptations and consequences.

In order to establish a stable and inducible knockdown system, the pSLIK lentiviral expression vector system was chosen [Hacke *et al*, 2009; Shin *et al*, 2006]. In this system, the RNF20 sequences are expressed as a short hairpin RNA (shRNA) that is incorporated into a natural micro RNA (miR) sequence for optimal incorporation into the cellular RNAi machinery. The miR-shRNA is located within the 3'UTR of a transgene encoding green fluorescent protein (GFP), which is under the control of a tetracycline response element (TRE) (Figure 3.18). A second transgene constitutively expresses a reverse tetracycline (Tet) transactivator (rtTA3) and a selection marker (the CD4 cell surface marker). The addition of the tetracycline analog

doxycycline (DOX) enables rtTA3 to switch on the expression of GFP and the linked RNF20 shRNA. The inducible expression of GFP can therefore be used as a marker for co-expression of RNF20 shRNA using a fluorescent microscope or flow cytometer.

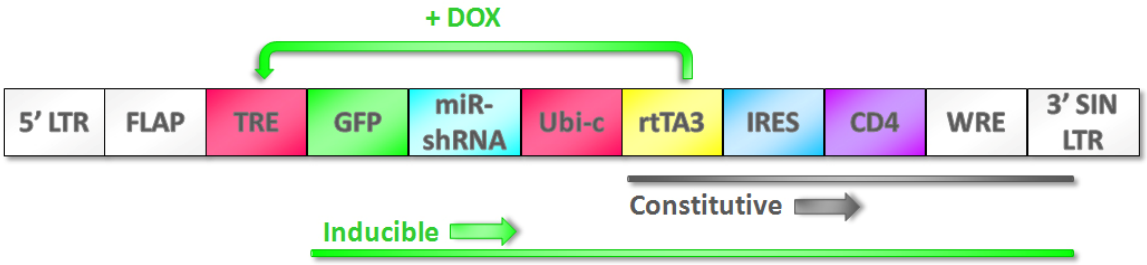

Figure 3.18 Schematic diagram of the recombinant pSLIK plasmid. miRNA expression accompanied with GFP was under the control of TRE that was activated by addition of DOX through inducing the expression of rtTA3. CD4 was supposed to be expressed constitutively. The figure is reproduced and modified from Shin *et al* (2006).

3.4.3 Establishment of clonal cell lines with inducible knockdown of RNF20

The preparation of the lentiviral vector that designed to mediate RNF20 knockdown was completed by Dr. Alan Hair (a colleague in Dr. West's group). The two RNF20 target sequences were firstly cloned into an entry vector containing the GFP transgene and linked miR sequence. The transgene was recombined into the pSLIK-CD4 destination vector (Figure 3.18) by Gateway cloning. Lentiviral particles were produced by co-transfection of the recombinant destination vector with third-generation lentivirus packaging (pMDLg/pRRE and pRSV-Rev) and pseudotyping (pCMV-VSV-G) vectors into the human 293T kidney cell line and collection of media supernatants [Dull *et al*, 1998]. Chicken 6C2 cells were then transduced with the pSLIK-RNF20 lentiviruses. The CD4 transgene was not expressed as expected for some unknown reason, so this could not be used to select for viral transduced cells. Clonal cell lines were generated by dilution. Lines which expressed GFP after DOX induction were selected for the analysis of RNF20 knockdown. 6C2 cell lines that are transduced with pSLIK lentiviruses that express shRNA targeting the *luciferase* gene were also generated for use as negative controls. However, these lines were discarded as the expression of this luciferase shRNA was

unexpectedly toxic to 6C2 cells, resulting in considerable cell death.

RNAi results in the degradation of mRNA that is homologous to siRNA. To examine whether the RNF20 mRNA levels decreased following DOX induced expression of RNF20-shRNA, RT-PCR was performed after 4-days of DOX administration (1 μg/ml). The expression of RNF20 in non-transduced wild type 6C2 cells was unaffected by DOX administration (wild type in Figure 3.19). However, RNF20 mRNA levels were reduced by up to 70% upon DOX administration in cell lines transduced with lentiviruses expressing the R2628 target sequence (Figure 3.19).

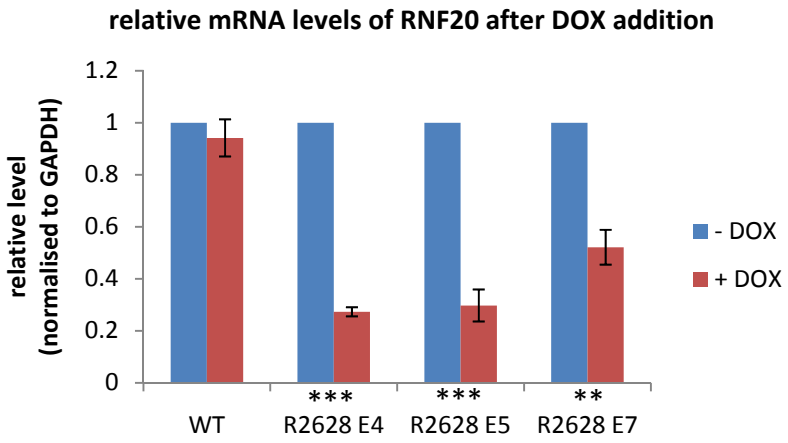

Figure 3.19 mRNA levels of RNF20 following DOX induced RNF20 knockdown for four days. RNA was extracted after DOX addition at the final concentration 1 μg/ml for four days for RT-PCR. The expression of RNF20 of DOX treated cell lines was compared with their respective no DOX controls. GAPDH served as a normaliser. P-values calculated from PCR triplicates with two-tailed student t-test assuming equal variance were introduced to test if differences of RNF20 mRNA levels between no DOX controls and induced knockdown cells were statistically significant. P-values that are smaller than 0.01 and 0.001 are indicated with two and three asterisks, respectively.

RNAi can also inhibit the translation of target mRNAs, resulting in further knockdown of target protein levels. Conversely, proteins with a long half life may reside for some time following mRNA degradation by RNAi. The levels of RNF20 protein in the nuclear extracts of 51 6C2 cell clones that inducibly express GFP were analysed before and after 4 days of DOX administration. Following the optimisation of western blotting, only one predominant band of the predicted size

of full length RNF20 was observed in these assays. This band decreased in intensity relative to a loading control upon RNF20 knockdown in pSLIK-RNF20 cell lines that have reduced RNF20 mRNA levels following DOX administration (e.g. Figure 3.20).

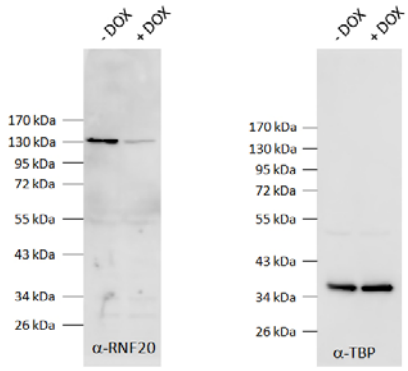

Figure 3.20 An example showing full blots of western images for RNF20 detection following the DOX induced RNF20 knockdown. TBP was a loading control. The two images were from the same blot that TBP was detected after stripping away the RNF20 antibodies.

In agreement with the RT-PCR analysis described above, the levels of RNF20 protein remain unchanged by DOX administration in non-transduced wild type 6C2 cells (Figure 3.21, top left). Out of the 51 lines, eight display substantial decreases in RNF20 protein levels following DOX administration. Seven of them were resulted from the target sequence R2628 while only one was from R1380 (Figure 3.21). The lentiviral system is prone to leaky expression, perhaps due to the preference for viral integration into open chromatin, which is typically transcriptionally active [Kafri *et al*, 2000]. Close inspection of RNF20 protein levels in the extracts of pSLIK-RNF20 cell lines in the absence of DOX relative to those of wild type 6C2 cells, indicates that some of the lines, R2628 G6 and R1380 H4 for instance, have leaky RNF20 shRNA expression (Figure 3.22).

R2628 E4, E5 and E7 are clones showing significant RNF20 knockdown with corresponding decrease in H2BK120ub1 (Figure 3.23), they are potentially for use in studying effects of H2BK120ub1 depletion. As the RNF20 protein level in R2628 D5 was not substantially following DOX induction, it was not included for further studies. FACS analysis found that R2628 E7 comprised of mixed populations of cells with different expression levels of RNF20-specific miRNA upon DOX induction, indicated by a wide range of GFP expression

level. The various knockdown levels would mask the real results in further investigations. Therefore, only R2628 E4 and E5 were chosen for subsequent analyses.

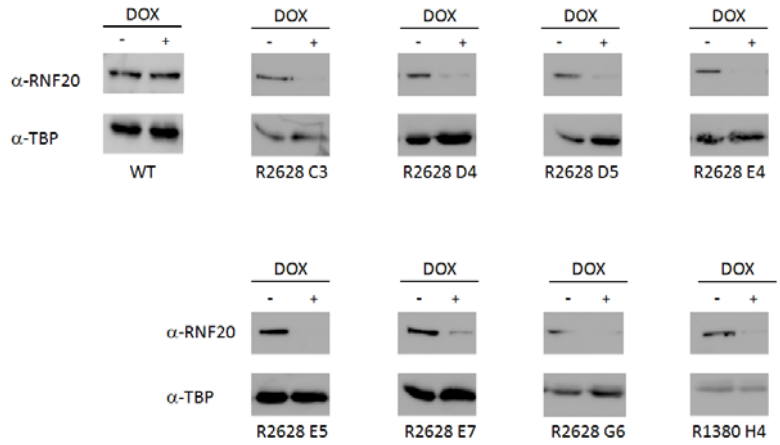

Figure 3.21 Western blotting analyses of RNF20 levels after DOX induction. Nuclear extracts from 51 potential clones were collected after addition of DOX (1 μg/ml) for four days. Cells growing alongside without DOX were served as controls to represent the basal *RNF20* expression levels. The eight clones demonstrating dramatic decreases in RNF20 are shown here. TBP was a loading control.

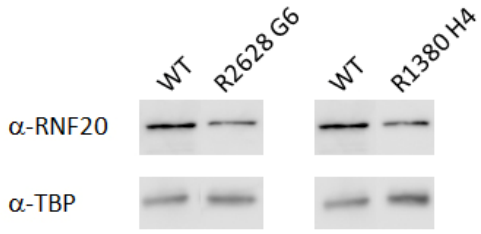

Figure 3.22 Examples of leaky RNF20 knockdown. Nuclear extracts were prepared from wild type and knockdown lines that were grown in DOX free medium to examine their basal levels of RNF20. Two examples of leaky lines R2628 G6 and R1380 H4 are shown.

3.4.4 H2B ubiquitination is RNF20 dependent in chicken

If RNF20 is a *bona fide* H2B-specific ubiquitination ligase in chicken, the knockdown of RNF20 should result in the decrease of H2BK120ub1. Native chromatin was prepared for global histone modification analysis using MNase digestion as described in the native ChIP method, but without size selection on sucrose density gradients. The levels of H2BK120ub1 in total chromatin from the 6C2 cell lines that displayed significant RNF20 knockdown were analysed. The pSLIK-RNF20 cell lines R2628 D5, E4, E5 and E7 displayed reliable RNF20 knockdown following DOX administration. It was found that H2BK120ub1 levels in total chromatin decreased upon RNF20 knockdown in these four independent cell lines (Figure 3.23). The level

of H2BK120ub1 did not alter in non-transduced wild type 6C2 cells upon DOX administration. These findings are consistent with RNF20 acting as an H2B-specific ubiquitin ligase like its mammalian counterparts.

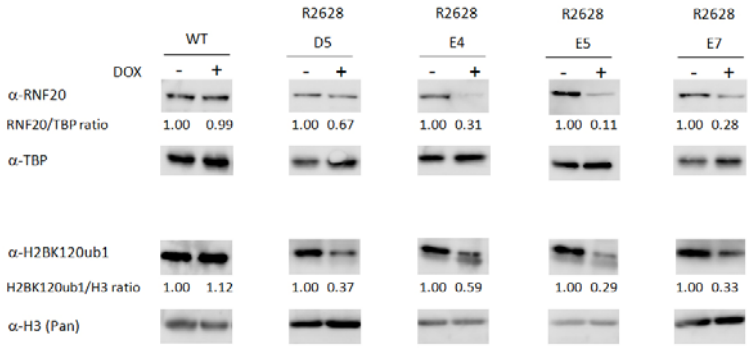

Figure 3.23 H2BK120ub1 levels decrease following RNF20 knockdown. Cells grown in the presence or absence of DOX for four days were harvested; chromatin and nuclear extracts were prepared for H2BK120ub1 and RNF20 detection, respectively. Chromatin and nuclear extract loading was monitored by H3 (Pan) and TBP respectively. The RNF20/TBP and H2BK120ub1/H3 ratios were calculated from band intensities measured with ImageJ and relative to their respective no DOX controls.

3.5 Discussion

The studies presented in this chapter addressed three objectives. Firstly, it was shown that the HSA/HSB and HS4 elements that flank a region of condensed heterochromatin are sites of H2B monoubiquitination. Secondly, it was found that the chicken paralog of mammalian RNF20/BRE1A is recruited to both of these elements. Thirdly, it was established that chicken RNF20 is required for H2B monoubiquitination. These findings are consistent with a role for RNF20-dependent H2B monoubiquitination at chromatin boundary elements. This hypothesis can be investigated in the next chapter following the establishment of the native ChIP assays and inducible RNF20 knockdown cell lines.

Chromatin boundaries are marked by H2B ubiquitination

Our starting hypothesis was that H2B ubiquitination may be required for H3K4 tri-methylation at the HS4 insulator element. The studies in this chapter have demonstrated that the HS4 insulator is marked by both H3K4me3 and H2BK120ub1. A chicken paralog of the yeast Bre1 and mammalian RNF20/BRE1A ubiquitin ligases was identified and found to interact with the HS4 element. These findings are consistent with the original hypothesis. RNAi inference was used to confirm that RNF20 is required for H2BK120ub1 in chicken. The development of inducible RNF20 knockdown cell lines will allow detailed analysis of the function of this modification at the HS4 chromatin boundary.

Unexpectedly, these studies revealed that the HSA and HSB regulatory elements of the *FOLR1* gene locus are also marked by H2BK120ub1. RNF20 has been also found to bind to bind to HSA, suggesting H2B ubiquitination at HSA may also be directed by RNF20. The HSA/HSB elements are not yet fully characterised, but are known to lie at the 5' boundary of the condensed heterochromatin domain that separates the *FOLR1* and *β-globin* gene loci. These elements may harbour chromatin barrier properties much like the HS4 insulator located at the 3' boundary of the same heterochromatin domain.

CHAPTER 4

Investigation of the interplay between H2B ubiquitination and other histone modifications at chromatin boundaries

4.1 Objectives

In the last chapter, it was determined that the boundaries of a heterochromatin domain between the *FOLR1* and *β-globin* gene loci are sites of H2B ubiquitination. Given the previous demonstrations that the bulk of H3K4 methylation requires prior H2B ubiquitination in yeast and mammals (Section 1.2.5), and that H3K4 methylation is required for the barrier activity of the HS4 insulator element [West *et al*, 2004], this chapter will describe the study of the role of H2B ubiquitination at chromatin boundary elements.

The HSA/HSB and HS4 chromatin boundaries are marked by several active histone modifications in addition to H3K4me (Section 1.5.1). This active chromatin signature includes the acetylation of H3 and H4, and the incorporation of H2A.Z, each of which have been linked to chromatin barrier activity in budding yeast (Sections 1.1.3.2 & 1.4.3.4). There is accumulating evidence that H3K4 methylation, H3K4me3 in particular, acts as a pivotal mark for active chromatin signature establishment by recruiting histone modifiers and chromatin remodelling enzymes (Sections 1.2.1.1 & 1.2.5). These observations lead to the hypothesis that H2B ubiquitination may be involved in the establishment of the active chromatin states of chromatin boundary elements by facilitating H3K4 methylation and subsequent chromatin modification and remodelling events. This hypothesis will be addressed in the following objectives.

Objective 1. Determine whether the *trans*-histone crosstalk pathway between H2B ubiquitination and H3K4 methylation is conserved in chicken

Analysis of histone modifications in total chromatin following RNF20 knockdown

Objective 2. Determine whether H2B ubiquitination is required for the active chromatin state at chromatin boundary elements

a) Native ChIP analysis of the following active histone marks across the *FOLR1* and *β-globin* loci before and after four days of RNF20 knockdown
    i. ubiquitinated histones and H2BK120ub1
    ii. H3K4 methylation
    iii. H3 and H4 acetylation
    iv. H2A.Z deposition and acetylation
b) Crosslinking ChIP analysis of insulator protein binding at chromatin boundaries following RNF20 knockdown

Objective 3. Determine whether H2B ubiquitination is required for chromatin boundary integrity

a) Native ChIP analysis of the following heterochromatin-associated histone marks across the *FOLR1* and *β-globin* loci before and after four days of RNF20 knockdown
    i. H3K9 di- and tri-methylation
    ii. H3K27me3
    iii. H4K20me3
b) Analysis of histone modifications in total chromatin following prolonged RNF20 knockdown
c) Native ChIP analysis of the following histone marks across the *FOLR1* and *β-globin* loci before and after prolonged RNF20 knockdown
    i. H3K4 di- and tri-methylation
    ii. H3K9me3
    iii. H4K20me3
d) Analysis of *FOLR1* gene expression following prolonged RNF20 knockdown

Objective 4. Determine whether H2B ubiquitination is required for the barrier activity of the HS4 insulator

Stable transgene assay for the barrier activity of HS4 in wild type and RNF20 knockdown cells

Objective 5. Investigate whether the presence of H2BK120ub1 is universal to chromatin boundary elements

Native ChIP analysis of H2BK120ub1 at human putative chromatin boundary elements

4.2 The *trans*-histone crosstalk pathway between H2B ubiquitination and H3K4 methylation is conserved in chicken

The first objective of this chapter is to determine whether the *trans*-histone crosstalk pathway between H2B ubiquitination and H3K4 methylation is conserved in chicken. To achieve this objective, western blotting analyses were performed on total chromatin collected from RNF20 knockdown cells. Histone modifications were profiled after four days of doxycycline-induced knockdown in the R2628 E5 and E4 cell lines, where RNF20 levels are reduced by 81% and 77%, respectively (Figure 4.1). The global levels of H2BK120ub1 were depleted by 74 and 58% in these lines, but H2AK119ub1 levels were unaffected. Chicken RNF20, like its yeast and mammalian RNF20/BRE1 orthologs, is specifically mediates the ubiquitination of histone H2B. It was notable that the depletion of H2BK120ub1 is greater in the E5 line compared with E4. This may reflect a greater level of knockdown in the E5 line than the Western analysis indicates or an increased susceptibility to RNF20 depletion in the E5 line.

The total levels of H3K4me3 in bulk chromatin were depleted by 71% and 41% in the E5 and E4 lines, respectively (Figure 4.1). This close correlation between H2BK120ub1 and H3K4me3 levels is consistent with a direct crosstalk between these modifications in chicken, as reported in other species [Briggs *et al*, 2002; Kim *et al*, 2005]. The levels of H3K79me2 also closely correlated with H2BK120ub1, with depletions of 33% and 22% in the E5 and E4 lines, respectively (Figure 4.1). However, the levels of H3K4me2 do not exhibit a linear correlation with H2B ubiquitination as H3K4me3 does. H3K4me2 levels were only depleted in the E5 line, which had the greatest depletion of H2BK120ub1 (Figure 4.1b). This suggests that H3K3me2 levels may be indirectly linked to prior H2BK120ub1 *via* a mechanism that is distinct from that which mediates crosstalk to H3K4me3 [Vitaliano-Prunier *et al*, 2008; Wu *et al*, 2008]. Other active or repressive histone modifications did not show any substantial changes in either RNF20 knockdown lines (Figure 4.1).

a

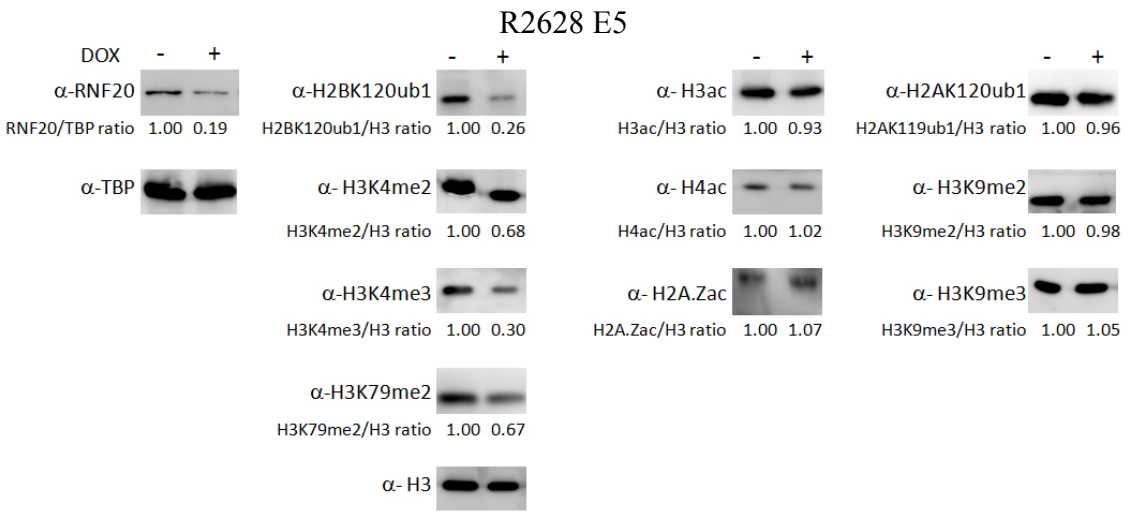

b

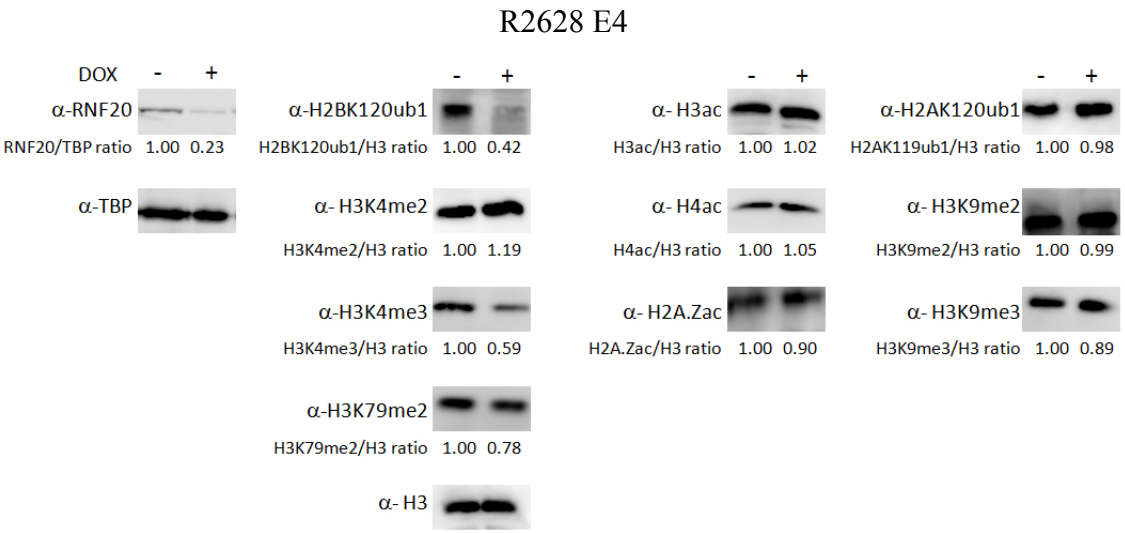

Figure 4.1 Western blotting analyses of histone modifications of R2628 E5 (**a**) and R2628 E4 (**b**) after four-day induction of RNF20-specific miRNA expression. RNF20 knockdown was induced by addition of DOX (+) for 4 days and then chromatin was extracted with MNase digestion for western blotting analyses. The same knockdown lines were also grown in DOX free condition to serve as controls (-). TBP and histone H3 (Pan) served as a loading controls for nuclear extract and total chromatin, respectively. Band intensities were measured and normalised to the loading controls with the RNF20/TBP and histone modification/H3 ratios set to one in no DOX controls.

4.3 Determine whether H2B ubiquitination is required for the active chromatin state at chromatin boundary elements

The second objective of this thesis is to determine whether the active chromatin state of chromatin boundary elements is established by H2B ubiquitination. Native ChIP was performed to study changes of active histone modifications, ubiquitinated histones, H3K4 methylation, H3 and H4 acetylation as well as H2A.Z deposition and acetylation, altogether indicating the active chromatin state, in knockdown lines R2628 E5 and R2628 E4 following short time course of RNF20 knockdown. Cells were induced to knock down RNF20 by DOX treatment (+DOX) for four days and the same lines grown in DOX free medium (-DOX) served as control to examine immediate effects of RNF20 depletion on the chromatin state of the chromatin boundaries at the chicken *β-globin* locus. Most ChIP experiments were performed with the same batch of cells for which global histone modifications were examined in Section 4.2. For repeated ChIP assays or those performed on other batches of chromatin, decreased levels of RNF20 and H2BK120ub1 of the cells were confirmed with western blotting following DOX induction to ensure significant and reproducible knockdown resulted.

The relative enrichments of genomic sequences following ChIP for each histone modification were normalised to the *ρ-globin 3'* (34.715) sequence using the ΔΔCt method described in Section 3.2.1.3. Normalisation was used to allow comparison between the different lines and immunoprecipitations. This region lacks any significant enrichment or depletion of the histone modifications studied here in 6C2 cells [Litt *et al*, 2001a; Litt *et al*, 2001b]. The choice of this region as a negative control minimises the chance that RNF20 knockdown may affect the normalisation. Student's t-tests were applied to all of the ChIP data to determine whether any changes in ChIP enrichments between control and knockdown cells were statistically significant.

4.3.1 RNF20 knockdown leads to a loss of ubiquitinated histones at chromatin boundaries

To determine whether the histone ubiquitination detected at the HSA/HSB and HS4 chromatin boundary elements is mediated by RNF20, native ChIP with anti-ubiquitin antibodies was performed after RNF20 knockdown. The histone ubiquitination at the HS4 element returned to background levels in both the E5 and E4 lines upon RNF20 knockdown (Figure 4.2). The histone ubiquitination at the HSA and HSB elements was also abolished upon RNF20 knockdown in the E5 cell line (Figure 4.2a). These findings are consistent with RNF20-mediated H2B ubiquitination at the HSA/HSB and HS4 chromatin boundary elements. However, the histone ubiquitination at the HSA was only reduced by ~30% and the modification of the HSB was unaffected following RNF20 knockdown in the E4 cell line (Figure 4.2b). Furthermore, histone ubiquitination at the *FOLR1* gene was observed to be entirely RNF20-dependent in the E5 line, but there is only a partial reduction in the E4 cell line. The differences between the two cell lines correlates with the more considerable depletion of H2BK120ub1 observed in the E5 line (section 4.2). It is possible that RNF20 binding to the HSA/HSB elements is more resistant to partial knockdown than the HS4 element. Crosslinking ChIP assays would be needed to confirm this explanation.

The availability of anti-H2BK120ub1 antibodies allowed the confirmation of whether the RNF20-dependent histone ubiquitination at the chromatin boundaries was H2BK120ub1. Depletions of H2BK120ub1 to close to background levels were observed at the HSA, HSB and HS4 elements (Figure 4.3).

a

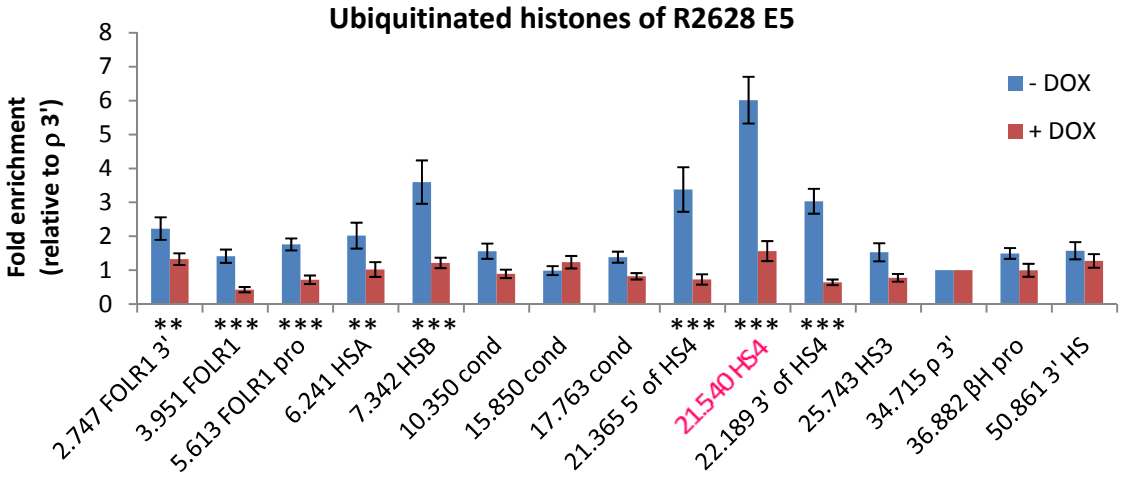

b

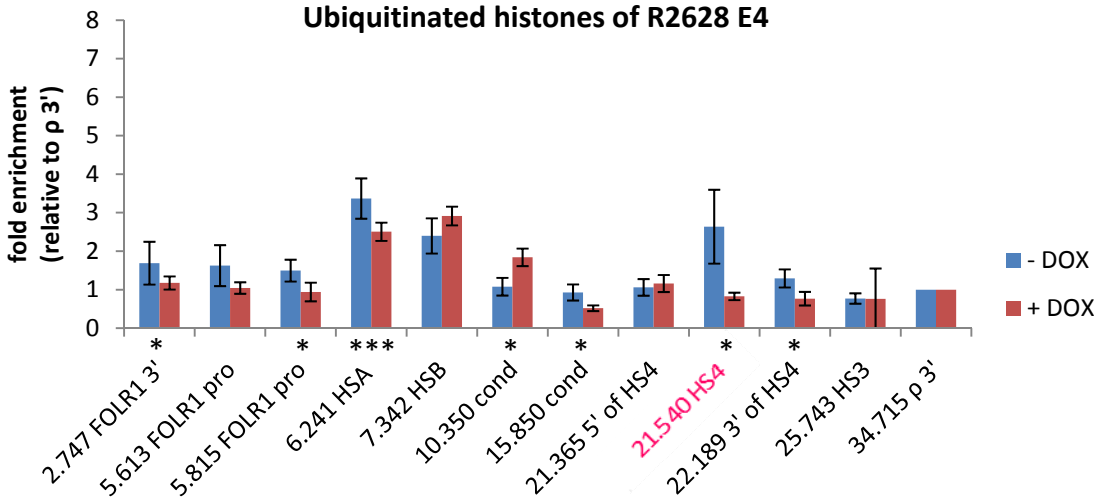

c

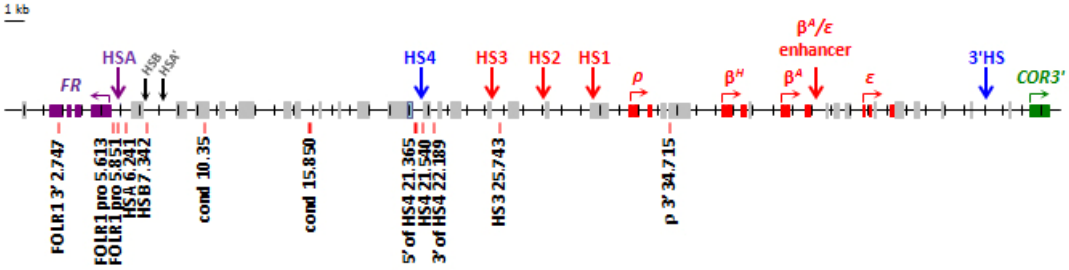

Figure 4.2 Native ChIP analyses of ubiquitinated histones across the chicken *β-globin* locus upon RNF20 knockdown. R2628 E5 **(a)** or R2628 E4 **(b)** cells were grown in the presence (+) or absence (-) of DOX for four days. Quantitative PCR was performed with primer sets indicated **(c)**. *ρ-globin* 3' (34.715) was set as a normalisation region. Significant changes following RNF20 knockdown with p-values smaller than 0.05, 0.01 and 0.005 are indicated with "*", "**" and "***", respectively.

a

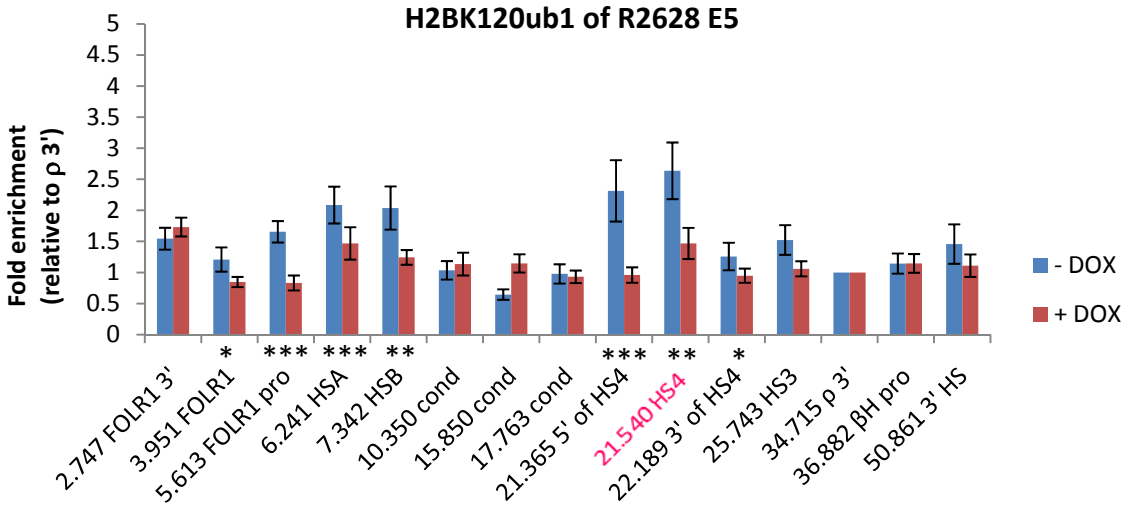

b

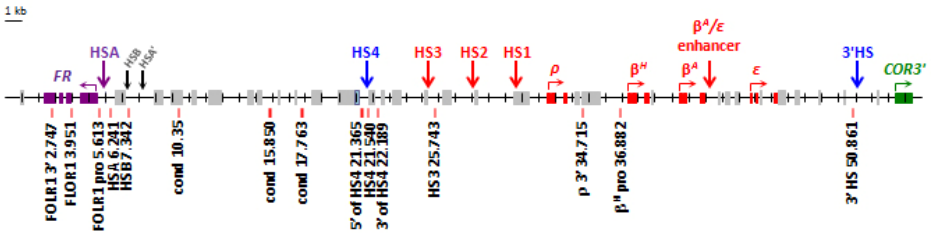

Figure 4.3 Native ChIP analysis of H2BK120ub1 in R2628 E5 after knocking down RNF20 for four days. Fold enrichments of H2BK120ub1 at examined sites were relative to *ρ-globin* 3' (34.715). Primer used for quantitative PCR is shown in **(b)**. Significant changes of the H2BK120ub1 levels following RNF20 knockdown are indicated with "*", "**" and "***" for p-values smaller than 0.05, 0.01 and 0.005, respectively.

4.3.2 H3K4 methylation at chromatin boundaries require prior H2B ubiquitination

The findings that the HSA/HSB and HS4 elements are sites of RNF20-dependent H2B ubiquitination and that this modification is required for global H3K4 methylation lead to a hypothesis that chromatin boundaries employ the H2B ubiquitination pathway to establish their active chromatin states. It is anticipated that the di-and tri-methylation of H3K4 at the chromatin boundaries would be diminished following the depletion of H2BK120ub1. Native ChIP was carried out in both the R2628 E5 and E4 cell clones to investigate changes of H3K4 methylation across the *FOLR1* and *β-globin* loci after just four days of induced RNF20 knockdown.

Substantial reductions in H3K4 tri-methylation at the chromatin boundaries was observed following RNF20 knockdown. H3K4me3 was depleted by ~70% and ~60% at the HS4 and HSB elements in the E5 cell line (Figure 4.4b, p-values of 0.0033 and 0.0017, respectively). H3K4me3 at the chromatin boundaries was also depleted following knockdown in the E4 cell line, albeit to a lesser degree (Figure 4.4d). These findings are consistent with *trans*-histone crosstalk, where the tri-methylation of H3K4 requires prior H2B ubiquitination. Statistically significant reductions in H3K4 di-methylation are also observed at the chromatin boundaries following RNF20 depletion, but these are more subtle. H3K4me2 was depleted by ~40% and ~30% at the HS4 and HSA elements in the E5 line, respectively (Figure 4.4a, p-values of 3.09E-06 and 6.28E-06, respectively). These findings are consistent with previous reports that H3K4me2 is not as tightly linked to prior H2B ubiquitination as H3K4me3 [Vitaliano-Prunier *et al*, 2008; Wu *et al*, 2008]. Collectively, these findings point to different molecular mechanisms governing the di- and tri-methylation of H3K4.

In contrast with the chromatin boundaries, H3K4 methylation of the *FOLR1* gene promoter was generally resistant to RNF20 knockdown. No changes in H3K4me2 or H3K4me3 were observed at the promoter in E5 line (Figure 4.4a & b). This is despite the depletion of H2BK120ub1 at the promoter in the same cell line (Figure 4.2 & Figure 4.3). These findings indicate that an H2BK120ub1-independent pathway contributes to H3K4 methylation of the *FOLR1* gene promoter.

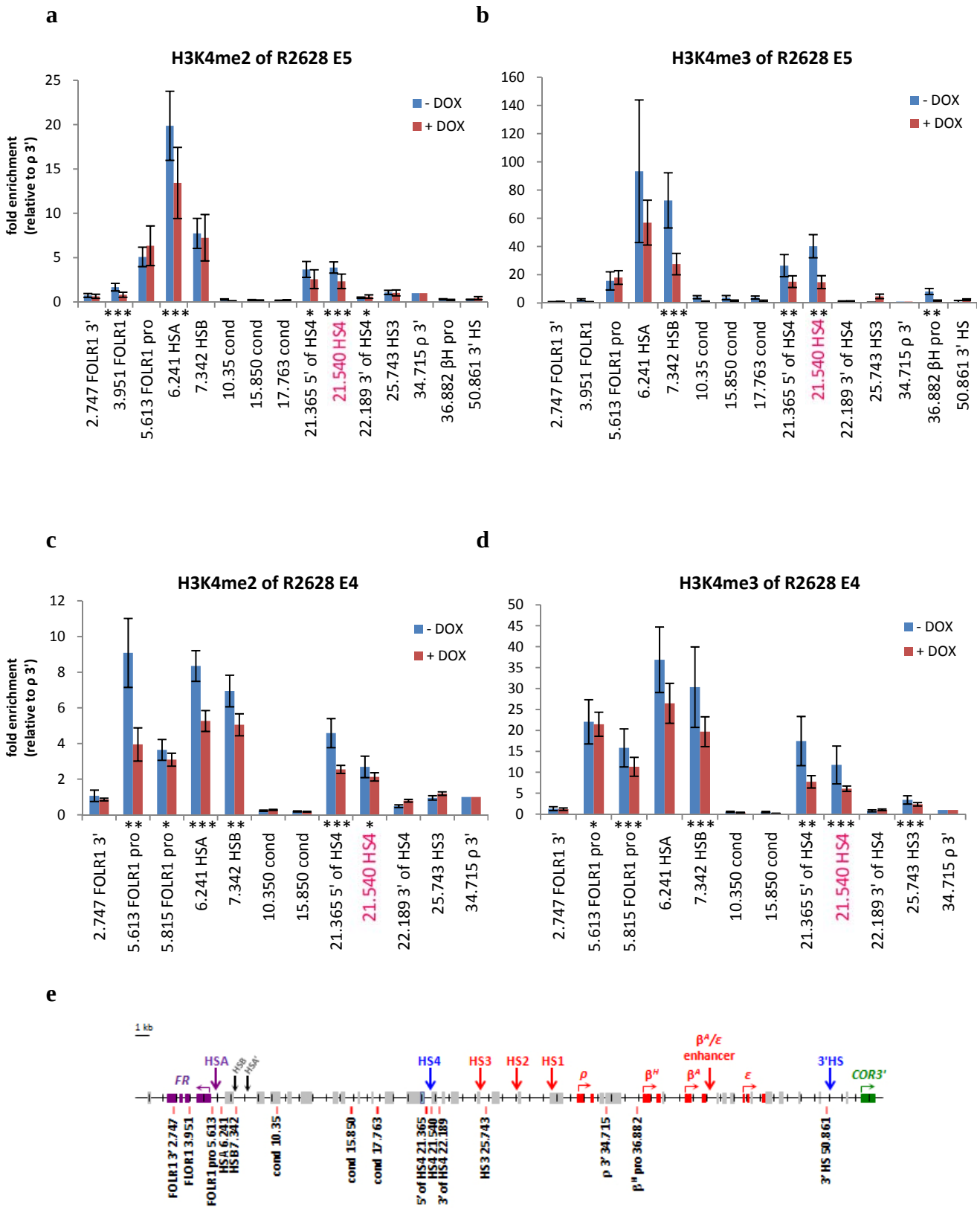

Figure 4.4 Native ChIP examinations of H3K4 di- and tri-methylation across the chicken *β-globin* locus in the RNF20 knockdown lines R2628 E5 (**a** and **b**) and E4 (**c** and **d**). **e**. Primers used for quantitative PCR. Normalisation of the quantitative PCR was carried out by using *ρ-globin 3'* (34.7) as a control region. P-values smaller than 0.05, 0.01 and 0.005 are indicated with "*", "**" and "***", respectively.

4.3.3 H2B ubiquitination may be required for acetylation of histones H3 and H4 at chromatin boundaries

In addition to H3K4me2 and H3K4me3, it has been shown that HS4 is enriched in hyperacetylated H3, H4 and H2A.Z [Bruce *et al*, 2005; Huang *et al*, 2005; Litt *et al*, 2001b; West *et al*, 2004]. It is known that hyperacetylated chromatin is generally accessible to proteins [Eberharter & Becker, 2002]. The multiple histone acetylation at HS4, therefore, may be crucial for maintaining the integrity of the HS4's permissive chromatin structure. If H2B ubiquitination is a master controller of HS4's active histone modifications, the levels of histone acetylation might be expected to decrease specifically at HS4 following RNF20 knockdown even though they do not change globally. Native ChIP was performed following RNF20 knockdown to study if histone acetylation at HS4 requires prior H2B ubiquitination.

Multiple acetylation of H3 and H4 was substantially depleted at the HSA/HSB and HS4 chromatin boundaries following the knockdown of RNF20 expression. H3ac was reduced by ~50% and ~60%, respectively, and H4ac was reduced by ~60% at the HSA/HSB and HS4 chromatin boundaries in the E5 line (Figure 4.5a & b; p-values for changes of H3ac at HSA, HSB and HS4 are 5.18E-05, 9.65E-05 and 0.0023, and those of H4ac at HSA, HSB and HS4 are 0.0075, 0.0056 and 0.0003, respectively). However, H3ac and H4ac were only substantially depleted at the HSB element in the E4 line (Figure 4.5c & d; reduced by ~60% with p-value 0.0075 and ~70% with p-value 0.032, respectively). Collectively, these observations indicate that H3ac and H4ac at the chromatin boundaries are greatly favoured by prior H2BK120ub1 and H3K4me2/3, but that the relationship between these modifications is indirect.

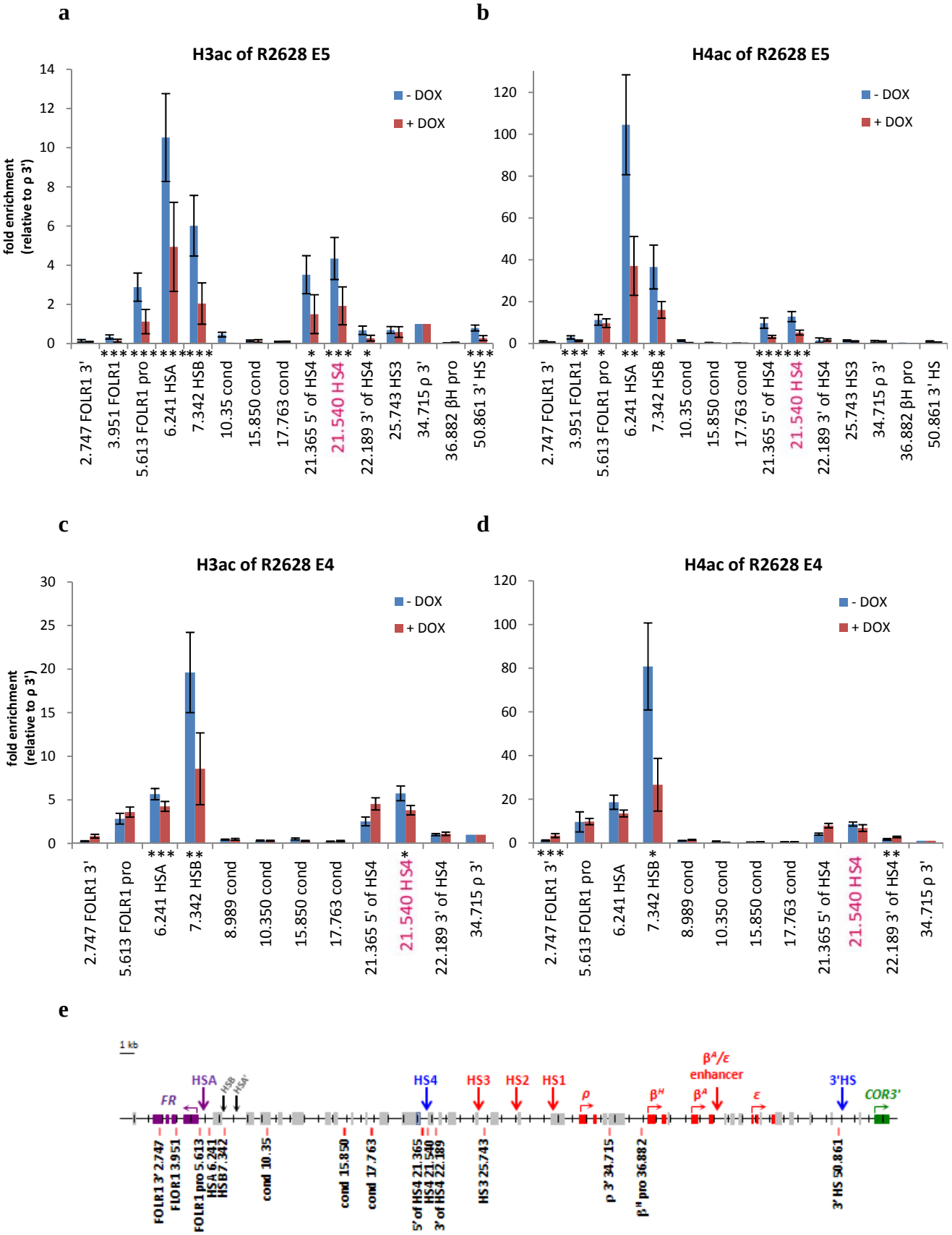

Figure 4.5 Examinations of H3 and H4 acetylation across the chicken *β-globin* locus following short time course of RNF20 knockdown in both R2628 E5 (**a** and **b**) and E4 (**c** and **d**). Quantitative PCR of ChIP was carried with primers indicated **(e)**, normalised to *ρ-globin 3'* (34.7). P-values obtained from a two-tail student t-test smaller than 0.05, 0.01 and 0.005 are indicated with "*", "**" and "***", respectively.

The discrepancy between the effects of RNF20 knockdown on histone acetylation in the E4 and E5 lines might be due to toxic or off-target effects of shRNA expression. The identity of the KATs that function at the *FOLR1* and *β-globin* loci have not been determined, so it is not possible to check whether off-site targeting of KAT expression, particularly in the E5 line, might be occurring following RNF20 knockdown. However, this appears to be unlikely as the E4 and E5 lines express the same shRNA sequence and the expression of the linked GFP gene is equivalent between the two lines (not shown). Moreover, the global levels of H3 and H4 acetylation in the two lines were not affected by RNF20 knockdown, so KAT expression does not seem to be susceptible to off-target effects. Rather, the discrepancy between the histone acetylation changes in the E4 and E5 lines might be explained by the fact that H2BK120ub1 is depleted to a greater extent in the E5 line than the E4 line (Figure 4.1). Partial depletion of H2BK120ub1 and methylated H3K4 might not be sufficient to disrupt KAT recruitment and function. If more knockdown lines with different degrees of RNF20 and H2BK120ub1 depletion were studied, the relationship between histone acetylation and prior H2BK120ub1 might become clearer.

4.3.4 Chromatin boundaries require H2BK120ub1 for H2A.Z acetylation

H2A.Z acetylation is of interest not only because it was shown to be enriched at the HSA/HSB and HS4 elements [Bruce *et al*, 2005], but also it is essential for the barrier activity of yeast chromatin boundaries [Babiarz *et al*, 2006]. Loss of H2A.Zac at the chromatin boundaries in cells lacking H2BK120ub1 could indicate the loss of their barrier activity. Native ChIP analyses were used to confirm that the HSA/HSB and HS4 elements are highly enriched in acetylated H2A.Z (Figure 4.6). In line with H3 and H4 acetylation, H2A.Z acetylation at the boundary elements requires prior H2BK120ub1 (Figure 4.6b & c). Depletions in H2A.Zac, by as much as 85%, are observed at the boundary elements following RNF20 knockdown in both the E4 and E5 cell lines.

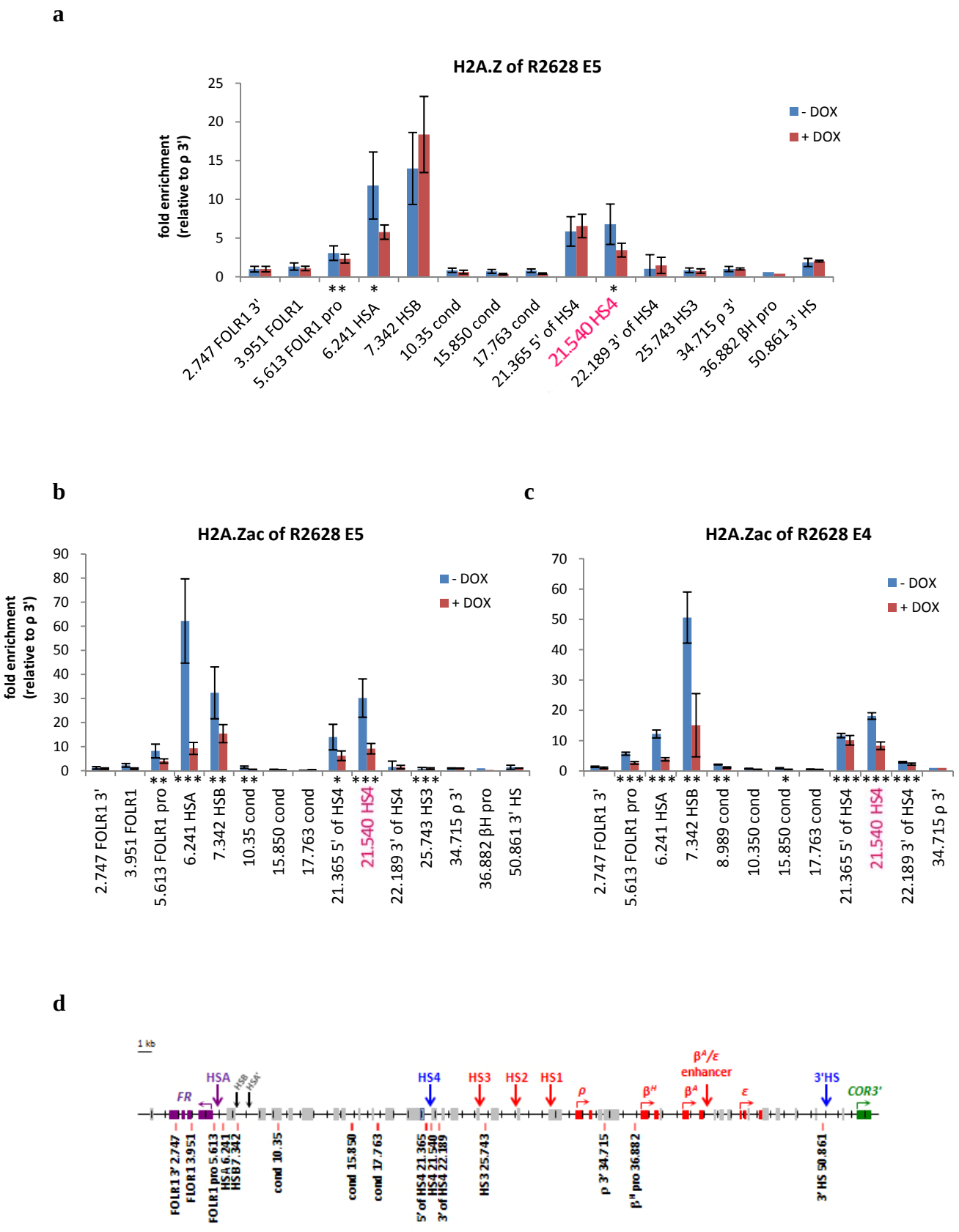

Figure 4.6 Native ChIP assays of H2A.Z and H2A.Zac across the chicken *β-globin* locus upon RNF20 knockdown in knockdown lines R2628 E5 (**a** for H2A.Z and **b** for H2A.Zac) and R2628 E4 (**c** H2A.Zac only) cells treated with DOX for four days. **d**. Primers used in quantitative PCR analyses in which *ρ-globin 3'* (34.715) was set as a normalisation region. P-values obtained from a two-tail student t-test smaller than 0.05, 0.01 and 0.005 are indicated with "*", "**" and "***", respectively.

The reduction of H2A.Zac could be because of reduced H2A.Z incorporation. The histone variant H2A.Z, unlike its canonical counterpart H2A, is not deposited into chromatin during replication [Hardy & Robert, 2010], but is selectively incorporated by specific chromatin remodelling complexes [Mizuguchi *et al*, 2004; Wong *et al*, 2007]. Although it is still not clear what the role of H2A.Z in vertebrate insulator barriers is, genome mapping of H2A.Z distribution found that DNaseI hypersensitive sites, and CTCF-bound elements in particular, are sites of H2A.Z incorporation [Barski *et al*, 2007; Jin *et al*, 2009]. Despite the depletion of H2BK120ub1 and multiple histone acetylation, H2A.Z incorporation remains at the HSA/HSB and HS4 chromatin boundaries, although there are ~50% reductions in H2A.Z levels at the HSA element and one of the HS4 nucleosomes (Figure 4.6a). There appears to be some requirement for prior H2B ubiquitination for H2A.Z incorporation, but this alone does not explain the very substantial depletions in H2A.Z acetylation following RNF20 knockdown. It is likely that the KATs which acetylate H2A.Z are in some way dependent upon prior H2BK120ub1-H3K4me3 modification.

4.3.5 Crosslinking ChIP analysis of insulator protein binding at chromatin boundaries following RNF20 knockdown

The proteins USF1, USF2 and VEZF1 bind to sites within the HS4 element and mediate its barrier activity (Figure 1.35) [Dickson *et al*, 2010; Huang *et al*, 2007; Recillas-Targa *et al*, 2002; West *et al*, 2004]. The single binding site for USF proteins has been found to be responsible for the recruitment of H3ac, H4ac, H3K4me2 and histone ubiquitination [West *et al*, 2004, Section 1.6.3]. Consistent with this, USF1 has been found to interact with H3K4-specific KMTs, SET1 and SET7/9, and a H3-specific KAT, PCAF, that mediate H3K4 methylation, H3 acetylation, respectively [Huang *et al*, 2007; West *et al*, 2004]. It is possible that the dramatic reductions of H2BK120ub1, H3K4me2/3, H3ac, H4ac and H2A.Zac at the HS4 element, and the HSA/HSB elements perhaps, could be due to reduced expression or binding of USF1 or the other insulator-binding proteins.

Western blotting analysis found that the expression levels of the HS4 binding proteins USF1, VEZF1 and CTCF were unchanged following RNF20 knockdown, ruling out off-target effects of the shRNA or RNF20-dependent expression of the insulator protein genes (Figure 4.7a). It is conceivable that the depletion of H2BK120ub1 might affect insulator protein binding to the HS4 element, perhaps as a result of altered nucleosome positioning, which in turn may affect the recruitment of histone modifying enzymes. Crosslinking ChIP analysis showed that the binding of USF1, VEZF1 and CTCF at HS4 was unaffected following RNF20 knockdown (Figure 4.7b-d). The loss of insulator protein binding and their potential to recruit histone modifying enzymes is therefore not responsible for the loss of active histone marks at the HS4 boundary element.

Crosslinking ChIP analysis was extended to the *FOLR1* regulatory elements, which revealed striking parallels with the HS4 element. USF1 was found to interact with the HSA, HSB and *FOLR1* promoter elements (Figure 4.7d). USF1 has been described to recognise the consensus sequence CAcgTG, although recognises the divergent site CACGGG at the HS4 element [Rada-Iglesias *et al*, 2005; West *et al*, 2004]. The HSA, HSB and *FOLR1* promoter elements contain the putative USF1 recognition motifs CACGaG, CcCGTG, and CAgGTG, respectively. It is possible that USF1 may be responsible for the recruitment of histone modifying enzymes to the *FOLR1* elements in a similar manner to the HS4 element. In another parallel with the HS4 element, VEZF1 binding was also observed at the *FOLR1* HSA and HSB elements, which contain the putative recognition motifs GGGGGGGGGGGG and CCCCatCtCCCCCC, respectively (Figure 4.7c). The binding of USF1 and VEZF1 to the HSA/HSB elements was unaffected by RNF20 knockdown (Figure 4.7c & d). The enhancer blocking protein CTCF did not bind to the *FOLR1* elements (Figure 4.7b).

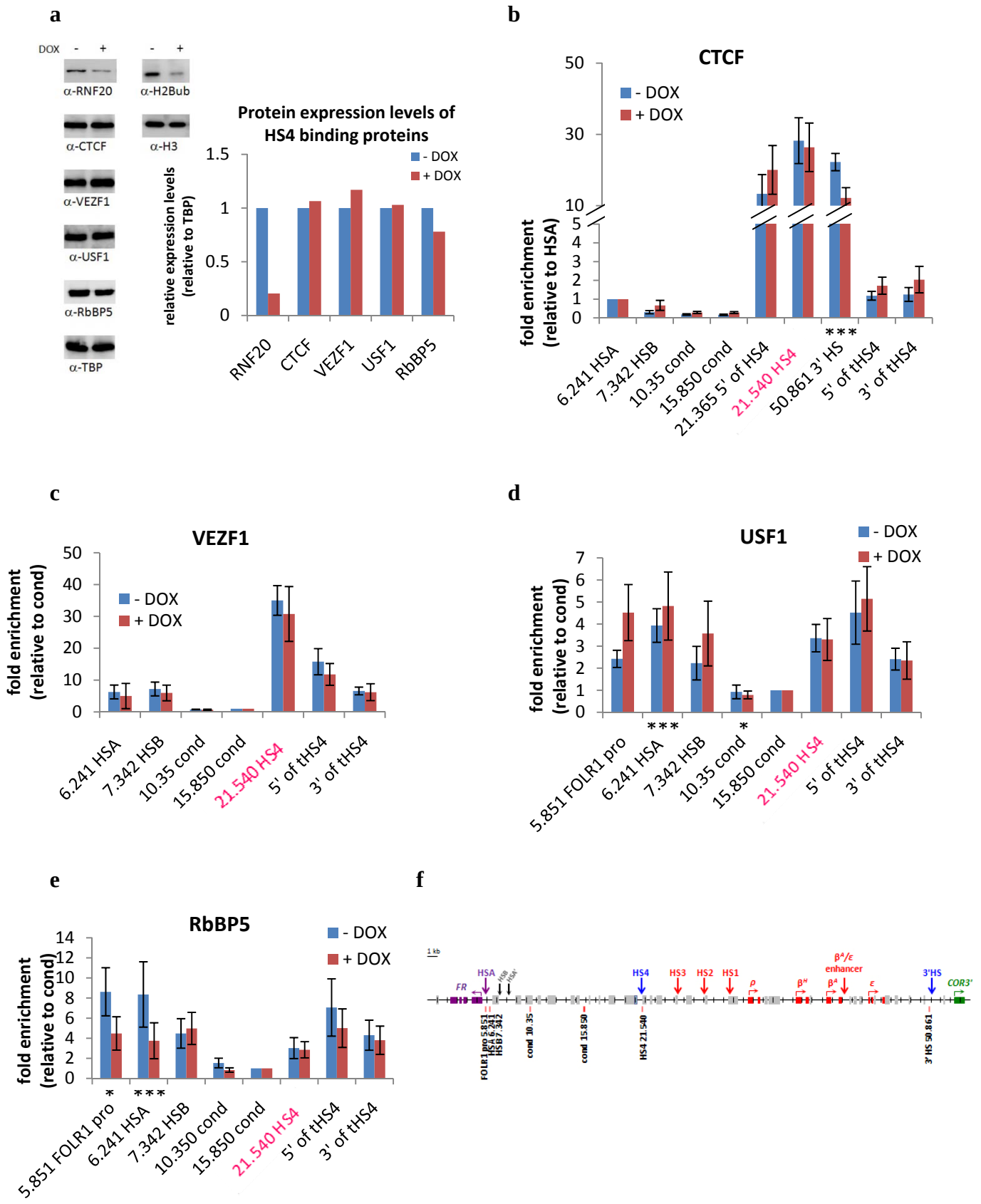

Figure 4.7 Western blotting **(a)** and crosslinking ChIP analyses **(b – e)** of HS4 binding proteins following RNF20 knockdown in R2628 E5. Fold enrichments of CTCF **(b)** of target sites were normalised to HSA (6.241) whereas those of VEZF1 **(b)**, USF1 **(c)** and RbBP5 **(e)** were relative to the condensed region (15.850). Significant changes with p-values smaller than 0.05, 0.01 and 0.005 are indicated with "*", "**" and "***", respectively. **f.** Primer sets used.

Several models have been proposed to explain the *trans*-histone crosstalk between H2B ubiquitination and H3K4 methylation, and recent results indicate that H2BK120ub1 mediates the binding of histone methyltransferase (KMT) complex factors to chromatin (discussed in section 1.2.4). There are several KMTs that mediate H3K4 methylation in mammals, including SET1A and B, as well as MLL 1 – 4, in vertebrates. Which of these KMTs functions at the HSA/HSB and HS4 boundary elements is yet to be determined, but USF1 has been shown to interact with the SET1 complex [Huang *et al*, 2007]. The proteins RbBP5, ASH2L and WDR5 are essential components of all the mammalian H3K4-specific SET1 and MLL HMT complexes, where RbBP5 is required for methyltransferase activity [Dou *et al*, 2006; Lee *et al*, 2007; Popovic *et al*, 2005; Steward *et al*, 2006]. Crosslinking ChIP was used to analyse the binding of RbBP5 across the *FOLR1* and *β-globin* loci. RbBP5 binding was detected at the *FOLR1* promoter, HSA, HSB elements and the HS4 element, consistent with each being sites of H3K4me2/3.

The total level of RbBP5 protein was found to be reduced by ~20% following RNF20 knockdown (Figure 4.7a). Despite this, the binding of RbBP5 was unaffected at the HSB and HS4 boundary elements (Figure 4.7e). The depletion of H3K4 methylation at the HSB and HS4 elements following RNF20 knockdown therefore cannot be explained by a loss of KMT complex binding. However, the scenario differed at the *FOLR1* promoter and HSA elements, where RbBP5 binding is reduced by ~50% following RNF20 knockdown (Figure 4.7e). It is unclear whether this reflects H2BK120ub1-dependent KMT recruitment or increased sensitivity to RbBP5 levels at these elements. The discrepancy between RNF20-independent USF1 binding and the partially RNF20-dependent binding of RbBP5, suggests that factors in addition to USF1 might recruit KMT complexes to the *FOLR1* promoter and HSA elements.

4.4 Determine whether H2B ubiquitination is required for chromatin boundary integrity

The HS4 barrier function in the chicken *β-globin* locus is speculated to protect the downstream *β-globin* domain from encroachment of the upstream repressive chromatin [Prioleau *et al*, 1999; West *et al*, 2004]. HSA/HSB is situated between the repressive chromatin and the *FOLR1* gene, and may protect the *FOLR1* gene from heterochromatin silencing. In order to study whether chromatin boundary integrity is abolished by H2BK120ub1 depletion, native ChIP was performed to study heterochromatin-associated histone marks H3K9me2, H3K9me3, H3K27me3 and H4K20me3 across the *β-globin* and *FOLR1* loci following RNF20 knockdown. The R2628 E5 line was employed for these experiments as it sustained high levels of RNF20 knockdown during long term culture, as described below.

4.4.1 The HS4 chromatin boundary is rapidly breached by H3K9me2 in the absence of H2BK120ub1

Chromosomal silencing has previously been shown to be a gradual process, as exemplified by the position effect silencing or reporter transgenes, which can take at least 30 days to occur [Recillas-Targa *et al*, 2002]. The severe disruption of the active signature at the HSA/HSB and HS4 elements following RNF20 knockdown might allow the intervening heterochromatin to breach these boundaries over a short period. To investigate this, native ChIP was performed to study heterochromatin associated histone modifications following four days of RNF20 knockdown. Fold enrichments were normalised to those at 3' of the ρ globin gene, which is neither enriched nor depleted in H3K9 methylation [Litt *et al*, 2001a]. Even at this early timepoint, spreading of one heterochromatin-associated mark into both the *FOLR1* and *β-globin* loci was observed. Statistically significant increased in H3K9me2 levels were observed from the HS4 element to almost as far as the ρ globin gene promoter following RNF20 knockdown (Figure 4.8a). Significant increases in H3K9me2 were also observed at the promoter and gene body of the *FOLR1* gene following RNF20 knockdown. However, unlike HS4, there was no significant elevation of H3K9me2 at HSB after RNF20 knockdown. We show that *FOLR1* does

not require RNF20 for its transcription later in the chapter, so the increase in H3K9me2 at *FOLR1* is not a consequence of its repression (Section 4.4.4).

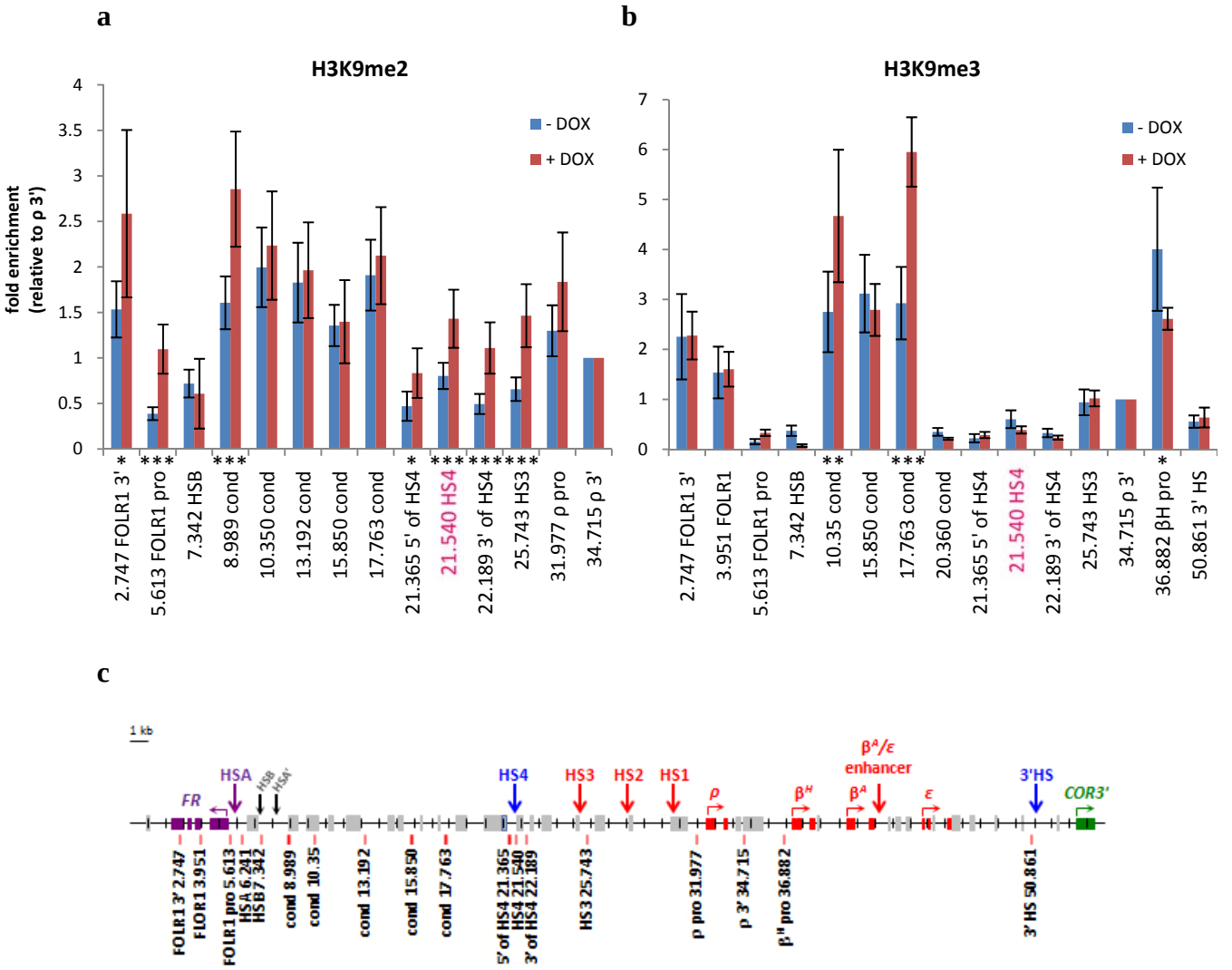

Figure 4.8 Examination of H3K9 methylation spreading by ChIP following short time course of RNF20 knockdown. Low salt ChIP was performed in R2628 E5 cells following four days of RNF20 knockdown to investigate the spreading of H3K9me2 **(a)** and H3K9me3 **(b)**. Significant changes with p values smaller than 0.05, 0.01 and 0.005 are indicated with "*", "**" and "***", respectively. All normalisation of the examined regions (**d**) was performed by using *ρ-globin 3'* (34.715) as a control region.

The HS4 barrier seemed not to be completely abolished at this stage that the spreading of H3K9me3 was still prohibited (Figure 4.8b). The levels of H3K9me3 across the *FOLR1* and *β-globin* gene bodies generally unchanged after 4-day of RNF20 knockdown. However, there was considerable consolidation of this mark at the flanks of the condensed chromatin region.

Native ChIP was also used to investigate the levels of another heterochromatin-associated mark, H4K20me3. H4K20me3 is often found with H3K9me3 at silenced genes and regions of constitutive heterochromatin [Nishioka *et al*, 2002; Schotta *et al*, 2004]. Fold enrichments across the locus were normalised to a site within the condensed chromatin region (10.350) as the ρ 3' used in the previous ChIP analyses exhibited an extremely low level of H4K20me3. This avoids exaggeration of enrichments and errors due to minor differences in ChIP efficiencies and PCR quantification of low abundance normaliser sequence. H4K20me3 is generally enriched at the condensed chromatin region and the gene body of *FOLR1* but it did not propagate beyond its normal limits following a short period of RNF20 knockdown (Figure 4.9). These results suggest that if heterochromatin does spread from the condensed region, H3K9me2 is the first mark in this process.

a

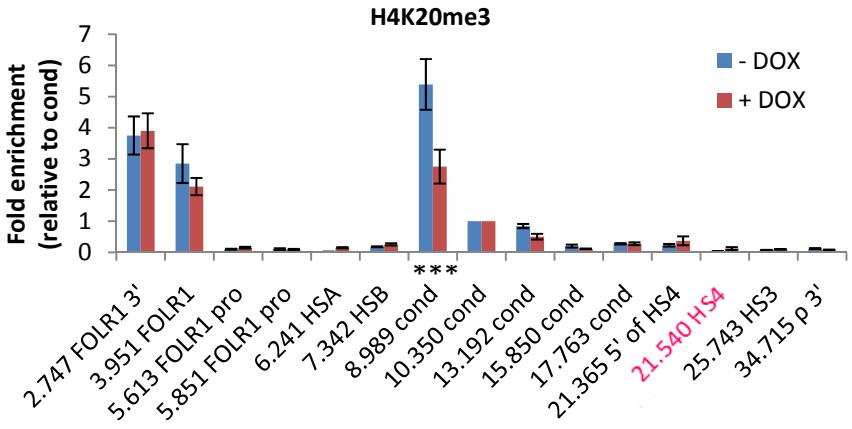

b

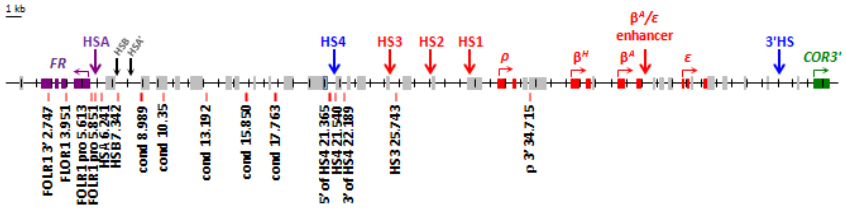

Figure 4.9 Examination of H4K20me3 across the chicken *β-globin* locus after RNF20 knockdown for four days in R2628 E5 **(a)**. Primers used for quantitative PCR **(b)**. Significant changes with p-values smaller than 0.05, 0.01 and 0.005 are indicated with "*", "**" and "***", respectively.

H3K27me3 is also associated with facultative heterochromatin-like gene silencing mediated by polycomb repressor complexes [Peters *et al*, 2003]. The enrichment of H3K27me3 across the condensed and *β-globin* loci was very low, with depletion evident at the *FOLR1* region (refer to the scale of the fold enrichment axis). There were no substantial increases in H3K27me3 enrichment across these loci after four days of RNF20 knockdown (Figure 4.10). It appears that the condensed region has the characteristics of constitutive heterochromatin marked by H3K9me3 and H4K20me3 and that H3K27me3 does not play as significant a role at this locus.

a

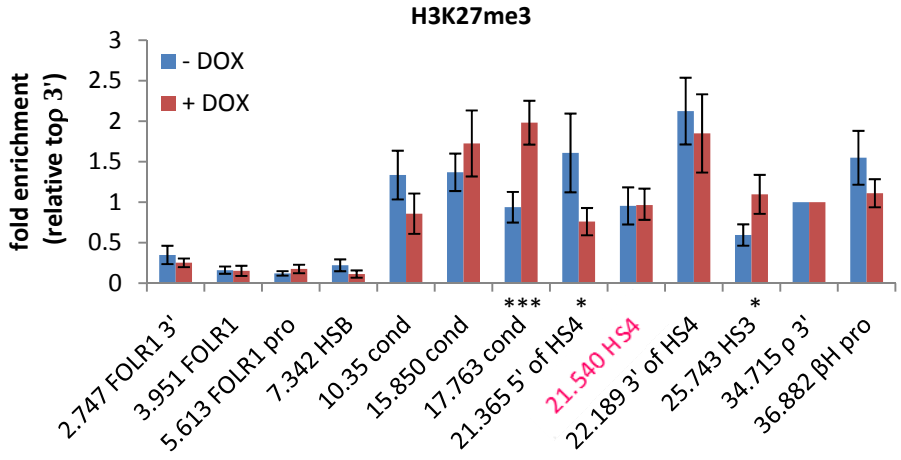

b

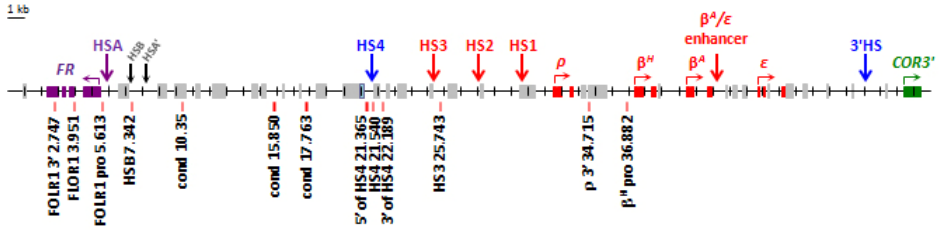

Figure 4.10 Examination of H3K27me3 across the *β-globin* locus after knocking down of RNF20 for four days in R2628 E5 **(a)**. Primer sets used for quantitative PCR **(b)**. Significant changes with p values smaller than 0.05, 0.01 and 0.005 are indicated with "*", "**" and "***", respectively.

4.4.2 Prolonged RNF20 knockdown leads to H3K4 methylation reduction

To observe whether other heterochromatin-associated marks would spread if active marks are depleted from chromatin boundaries for longer periods, native ChIP analyses were performed

after 30 days of RNF20 knockdown. This presented a technical challenge as FACS analysis showed that the fraction of E5 cells that express GFP-RNF20-shRNA following DOX treatment steadily decreased with time in culture (not shown). The E5 line is not maintained with drug selection, so the lentiviral construct may be subject to progressive chromosomal position effect silencing. GFP expressing E5 cells were therefore re-cloned by serial dilution.

However, the resulting sub-clones were found to have leaky RNF20 shRNA expression in the absence of DOX treatment. RT-PCR analysis determined that RNF20 mRNA levels were reduced by ~20% in E5 sub-clones compared to wild type 6C2 cells (Figure 4.11). The addition of DOX reduced RNF20 mRNA levels by 65-75%. The apparent leaky RNF20 knockdown affects active histone marks in total chromatin. H2BK120ub1, H3K4me2 and H3K4me3 levels were all reduced in E5 sub-clones in the absence of DOX when compared with wild type 6C2 cells (Figure 4.11a). Therefore, the ChIP analysis of histone modification profiles following long term RNF20 knockdown in E5 sub-clones were compared to those in wild type 6C2 cells as untreated E5 cells were not a suitable negative control. Interestingly, prolonged RNF20 knockdown appeared to alter global histone modifications other than H3K4 methylation and H2B ubiquitination. There was a global increase in H2A.Z, H3K9me3 and H4K20me3 after long term RNF20 knockdown (Figure 4.11).

Native ChIP analyses of active histone marks following long term RNF20 knockdown were completed using sequences 3' of the ρ globin gene as a neutral site for normalisation as described above (Section 4.3). In agreement with the effects of a short period of RNF20 knockdown, the levels of H3K4me2 and H3K4me3 at the *FOLR1* and HS4 elements were depleted following long term RNF20 knockdown (Figure 4.12).

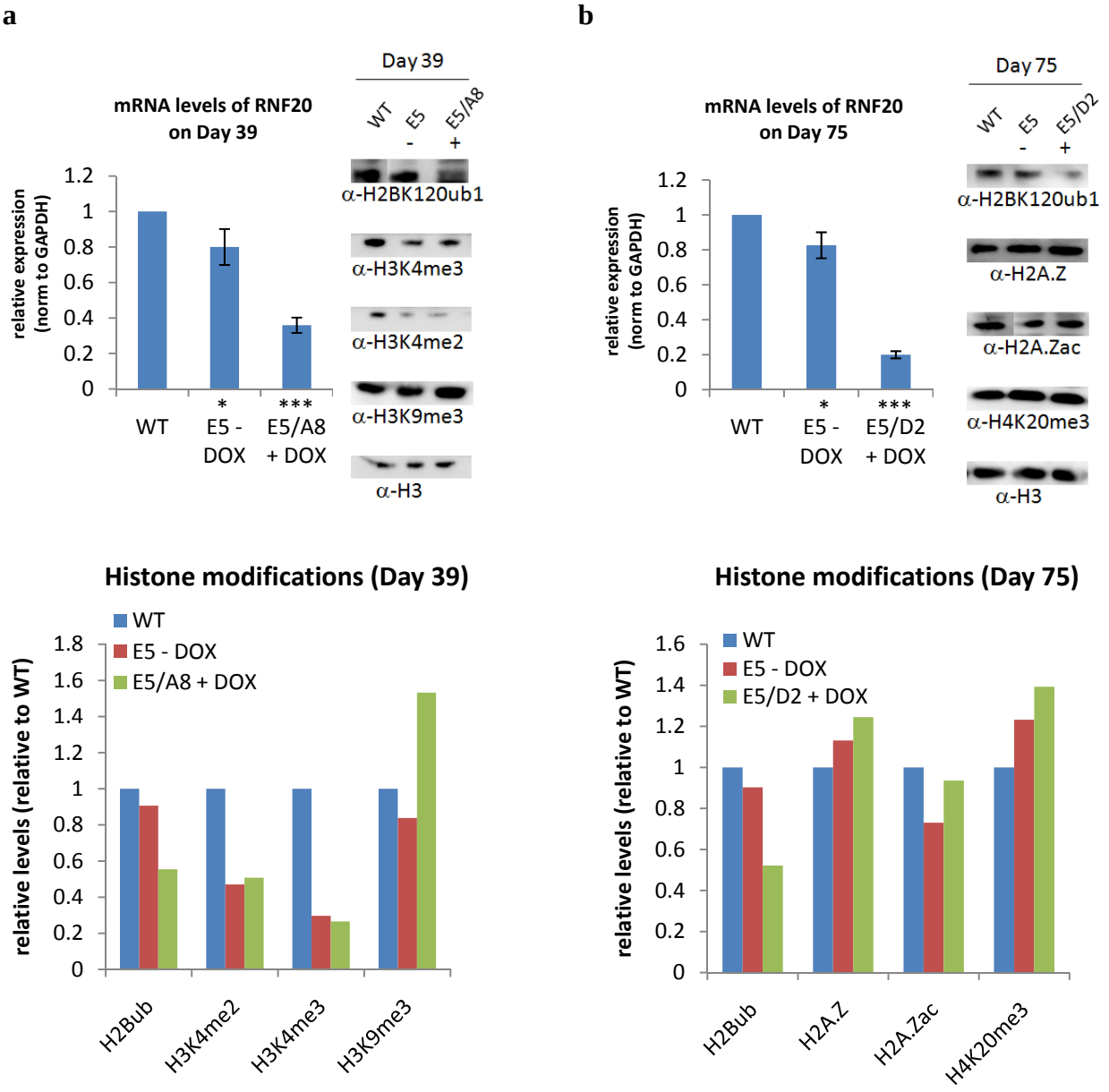

Figure 4.11 RT-PCR analysis of RNF20 expression levels and western blotting of histone modifications after prolonged RNF20 knockdown. Sub-clones showing RNF20 knockdown after long time course were selected and grown in larger scales. R2628 E5/A8 and R2628 E5/D2 were sub-clones screened from two separate experiments while cells were harvested on Day 39 for R2628 E5/A8 **(a)** and on Day 75 for R2682 E5/D2 **(b)**. Untreated R2628 E5 and wild type cells were grown alongside. mRNA expression of RNF20 of no DOX controls and DOX induced RNF20 knockdown cells was relative to wild type and significant differences compared with wild type are indicated with "*" and "***" for p-values small than 0.05 and 0.001, respectively. Relative histone modification levels in wild type (WT), untreated R2628 E5 (E5 –DOX) and DOX treated R2628 E5/A8 or E5/D2 cells were calculated by their corresponding band intensities in western blotting and then normalised to the H3 loading control. Some of the lanes obtained from the same western image were rearranged for representation. All wild type levels were set to one.

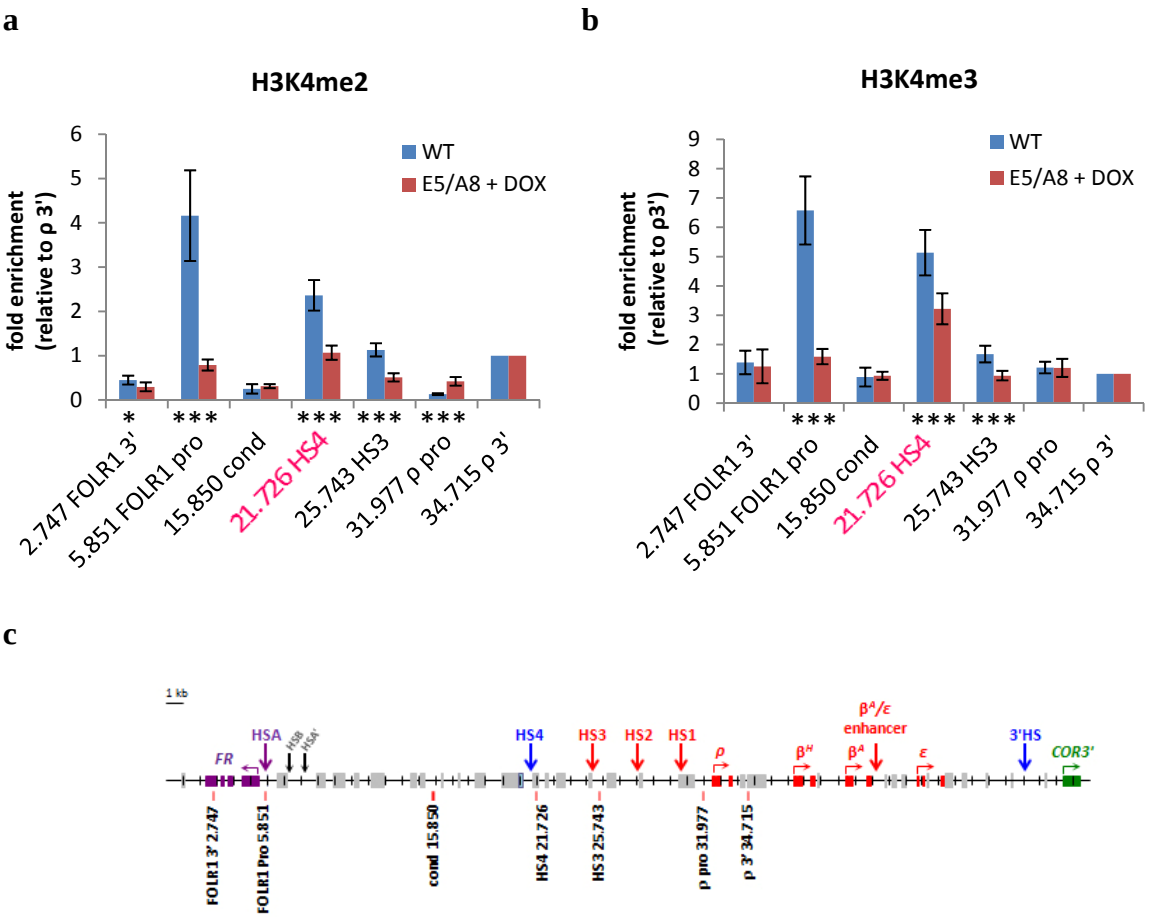

Figure 4.12 ChIP analyses of H3K4 methylation across the chicken *β-globin* and *FOLR1* loci after a long time course knockdown of RNF20. Wild type 8103 (6C2 harbouring transgenic HS4) and DOX treated R2628 E5/A8 were harvested on Day 39, chromatin was extracted for low salt ChIP analyses of H3K4 di- **(a)** and tri-methylation **(b)**. Fold enrichments at examined regions **(c)** were normalised to that at *ρ 3'* (34.715). Significant changes with p-values smaller than 0.05 and 0.005 are indicated with "*" and "***", respectively.

4.4.3 Prolonged RNF20 knockdown allows spreading of repressive histone marks across the entire *chicken β-globin* locus

Native ChIP analyses of active histone marks following long term RNF20 knockdown were completed using sequences within the condensed region for normalisation as a positive control, as described above (Section 4.4.1). A striking propagation of H3K9me3 was observed following 39 days of RNF20 knockdown. Statistically significant increases in H3K9me3 were observed at the *FOLR1* gene and from the HS4 element to most of the sites across the *β-globin* locus (Figure 4.13a). There is also a dramatic spread of H4K20me3, with significant increases in this mark at the *FOLR1* gene and from the HS4 element to sites as far as the *ρ* gene promoter (Figure 4.13b).

Collectively, these results show that i) the heterochromatin within the condensed region is capable of spreading into neighbouring gene loci, ii) the HSA/HSB and HS4 boundary elements function to provide limits to this heterochromatin and iii) the boundary elements require active histone modifications that are dependent on H2B ubiquitination.

a

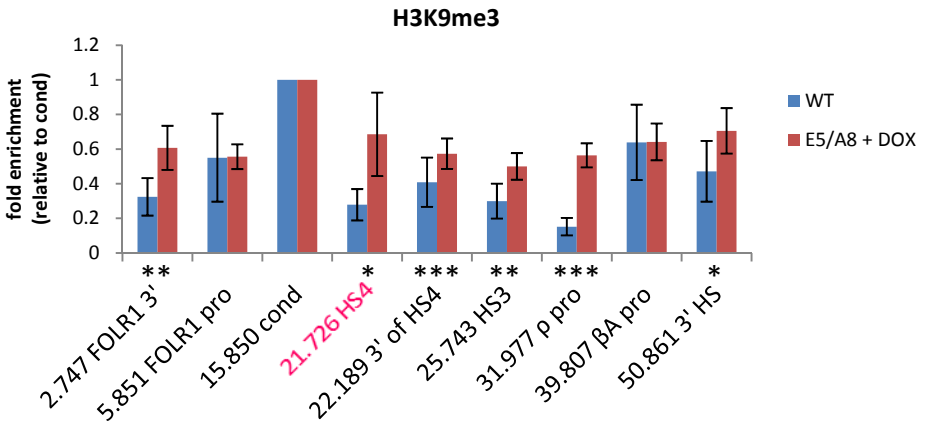

b

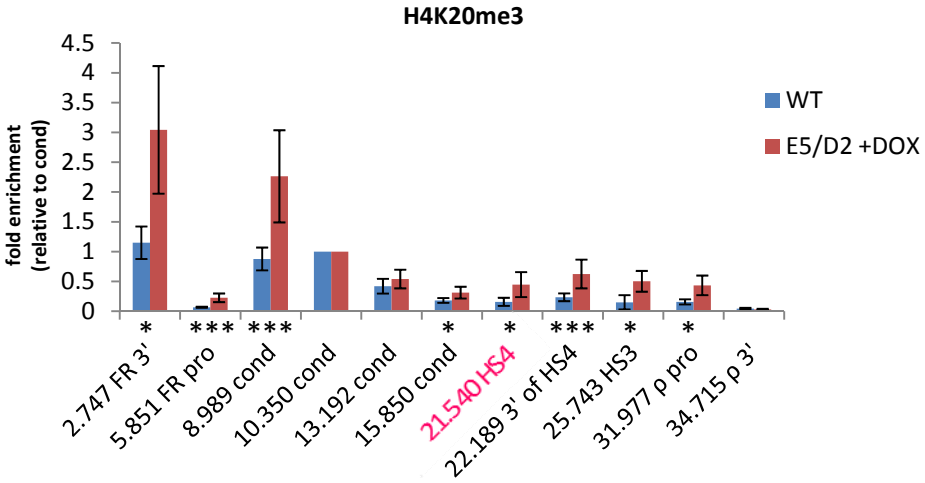

c

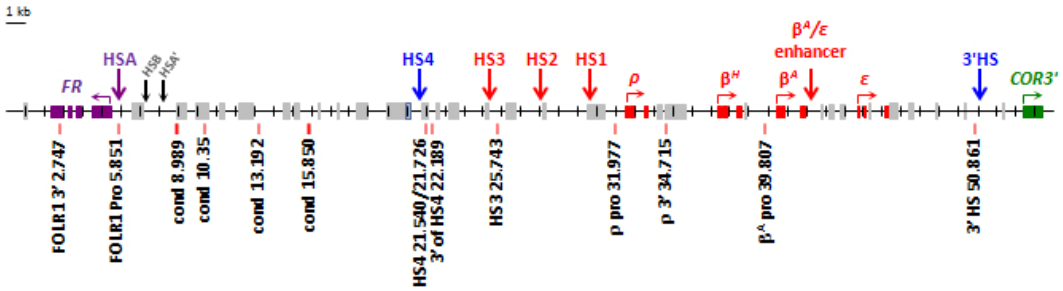

Figure 4.13 ChIP analyses of H3K9me3 and H4K20me3 on the chicken *β-globin* locus following long-term knockdown of RNF20. Cells of the subclone R2628 E5/A8 cells were treated by DOX for 39 days for H3K9me3 ChIP analysis **(a)** while cells of the subclone R2628 E5/D2 were treated for 75 days for H4K20me3 ChIP analysis **(b)**. Untreated R2628 E5 and wild type cells were grown alongside to serve as control. **c**. Primers used in quantitative PCR. Fold enrichments were normalised to a condensed chromatin region 15.850 and 10.350 for H3K9me3 and H4K20me3, respectively.

4.4.4 Prolonged RNF20 knockdown leads to silencing of the *FOLR1* gene

The encroachment of heterochromatin-associated marks over the *FOLR1* and *β-globin* genes following RNF20 depletion may result in the silencing of their transcription. While the *β-globin* locus is becoming primed for expression at the CFU-E progenitor stage represented by 6C2 cells, the *β-globin* genes themselves are not expressed until terminal differentiation [Groudine & Weintraub, 1981; Prioleau *et al*, 1999]. 6C2 cells cannot be induced to terminally differentiate, so we are unable to study the impact of heterochromatin spreading on the activation of *β-globin* gene transcription in this system. The *FOLR1* gene is active in 6C2 cells, however.

RT-PCR analysis was performed to monitor *FOLR1* expression following a time course of RNF20 knockdown. *FOLR1* mRNA levels were normalised to either the *GAPDH* or *ACTB* housekeeping genes as loading controls. It has previously been found that the transcription of *GAPDH* in human cells does not rely on H2B ubiquitination [Shema *et al*, 2008]. Despite the spreading of H3K9me2, *FOLR1* expression was not silenced following four days of RNF20 knockdown (Figure 4.14). In fact, *FOLR1* expression appears to increase following RNF20 knockdown, but a Student's t-test found that this increase was not statistically significant compared with wild type. This result indicates that the expression of *FOLR1* does not dependent upon H2B ubiquitination and that the early onset of heterochromatin spreading marked by H3K9me2 is not capable of causing *FOLR1* gene silencing.

However, *FOLR1* expression is progressively silenced following prolonged periods of RNF20 knockdown (Figure 4.14). *FOLR1* mRNA levels are reduced by 60% and 95% following 30 and 75 days of RNF20 knockdown, respectively. The progressive silencing of *FOLR1* is consistent with the spread of the heterochromatin-associated marks H3K9me3 and H4K20me3 across the gene. These results support the hypothesis that the active histone modifications at the HSA/HSB chromatin boundary elements act to insulate the *FOLR1* gene from repressive heterochromatin located a few kilobases upstream of the gene.

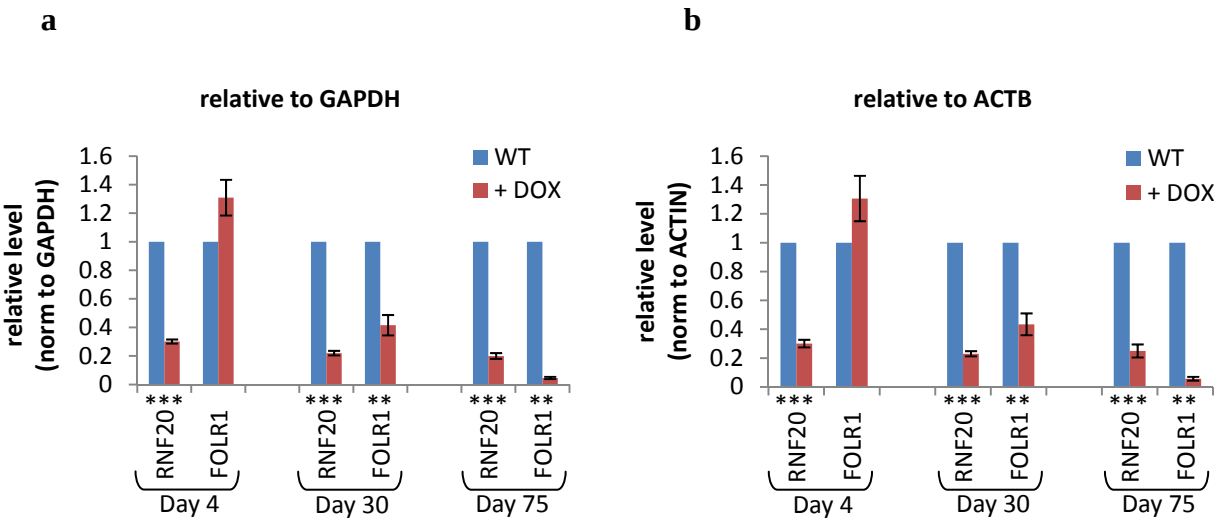

Figure 4.14 mRNA levels of *FOLR1* after 4, 30 and 75 days of RNF20 knockdown. RNF20 knockdown was induced by addition of DOX to R2628 E5 cells. RT-PCR was performed on RNA of subclones of R2628 E5 on Day 30 and 75 which had at least 90% of green cells indicating the expression of the RNF20-shRNA-GFP cassette. The relative expression was normalised to that of *GAPDH* **(a)** or *ACTB* **(b)**. The *FOLR1* expression in control cells was set to one. Significant differences of expression between wild type and knockdown cells are indicated with "**" and "***" if their p values from a two-tailed student t-test are less than 0.01 and 0.001, respectively.

4.5 Determine whether H2B ubiquitination is required for the barrier activity of the HS4 insulator

The fourth object of this chapter is to test the direct effect of RNF20 knockdown on the HS4 barrier activity. We made use of the well established reporter assay system [Pikaart *et al*, 1998], which has been employed in several studies to examine the HS4 barrier activity [Huang *et al*, 2007; Pikaart *et al*, 1998; Recillas-Targa *et al*, 2002]. The reporter gene, *interleukin 2 receptor* (*IL2R*, also known as *CD25*), its expression driven by the chicken β^A*-globin* promoter and strong *β/ε* enhancer, was flanked by two copies of HS4 at each side (Figure 4.15). The entire cassette was integrated into the genome of 6C2 cells and individual clones were isolated. IL2R is expressed on the cell membrane and acts as a surface antigen that can be detected by fluorescence-activated cell sorter (FACS) analysis following immunostaining. The whole cassette was flanked by HS4, therefore unlike non-insulated transgenes, the IL2R expression would not be silenced by the genomic environment even when the cell line was cultured for a long period of time (more than 90 days) [Pikaart *et al*, 1998]. One of the previously characterised lines, 8103, was used in this study [Recillas-Targa *et al*, 2002].

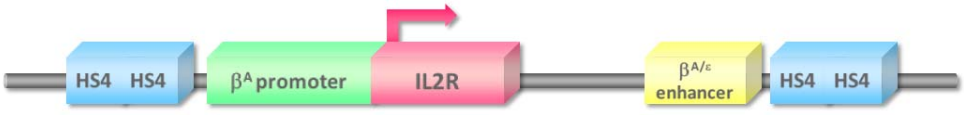

Figure 4.15 Schematic diagram of the *IL2R* reporter construct.

The parent of the E4 and E5 cell lines expressing R2628 RNF20 shRNA described above is 8103 6C2 cells. These characterised lines can therefore be used to monitor the effect of RNF20 knockdown on the barrier activity of the HS4 insulator element using the *IL2R* reporter transgene assay. IL2R expression was monitored by flow cytometry following the staining of cells with an anti-IL2R antibody conjugated to the red fluorescent dye Phycoerythrin (PE). During FACS analysis, only viable cells were gated for further analyses. As the RNF20-shRNA was expressed as a conjugate with GFP (Figure 3.18), RNF20 knockdown cells were gated as GFP expressing

cells for examination of their IL2R expression (Figure 4.16). The mean and median of red fluorescent intensity of this RNF20 knockdown population reflected the expression levels of *IL2R*. The expression level of IL-2R in RNF20 knockdown cells was relative to that of 8103 wild type or no DOX control of the knockdown lines. In order to ensure results were statistically reliable, 10^4 green cells indicating RNF20 knockdown were collected for IL2R expression measurement. For the case of 8103 wild type or no DOX controls, 10^4 viable cells were collected. To determine with the anti-IL-2R antibody was specific, 6C2 cells without integration of the *IL2R* reporter cassette were stained with the antibody and no significant fluorescent signal was detected (Figure 4.17a).

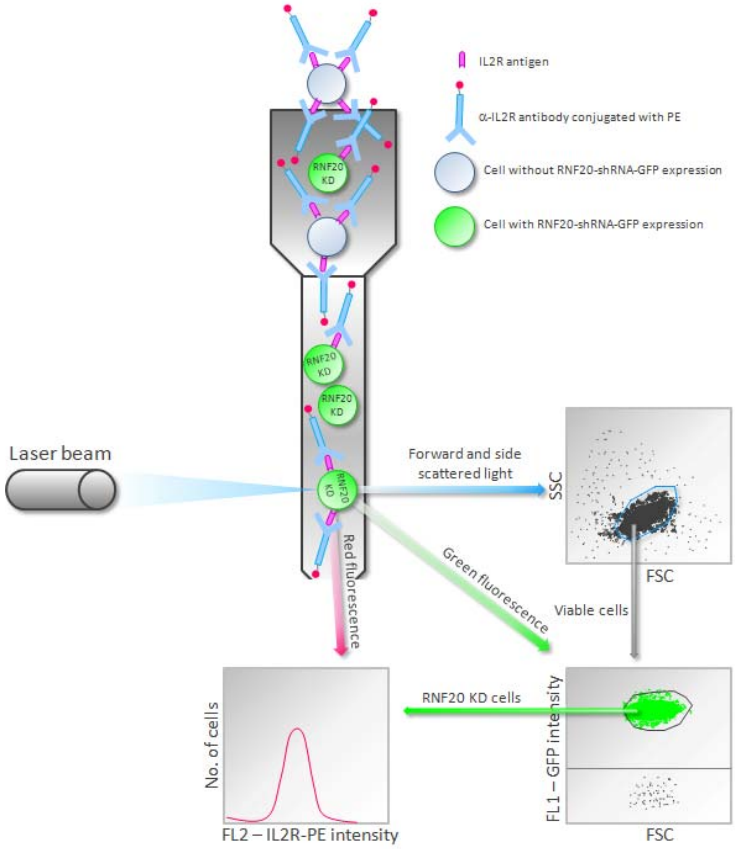

Figure 4.16 Schematic diagram showing FACS analysis of IL2R expression in RNF20 knockdown cells.

RNF20 knockdown was maintained for up to 80 days, to allow occurrence of gene silencing. Experiments with two clones, R2628 E4 and E5, were carried out in parallel to observe changes of IL-2R expression at different time points. The GFP signals of wild type and no DOX treated

RNF20 knockdown cells were measured along the time course to monitor the background noise and leakage of RNF20-specific miRNA in the non-induced conditions (refer to Appendix II for GFP intensities). Due to the unexpected reduction of H3K4me2 and H3K4me3 in untreated R2628 E5 cells following long-term RNF20 knockdown (Figure 4.11), the IL-2R expression level in knockdown cells were compared with wild type 8103 cells. The IL-2R expression in the induced knockdown R2628 E4 clone was compared with that in the uninduced R2628 E4 cells.

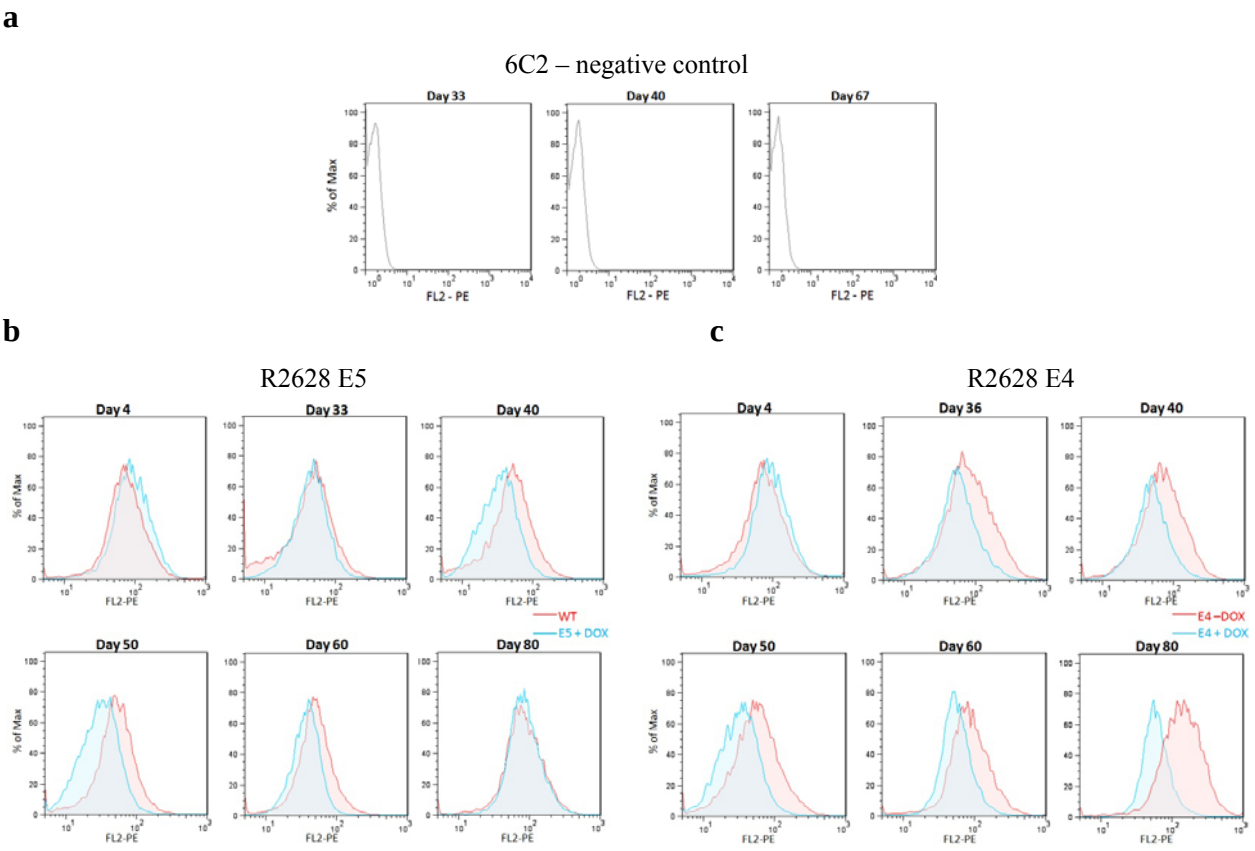

Figure 4.17 FACS analyses of *IL2R* expression in RNF20 knockdown cells. RNF20 knockdown in R2628 E5 and E4 cells was induced by DOX and cells were collected at different time points for *IL2R* expression assessment. Collected cells were stained by IL2R-PE antibody and then subjected to FACS analyses. 6C2 and 8103 wild type cells were grown in parallel as controls. The antibody specificity was examined by 6C2 cells that have no expression of *IL2R* on the cell membrane **(a)**. Only green cells from knockdown cell clones were gated for *IL2R* expression examination so graphs (**b** and **c**) of DOX treated cells showing *IL2R* expression came from 10^4 green cells.

No silencing of the *IL-2R* transgene was observed during the early stages of RNF20 knockdown (Figure 4.17 & Figure 4.18). The transcription of the *IL-2R* transgene is therefore not dependent

upon RNF20 and H2B ubiquitination. However, IL-2R expression in both the E4 and E5 cell lines was progressively repressed with prolonged RNF20 knockdown. IL-2R repression only becomes evident after 30 days of RNF20 knockdown. This is consistent with a previous study, which found that the chromosomal position effect silencing of IL-2R expression from non-insulated transgenes only occurs after 20-40 days of culture in this system [Recillas-Targa *et al*, 2002]. These results are consistent with a disruption of HS4's barrier function following the knockdown of RNF20. The level of IL-2R expression following 80 days of knockdown reached ~65% at the most (Figure 4.18). This level is less than the near total silencing of *IL-2R* transgenes that are flanked by HS4 elements that carry a deletion of the USF binding site [Recillas-Targa *et al*, 2002]. However, the partial repression of insulated *IL-2R* transgenes observed following RNF20 knockdown compares well with that observed in cells transfected with AUSF, a truncated form of USF1 that dominantly inhibits USF1 function [Huang *et al*, 2007]. It can be concluded that constant H2B ubiquitination is required for HS4 to act as a stable barrier to chromosomal silencing.

a

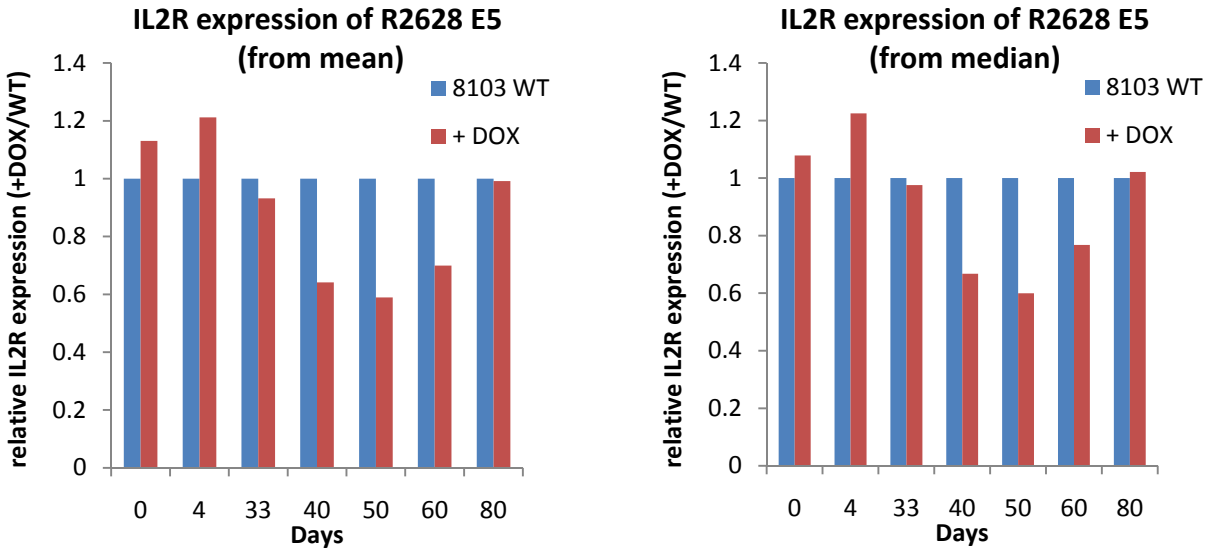

b

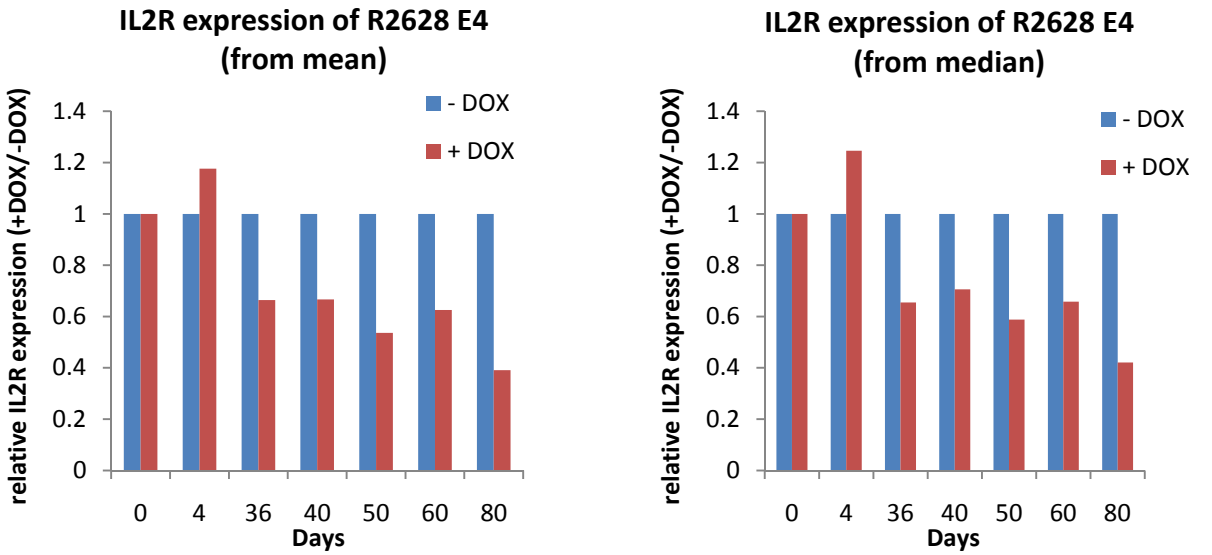

Figure 4.18 Bar chart representations of barrier assay results. Bar charts show the relative expression of *IL2R* in R2628 E5 **(a)** and in R2628 E4 **(b)** where E5 was relative to 8103 wild type and E4 relative to its DOX untreated control. The relative expression was calculated by the mean (left panels) or median (right panels) of the PE fluorescent intensity. The raw fluorescent intensities are shown in Appendix II.

Unexpectedly, the expression *IL2R* in R2628 E5 knockdown cells decreased from Day 33 and to the lowest level on Day 50 but it increased afterwards and reached the level similar to that of wild type on Day 80 (Figure 4.17b & Figure 4.18a). These knockdown cells might have developed an adaption towards the lowered levels of H2BK120ub1 or H3K4me2/3 so that *IL2R* could be fully expressed again.

4.6 The presence of H2BK120ub1 may be universal to chromatin boundary elements

The binding sites of the HS4-binding proteins CTCF, USF1, USF2 and VEZF1 were mapped across the human genome in a previous study in the West laboratory. The identified binding sites are different regulatory elements including promoters, enhancers and putative boundary elements (R. Strogantsev, unpublished data). The positions of insulator protein binding and histone modification profiling were used to identify novel regulatory elements that may function as chromatin boundary elements. These elements contain very similar active chromatin hallmarks to the chicken HS4 boundary element and are located close to the boundaries of heterochromatin-like regions (Table 4.1). These elements have recently been demonstrated to harbour chromatin barrier activity using the *IL-2R* reporter assay described above (G. Barkess, unpublished data).

Putative Boundary Elements	Coordinates	Descriptions
***FLNA* (*filamin A, alpha*) inverted repeat**	Chr X: 153222742 – 153224663 Chr X: 153270597 – 153272488	- CpG islands flanking the *FLNA-EMD* locus - Enriched in H3K4me1/2/3 - CTCF bound
***GMPPA-ACCNA* (*GDP-mannose pyrophosphorylase A – amiloride-sensitive cation channel 4*) locus DHS**	Chr 2: 220081805 – 220084838	- 3 kb long DHS separating two differentially expressed genes *GMPPA* and *ACCN4* - Enriched in H3K4me1/2/3 and H4ac - CTCF bound
***CKMT* (*creatine kinase*) 5' DHS**	Chr 15: 41668992 – 41669954 Chr 15: 41768824 – 41769786	- CpG islands located upstream of the *CKMT* gene - Enriched in H3K4me1/2/3, H3ac and H4ac - CTCF and USF bound
***IGF2* (*insulin-like growth factor 2*) 5' DHS**	Chr 11: 2129014 – 2130307	- DHS separating *IGF2* and *INS* - Enriched in H3K4me1/2 - CTCF bound
***NRXN2* (*neurexin 2*) intragenic DHS**	Chr 11: 64176954 – 64178673	- DHS located in the *NRXN2* gene - Enriched in H4ac - CTCF and USF bound
***EHD1* (*EH-domain containing 1*) 5' DHS C66/16**	Chr: 11: 64411899 – 64412736	- DHS separating *EHD1* and *ATG2A* - Enriched in H3K4me1/2/3 - CTCF bound
SPA1 DHS	Chr 11: 63972553 – 63973655	- CpG island located in a gene poor region identified by ChIP-chip with SPA-tagged VEZF1 - Enriched in H3K4me1/2/3 - CTCF and USF bound

Table 4.1 Descriptions of VEZF1 bound putative boundary elements. Histone modification profiles of these elements aroused from the ENCODE (Encyclopaedia of DNA Elements) project and Dr David Vetrie's group (unpublished data).

Native ChIP analysis of H2BK120ub1 at these putative chromatin boundary elements was performed in transgenic human K562 erythroleukemia cells. The K562 cells were stably transfected with a transgene that contained the HS4 insulator, which can be used as a positive control reference. Other known enhancer and promoter elements were also studied for comparison. It was found that all of the putative barrier elements were enriched with H2BK120ub1 (Figure 4.19). The enrichments were lower than expected from experiments in 6C2 cells, especially at the transgenic HS4 element, indicating this was not a particularly efficient ChIP. The enhancer and promoter of the *SCL* gene, which is actively expressed in K562 cells, are substantially enriched with H2BK120ub1. The promoter and enhancer of the *IL-3* gene,

which is poised for expression in K562 cells, were also enriched with H2BK120ub1. Sites at the *MeCP2*, *KDR* and *CKDN1A* genes, which are not expressed in K562 cells, served as negative controls. These findings suggest that the chromatin boundary elements in human cells may employ H2B ubiquitination in their heterochromatin barrier activity in a manner similar to that of the HS4 element in chicken.

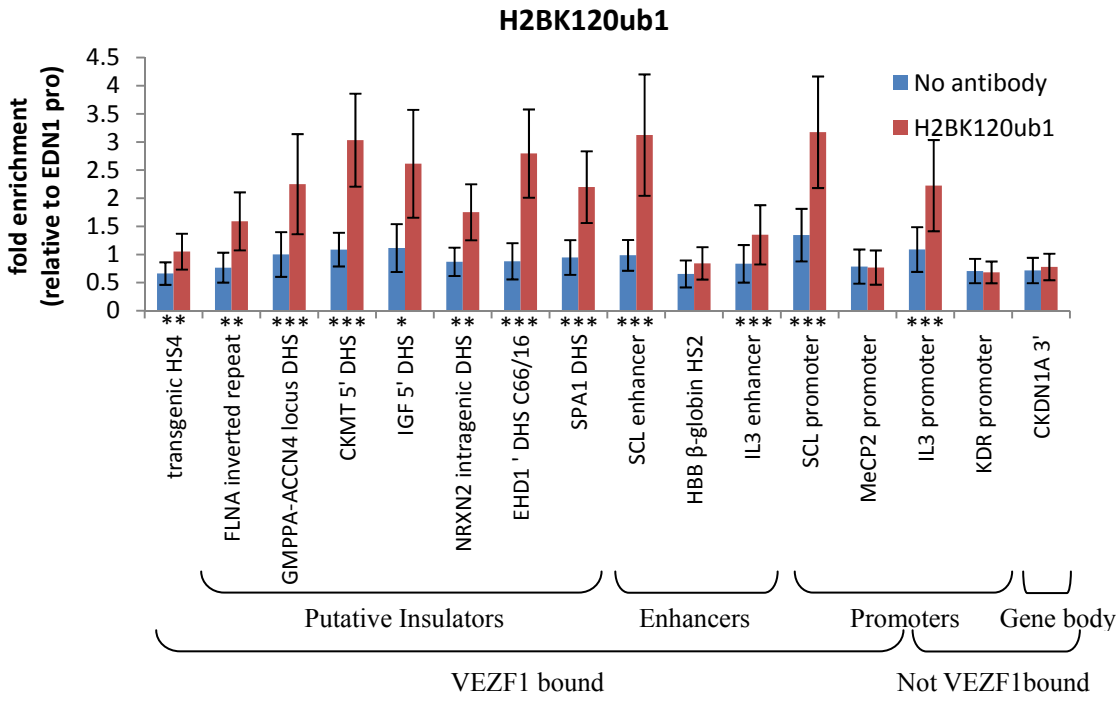

Figure 4.19 Native ChIP analysis with H2BK120ub1-specific antibody in human erythroid K562 cells. The quantitative PCR results were normalised to the promoter of the inactive *EDN1* gene for fold enrichment calculations. Significant differences in fold enrichments between no antibody control and H2BK120ub1 IP with p-values smaller than 0.05, 0.01 and 0.005 are indicated with "*", "**" and "***".

4.7 Discussion

4.7.1 *Trans*-histone crosstalk between H2B ubiquitination and H3K4 methylation occurs at chicken chromatin boundary elements

It has previously been shown that the barrier activity of the HS4 insulator requires active histone modifications, including H3K4 methylation [West *et al*, 2004]. Based on the observations that prior H2B ubiquitination is required for H3K4me2/3 from yeast to mammals, we hypothesised that H2B ubiquitination could be a key component of barrier activity. This study demonstrated that the *FOLR1* HSA/HSB and *β-globin* HS4 elements, located at the boundaries of a region of heterochromatin, are sites of H2B ubiquitination. H2B ubiquitination at these chromatin boundaries was found to be dependent upon the ubiquitin ligase RNF20. Consistent with conserved *trans*-histone crosstalk, H3K4me2 and H3K4me3 were found to decrease globally and locally at the chromatin boundaries upon the knockdown of RNF20.

To examine whether the recruitment of H3K4-specific KMTs to the chromatin boundary elements is lost following H2B ubiquitination depletion, the binding of RbBP5, a shared subunit of the SET1 and MLL complexes, was investigated. Perhaps counter-intuitively, the recruitment of KMT complexes responsible for H3K4 methylation remains intact despite the depletion of H3K4me2/3 in the absence of H2B ubiquitination. This finding is consistent with recent studies of the Set1 complex in budding yeast. It has been shown that H2B ubiquitination facilitates the binding and ubiquitination of Cps35 (also known as Swd2), a subunit of the COMPASS, which augments the processive methyltransferase activity of Set1 to mediate di- and tri-methylation of H3K4 *in vivo* [Lee *et al*, 2007; Vitaliano-Prunier *et al*, 2008]. The Swd2 homolog WDR82 mediates the H2BK120ub1 augmentation of the SET1 complex's activity in humans [Wu *et al*, 2008]. It appears likely that chickens also adopt the same mechanism of H2BK120ub1-mediated H3K4 methylation. Nevertheless, the binding of H3K4 KMTs might depend on H2B ubiquitination at some regulatory elements such as the *FOLR1* HSA and promoter elements, where the binding of RbBP5 reduces following H2BK120ub1 depletion. It also implies the

existence of two or more mechanisms by which H2B ubiquitination can regulate H3K4 methylation. One of them is the identified pathway where H2BK120ub1 stimulates the di- and tri-methylation activity of chromatin bound H3K4 KMTs, whereas the other one may be an unidentified pathway in which H2BK120ub1 is a prerequisite for the binding of some H3K4 KMTs.

4.7.2 H2B ubiquitination may mediate histone acetylation *via* H3K4 methylation to establish the active chromatin signature of chromatin boundaries

This study unexpectedly found that the establishment of multiple histone acetylation marks at chromatin boundaries was also dependent upon prior H2B ubiquitination. The *FOLR1* HSA/HSB elements are highly acetylated and are particularly sensitive even to moderate depletion of RNF20. Whereas the HS4 element requires more substantial RNF20 depletion to result in the loss of its histone acetylation, there are no reports showing H2B ubiquitination is directly linked to histone acetylation and our global histone modification analysis also suggests there is no direct linkage because no significant change of histone acetylation was observed following RNF20 knockdown. A number of KAT complexes have been shown to recognise methylated H3K4, particularly H3K4me3, so the loss of acetylation at chromatin boundary elements may be a consequence of H3K4me3 depletion upon RNF20 knockdown (Section 1.2.5). However, the lack of an effect of RNF20 knockdown on global histone acetylation suggests that other means of histone crosstalk may exist at specific elements such as chromatin boundaries.

Although the loss of H4ac at HS4 following RNF20 knockdown was only observed in the R2628 E5 line but not the R2628 E4 line, the effect does not seem to be due to off target effects of the shRNA. Except the RNF20-dependent marks H2BK120ub1, H3K4 and H3K79 methylation, there were no significant changes of H4 acetylation and other histone modifications in total chromatin (Section 4.2). The protein expression of the insulator proteins that direct H4 acetylation at the chromatin boundaries also unchanged (Section 4.3.5) Ideally, more lines with

different degrees of knockdown and from different potential triggers should be employed in the study so that a more solid conclusion could be drawn. Unfortunately, the other potential trigger R1380 only resulted in one potential clone and it was found to be leaky. Many leaky lines were also resulted from the R2628 trigger so only two lines from this trigger were selected for further study (Section 3.4.3).

H3K9me3 plays a central role in heterochromatin propagation. HP1 acts as an adapter protein that helps H3K9me3 spreading by binding to methylated H3K9 and recruiting H3K9 KMTs. The interaction between HP1 and DNMTs facilitates DNA methylation, which in turn reinforce the H3K9 spreading as the MBDs that bind to methylated DNA associate with H3K9 KMTs and HP1. Moreover, the chromodomain of the SUV39 family of H3K9 KMTs recognising H3K9me3 is another self-reinforcing mechanism (Section 1.3.2.3). H4K20me3 is also associated with heterochromatin and its appearance seems to require prior H3K9me3 as SUV4-20H responsible for H4K20 trimethylation is directed to chromatin regions by HP1, which appears to bridge H3K9 and H4K20 methylation together for heterochromatin spreading [Hines *et al*, 2009; Schotta *et al*, 2004].

To efficiently halt heterochromatin spreading, chromatin barriers need to block H3K9 methylation. As prior deacetylation of H3K9 is required for H3K9 methylation, chromatin barriers could utilise H3K9 acetylation to interrupt the formation of heterochromatin. Consistent with this, it has been shown that USF1 interacts with the H3K9-specific KAT PCAF, which is recruited to the HS4 insulator [West *et al*, 2004]. The methylation of H3K4 also facilitates the acetylation of H3K9 and other histone residues as chromodomain containing proteins present in the SAGA, TAC and TIP60 KAT complexes specifically interact with H3K4me3 (Section 1.2.4). Alternatively, the binding of co-repressor complexes that modify H3K9 can be inhibited by H3K4 methylation. The NuRD and SUV39H1 complexes, which deacetylate and methylate H3H9 respectively, both bind to the N-terminus of H3 that is unmethylated at K4 [Lachner &

Jenuwein, 2002]. In addition, the acetylation of H3, H4 and H2A.Z found at the HSA/HSB and HS4 chromatin boundaries can favour H3K9 acetylation as several KATs that target H3K9 contain bromodomains that bind to acetyl-lysines on other histone tails (Section 1.2.2). The study of the binding of histone modifying enzymes and adaptor proteins such as HP1 following RNF20 knockdown would provide insight into the specific mechanisms adopted by chromatin barriers to prevent H3K9 methylation.

4.7.3 Heterochromatin spreading appears to be initiated promptly following the collapse of chromatin boundaries but takes time to complete

Heterochromatin-associated histone marks were found to propagate in large continuous domains across the *FOLR1* and *β-globin* gene loci following RNF20 knockdown. H3K9me2, H3K9me3 and H4K20me3 were found to propagate in a sequential manner, and the pattern of their propagation is consistent with their spread from the condensed chromatin region flanked by the HSA/HSB and HS4 elements. H3K9me2 was found to rapidly propagate across the *β-globin* and *FOLR1* loci following RNF20 knockdown. This propagation did not affect the expression of the *FOLR1* gene. Given this finding and the fact that the *IL-2R* reporter transgene only becomes repressed after more than 30 days of RNF20 knockdown, suggests that H3K9me2 is not a repressive mark at these loci. Whole genome maps of H3K9me2 show that this mark is more widely distributed than H3K9me3 and is found at euchromatic and heterochromatic loci [Barski *et al*, 2008; Rice *et al*, 2003]. H3K9me3 and H4K20me3 were only found to have spread across the *β-globin* and *FOLR1* loci after 40 days of RNF20 knockdown. H4K20me3 did not spread as far across the *β-globin* locus as H3K9me3 by this stage. The spreading of these marks was coincident with the silencing of *FOLR1* gene expression. This timing also coincides with the repression of the *IL-2R* reporter transgene in the same cells.

The sequential nature of repressive histone mark spreading implies that different KMT complexes mediate each mark, and that the modifications may be pre-requisites for each other.

The identity of the KMT complexes that mediate heterochromatin spreading at the *β-globin* and *FOLR1* loci remains to be determined. H3K9me2-specific KMTs such as G9a and G9a-like protein (GLP) may be recruited immediately upon RNF20 knockdown, leading to H3K9me2 spreading over the entire *FOLR1* gene and ~14 kb into the *β-globin* gene locus. As the binding affinity of HP1 and SUV39H1 to unmethylated H3K9 is low [Stewart *et al*, 2005; Zhang *et al*, 2008], H3K9 trimethylation might not be initiated immediately after the deacetylation of H3K9 at the disrupted HS4 and HSA/HSB barriers. Nevertheless, H3K9me3 is consolidated at the flanks of the condensed chromatin region at this stage. The elevated H3K9me2 at the *FOLR1* and *β-globin* loci may switch on the self-reinforcing H3K9 spreading and then heterochromatin propagation from the condensed chromatin region later on, resulting in the spreading of H3K9me3 to almost the entire ~50 kb *FOLR1* and *β-globin* region after about 40 days of RNF20 knockdown. The spreading of another repressive histone mark, H4K20me3, appears to be the slowest process as it only encompasses the *FOLR1* gene body and ~20 kb *β-globin* region even after 75 days of RNF20 knockdown. It agrees to the previous finding that prior H3K9me3 is required for H4K20 trimethylation [Schotta *et al*, 2004]. The binding of HP1 *via* H3K9me3 to the *FOLR1* and *β-globin* loci may recruit SUV4-20H for H4K20 trimethylation [Hines *et al*, 2009]. The trimethylated state of H4K20 may eventually facilitate chromatin folding leading to the formation of heterochromatin [Lu *et al*, 2008]. Interestingly, the global levels of H3K9me3 and H4K20me3 increase following prolonged RNF20 knockdown. It suggests that not only the chromatin boundaries at the *β-globin* and *FOLR1* loci, but those distributed in the genome rely on H2B ubiquitination to maintain their barrier structures. Collapse of these boundaries resulting from the lowered level of H2BK120ub1 could lead to comprehensive propagation of heterochromatin within the genome.

4.7.4 H2B ubiquitination marks potential chromatin boundary elements

Two other DNase hypersensitive sites HSA and HSB shared similar histone modification profiles with HS4; they are enriched in all active histone modifications examined including

H2BK120ub1. Similar to HS4, many of the active histone modifications of HSA/HSB cannot be maintained in the H2BK120ub1 depleted condition, suggesting the necessity of H2B ubiquitination for the establishment of the active chromatin structure of HAS/HSB. Moreover, USF1, VEZF1 and H3K4-specific KMT (RbBP5) binding to HS4 also appear to be recruited to these two sites. Therefore, it is possible that HSA and HSB function as insulator barriers, maybe for the protection of the upstream *FOLR1* gene from the nearby condensed chromatin region. However, in this study, we could not distinguish whether HSA and HSB cooperate together to form one insulator barrier or they are two separate regulatory elements. HSA is suggested to be a regulatory element of the *FOLR1* gene because unlike HS4, HSA is not constitutively hypersensitive in different cells types and is linked to the *FOLR1* expression, only being permissive in erythroid progenitors that express *FOLR1* [Prioleau *et al*, 1999].

The similarity of histone modification and binding protein profiles between HSA/HSB and HS4 suggests there is a possibility that, HSA/HSB interacts with HS4 physically to loop out the 16 kb condensed chromatin region between them. HSA/HSB and HS4 flank the condensed chromatin region and their interaction could reinforce the blocking of heterochromatin. While chromosomal looping is currently linked to the separable enhancer blocking activity of insulators, it might also occur for insulator barriers. It was shown in yeast that artificial tethering to nuclear pore complexes can support heterochromatin barrier activity [Ishii *et al*, 2002]. The condensed chromatin region separating the *FOLR1* and *β-globin* loci is present in all developmental stages of erythroid cells while HSA is absent in terminally differentiated erythroid cells that do not express *FOLR1* [Prioleau *et al*, 1999]. It suggests that this silent chromatin region may act as a source of silencing and ensure the two loci can be regulated independently. If it is the case, the looping model seems to be unlikely as the condensed chromatin region could not afford to be looped out. As HS4 is constitutively hypersensitive, silencing of the *β-globin* genes may not be dependent on the condensed chromatin region and more importantly, HS4 cannot rely on HSA to maintain its permissive chromatin structure during different developmental stages. If HSA/HSB

does not form a loop with HS4, HSA/HSB and HS4 might function separately by forming two independent barriers. Examination of the HSA and HSB barrier activity with barrier assay would unravel their functioning mechanism and determine whether they can independently function as a heterochromatin barrier.

Native ChIP analysis also demonstrated that all examined putative chromatin boundaries are enriched in H2BK120ub1, this scenario is not observed in other regulatory elements, suggesting that H2B ubiquitination is not unique to HS4; other chromatin boundaries may also require H2B ubiquitination. The similar histone modification profiles between HSA/HSB and HS4 suggest that histone modification profiling would help identify new chromatin barrier.

CHAPTER 5

Deposition and acetylation of H2A.Z at insulator elements by VEZF1

5.1 Objectives

It was demonstrated in the last chapter that the HSA/HSB and HS4 chromatin boundaries are both sites of H2A.Z incorporation (Section 4.3.4). A role for the htz1 paralog in chromatin barrier activity has been demonstrated in budding yeast (Section 1.1.2.2), but the role of H2A.Z at vertebrate chromatin barriers is undetermined. We have found that while the acetylation of H2A.Z is linked to the histone modification pathways that are dependent on RNF20, its deposition does not appear to be strictly dependent upon these processes (Section 4.3.4). It is therefore of interest to determine how H2A.Z is deposited at chromatin boundaries and whether it plays a critical role in boundary formation and stability.

The barrier activity of the HS4 insulator element requires both the binding sites for VEZF1 and USF proteins. While USF proteins direct histone modification, VEZF1 is associated with the control of DNA methylation (Section 1.5.4). To better understand the role of VEZF1 in barrier activity, Dr. Dan Li in the group of Dr. Adam West has identified VEZF1 binding proteins using mass spectrometry analysis of purified complexes. No factors with an obvious role in DNA demethylation were identified, but VEZF1 was found to interact with many histone modifying enzymes and chromatin remodelling complexes. Of which, several components of complexes involved in the deposition and acetylation of histone variant H2A.Z were identified (Figure 5.1) (D. Li, unpublished observations).

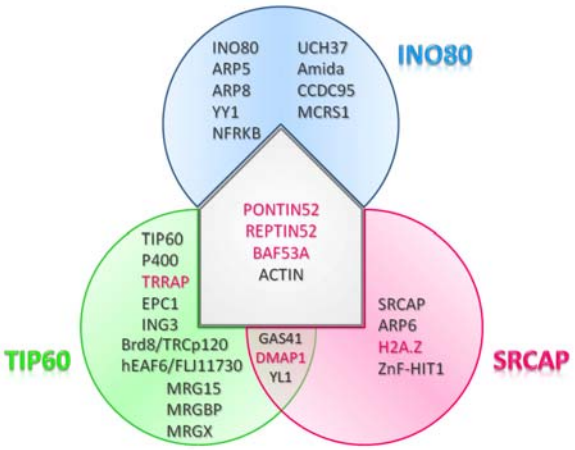

Figure 5.1 Mammalian protein complexes involved in H2A variant deposition. The INO80 (Inositol-requiring protein 80) complex is required for H2A.X incorporation and yeast H2A.Z deposition while TIP60 (Tat interacting protein 60 kDa) and the SRCAP (Snf-2-related CREB-binding protein activator protein) complexes are responsible for H2A.Z deposition [Jin *et al*, 2005; Papamichos-Chronakis *et al*, 2011; Ruhl *et al*, 2006]. TIP60 can acetylate H2A.Z, H2A and H4. The protein subunits shown in red are identified as VEZF1 interacting partners using mass spectrometry (D. Li, unpublished data). These three protein complexes are ATP-dependent chromatin remodelling complexes and share the subunits PONTIN52, REPTIN52 (also known as RUVBL1 and RUVBL2 respectively), BAF53A (BRG1/brm-associated factor (BAF) complex 53 kDa subunit) and ACTIN.

It has been previously found that there is an inverse correlation between DNA methylation and H2A.Z occupancy in plants and vertebrates (Section 1.1.2.2). Collectively, these observations lead to the hypothesis that VEZF1 may contribute barrier activity at chromatin boundaries by facilitating deposition of H2A.Z. This chapter addresses this hypothesis in the following objectives.

Objective 1. Determination whether VEZF1 recruits H2A.Z deposition complexes to the HS4 insulator

a) Analysis of proteins immunoprecipitated with FLAG tagged VEZF1

b) Analysis of SRCAP/TIP60 subunit binding to the transgenic HS4 element in human K562 cells

c) Analysis of H2A.Z deposition and acetylation at HS4 mutants with protein site deletions

Objective 2. Determine whether H2A.Z deposition/acetylation is a common feature at human chromatin boundary elements

a) Analysis of H2A.Zac at human chromatin boundary elements bound by VEZF1

b) Analysis of the SRCAP/TIP60 subunit at human chromatin boundary elements

Objective 3. Determine whether VEZF1 is required for H2A.Z incorporation at human chromatin boundaries

a) Development of clonal human cell lines that carry inducible and stable VEZF1 knockdown vectors

   i. Analysis of VEZF1 protein levels

   ii. Analysis of VEZF1 binding to characterised target sites

   iii. Analysis of global histone modification levels following VEZF1 depletion

b) Analysis of the following histone modifications at human chromatin boundary elements before and after VEZF1 knockdown

   i. H2A.Z deposition and acetylation

   ii. H3 acetylation and H3K4 dimethylation

5.2 Determine whether VEZF1 recruits H2A.Z deposition complexes to the HS4 insulator

5.2.1 Analysis of proteins immunoprecipitated with FLAG tagged VEZF1

Peptides from H2A.Z and the proteins of the SRCAP/TIP60 complexes, PONTIN52, REPTIN52, BAF53A, TRRAP and DMAP1, were identified in VEZF1 protein complexes (D. Li, unpublished data). To further validate the interaction between VEZF1 and the SRCAP/TIP60 complexes, co-immunoprecipitation (Co-IP) experiments were performed and the presence of complex subunits was assessed by western blotting analyses. Co-IP experiments were performed in human cells as the antibodies used in western blotting analyses were all raised against human protein peptides and a stable cell line expressing tagged VEZF1 had been available.

A stable cell line D3/6, originated from human myelogenous leukaemia line K562 carrying a SPA (sequential purification affinity) tagged version of VEZF1, had been generated and routinely maintained in the lab. The SPA tag consisting of CBP (calmodulin-binding peptide) and FLAG tags was conjugated at the C-terminal of VEZF1 to allow sequential purification steps (Figure 5.2). VEZF1-SPA in the cell line was expressed at the level around 50% of the endogenous one. Such double tag system is a widely used approach for purification of protein complexes because of the higher purity compared with the single individual purification [Rigaut *et al*, 1999]. Another cell line, S3F1, was a vector control line that only expressed the SPA tag. Nuclear extracts prepared from these two lines were subject to FLAG affinity immunoprecipitation to test whether the SRCAP and TIP60 complex factors interact with VEZF1 *in vivo*.

Figure 5.2 SPA tagged VEZF1 protein expressed in the D3/6 line. The two tags, CBP and 3X FLAG, were expressed at the C-terminal of VEZF1. A TEV cleavage site located in between the tags allowed FLAG tag removal by TEV protease.

The SRCAP, TIP60 and INO80 shared protein subunits, PONTIN52, REPTIN52 and BAF53A, were detected in the FLAG-VEZF1 immunoprecipitates. H2A.Z was also pulled down with VEZF1 (Figure 5.3). However, H2A.Z and PONTIN52 were detected in the negative control SPA immunoprecipitates but the levels were much lower. Another SRCAP subunit, ARP6 (Actin-related protein 6) [Altaf *et al*, 2009], was enriched in the immunoprecipitates of FLAG-VEZF1 so VEZF1 may recruit the SRCAP complex to its binding sites (Figure 5.3), although the recruitment may not be necessarily to be *via* ARP6. To minimise non-specific binding detected in the control immunoprecipitates, optimisation of Co-IP conditions for PONTIN52, H2A.Z and ARP6 is required. Although VEZF1 appears to interact with the H2A.Z deposition complexes, the interaction between VEZF1 and SRCAP could not be detected in this study (Figure 5.3). There were technical difficulties in western blotting detection of SRCAP due to its large molecular weight. The expected SRCAP molecular weight is 344 kDa, such large molecular weight protein is not easy to be transferred to a membrane from a SDS-PAGE in western blotting assay. Moreover, the putative SRCAP band detected in the input materials was larger than expected; it migrated slower than the 460 kDa protein marker. It might be due to post-translational modifications that increase the actual size of SRCAP or the band might not be *bona fide* SRCAP.

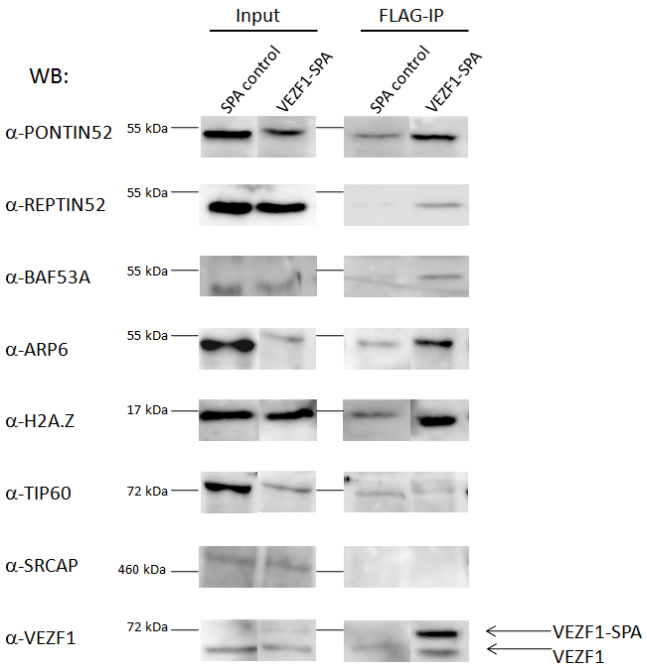

Figure 5.3 Interaction between VEZF1 and SRCAP/TIP60 complexes' subunits. Nuclear extracts of VEZF1-SPA (D3/6 line) and SPA alone expressing (S3F1 line) K562 cells were prepared for immunoprecipitation using FLAG affinity agarose. After extensive washing, bound proteins were eluted by boiling with 2X SDS loading buffer for 10 minutes. The presence of target proteins was examined by western blotting with protein-specific antibodies. All blots for detection of the same protein were run on the same gel and bands were visualised under the same exposure conditions. Some lanes were rearranged for presentation.

Despite the high H2A.Zac level at the HS4 insulator element (see no DOX controls in Figure 4.6b & c), no TIP60-VEZF1 interaction was identified in the previous mass spectrometry analysis (D. Li, unpublished data) and in this Co-IP experiment (Figure 5.3). TIP60 is the catalytic subunit of the TIP60 complex, capable of acetylating H2A, H4 and H2A.Z [Ikura *et al*, 2000]. The failure of detecting TIP60 in VEZF1-SPA immunoprecipitate might be because less input material was used (see input of SPA control and VEZF1-SPA lines for TIP60 detection in Figure 5.3) or because the interaction is transient that it is easy to be disrupted during cell lysis. The tagged version of VEZF1 might induce improper folding of the VEZF1 protein or block the binding to some interacting proteins such that the interaction between TIP60 or other undetectable protein subunits are interrupted. Performing immunoprecipitation with anti-VEZF1 or anti-complex subunit antibodies may help resolve these potential problems. Nevertheless, the interaction of VEZF1 with several SRACP subunits and H2A.Z suggests that VEZF1 is at least involved in H2A.Z deposition.

5.2.2 The shared subunits of TIP60 and SRCAP complexes are detected at HS4

To study whether H2A.Z deposition and acetylation at HS4 were mediated by the TIP60 and SRCAP complexes, crosslinking ChIP was performed. Ideally, the assay performed in chicken 6C2 cells would reflect the real scenario at HS4 in the genomic contexts. Unfortunately, no antibodies had been confirmed to be specific to the chicken orthologs. To minimise non-specific binding of antibodies to chicken proteins leading to false positive or negative results, crosslinking ChIP was then performed in human K562 cells carrying transgenic HS4, which had been shown to be enriched in H2A.Zac (Figure 5.6).

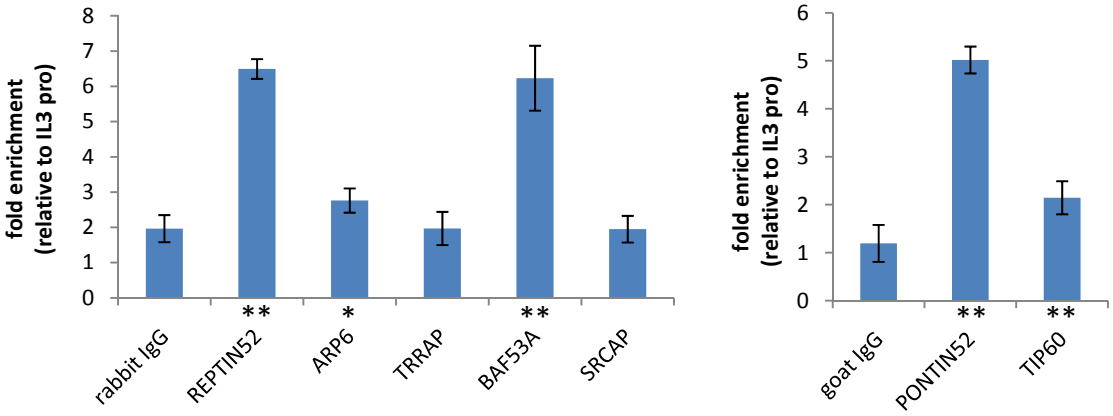

Figure 5.4 Detection of the protein subunits of TIP60 and SRCAP complexes at HS4 using crosslinking ChIP. K562 cells carrying the transgenic HS4 element (S3F1 cell line) were crosslinked with 1% formaldehyde at room temperature for 30 minutes. Chromatin was sonicated and immunoprecipitation with specific antibodies followed. Fold enrichments of HS4 sequences immunoprecipitated from ChIP were normalised to that of *IL3* (*interleukin-3)* promoter where H2A.Zac was at a low level (Figure 5.6). Significant enrichments, compared with the non-immunised antibody controls, with p-values smaller 0.01 and 0.005, are indicated with "*" and "**", respectively.

The shared subunits of TIP60 and SRCAP complexes, REPTIN52, BAF53A and PONTIN52, were found at HS4 (Figure 5.4). TIP60 and ARP6 were also detected although the level was low but still statistically significant. It suggests that H2A.Z deposition and acetylation at HS4 are mediated by the TIP60/SRCAP complexes. However, SRCAP and TRRAP were undetectable at HS4 in this assay (Figure 5.4 right panel). The crosslinking condition might not be optimal for their detection or the antibodies did not perform well in immunoprecipitation. SRCAP and TRRAP in particular, they are large proteins so there were always some difficulties in western blotting analyses (see SRCAP in input lanes Figure 5.3). Therefore, it is still not clear whether they can detect the specific proteins in human nuclear extracts. Further optimisation of crosslinking ChIP assays is needed to confirm these two structural subunits of the TIP60 and SRCAP complexes are recruited to HS4 because REPTIN52, PONTIN52 and BAF53A are not only present in the TIP60, SRCAP and INO80 complexes. These protein subunits are associated with many other chromatin protein complexes involved in different chromatin accessing abilities such as transcription and DNA repair [Jha & Dutta, 2009].

5.2.3 The VEZF1 and USF binding sites are required for the H2A.Z deposition of HS4

It has been shown that HS4 and HSA/HSB are enriched in H2A.Zac in a H2B ubiquitination-dependent manner [Bruce *et al*, 2005] (Figure 4.6). However, H2A.Zac is not enriched at the CTCF bound 3' HS enhancer blocker, suggesting that H2A.Z and H2A.Zac does not simply flank DNase I hypersensitive sites. CTCF bound enhancer blockers may not rely on H2A.Z incorporation for the enhancer blocking activity although there is a genome-wide correlation of the CTCF and H2A.Z occupancies [Barski *et al*, 2007; Fu *et al*, 2008]. H2A.Z, rather, may be more closely associated active histone modifications.

VEZF1 is not required for H2B ubiquitination at HS4 as it has been shown that deletion of one of the VEZF1 binding sites does not result in a loss of histone ubiquitination (Figure 1.39). Nevertheless, the H2A.Z deposition and acetylation at HS4 may be recruited by VEZF1 when signalled by H2B ubiquitination. In order to examine whether the VEZF1 binding sites are required for the H2A.Z deposition and acetylation, native ChIP was performed in 6C2 cell lines integrated with the transgenic HS4 elements carrying footprint deletions. The constructs were similar to those for the reporter assay carried out in Section 4.5. The entire transgenic cassette was flanked by two copies of HS4 at each side while a footprint was deleted at each copy of HS4 (Figure 5.5c). Fold enrichments of H2A.Z and H2A.Zac at examined sites were relative to the *FOLR1* promoter, which is enriched in both H2A.Z and H2A.Zac [Bruce *et al*, 2005] (see no DOX in Figure 4.6). The endogenous HS4 element served as an internal control to indicate whether there was dramatic difference in ChIP efficiency between cell lines.

H2A.Z deposition appears to require both VEZF1 and USF binding but not that of CTCF. VEZF1 binding sites (FI, FIII and FV) were crucial for the H2A.Z deposition of HS4, although the effect of footprint III deletion was relatively mild (Figure 5.5a). Deletion of one of the VEZF1 binding sites could not abolish the H2A.Z incorporation at the transgenic HS4 element completely; it may be due to the residual VEZF1 binding from the other two binding sites.

Contrastingly, the USF binding site, the one essential for H3K4 dimethylation at HS4, was of particular importance to H2A.Z deposition. Deletion of the USF site led to an almost complete loss of H2A.Z at both the 5' and 3' transgenic HS4 elements (Figure 5.5a). The result also suggests that H2A.Z deposition might interplay with other active histone modifications. Deletion of footprint II, the CTCF binding site, only caused a mild loss of H2A.Z at the 5' transgenic HS4 while the H2A.Z level at the 3' transgenic HS4 remained unchanged (Figure 5.5a). Taken together with the absence of H2A.Z at 3' HS, another CTCF binding site at the *β-globin* locus, it suggests that CTCF may not be responsible for the H2A.Z deposition although the binding sites of CTCF show overlapping with the H2A.Z sites in genome-wide studies [Barski *et al*, 2007; Fu *et al*, 2008].

Given a general positive correlation between transcription activity and H2A.Z occupancy, deletion of any footprint binding sites except the CTCF binding site resulted in a loss of H2A.Z at the *IL2R* coding region is in agreement with the silencing effects of footprint deletions on the *IL2R* expression [Barski *et al*, 2007; Recillas-Targa *et al*, 2002].

Unexpectedly, the patterns of H2A.Z acetylation at HS4 mutants did not correlate with the H2A.Z deposition. Although all HS4 mutants located at the 5' end of the cassette had lower levels of H2A.Z compared with wild type, there were only moderate reductions in H2A.Zac at the HS4 mutants missing either the VEZF1 (FV) or USF (FIV) binding sites. H2A.Zac of HS4 mutants without one of the VEZF1 binding sites, FI and FIII, even retained at similar levels compared with wild type (Figure 5.5b). The discrepancy between the H2A.Zac and H2A.Z may be because ChIP of H2A.Zac did not perform equally well in all cell lines, suggested by an observation that H2A.Zac at the internal control, the endogenous HS4 elements, varied between the lines (Figure 5.5b). Nevertheless, the H2A.Zac level across the transgenic cassette did not decrease if there was no CTCF binding site at the HS4 mutant, consistent with the pattern of H2A.Z deposition.

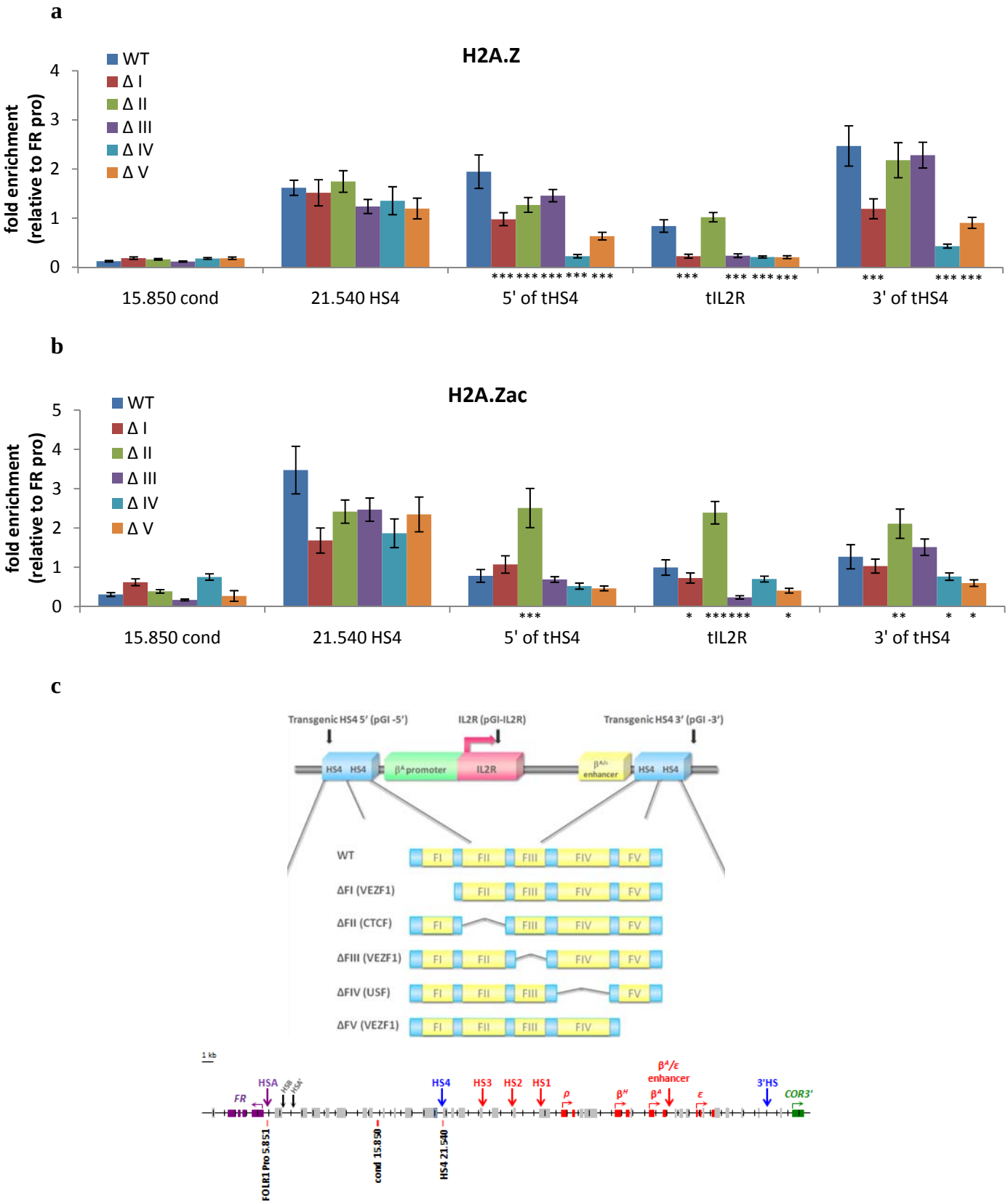

Figure 5.5 Native ChIP analyses of H2A.Z **(a)** and H2A.Zac **(b)** at the footprint deleted HS4 elements. Fold enrichments were relative to the *FOLR1* promoter (5.851). Significant differences in fold enrichments between wild type and footprint deleted HS4 with p-values smaller than 0.05, 0.01 and 0.005 are indicated with "*", "**" and "***", respectively. **c**. Schematic diagram of the footprint deletion constructs. Primers used for studying the transgenic reporter cassette (upper panel) and the chicken *β-globin* locus (lower panel).

5.3 Determine whether H2A.Z deposition is a common feature at human chromatin boundary elements

5.3.1 Analysis of H2A.Zac at human chromatin boundary elements bound by VEZF1

The results of the Co-IP assay and native ChIP study at the footprint deletion HS4 elements suggest that VEZF1 plays a role in H2A.Z deposition. It was shown that H2A.Zac is of particular importance for chromatin barriers to block heterochromatin spreading in yeast [Babiarz *et al*, 2006] but whether H2A.Zac is essential for vertebrate chromatin boundaries remains unclear. Native ChIP with H2A.Zac-specific antibody was carried out to study whether H2A.Zac is enriched at the VEZF1 bound chromatin barriers (refer to Table 4.1 for description of the barriers). Result showed that H2A.Zac was enriched at some but not all VEZF1 bound putative barriers (Figure 5.6). Only the *FLNA* inverted repeat, *GMPPA-ACCNA* locus DHS, *CKMT* 5' DHS, *EHD1* 5' DHS and SPA1 DHS had higher or similar levels of H2A.Zac compared with HS4. Like HS4, all of these five elements are able to protect a transgene from silencing in long term culture (G. Barkess, unpublished data). However, acetylation of H2A.Z did not appear to be a universal signature for the VEZF1 binding sites that the function of VEZF1 could be site-specific. Two of the examined putative insulators, the *IGF2* 5' DHS and the *NRXN2* intragenic DHS, the *β-globin* HS2 and the *IL3* enhancers, were not enriched in H2A.Zac. The *IGF2* 5' DHS was not able to protect a transgene from chromatin silencing in the barrier assay, suggesting that it may not be a genuine chromatin barrier (G. Barkess, unpublished data). The full length *NRNX2* intragenic DHS element encompassing > 1000 bp can maintain expression of a transgene in a reporter assay (G. Barkess, unpublished data) despite of that H2A.Zac was not detected. It is possible that the short PCR amplicon (~170 bp) might have missed the site enriched in H2A.Zac. Alternatively, this putative barrier may not require H2A.Zac for its barrier activity. More sites of the *NRNX2* intragenic DHS element need to be studied to determine which scenario is more likely.

Consistent with the previous genome-wide study in yeast showing that transcription activity is positively correlated with H2A.Zac [Millar *et al*, 2006], the actively expressing *SCL* (stem cell leukemia) gene in K562 [Rath *et al*, 1997] was also enriched in H2A.Zac at its promoter and enhancer. *MeCP2* (*methyl CpG binding protein 2*), *IL3* and *β-globin* silent in K562 cells [Chen *et al*, 1994; Fordis *et al*, 1984; Weber-benarous *et al*, 1988; biogps.gnf.org] had low levels of H2A.Zac at their promoters or enhancers. However, the low levels of H2A.Zac at these sites do not seem to be because of reduced VEZF1 binding as the *MeCP2* promoter is still bound by VEZF1 at a high level in K562 cells (see no DOX in Figure 5.9). These results suggest that VEZF1 play different roles at different binding sites, not only restricted to facilitate H2A.Z deposition and acetylation.

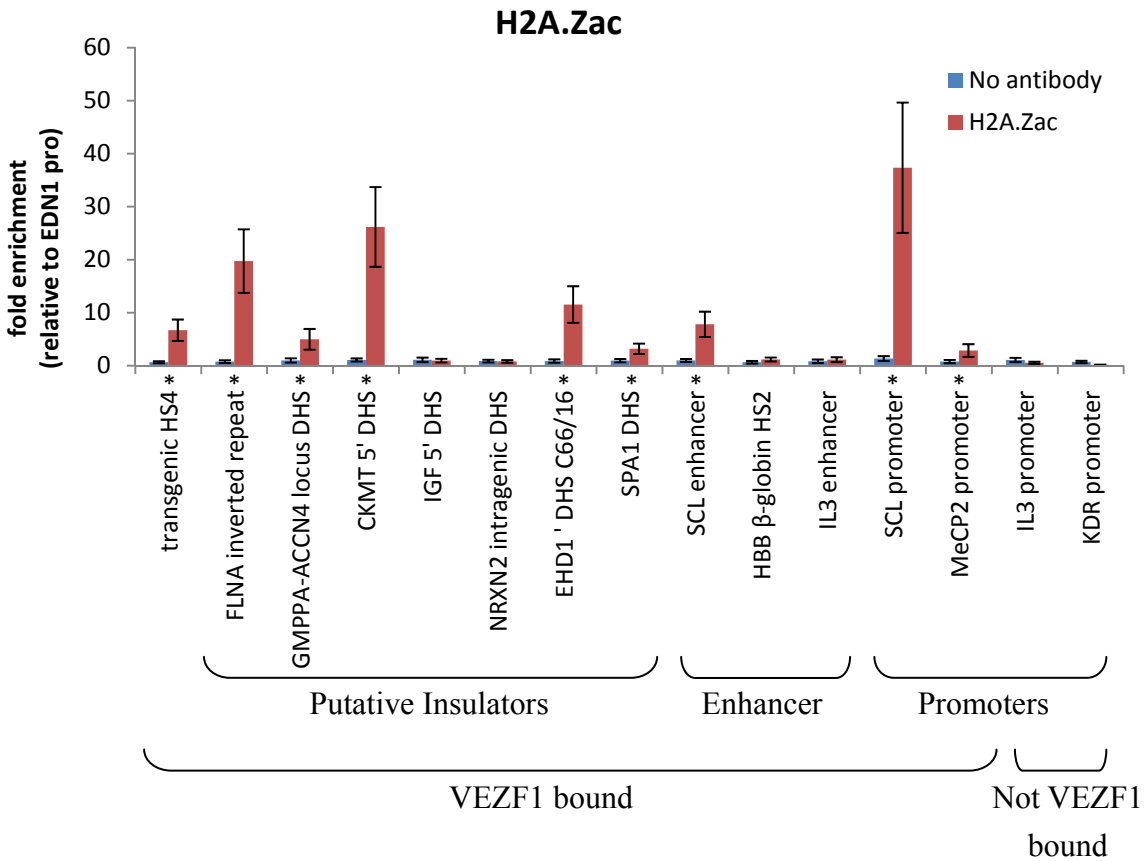

Figure 5.6 ChIP analysis of H2A.Zac at transgenic HS4 and the VEZF1 bound elements. Low salt ChIP was performed in K562 cells incorporated with transgenic HS4. Fold enrichments of H2A.Zac were calculated by normalising to the *EDN1* (*endothelin 1*) promoter, which is supposed to be inactive due to the low expression of *EDN1* in K562 cells. VEZF1 does not bind to the *EDN1*, *IL3* and *KDR* (*kinase insert domain receptor*) promoters in K562 cells. Significant enrichments ($p<0.001$) are asterisked.

5.3.2 Analysis of the SRCAP/TIP60 subunit at human chromatin boundary elements

To determine if VEZF1 directs H2A.Z acetylation at the putative boundary elements by recruiting the SRCAP and TIP60 complexes, crosslinking ChIP was performed. The binding of PONTIN52, REPTIN52 and BAF53A were examined at the VEZF1 bound putative boundaries as an indicator of the recruitment of the SRCAP or TIP60 complexes because crosslinking ChIP with these three antibodies seemed to perform better than the others (Figure 5.4).

Similar to HS4, H2A.Z deposition and acetylation at the VEZF1 bound putative chromatin boundaries seems to be mediated by the SRCAP or TIP60 complexes. In general, sites enriched in H2A.Zac had significant high levels of REPTIN52 and PONTIN52, and some but not all of them were also bound by BAF53A. REPTIN52 and PONTIN52 were recruited to the *FLNA* inverted repeat, *GMPPA-ACCN4* locus DHS, *CKMT* 5' DHS and the *SCL* enhancer and promoter, mirroring the substantial enrichments of H2A.Zac (Figure 5.7a & b for PONTIN52 and REPTIN52, Figure 5.6 for H2A.Zac). Contrastingly, the *NRXN2* intragenic DHS and the *KDR* promoter showing low H2A.Zac levels did not recruit these remodelling proteins. However, the recruitment of BAF53A did not follow the H2A.Zac pattern. BAF53A bound to the *FLNA* inverted repeat and slightly to the *GMPPA-ACCN4* locus DHS and *SCL* promoter, while the *CKMT* 5' DHS and *SCL* enhancer did not have detectable BAF53A despite of their recruitment of REPTIN52 and PONTIN52 as well as high levels of H2A.Zac (Figure 5.7c). This suggests that BAF53A might not be essential for the H2A.Z deposition or acetylation although it is always present in the complexes responsible for that. Alternatively, REPTIN52 and PONTIN52 might work at those elements with other complexes that BAF53A is not involved. It might be also because BAF53A was not be accessed by the antibody equally at all sites due to the presence of other complex subunits. Optimisation of ChIP condition may help the detection as the ChIP efficiency was not indeed very high, suggested by the low enrichments at the sites with detectable BAF53A.

a

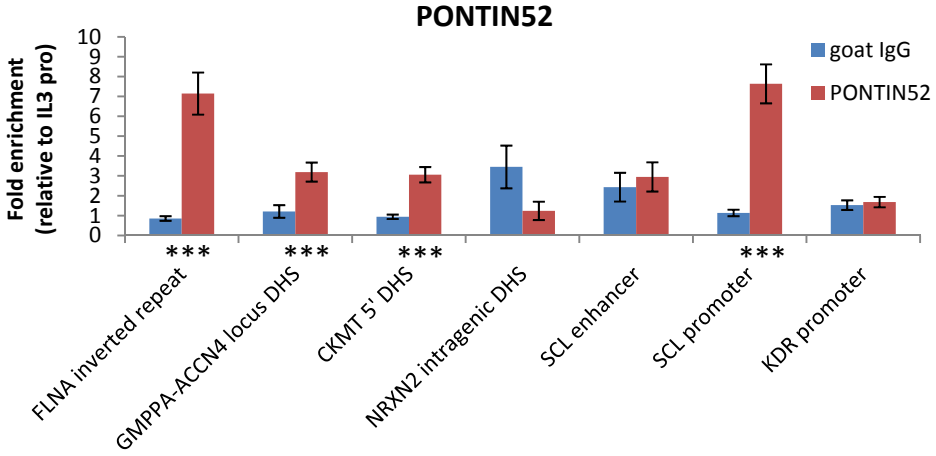

b

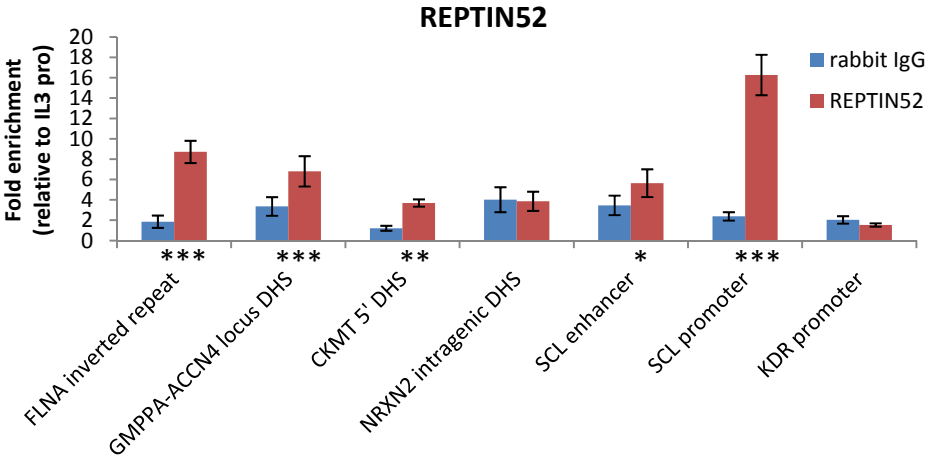

c

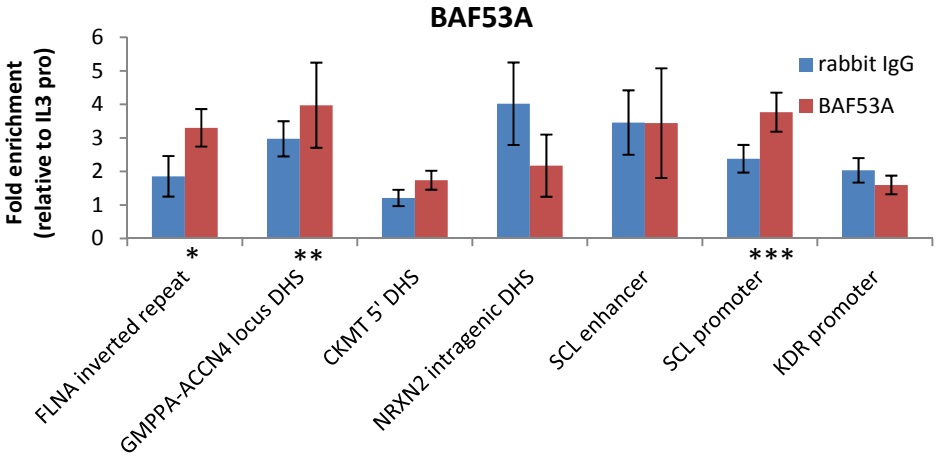

Figure 5.7 Crosslinking ChIP analyses of recruitment of PONTIN52 **(a)**, REPTIN52 **(b)** and BAF53A **(c)** at VEZF1 bound elements. Normalisation of quantitative PCR data was performed by choosing the *IL3* promoter as a control region where H2A.Zac was not enriched as shown inFigure 5.6. Significant enrichments are represented with asterisks (*=p<0.05,**= p<0.01 and ***=p<0.005).

5.4 Determine whether VEZF1 is required for H2A.Z incorporation at human chromatin boundaries

5.4.1 Development of clonal human cell lines that carry inducible and stable VEZF1 knockdown vectors

Our results have demonstrated that the VEZF1 bound insulator elements are generally enriched in H2A.Zac. To study if VEZF1 plays a major role in the H2A.Z deposition and acetylation, inducible VEZF1 knockdown K562 cell lines had been established by Dr. Alan Hair and Dr. Ruslan Strogantsev. The design of VEZF1 shRNA triggers for VEZF1 knockdown was based on the same criteria used for the RNF20 shRNA design (Section 3.4.1) (R. Strogantsev, unpublished data). The potential shRNA triggers were cloned into the lentiviral shRNA expression vector system (Figure 3.18) and lentiviral particles containing the vector cassette were used to transduce human K562 cells. The expression of VEZF1-specific miRNA was induced by DOX addition and indicated by GFP expression. Potential clones were screened by Dr. Ruslan Strogantsev using RT-PCR and western blotting analyses.

5.4.1.1 Analysis of VEZF1 protein levels

To further confirm the selected clone was effective in VEZF1 knockdown and the expression of VEZF1 could be recovered after DOX removal, western blotting analysis of VEZF1 was performed. VEZF1 knockdown was induced by DOX addition for two days and a portion of cells was transferred to DOX free medium and then kept growing for seven days to allow recovery of the expression of VEZF1 while the rest of the cells continued to be grown in the presence of DOX. Nuclear extracts prepared from cells harvested on Day 2 and 9 were subject to western analysis. Result of western blotting showed that VEZF1 knockdown was significant upon DOX induction, VEZF1 was knocked down by 80% following two-day induction (**Figure 5.8**). Moreover, the VEZF1 knockdown was reversible although the recovery was not complete that only 60% of VEZF1 was expressed in recovered cells compared with uninduced cells (-DOX) (Figure 5.8).

a

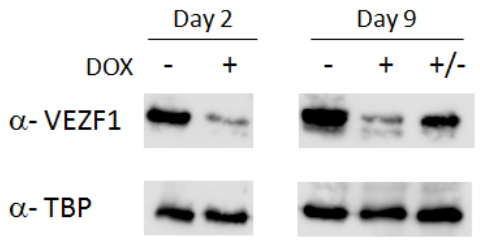

b

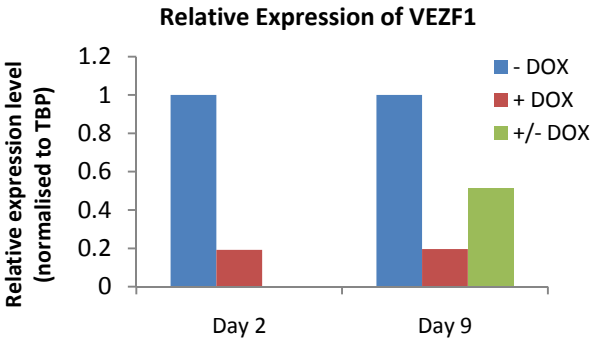

Figure 5.8 Western blotting analysis of VEZF1 expression following DOX induced knockdown. The expression of VEZF1-specific miRNA was induced by DOX (+ DOX) for two days and then half of the knockdown cells were grown in DOX free medium for seven days to rescue the VEZF1 expression (+/- DOX). Cells without DOX treatment (- DOX) were grown in parallel as a control. Cells were harvested on Day 2 and Day 9 for nuclear extraction to examine their VEZF1 protein level by western blotting **(a)**. TBP served as a loading control for normalisation. Relative protein expression was calculated from band intensities **(b)**.

5.4.1.2 Analysis of VEZF1 binding to characterised target sites

Although the protein level of VEZF1 was significantly reduced following knockdown, the remaining VEZF1 in cells might still give rise to substantial binding to the target sites, potentially diluting the knockdown effects in further studies. To examine whether the binding of VEZF1 at its target sites was significantly reduced following knockdown, crosslinking ChIP was carried out with anti-VEZF1 antibody after nine days of VEZF1 knockdown. Consistent with the VEZF1 protein level, VEZF1 binding to all examined binding sites were reduced in knockdown cells and it increased after recovery (Figure 5.9). The VEZF1 binding, however, could not be fully rescued in the recovered cells, possibly due to the incomplete recovery of the VEZF1 expression (Figure 5.8).

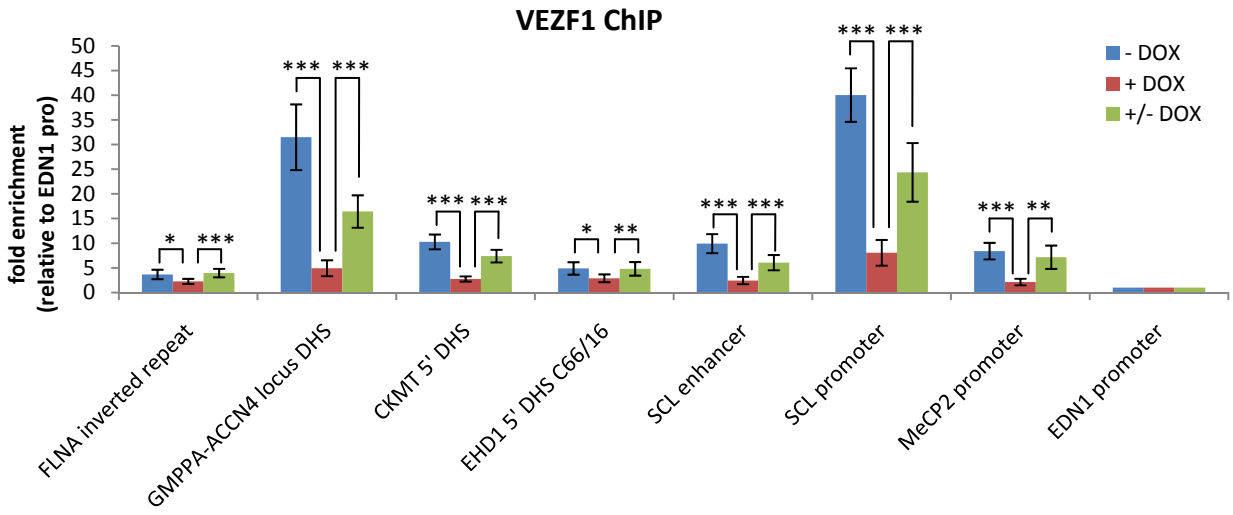

Figure 5.9 ChIP analysis of VEZF1 binding following VEZF1 knockdown and expression recovery. DOX was administrated to induced VEZF1 knockdown for nine days (-DOX) while recovery cells (+/- DOX) were firstly treated with DOX for two days and then DOX was removed for seven days to allow expression recovery. All cells including the untreated control were harvested and crosslinked on Day 9 for ChIP analysis. The relative enrichment was normalised to the *EDN1* promoter where had no VEZF1 binding in K562 cells. Significant changes of VEZF1 binding following knockdown and expression recovery are indicated with asterisks (*=p<0.05, **=p<0.01 and ***=p<0.005).

5.4.1.3 Analysis of global modification levels following VEZF1 depletion

There is emerging evidence that proteins physically interact are sometimes correlated genetically. They could be involved in the regulation of gene expression of their interacting partners [Walhout & Vidal, 2001]. While VEZF1 is a transcription factor, VEZF1 physically interacts with H2A.Z and complexes responsible for H2A.Z deposition and acetylation, and might also directly regulate the expression of H2A.Z and the complex components. To study whether the global levels of H2A.Z and H2A.Zac were altered following VEZF1 knockdown, western blotting analysis of total chromatin was performed. There was downregulation of H2A.Z following VEZF1 knockdown and the level could be restored after VEZF1 expression recovery (Figure 5.10). Even though the global level of H2A.Z was downregulated, the H2A.Zac level was upregulated following VEZF1 knockdown and again, the effect was reversible after re-expression of VEZF1 (Figure 5.10). Given that H2A.Z, H2A.Zac, H3ac and H3K4me2 are all associated with euchromatin, the elevated H2A.Z acetylation might counteract effects of the

reduction of H2A.Z, H3ac and H3K4me2 on chromatin following VEZF1 knockdown. The global level of H3ac decreased after VEZF1 knockdown but it could not come back to the normal level even the expression of VEZF1 was rescued (Figure 5.10), suggesting that there might be some irreversible changes at some chromatin regions caused by VEZF1 depletion.

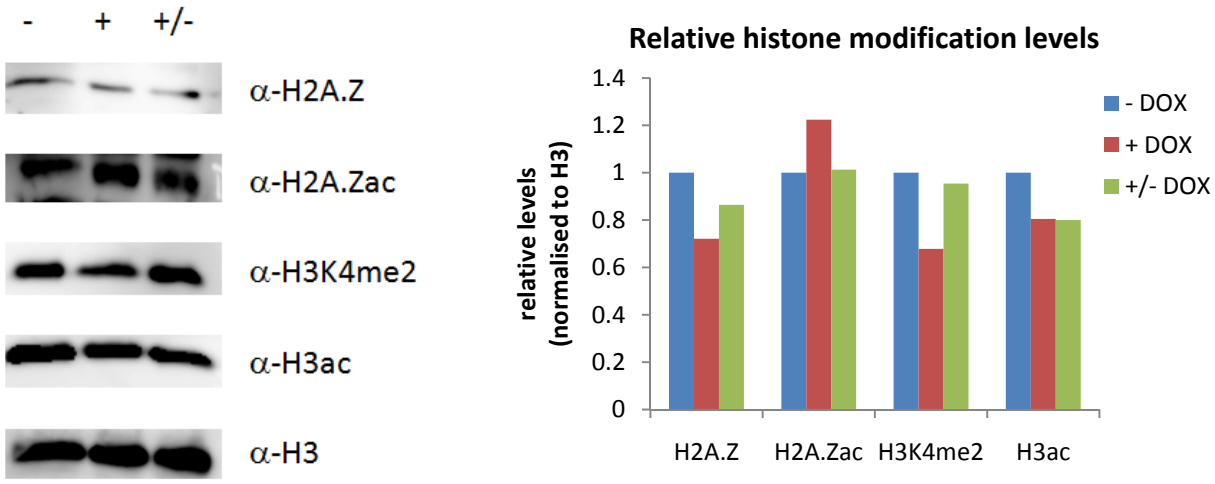

Figure 5.10 Global histone modification analyses following VEZF1 knockdown. VEZF1 knockdown was induced by DOX for nine days (+DOX) and two-day DOX treatment followed by seven-day removal was carried out in recovery cells (+/- DOX). Cells including untreated control were collected on Day 9 for histone modification examination. Total chromatin was extracted for western blotting analyses to examine the global levels of H2A.Z, H2A.Zac, H3ac and H3K4me2 (left panel) and the relative levels are presented with a histogram (right panel). The relative levels were measured from the band intensities of the western blotting analyses and normalised to that of histone H3. The levels in no DOX cells were set to one.

5.4.2 Analysis of histone modifications at human chromatin boundary elements before and after VEZF1 knockdown

The global changes of histone modifications following VEZF1 knockdown suggest histone modifications at VEZF1 binding sites might be altered. To study changes of histone modification at putative chromatin boundaries, native ChIP was performed following VEZF1 knockdown and expression recovery. Fold enrichments of examined histone modifications at target sites were relative to those at the promoter of *EDN1*, which is a silent promoter with no VEZF1 binding in K562 cells. Due to its promoter nature, histone modifications examined, H2A.Z, H2A.Zac, H3K4me2 and H3ac may not be depleted but the levels should remain unchanged following

VEZF1 knockdown.

5.4.2.1 H2A.Z deposition and acetylation

To study whether VEZF1 is responsible for the H2A.Z deposition and acetylation, native ChIP was performed following VEZF1 knockdown and expression recovery. H2A.Z is commonly found at promoters of active and inactive genes [Albert *et al*, 2007; Barski *et al*, 2007; Mavrich *et al*, 2008; Raisner *et al*, 2005]. Consistent with this, the silent *EDN1* gene employed as a normaliser also appeared to have a substantial enrichment of H2A.Z suggested by the ΔCt relative to input (not shown). Therefore, fold enrichments of H2A.Z below one at examined chromatin boundaries did not represent undetectable H2A.Z. It is notably that the *EDN1* promoter is not bound by VEZF1 in K562 cells (Figure 5.9) which histone modifications should not be affected by VEZF1 knockdown. Although VEZF1 interacts with several subunits involved in H2A.Z deposition as shown in Section 5.2.1 and there was a global reduction of H2A.Z following VEZF1 knockdown (Figure 5.10), the H2A.Z deposition at many VEZF1 binding sites was not affected by VEZF1 depletion. Only three of the examined sites *GMPPA-ACCN4* locus DHS, SPA1 DHS and *SCL* enhancer exhibited a slight decrease in H2A.Z following VEZF1 knockdown and the H2A.Z deposition was back to normal when VEZF1 was expressed again (Figure 5.11a). Two of the putative chromatin boundaries, *IGF2* 5' DHS and *EHD1* 5' DHS, were unexpectedly had higher levels of H2A.Z after VEZF1 knockdown while the increased level retained despite of the restored VEZF1 expression, suggesting that VEZF1 at these two sites are not responsible for H2A.Z deposition. The elevated H2A.Z might be compensation of chromatin state alteration after VEZF1 knockdown while the alteration might be quite stable that even the re-expression of VEZF1 could not restore it.

Acetylation of H2A.Z was reduced at some, but not all, at the VEZF1 binding sites upon VEZF1 knockdown and the reduction could be relieved when DOX was removed. The *FLNA* inverted repeat, *GMPPA-ACCN4* locus DHS and *SCL* enhancer exhibited lowered levels of H2A.Zac in

knockdown cells but the re-expression of VEZF1 could rescue them (Figure 5.11b). Notably, VEZF1 knockdown did not result in a complete loss of H2A.Z acetylation at these sites; rather, they still exhibited significant enrichments. This might be because the residual VEZF1 binding was still able to recruit the responsible enzymes. Alternatively, other transcription factors such as USF or CTCF binding on these elements might share the role of directing histone modifications with VEZF1. Reduced H2A.Zac was also observed at some VEZF1 binding sites including the HBB *β-globin* enhancer HS2, and the promoters of *SCL* and *MeCP2* following VEZF1 knockdown. However, the H2A.Zac levels could not be replenished significantly after recovery of the VEZF1 expression (Figure 5.11b). There might be irreversible chromatin state alteration at these sites induced by VEZF1 depletion. Collectively, VEZF1 appeared to regulate the H2A.Z acetylation and/or deposition at the boundary elements *FLNA* inverted repeat and *GMPP-ACCN4* locus DHS.

a

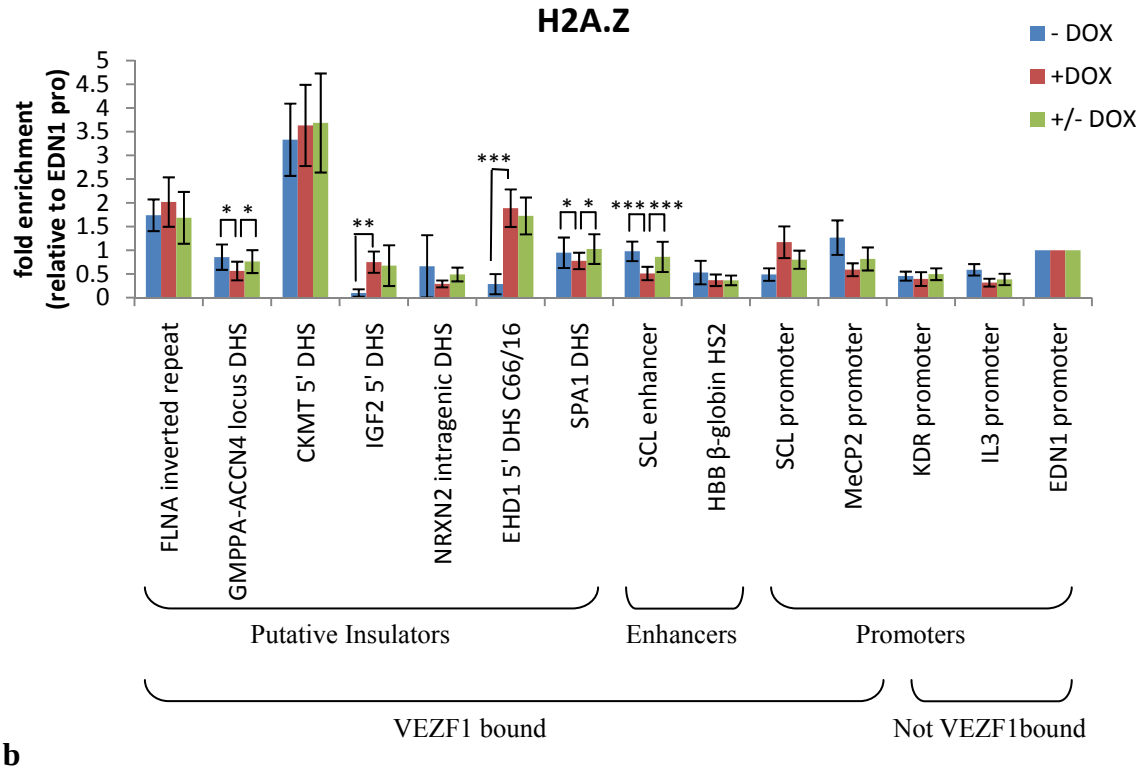

b

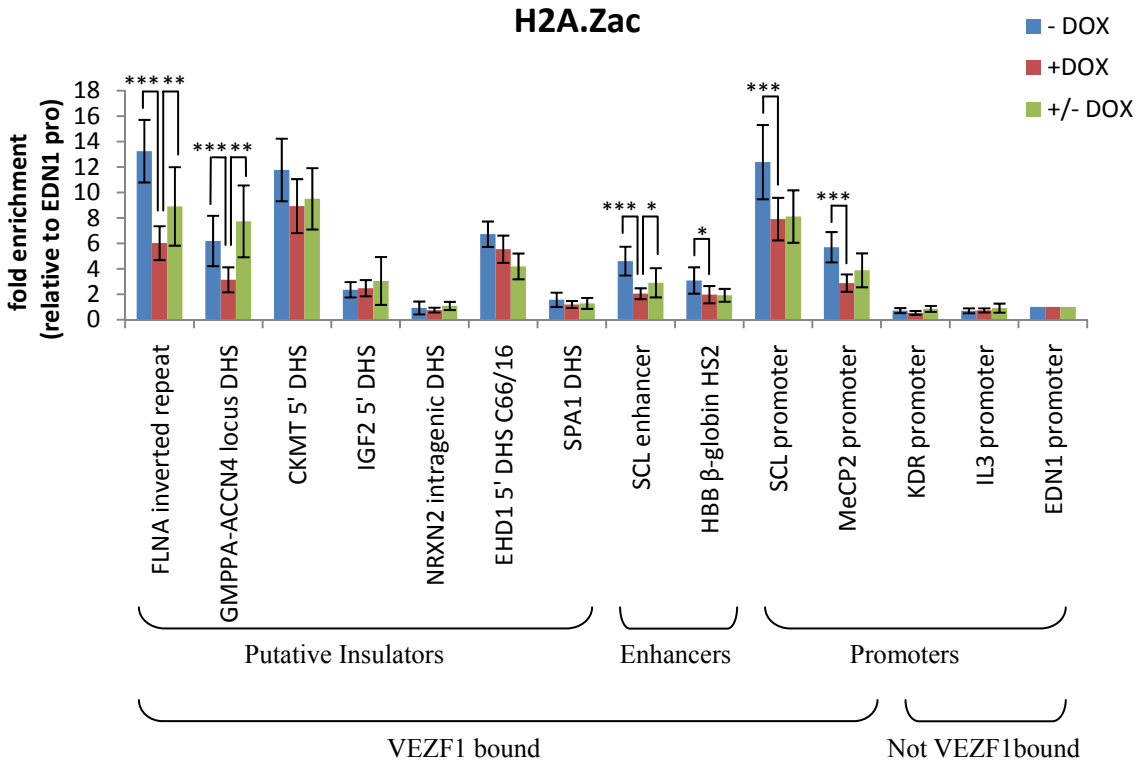

Figure 5.11 Native ChIP analyses of H2A.Z **(a)** and H2A.Zac **(b)** at VEZF1 binding sites upon VEZF1 knockdown. VEZF1 knockdown was induced by DOX for nine days (+DOX) and two days followed by seven-day removal in recovery cells (+/- DOX). Fold enrichments were relative to the *EDN1* promoter. Significant changes following VEZF1 knockdown and expression recovery are represented with asterisks (*=p<0.05, **=p<0.01 and ***=p<0.005).

5.4.2.2 H3 acetylation and H3K4 dimethylation

H3K4 methylation and histone acetylation were also studied because they were enriched at the insulator paradigm chicken HS4 element and HSA/HSB boundary, and appear to be essential for anti-silencing in yeast [Ladurner *et al*, 2003; Santos-Rosa *et al*, 2004; Venkatasubrahmanyam *et al*, 2007]. Like H2A.Z, the distribution of H3K4me2 is broad that it is not only restricted to active promoters [Barski et al, 2007] so the fold enrichments relative to the *EDN1* promoter below one did not mean there were no H3K4me2. Similar to H2A.Z acetylation, H3 acetylation and H3K4 dimethylation displayed a slightly but reversible reduction at some of the binding sites upon VEZF1 knockdown and again, changes were mostly observed at the *FLNA* inverted repeat, the *GMPPA-ACCN4* locus DHS and the *SCL* enhancer (Figure 5.12). Such changes were not seen at all VEZF1 binding sites and not dependent on the VEZF1 binding affinity, suggesting diverse functions of VEZF1. All histone modifications examined at the *SCL* promoter that has the highest VEZF1 binding affinity (see no DOX in Figure 5.9) did not exhibit a significant change of histone modification examined upon knockdown and recovery, suggesting that VEZF1 regulates the *SCL* promoter through a mechanism independent on the active histone modifications.

Taken together, VEZF1 appears to have different functions at the putative chromatin boundaries. Of which, VEZF1 plays a partial role in directing histone modifications, H2A.Z deposition and acetylation, H3 acetylation and H3K4 dimethylation, at the chromatin boundaries *FLNA* inverted repeat and *GMPPA-ACCN4* locus DHS. But notably, VEZF1 alone may not be sufficient for the active histone mark establishment as the levels of these marks at the *FLNA* inverted repeat and *GMPPA-ACCN4* locus DHS decreased but still substantially high although the VEZF1 binding was significantly reduced after knockdown.

a

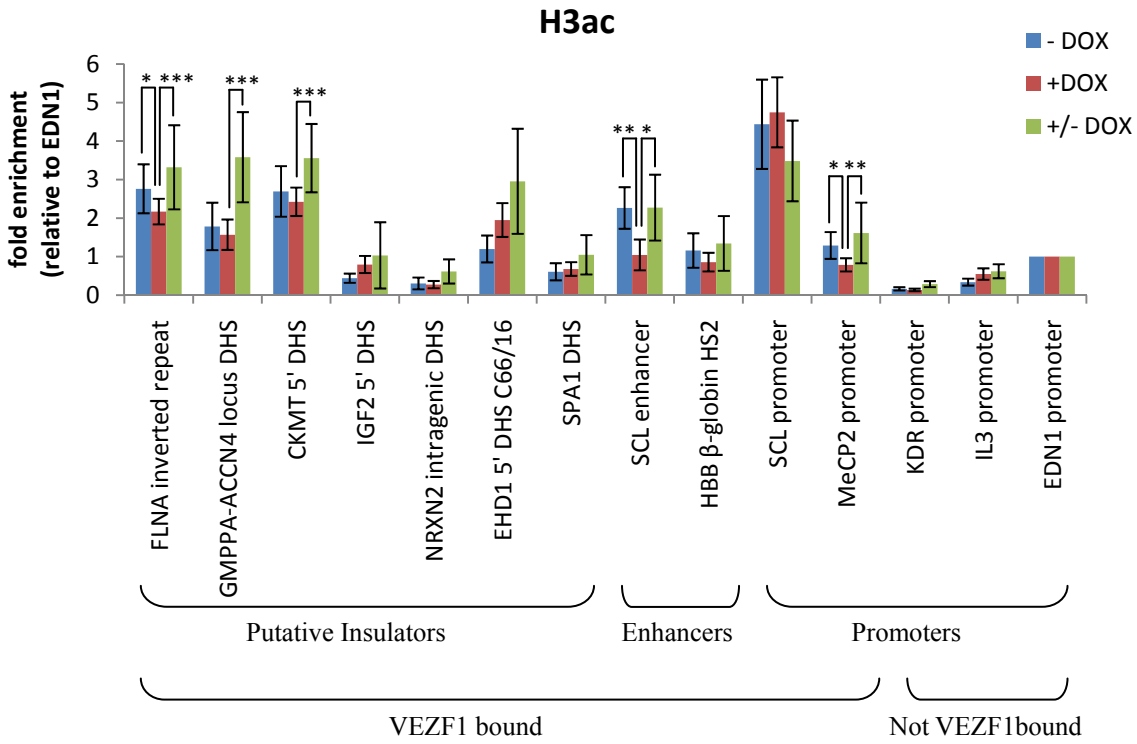

b

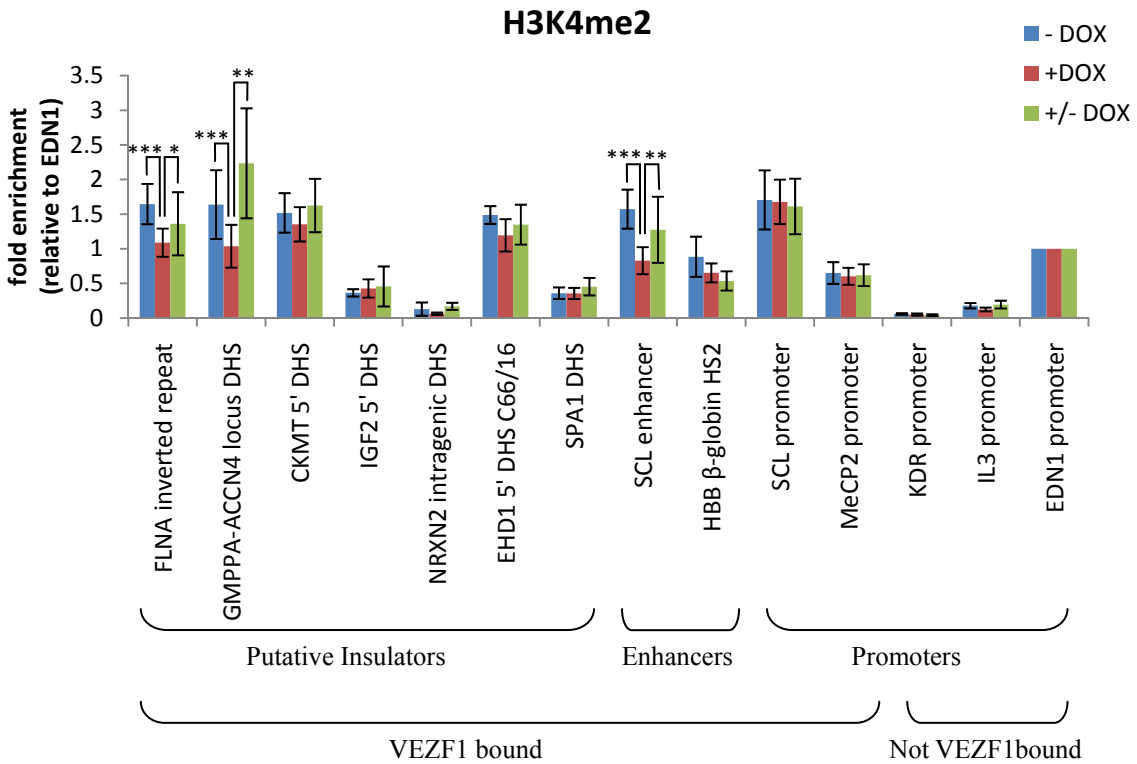

Figure 5.12 Native ChIP analyses of H3ac **(a)** and H3K4me2 **(b)** at VEZF1 binding sites upon VEZF1 knockdown. VEZF1 knockdown was induced by DOX for nine days (+DOX) and two days followed by seven-day of DOX removal in recovery cells (+/- DOX). Fold enrichments were relative to the *EDN1* promoter. Significant changes following VEZF1 knockdown and expression recovery are represented by asterisks (*=p<0.05, **=p<0.01 and ***=p<0.005).

5.5 Discussion

Nucleosome-free regions including transcription start sites (TSS) and boundaries elements are commonly decorated by H2A.Z that promotes transcription and counteracts heterochromatin propagation, respectively [Jin *et al*, 2009; Meneghini *et al*, 2003; Zhang *et al*, 2004]. However, it remains unclear that how the H2A.Z deposition is regulated and what is the function of H2A.Z at boundaries.

5.5.1 H2A.Z deposition and acetylation may be a signature of vertebrate insulators

Chromatin barriers in vertebrates may be like in yeast that H2A.Z, particularly its hyperacetylated form, is required for the barrier activity. H2A.Zac is substantially enriched at the chromatin boundaries at the chicken *β-globin* and *FOLR1* loci and the human putative chromatin barriers, the *FLNA* inverted repeat, *GMPPA-ACCN4* locus DHS and *CKMT* 5' DHS, possessing barrier activity. H2A.Z deposition at these sites is further confirmed by the recruitment of PONTIN52, REPTIN52 and BAF53A that constitute the shared module of the SRCAP, TIP60 and INO80 complexes but they are not recruited to the *NRXN2* intragenic DHS with a low level of H2A.Zac. SRCAP and TIP60 are responsible for H2A.Z deposition and acetylation in human while yeast INO80 was also recently found to be involved in the global H2A.Z localisation [Jin *et al*, 2005; Papamichos-Chronakis *et al*, 2011]. The other two putative barriers, the *IGF* 5' DHS and the SPA1 DHS, exhibiting relatively lower levels of H2A.Zac are unable to protect a transgene from chromosomal silencing (G. Barkness, unpublished data).

In this study, all tested putative chromatin boundary elements are DNase hypersensitive sites where nucleosomes are usually depleted. H2A.Z indeed always decorates nucleosome-free regions together with the histone variant H3.3 in the human genome [Jin *et al*, 2009]. Nucleosomes at the boundary elements may be unstable although the presence of H3.3 is yet to be confirmed. The unstable nature of nucleosomes may contribute the barrier activity by inhibiting the binding of repressive complexes responsible for heterochromatin propagation as in

yeast [Babiarz *et al*, 2006; Meneghini *et al*, 2003; Venkatasubrahmanyam *et al*, 2007; Zhang *et al*, 2004] and/or by preventing nucleosome oligomerisation for the formation of heterochromatin [Fan *et al*, 2002]. Moreover, the refractory profiles of H2A.Z and DNA methylation [Zilberman *et al*, 2008] raises the possibility that H2A.Z is deposited into these barrier elements to prevent DNA methylation, which is one of the events commonly associated with chromatin silencing [Fuks, 2005; Newell-Price *et al*, 2000]. It is supported by the capability of the H2A.Z enriched insulator paradigm HS4 element protecting the flanking transgene from DNA methylation [Dickson *et al*, 2010; Mutskov *et al*, 2002].

5.5.2 VEZF1 is necessary but not sufficient for H2A.Z deposition

Although the Co-IP experiment demonstrated that VEZF1 interacts with several subunits of the SRCAP and TIP60 complexes, VEZF1 alone is not sufficient for H2A.Z deposition. In the ChIP analyses on footprint deleted transgenic HS4, H2A.Z reduced dramatically not only if VEZF1 binding sites (footprint I, III and V) were deleted, but also in the case with USF binding site deletion. The results indicate that both VEZF1 and USF are needed for H2A.Z deposition while their roles may be different. VEZF1, as we suggested, it may be involved in recruiting H2A.Z deposition responsible protein complexes. USF at HS4 may mediate H2A.Z deposition through regulation of histone modifications, in which histone acetylation in particular, that are essential for H2A.Z incorporation. It has been shown in yeast that H4K16 acetylation is a prerequisite of H2A.Z incorporation [Shia *et al*, 2006]. USF is essential for H4 acetylation at HS4 and the process may be RNF20 dependent [Huang *et al*, 2007] (Section 4.3.3). The active histone modifications at HS4 may interplay with H2A.Z to eventually maintain the active state of HS4 to counteract the repressive histone marks and DNA methylation associated with heterochromatin propagation.

In the case of the putative boundary elements of our interest, all of them display a much higher level of H2BK120ub1 compared with other regulatory elements, suggesting that H2A.Z

deposition at these elements may require H2B ubiquitination. However, the ENCODE data shows that not all of these putative insulators are USF bound. The requirement of USF binding is thus not universal that other transcription factors such as CTF1 might recruit histone modification enzymes to generate the active chromatin environment for H2A.Z deposition [Esnault *et al*, 2009]. Histone modification profiling showed colocalisation of H3K4 methylation, the trimethylated state in particular, with H2A.Z, [Barski *et al*, 2007], implying that H2A.Z deposition is linked to or even signalled by active histone modifications. Of these putative insulator barriers, the *NRXN2* intragenic DHS lacks H3K4me3 (ENCODE project) as well as H3K4me2 (see no DOX control of Figure 5.12d), this might explain why this site does not favour H2A.Z deposition, disproving its barrier element identity.

Although the genomic CTCF distribution correlates with that of H2A.Z [Barski *et al*, 2007; Fu *et al*, 2008], loss of the CTCF binding site does not result in depletion of H2A.Z at HS4. Therefore, the relationship between CTCF and H2A.Z occupancies seems not to be absolute, at least this does not apply to HS4 and the 3' HS enhancer blocker at the chicken *β-globin* locus. The H2A.Z and CTCF occupancy could be simply a consequence that both of them are commonly found at nucleosome-free regions [Barski *et al*, 2007; Kim *et al*, 2007; Jin *et al*, 2009] while insulators, perhaps not as previously thought, they may be regulated by more than CTCF.

5.5.3 The dual role of VEZF1 in *de novo* DNA methylation

The previous bisulfite sequencing result demonstrated the necessity of all the three VEZF1 binding sites for HS4 to protect the flanked transgene from *de novo* DNA methylation mediated silencing (Section 1.5.5). The interaction between VEZF1 and the chromatin remodelling complexes responsible for H2A.Z deposition suggests the possibility that VEZF1 directs the H2A.Z deposition at HS4 to inhibit the DNA methylation. Consistent with the DNA bisulfite sequencing that the transgene is heavily methylated in the absence any of the VEZF1 binding sites (FI, FIII and FV) [Dickson *et al*, 2010], deletion of any of the binding sites leads to a

reduction in H2A.Z at the *IL2R* transgene and HS4 elements. However, more Co-IP and crosslinking assays are required to determine whether VEZF1 mediates the H2A.Z deposition by recruiting the TIP60 and SRCAP complexes as PONTIN52 and REPTIN52 are not specific for H2A.Z deposition [Jin *et al*, 2005].

The hypothesis that VEZF1 is required for H2A.Z deposition, however, is challenged by the histone modification profiling on the putative barrier elements performed in VEZF1 knockdown cells. VEZF1 knockdown leads to a loss of H2A.Z acetylation at the *FLNA* inverted repeat and the *GMPPA-ACCN4* locus DHS whilst the deposition is not affected. VEZF1 might facilitate H2A.Z acetylation by recruiting the TIP60 complex containing PONTIN52, REPTIN52 and BAF53A. The putative barriers, other than the *FLNA* inverted repeat and the *GMPPA-ACCN4* locus DHS, do not show any changes in H2A.Z incorporation and acetylation although VEZF1 is substantially depleted, suggesting that other binding proteins may share the role of H2A.Z deposition/acetylation. It supports by an observation that the HS4 mutant missing the USF binding site is depleted in H2A.Z. However, the *FLNA* inverted repeat and the *GMPPA-ACCN4* locus DHS are not bound by USF so other proteins may be involved instead (ENCODE Project).

Although the previous finding implies a negative correlation between VEZF1 binding and DNA methylation [Dickson *et al*, 2010], VEZF1 was found to regulate the genome-wide DNA methylation positively in mouse ES cells [Gowher *et al*, 2008]. Knockout of VEZF1 causes a loss of genomic DNA methylation as a result of substantial decreased expression of a *de novo* DNA methyltransferase Dnmt3b. The reduced expression is probably resulted from alternative splicing leading to reduced production of the catalytically active form of Dnmt3b. Even so, it does not mean that our working hypothesis is contradicted. VEZF1 could play a dual role in DNA methylation in a site specific manner and/or *via* cooperation with other binding proteins.

5.5.4 VEZF1 plays a role in active histone modification recruitment at its binding sites

VEZF1 also appears to regulate histone modifications at some binding sites. VEZF1 knockdown leads to depletion of several active histone modifications including acetylation of H2A.Z and H3, as well as H3K4me2. However, the loss of these marks is not complete and universal at all the binding sites, suggesting that the functions of VEZF1 are diverse that regulation of histone modification is apparently not the only role. Identification of VEZF1 binding proteins may give us a clue. VEZF1 has been found to interact with proteins responsible for histone modifications, chromatin remodelling and DNA replication (D. Li, unpublished). Although no direct interaction has been detected between VEZF1 and H3K4 KMTs and H3 KATs, VEZF1 might promote these modifications by providing an active open chromatin environment through rapidly exchanging nucleosomes. Several subunits of the BAF (Brahma-related gene/Brahma-associated factor) and NURF (nucleosome remodelling factor) complexes mediating chromatin remodelling have been found to interact with VEZF1. The loss of H3K4me2 and H3ac at some binding sites in VEZF1 lacking condition, thus, might be because of the more compact chromatin structure that is unfavourable for active histone modification enzymes.

The variety of VEZF1 binding proteins could also explain the diversity of binding sites. Like the *SCL* promoter and enhancer, VEZF1 tightly binds to these sites in K562 cells, however, in the absence of VEZF1, loss of active histone modifications is only observed at the enhancer but not the promoter. It suggests that VEZF1 may function differently at enhancers and promoters by recruiting different binding proteins to the binding sites, such process could be achieved by cooperation with other proteins or even the transcription machinery. Notably, two of the putative insulators, the *FLNA* inverted repeat and the *GMPPA-ACCN4* locus DHS, exhibit lower levels of H3K4me2 and H3ac in the VEZF1 depleted condition, suggesting a potential histone modification regulatory role of VEZF1. These active histone modifications may in turn act as a signal for H2A.Z deposition/acetylation, which might be essential for prohibiting *de novo* DNA methylation. Moreover, the loss of H3K4 methylation at these two sites may reflect the gain of

DNA methylation. It has been shown that a *de novo* methyltransferase DNMT3L has a higher affinity to K4 unmethylated histone H3 [Ooi *et al*, 2007]. If this is the case, VEZF1 may protect insulators and insulated regions from DNA methylation by facilitating H2A.Z incorporation as well as H3K4 methylation. In contrast, other putative insulator elements such as the *CKMT* 5' DHS and the *EDH1* 5' DHS do not appear to require VEZF1 to maintain or establish the active histone modification patterns. The role of VEZF1 in the barrier activity of these elements, thus, remains enigmatic. Characterising the barrier activity, DNA methylation and full histone modification patterns of these elements in VEZF1 knockdown cells would gain an insight into it.

CHAPTER 6

Conclusions and Future Perspectives

In this study, the regulation of histone modifications at the HS4 insulator element has been studied in depth. HS4 lies between a condensed chromatin region and the *β-globin* gene locus. I postulated that HS4 protects the *β-globin* genes from chromatin silencing that may spread from the condensed region [Prioleau *et al*, 1999]. The open chromatin structure of HS4 was previously linked to its barrier activity against heterochromatin propagation. Active histone modifications including H3K4 methylation and multiple histone acetylation are crucial to maintain such permissive chromatin structure [Huang *et al*, 2005; Huang *et al*, 2007; West *et al*, 2004], but little was known about how these marks are established. In this study, it has been found that H2B ubiquitination is a master regulator of an active histone modification cascade required for the barrier activity of HS4. Knockdown of the H2B-specific ubiquitination E3 ligase RNF20 leads to depletion of H2BK120ub1 and abolishes a series of active histone marks at HS4. This resulted in a breach of the HS4 barrier by heterochromatin-associated histone marks, which eventually spread across the entire *β-globin* domain. H2BK120ub1-dependent barrier activity may happen at other insulators such as the HSA/HSB barrier at the *FOLR1* locus. Several human putative chromatin barriers are also found to be enriched in H2BK120ub1. Collectively, a novel histone crosstalk regulated by H2B ubiquitination may be required for barrier activity.

Besides active histone modifications, HS4 is particularly enriched in the histone variant H2A.Z. H2A.Z has been found to be essential for yeast boundary elements to delimit the spread of heterochromatin [Babiarz *et al*, 2006; Meneghini *et al*, 2003; Venkatasubrahmanyam *et al*, 2007]. However, the function of this histone variant at vertebrate chromatin boundaries is not clearly understood although genome wide mapping has shown an enrichment of H2A.Z at CTCF elements [Barski *et al*, 2007; Jin *et al*, 2009]. However, our results found that the CTCF binding site is dispensable for H2A.Z deposition at HS4. Rather, the USF and VEZF1 binding sites are

essential for the deposition, possibly due to the recruitment of the active histone modification regulator H2B ubiquitination and H2A.Z deposition responsible chromatin remodelling complexes, respectively. Although some VEZF1 binding sites in the genome are enriched in these chromatin remodelling protein factors, H2A.Z deposition does not seem to be the only functional mechanism of VEZF1 as there is no universal decrease in H2A.Z and H2A.Zac at the binding sites following VEZF1 knockdown. Changes in other histone modifications at some but not all of the binding sites upon VEZF1 depletion suggest diverse functions of VEZF1.

6.1 Overview of histone modifications at insulator elements

In this study, histone modifications at the paradigm insulator element HS4, newly identified HSA/HSB boundary and some putative chromatin barriers in human have been profiled in Chapter 4 and 5 (Sections 4.3 & 5.4.2). HS4 and HSA/HSB, consistent with other previous studies, it is enriched in active histone modifications including H3K4me2, H3K4me3 and multiple acetylations of H3, H4 and H2A.Z. Moreover, native ChIP with anti-ubiquitin and anti-H2BK120ub1 antibodies found that HS4 and HSA/HSB are also sites of H2B ubiquitination. It is the first report showing H2B ubiquitination is linked to chromatin boundary elements.

Several putative insulators identified by profiling of genomic binding sites of HS4 binding proteins (R. Strogantsev, unpublished data) have been characterised in Chapter 5. All these putative insulators are bound by VEZF1; some of them are also binding sites for CTCF and USF proteins. All of the putative chromatin barriers, the *FLNA* inverted repeat, *GMPPA-ACCN4* locus DHS, *CKMT* 5’ DHS and *EHD1* 5’ DHS C66/16, are enriched in H2A.Zac, H2A.Z, H3ac, H3K4me2 and H2BK120ub1 (Sections 4.6 & 5.4.2). This histone modification pattern is similar to that of HS4 and HSA/HSB. Therefore, histone modification profiling may be one of the approaches to identify novel insulator barriers. DNase hypersensitive sites that demarcate boundaries between euchromatin and heterochromatin that are enriched in active histone modifications may be potential insulator barriers.

6.2 The histone modification cascade switched on by H2B ubiquitination at HS4 may occur at other insulator barriers

H2B ubiquitination found at HS4 appears to be a master switch of active histone modifications to counteract encroachment of repressive ones. RNF20 knockdown results in a loss of several active histone modifications at HS4 promptly. In agreement with other studies [Briggs *et al*, 2002; Kim *et al*, 2005], the loss of H2B ubiquitination at HS4 causes a local depletion of H3K4 methylation. However, despite the H2BK120ub1 depletion, the binding of a shared structural subunit of several SET1 and MLL KMTs to HS4 remains unchanged, suggesting that the activity rather than the recruitment of H3K4 KMTs is regulated by H2B ubiquitination.

Besides H3K4 methylation, histone acetylation at HS4 may be dependent on prior H2B ubiquitination. Multiple acetylations of H3, H4 and H2A.Z are specifically reduced at HS4 following H2BK120ub1 depletion. This is the first report showing that there is a crosstalk between H2B ubiquitination and histone acetylation. This crosstalk seems to be indirect or site-specific as the global levels of histone acetylation in H2BK120ub1 depleted cells are largely unaffected. The presence of chromodomain recognises H3K4me3 in HAT complexes suggests that H3K4me3 may be the mediator linking H2B ubiquitination and histone acetylation together. Interestingly, a similar loss of active histone modifications at HSA/HSB is also observed after RNF20 knockdown (Section 4.3). Moreover, H2BK120ub1 is detected at all the examined human chromatin boundary elements (Section 4.6). These results indicate that the histone crosstalk regulated by H2B ubiquitination may be adopted by a subset of vertebrate chromatin boundary elements to establish an active chromatin state.

In the absence of H2B ubiquitination, spreading of repressive H3K9me2 is rapidly initiated at the *β-globin* and *FOLR1* loci (Section 4.4.1). H3K9me2 is widely distributed but more likely to be found at silencing chromatin [Rice *et al*, 2003]. However, constitutive heterochromatin histone marks H3K9me3 and H4K20me3, can only breach the HS4 and HSA/HSB boundaries and

propagate along the chromatin after prolonged depletion of H2B ubiquitination (Sections 4.4.3 & 4.4.4). The spreading of H3K9me3 seems to precede that of H4K20me3 as the propagation of H4K20me3 is slower than H3K9me3 following RNF20 knockdown. Consistent with the slow spreading of H3K9me3 and H4K20me3, significant silencing of the *FOLR1* gene and repression of the HS4 flanked transgene is only observed after knockdown RNF20 for more than 30 days (Section 4.4.4 & 4.5). Collectively, H2B ubiquitination is a master regulator H3K4 methylation at HS4 and HSA/HSB. It may in turn switch on multiple acetylation. These active histone marks are essential for the barrier activity against heterochromatin spreading (Figure 6.1). The presence of H2BK120ub1 at the human putative chromatin barriers suggest that such histone crosstalk may be employed by other chromatin boundary elements.

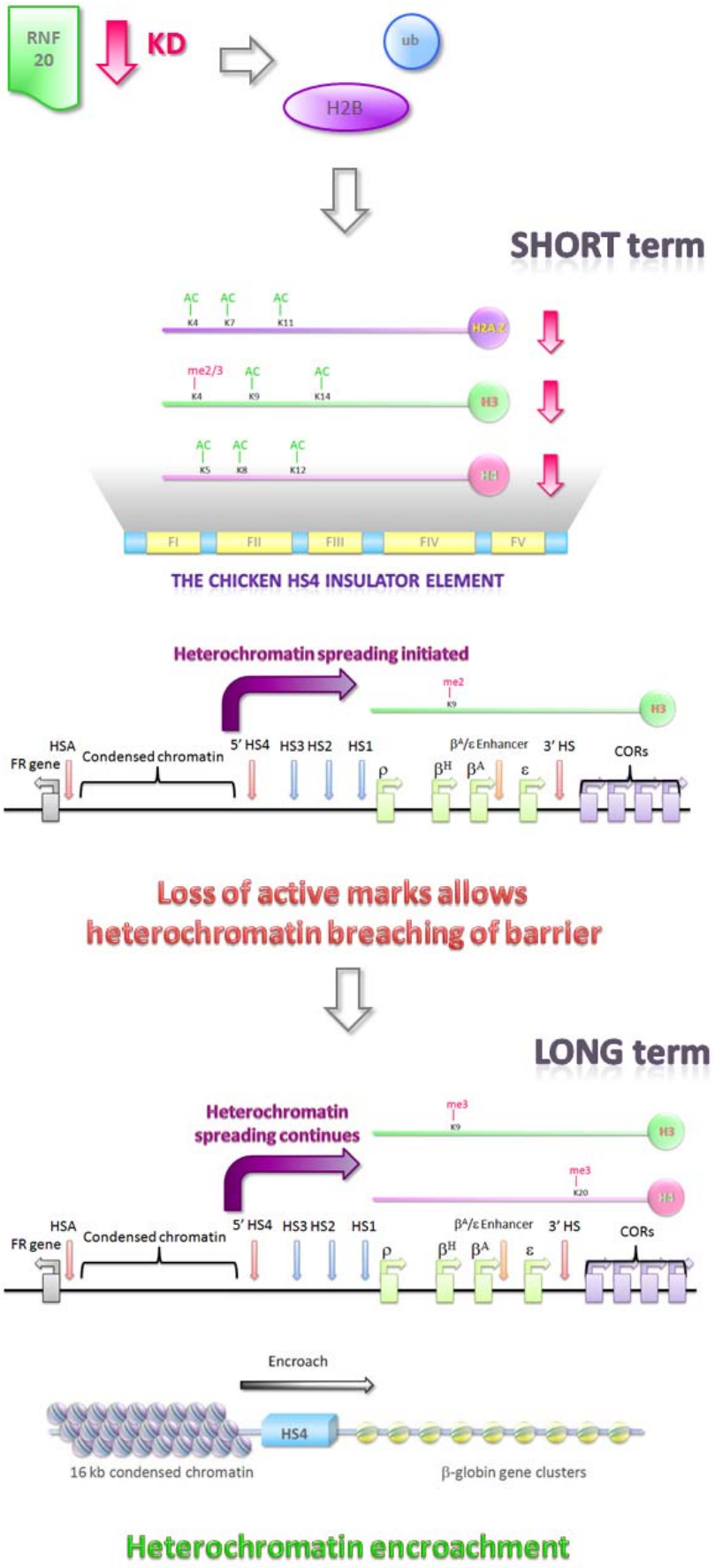

Figure 6.1 Schematic diagram of effects on the HS4 barrier and the entire chicken *β-globin* locus upon RNF20 knockdown caused H2B ubiquitination depletion.

6.3 Binding of transcription factors is crucial for the activity of insulator barriers

It has been found that at least three transcription factors bind to the chicken HS4 element; they are CTCF, USF and VEZF1 [Bell *et al*, 1999; West *et al*, 2004; Dickson *et al*, 2010]. They are responsible for the two separable insulator activities, enhancer-blocking and barrier activity. CTCF is a best known transcription factor associated with insulators [Wallace & Felsenfeld, 2007]. However, its binding to HS4 is only essential for the enhancer-blocking activity but not the barrier activity [Bell *et al*, 1999; Recillas-Targa *et al*, 2002]. ChIP analyses on HS4 binding site deletion mutants reveal that the CTCF site is dispensable for HS4's H2B ubiquitination [Ma *et al*, 2011] and its binding to HS4 is not H2B ubiquitination dependent (Section 4.3.5). Thus, it was not investigated deeply in this study. Contrastingly, the binding sites for USF proteins and VEZF1 are crucial for the HS4's barrier activity [Recillas-Targa *et al*, 2002; Huang *et al*, 2005; Huang *et al*, 2007; West *et al*, 2004]. These two proteins are also found to bind to the chicken HSA/HSB element and several human putative insulators, suggesting a conserved mechanism for barrier activity for at least a subset of insulator barriers.

6.3.1 Role of USF proteins

USF1/2 proteins interact with histone modification enzymes such as KMTs and KATs so that knockdown of USF1 leads to a loss of multiple active histone modifications at HS4, allowing the spreading of H3K9me2 and H3K27me3 beyond the HS4 boundary [Huang *et al*, 2007; West *et al*, 2004]. ChIP data on HS4 mutants showing that the level of ubiquitinated histones is reduced only if the USF binding site is deleted, further confirming the crucial role of USF at HS4 [Ma *et al*, 2011]. Besides H2B ubiquitination, H2A.Z deposition at HS4 is also dependent on the USF binding site. The H2A.Z deposition/acetylation seems to be in a RNF20-dependent manner. It might be postulated that the USF proteins recruit the H2B ubiquitination machinery to HS4 in the first place so the H2BK120ub1 enriched environment may favour the activity or recruitment of other histone modifiers (Figure 6.2). However, the precise interactions between USF and H2B ubiquitination essential factors remain to be identified.

6.3.2 Role of VEZF1

This study reveals that VEZF1 is responsible for the recruitment of the SRCAP and TIP60 complexes for H2A.Z deposition and acetylation at HS4 and some of the human putative chromatin barriers. VEZF1 interacts with the shared module of the two complexes and also H2A.Z (Section 5.2.1). ChIP analyses on HS4 footprint deletion mutants also further confirms the indispensible role of VEZF1 in H2A.Z incorporation although USF is also required (Section 5.2.3) (Figure 6.2). Deletion of the VEZF1 binding sites results in a loss of H2A.Z at HS4 itself and the HS4 flanked transgene, consistent with the appearance of DNA methylation [Dickson *et al*, 2010]. Given that H2A.Z and DNA methylation is mutually exclusive [Conerly *et al*, 2010; Zemach *et al*, 2010; Zilberman *et al*, 2008], VEZF1 may contribute the HS4 barrier activity by recruiting H2A.Z to prohibit DNA methylation. However, VEZF1 appears to have diverse functions at its binding sites that H2A.Z deposition/acetylation might not be its only role. Knockdown of VEZF1 only results in a mild reduction in H2A.Zac locally at the *FLNA* inverted repeat and *GMPPA-ACCN4* locus DHS (Section 5.4.2.1), suggesting the involvement of other factors to mediate the H2A.Z deposition and modification. Intriguingly, VEZF1 appears to regulate histone modifications, H3K4 dimethylation and H3 acetylation, at its binding sites. Taken together, functions of VEZF1 appear to be site specific that it may exert different effects at different binding sites, maybe *via* interaction with various protein factors.

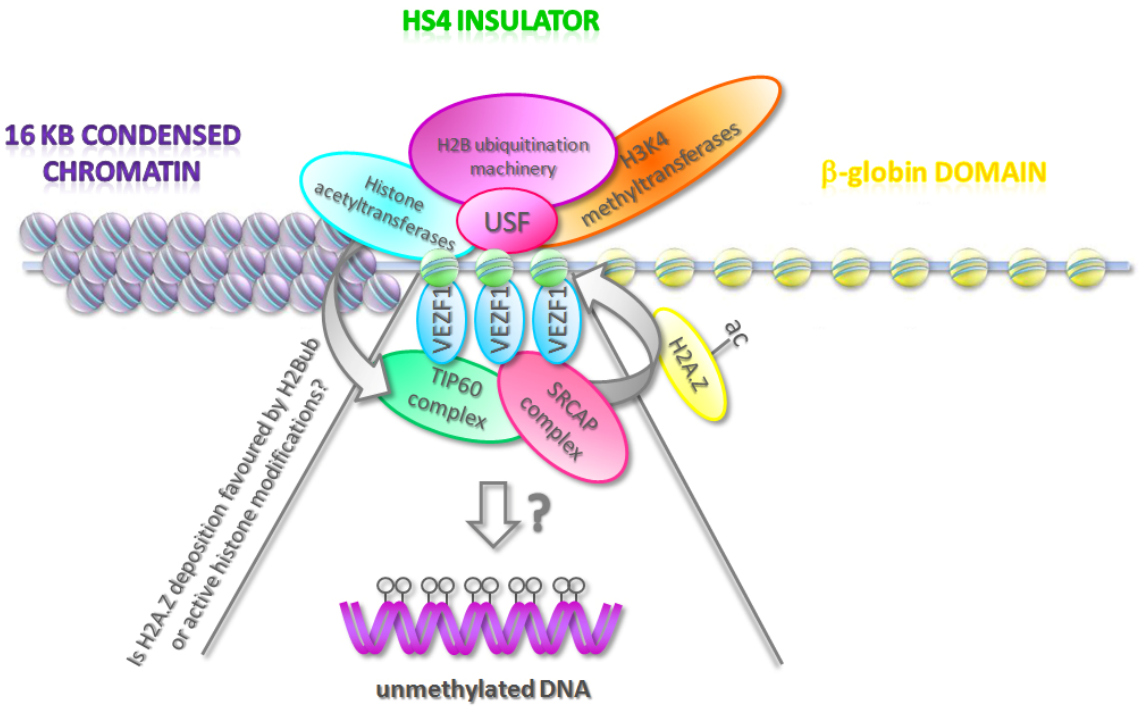

Figure 6.2 Schematic diagram showing the roles of USF and VEZF1 proteins at the HS4 insulator element. USF recruits the H2B ubiquitination machinery to promote H2B ubiquitination, which may in turn augment the di- and tri-methylation activity of H3K4- specific KMTs to HS4 (green nucleosomes). The methylated H3K4 histone tails may be a recognition mark for KATs. The recruitment of H3K4-specific KMTs and KATs also depends on USF proteins. H2BK120ub1 itself or its triggered active histone modification may also favour H2A.Z deposition and acetylation. Even so, VEZF1 is needed for the incorporation of this histone variant as the SRCAP and TIP60 complexes appear to be recruited to HS4 by VEZF1. H2A.Z incorporation may eventually prevent the HS4's DNA from methylation. These events are collectively considered to be required to maintain the open chromatin barrier to heterochromatin spreading.

6.4 Potential roles of H2A.Z at heterochromatin barrier elements

It has been found that deposition of histone variant H2A.Z can alter nucleosome stability. Nucleosomes with two histone variants H2A.Z and H3.3 are very labile so these nucleosomes dissociate easily in modest ionic conditions *in vitro* [Jin *et al*, 2007]. Unstable nucleosomes would disrupt higher-order of chromatin structure, suggesting why insulator barriers are commonly decorated by H2A.Z [Barski *et al*, 2007; Jin *et al*, 2009]. Perhaps not surprisingly, HS4, HSA/HSB and several putative human barriers are enriched in H2A.Z and H2A.Zac (Section 4.3.4 & 5.4.2.1).

Our ultimate goal is to determine whether H2A.Z contributes barrier activity by preventing DNA methylation. However, it is still not known whether knockdown of H2A.Z expression would lead to DNA methylation at insulator elements. More studies are required before drawing a conclusion that HS4 and other insulator elements recruit H2A.Z to interfere with DNA methylation although most of them are enriched in this histone variant.

6.5 Future Perspectives

6.5.1 Is H2B ubiquitination is a common feature of insulator elements?

The ChIP result showing that H2BK120ub1 is enriched in several insulator barriers inspired us to ask whether this histone modification is a universal regulator of insulator barriers. Knockdown of RNF20 could be carried out in human cells and the whole genome histone modification profiling for H2BK120ub1, active and repressive histone marks could be followed. Results would reveal if RNF20-dependent histone modifications are required for barrier activity.

6.5.2 Is VEZF1 required for H2A.Z recruitment?

Although it has been found that VEZF1 interacts with H2A.Z and the SRCAP/TIP60 complex subunits, it is still not clear whether VEZF1 recruits these complexes for H2A.Z deposition and acetylation to its binding sites. We hypothesised that VEZF1 counteracts DNA methylation *via* recruitment of these complexes. Inducible VEZF1 knockdown lines have been established and characterised that the VEZF1 protein level and its binding to target sites are substantially reduced following DOX induction. Therefore, these lines would be a potential model to study whether the recruitment of the SRCAP and TIP60 complexes to the putative insulator barriers is abolished in the absence of VEZF1. To further confirm the role of VEZF1 in preventing DNA methylation, MeDIP (methylated DNA immunoprecipitation) would be carried out to study changes in DNA methylation at its bound chromatin barriers before and after VEZF1 knockdown. Techniques involved would be similar to ChIP that enrichment of methylated DNA after immunoprecipitation with methylated DNA-specific antibodies would be measured with real-time PCR. The only difference is that immunoprecipitation would be performed on DNA but not on chromatin. If VEZF1 facilitates H2A.Z deposition to block DNA methylation, a loss of the SRCAP and TIP60 complex recruitment in VEZF1 knockdown cells would in turn allow DNA methylation to occur at insulator barriers and their surrounding regions.

6.5.3 What is the role of H2A.Z at insulator elements?

Insulators especially barrier elements are commonly incorporated with H2A.Z. However, the role of H2A.Z in barrier activity, especially in vertebrate barriers, is still not clearly understood. H2A.Z induced nucleosome instability may facilitate nucleosome exchange to achieve and maintain the open chromatin structure, or H2A.Z may prevent DNA from methylation. Knockdown of H2A.Z or the SRCAP complex subunits may be able to give us a clue. The chromatin structure of barrier elements following knockdown could be studied by DNase digestion. Also, MeDIP would be performed in cells lacking H2A.Z deposition. Both well-known and putative insulator elements, as well as their surrounding regions would be examined to figure out whether H2A.Z incorporated at insulator barriers is a means to prevent DNA methylation. Moreover, in order to study whether H2A.Z is necessary for barrier activity, barrier assays could be also performed in H2A.Z knockdown cells. Our colleague, Dr Grainne Barkess, has been recently developing the barrier assay by integrating a transgene cassette flanked by putative barrier elements into a genome systematically. These stable lines with the transgenic reporter cassette would allow us to investigate whether barrier elements can function properly in the absence of H2A.Z.

APPENDIX I

Primer sequences

Abbreviations: “F” and “R” represent forward and reverse primers, respectively. “T” indicates Taqman probe.

I. 1 Primers for the chicken *β-globin* locus

2.747 FOLR1 3’	F	5’ – CCTGGCAGGAGAGGATCTCTT – 3’
	R	5’ – CCAACTCCTACAAATACACCACAGAA – 3’
	T	5’ – FAM-TCAAACCACATCTGGATCAGGCGC-TAMRA – 3’
3.951 FOLR1	F	5’ – CAGCAAAGAGTCCTTTCCCTTCT – 3’
	R	5’ – TTCAACACCATCTTGCTGCAAT – 3’
	T	5’ – FAM-CAAAACACCCGAGGGCTGCCTG-TAMRA – 3’
5.613 FOLR1 pro	F	5’ – AACATTACCTGCCTAGAGACTATCCA – 3’
	R	5’ – CTGTGTCAGAAGGCTTTCCTGTTA – 3’
	T	5’ – FAM-CCACAACAACACTCAGAACAGCAGCCTC-TAMRA – 3’
5.851 FOLR1 pro	F	5’ – GAAGGGCTGGGCTCTTATCTG – 3’
	R	5’ – TGCCTGGTGGGAAGCAAA – 3’
	T	5’ – FAM-ATGGCCACACACACAAAGCCCTTCTC-TAMRA – 3’
6.241 HSA	F	5’ – GGGTCCGACCAGGAAGGA – 3’
	R	5’ – TCAGTGCCAGGATTGAAGCA – 3’
	T	5’ – FAM-ACAGACCAGCAGATCTTCCTATTGGCACA-TAMRA – 3’
7.342 HSB	F	5’ – CACAGCACTGCAGCAGCATT – 3’
	R	5’ – ATCCAAAAACAAACCCGATATCA – 3’
	T	5’ – FAM-CTCTGTTTTCTGTTCCTCGCCGAGGA-TAMRA – 3’
8.989 cond	F	5’ – GGGCCCAATGAACCAGAAA – 3’
	R	5’ – TGTTCCCCAGCAACGCA – 3’
	T	5’ – FAM-AAATGGCAAACTGTTGATGGGAACGC-TAMRA – 3’
10.350 cond	F	5’ – GGAACAAGTTGGCAAGGTCCTAT – 3’
	R	5’ – TCTTCTGCCCTGCCCGTAT – 3’
	T	5’ – FAM-TGCAGTTCCCTGTTCATGTGCTTTTCG-TAMRA – 3’

13.192 cond	F	5’ – GAATGTGTCCATCTGCCCTCAT – 3’
	R	5’ – GGGAAGCCATCCCTGCA – 3’
	T	5’ – FAM-TGCTGAGCATGTGGCTGCCTCC-TAMRA – 3’
15.850 cond	F	5’ – CAGCAGACGCTGTGGTGAA – 3’
	R	5’ – CTTGCAGGATGCAGACTGGA – 3’
	T	5’ – FAM-ATCCCATCGGTGCCACCCTGAG-TAMRA – 3’
17.763 cond	F	5’ – TGTTATCGCACACACACACACTTT – 3’
	R	5’ – GACAGGGATGTTCTTCCTCTGAA – 3’
	T	5’ – FAM-TCGTCTGATGCAGACAATTTCTCTGTGATCTC-TAMRA – 3’
20.360 cond	F	5’ – GCTCTGCGAGGGCTCTCTTT – 3’
	R	5’ – CCTCTCCTCACCCACCTGTTT – 3’
	T	5’ – FAM-TTCCCGCTCTCTGTTAATATTGGATTTCCTTTTT-TAMRA – 3’
21.365 5’ of HS4	F	5’ – CTCTGTGCTCAGCATCCTTCAAT – 3’
	R	5’ – CCTTTCGGCACTTTCTTCCTTT – 3’
	T	5’ – FAM-CTCCGCTGCACCTCCTCTGCAAA-TAMRA – 3’
21.540 HS4	F	5’ – TCCTGGAAGGTCCTGGAAG – 3’
	R	5’ – CGGGGGAGGGACGTAAT – 3’
	T	5’ – FAM-CCCAAAGCCCCCAGGGATGT-TAMRA – 3’
21.726 HS4	F	5’ – CGGGATCGCTTTCCTCTGA – 3’
	R	5’ – CCGTATCCCCCCAGGTGTCT – 3’
	T	5’ – FAM-CGCTTCTCGCTGCTCTTTGAGCCTG-TAMRA – 3’
22.189 3’ of HS4	F	5’ – CAGGACAGCATGGACGTGG – 3’
	R	5’ – TTCTGAACGCTGTGACTTGGA – 3’
	T	5’ – FAM-CATGCAGGTGTTGAGGCTCTGGACA-TAMRA – 3’
25.743 HS3	F	5’ – GCCCGTGCTGTTTGCAC – 3’
	R	5’ – TGAGTCACGGTTGTGTGTGGT – 3’
	T	5’ – FAM-AGCCGTGTTATCGCCCCATGGC-TAMPA – 3’
31.977 ρ pro	F	5’ – CAGAGGAGCCAACATTTGGG – 3’
	R	5’ – CCCCTCTGGGTGATGCATT – 3’
	T	5’ – FAM-CGCTGCAGGCGTGAAGCCATT-TAMPA – 3’

34.715 ρ 3’	F	5’ – CGTGTTCTGGAGGAGAGAGAAGA – 3’
	R	5’ – CTTATCAGCAAGACTGGCAGATGT – 3’
	T	5’ – FAM-TGACTGGCTGTGGTCCAGAGGCTG-TAMRA – 3’
36.882 β^H pro	F	5’ – TGACACTGGAAACCTATGGCC – 3’
	R	5’ – AGCCCCGAGTGCAGGTG – 3’
	T	5’ – FAM-TGGAGGAGCCATGCAGGCAGC-TAMRA – 3’
39.807 β^A pro	F	5’ – CTGTGGTCTCCTGCCTCACA – 3’
	R	5’ – AGGCTGGGTGCCCCTC – 3’
	T	5’ – FAM-CAATGCAGAGTGCTGTGGTTTGGAACTG-TAMRA – 3’
42.112 β^A 3’	F	5’ – CCTTGTTTATGCACTTCTTCACCC – 3’
	R	5’ – AACCCCCTCTCTTCCCTCAC – 3’
	T	5’ – FAM-CGCTGCCCATTCTGCTGCTCTG-TAMRA – 3’
50.861 3’ HS	F	5’ – TTCACAAAACACCAGTTATGCTCC – 3’
	R	5’ – ACCTGCTGCTTCAGAGGCA – 3’
	T	5’ – FAM-TCTGCTGGTGAGATGGCGTCTGCT-TAMRA – 3’

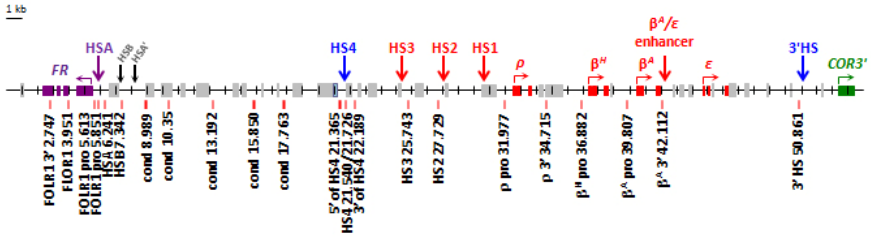

Figure I.1 Primer used for studying the chicken *β-globin* locus.

Transgenic HS4 5’	F	5’ – CACAGGAAACAGCTATGACATGATT – 3’
	R	5’ – TCTGCCTTCTCCCTGATAACG – 3’
	T	5’ – FAM-AATTCCTGCCCACACCCTCCTGC-TAMRA – 3’
IL2R	F	5’ – GGGACTCTCACGTTCATCA – 3’
	R	5’ – AATGTGGCGTGTGGGATCTC – 3’
	T	5’ – FAM-AGAGCTCTGTGACGATGACCCGCC-TAMRA – 3’
Transgenic HS4 3’	F	5’ – GCTTGTCTCCCTATAGTGAGTCGTATT – 3’
	R	5’ – TGTGAGCGGATAACAATTTCACA – 3’
	T	5’ – FAM-TTGGCGTAATCATGGTCATAGCTGTTTCCT-TAMRA – 3’

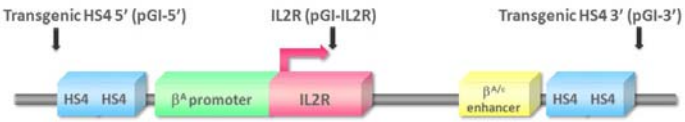

Figure I.2 Primers used for studying the transgenic *IL2R* reporter construct.

I. 2 Primers for ChIP assays in human K562 cells

I. 2.1 TaqMan based primers

CKMT 5' DHS	F	5' – CCCTCCTCGGTACTCTCCTC – 3'
	R	5' – GGGCCTTAGTGTCAGCGTAG – 3'
	T	5' – FAM-CTCGCATCCCGACTCCACTAGCCTT-TAMRA – 3'
EDN1 promoter	F	5' – TGCCCCCGAATTGTCAGA – 3'
	R	5' – CAGGCCCGAAAGGAAATCA – 3'
	T	5' – FAM-CGGGCGTCTGCCTCTGAAGTTAGCA-TAMRA – 3'
FLNA inverted repeat	F	5' – CCTTGTGTTTTGGGTGTGG – 3'
	R	5' – CACGACCTCTGGACGTTTCT – 3'
	T	5' – FAM-TGCGCTTCTCTAAGCGTTCCATTCC-TAMRA – 3'
GMPPA-ACCN4 locus DHS	F	5' – TGTCTTGCCCTCAACCTTCT – 3'
	R	5' – AGCTGCTGGGAGCAGATAAG – 3'
	T	5' – FAM-CTCTAATCCCTCCTGCTGCTGTGCC-TAMRA – 3'
IL3 enhancer	F	5' – ACAGCAGTCAGGAACCCCTTT – 3'
	R	5' – CCCCACAACAACACCATTATAGG – 3'
	T	5'–FAM-CCACCCACTGCAGAAAGGATGGCTAA-TAMRA– 3'
IL3 promoter	F	5' – GGTTGTGGGCACCTTGCT – 3'
	R	5' – TCTGTCTTGTTCTGGTCCTTCGT – 3'
	T	5' – FAM-ACATATAAGGCGGGAGGTTGTTGCCAA-TAMRA – 3'
KDR promoter	F	5' – GGCTAGGCAGGTCACTTCAA – 3'
	R	5' – AGTGCGTTTTCTGATTAAGAGCA – 3'
	T	5' – AAATAGCGGGAATGTTGGCGAACTGG – 3'
SCL enhancer	F	5' – TTACAGCCCTTCACCCTCAC – 3'
	R	5' – TGGGAATGAGCGATAAGGAT – 3'
	T	5' – FAM-ATGTTCCTGCCCTGATCCAGAGGG-TAMRA – 3'
SCL promoter	F	5' – AGGAAAGGCTCCAAACACCT – 3'
	R	5' – ATGGCTGGGAATTACCTCCT – 3'
	T	5' – FAM – CGATTCCCTGGACTGGTTGGTCG –TAMRA – 3'

I. 2.2 SYBR® Green based primers

CKDN1A 3'	F	5' – CCAGGGCTGCGATTAGGAA – 3'
	R	5' – GTGTCCCTCATGGGTGTGAAT – 3'

CKDN1A promoter	F	5’ – AGCAGGCTGTGGCTCTGATT – 3’
	R	5’ – CAAAATAGCCACCAGCCTCTTCT – 3’
EHD1’ DHS C66/16	F	5’ – AGCCAGTGAGTGGGGTAATG – 3’
	R	5’ – CCCCTCTCAGAACTCCTCAA – 3’
HBB β-globin HS2	F	5’ – ATCTGGGCACACACCCTAAG – 3’
	R	5’ – AAGCAAACCTTCTGGCTCAA – 3’
IGF 5’ DHS	F	5’ – TCCACCTGTAAAGCGGAGAT – 3’
	R	5’ – TGGGTCATGGCAATATGGAT – 3’
NRXN2 intragenic DHS	F	5’ – TAGGACCACAGGTGCTACCC – 3’
	R	5’ – AAATGAAGCAGAGCCAAGGA – 3’
SPA1 DHS	F	5’ – GGAGGGGGTGAATGTCACTA – 3’
	R	5’ – TTCCAAGGAAAGGGGTAAGG – 3’
MeCP2 promoter	F	5’ – CAATTGGCGAGATTTCCTGT – 3’
	R	5’ – TCAAATTCCGCCCACTAAAC – 3’
KRT35 promoter	F	5’ – GAGGAGGCTTGGACTGTTTC – 3’
	R	5’ – AGCACCTTTCTATCCACGA – 3’
NPY5R 3’	F	5’ – AAGCACCAGTCAAAGCTGTTT – 3’
	R	5’ – TCATATTCCCAGTCAATGGC – 3’

I. 3 Primers for RT-PCR in chicken 6C2 cells

ACTB	F	5’ – TGCTGCGCTCGTTGTTGA – 3’
	R	5’ – CATCGTCCCCGGCGA – 3’
GPADH	F	5’ – ATGGGCACGCCATCACTATC – 3’
	R	5’ – AACATACTCAGCACCTGCATCTG – 3’
FOLR1	F	5’ – GATTCTGCATGTGCCACTGT – 3’
	R	5’ – AAGACCTGGGTGAAGGGTCT – 3’
RNF20	F	5’ – ATGCGTCATCTCATCAGCAG – 3’
	R	5’ – TTGGGAAGAAGGGTCATCAG – 3’

As primers specific to RNF20 and FOLR1 were newly designed for RT-PCR with SYBR® Green chemistry that gives fluorescent signal for both specific and non-specific PCR products, the end PCR products were analysed with 2% TBE gel to ensure a single band with predicted size resulted. The expected sizes of PCR products are 65 bp for GAPDH, 162 bp for FOLR1, 93 bp for ACTB and 212 bp for RNF20 (Figure I.3). Although primer dimers were formed in the PCR reactions, they did not contribute fluorescent signals in real-time PCR assays as shown in negative controls without cDNA templates.

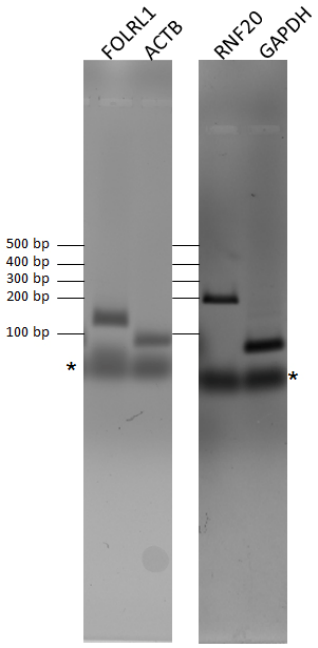

Figure I.3 Sizes of RT-PCR products. 20 µl of PCR reaction was analysed with 2% TBE gel after 40 cycles of PCR amplification. Primer dimers are asterisked.

APPENDIX II
Raw FACS data

Clone	DOX (-/+)	Day	% of green cells	Mean of GFP fluorescence intensity	Median of GFP fluorescence intensity
8103	-	0	---	1.84	1.55
	-	40	---	3.31	3.15
	-	60	---	3.17	3.00
	-	80	---	2.90	2.76
R2628 E5	-	0	---	1.85	1.54
	-	4	---	4.30	3.03
	-	33	---	2.74	2.59
	-	40	---	2.41	2.24
	-	50	---	2.80	2.58
	-	60	---	3.02	2.89
	-	80	---	2.30	2.12
	+	4	95.4%	824	824
	+	33	22.6%	766	719
	+	40	45.5%	577	542
	+	50	66.6%	633	601
	+	60	75.0%	616	585
	+	80	53.9%	811	780
R2628 E4	-	0	---	1.66	1.34
	-	4	---	3.20	2.99
	-	36	---	3.18	2.94
	-	40	---	3.30	3.06
	-	50	---	3.02	2.85
	-	60	---	2.81	2.66
	-	80	---	2.30	2.15
	+	4	89.5%	623	628
	+	36	4.23%	864	812
	+	40	4.56%	789	735
	+	50	6.03%	824	786
	+	60	7.96%	818	799
	+	80	5.22%	834	815

Table II.1 Table showing percentages and GFP fluorescence intensities of green cells of RNF20 knockdown clones R2628 E5 and R2628 E4. 8103 and no DOX treated R2628 E5 and E4 cells were served as controls to determine the background green signals. All mean/median of fluorescence intensities was only calculated from green cell population.

Clones	DOX (+/-)	Day	Mean of PE fluorescent intensity	Median of PE fluorescent intensity
6C2	-	33	1.6	1.5
	-	40	1.8	1.7
	-	67	2.5	1.6
8103	-	33	41.8	36.5
	-	36	52.8	45.5
	-	40	65.7	53.9
	-	50	59.1	49.9
	-	60	58.7	50.7
	-	67	72.8	60.9
	-	80	97.0	80.2
R2628 E5	+	33	49.2	44.4
	+	40	37.9	33.3
	+	50	34.6	30.4
	+	60	39.8	37.3
	+	80	96.2	81.9
R2628 E4	-	36	73.9	64.8
	-	40	104.0	77.0
	-	50	84.3	68.3
	-	60	69.9	54.6
	-	80	103.0	81.8
	+	36	69.1	50.4
	+	40	56.2	48.2
	+	50	37.5	32.1
	+	60	64.4	53.8
	+	80	65.3	57.7

Table II.2 Table showing fluorescent intensities of PE of the time course barrier assay experiment by examining the transgene *IL2R* expression. Only PE signals from green cell populations of DOX treated cells were taken for the *IL2R* expression examination. 6C2 served as a control to determine the antibody specificity, given no *IL2R* expression in this cell line.

REFERENCES

Aagaard L, Laible G, Selenko P, Schmid M, Dorn R, Schotta G et al. Functional mammalian homologues of the Drosophila PEV-modifier Su(var)3-9 encode centromere-associated proteins which complex with the heterochromatin component M31. EMBO J 1999; 18(7):1923-1938.

Adam M, Robert F, Larochelle M, Gaudreau L. H2A.Z is required for global chromatin integrity and for recruitment of RNA polymerase II under specific conditions. Mol Cell Biol 2001; 21(18):6270-6279.

Agalioti T, Chen G, Thanos D. Deciphering the transcriptional histone acetylation code for a human gene. Cell 2002; 111(3):381-392.

Agger K, Christensen J, Cloos PA, Helin K. The emerging functions of histone demethylases. Curr Opin Genet Dev 2008; 18(2):159-168.

Albert I, Mavrich TN, Tomsho LP, Qi J, Zanton SJ, Schuster SC et al. Translational and rotational settings of H2A.Z nucleosomes across the Saccharomyces cerevisiae genome. Nature 2007; 446(7135):572-576.

Alberts B, Johnson A, Lewis J, Raff M, Roberts K, Walter P. Molecular biology of the cell. 5th Ed. New York: Garland Science; 2008.

Allis CD, Berger SL, Cote J, Dent S, Jenuwien T, Kouzarides T et al. New nomenclature for chromatin-modifying enzymes. Cell 2007; 131(4):633-636.

Altaf M, Auger A, Covic M, Cote J. Connection between histone H2A variants and chromatin remodeling complexes. Biochem Cell Biol 2009; 87(1):35-50.

Arents G, Burlingame RW, Wang BC, Love WE, Moudrianakis EN. The nucleosomal core histone octamer at 3.1 A resolution: a tripartite protein assembly and a left-handed superhelix. Proc Natl Acad Sci U S A 1991; 88(22):10148-10152.

Arents G, Moudrianakis EN. The histone fold: a ubiquitous architectural motif utilized in DNA compaction and protein dimerization. Proc Natl Acad Sci U S A 1995; 92(24):11170-11174.

Arya M, Shergill IS, Williamson M, Gommersall L, Arya N, Patel HR. Basic principles of real-time quantitative PCR. Expert Rev Mol Diagn 2005; 5(2):209-219.

Baarends WM, Hoogerbrugge JW, Roest HP, Ooms M, Vreeburg J, Hoeijmakers JH et al. Histone ubiquitination and chromatin remodeling in mouse spermatogenesis. Dev Biol 1999; 207(2):322-333.

Baarends WM, Wassenaar E, van der LR, Hoogerbrugge J, Sleddens-Linkels E, Hoeijmakers JH et al. Silencing of unpaired chromatin and histone H2A ubiquitination in mammalian meiosis.

Mol Cell Biol 2005; 25(3):1041-1053.

Babiarz JE, Halley JE, Rine J. Telomeric heterochromatin boundaries require NuA4-dependent acetylation of histone variant H2A.Z in Saccharomyces cerevisiae. Genes Dev 2006; 20(6):700-710.

Balakrishnan L, Milavetz B. Decoding the histone H4 lysine 20 methylation mark. Crit Rev Biochem Mol Biol 2010; 45(5):440-452.

Bannister AJ, Zegerman P, Partridge JF, Miska EA, Thomas JO, Allshire RC et al. Selective recognition of methylated lysine 9 on histone H3 by the HP1 chromo domain. Nature 2001; 410(6824):120-124.

Barak O, Lazzaro MA, Lane WS, Speicher DW, Picketts DJ, Shiekhattar R. Isolation of human NURF: a regulator of Engrailed gene expression. EMBO J 2003; 22(22):6089-6100.

Bartolomei MS, Zemel S, Tilghman SM. Parental imprinting of the mouse H19 gene. Nature 1991; 351(6322):153-155.

Batsche E, Yaniv M, Muchardt C. The human SWI/SNF subunit Brm is a regulator of alternative splicing. Nat Struct Mol Biol 2006; 13(1):22-29.

Bao Y, Shen X. SnapShot: chromatin remodeling complexes. Cell 2007; 129(3):632.

Baumann C, Viveiros MM, De La FR. Loss of maternal ATRX results in centromere instability and aneuploidy in the mammalian oocyte and pre-implantation embryo. PLoS Genet 2010; 6(9).

Bayne EH, White SA, Kagansky A, Bijos DA, Sanchez-Pulido L, Hoe KL et al. Stc1: a critical link between RNAi and chromatin modification required for heterochromatin integrity. Cell 2010; 140(5):666-677.

Bell AC, Felsenfeld G. Methylation of a CTCF-dependent boundary controls imprinted expression of the Igf2 gene. Nature 2000; 405(6785):482-485.

Bell AC, West AG, Felsenfeld G. The protein CTCF is required for the enhancer blocking activity of vertebrate insulators. Cell 1999; 98(3):387-396.

Belotserkovskaya R, Oh S, Bondarenko VA, Orphanides G, Studitsky VM, Reinberg D. FACT facilitates transcription-dependent nucleosome alteration. Science 2003; 301(5636):1090-1093.

Bernard P, Maure JF, Partridge JF, Genier S, Javerzat JP, Allshire RC. Requirement of heterochromatin for cohesion at centromeres. Science 2001; 294(5551):2539-2542.

Bernstein BE, Mikkelsen TS, Xie X, Kamal M, Huebert DJ, Cuff J et al. A bivalent chromatin structure marks key developmental genes in embryonic stem cells. Cell 2006; 125(2):315-326.

Bernstein BE, Kamal M, Lindblad-Toh K, Bekiranov S, Bailey DK, Huebert DJ et al. Genomic maps and comparative analysis of histone modifications in human and mouse. Cell 2005; 120(2):169-181.

Barski A, Cuddapah S, Cui K, Roh TY, Schones DE, Wang Z et al. High-resolution profiling of histone methylations in the human genome. Cell 2007; 129(4):823-837.

Beug H, Doederlein G, Freudenstein C, Graf T. Erythroblast cell lines transformed by a temperature-sensitive mutant of avian erythroblastosis virus: a model system to study erythroid differentiation in vitro. J Cell Physiol Suppl 1982; 1:195-207.

Bi X, Yu Q, Sandmeier JJ, Zou Y. Formation of boundaries of transcriptionally silent chromatin by nucleosome-excluding structures. Mol Cell Biol 2004; 24(5):2118-2131.

Bird A. DNA methylation patterns and epigenetic memory. Genes Dev 2002; 16(1):6-21.

Bird AP, Wolffe AP. Methylation-induced repression--belts, braces, and chromatin. Cell 1999; 99(5):451-454.

Boa S, Coert C, Patterton HG. Saccharomyces cerevisiae Set1p is a methyltransferase specific for lysine 4 of histone H3 and is required for efficient gene expression. Yeast 2003; 20(9):827-835.

Boardman PE, Sanz-Ezquerro J, Overton IM, Burt DW, Bosch E, Fong WT et al. A comprehensive collection of chicken cDNAs. Curr Biol 2002; 12(22):1965-1969.

Boyer LA, Latek RR, Peterson CL. The SANT domain: a unique histone-tail-binding module? Nat Rev Mol Cell Biol 2004; 5(2):158-163.

Brasher SV, Smith BO, Fogh RH, Nietlispach D, Thiru A, Nielsen PR et al. The structure of mouse HP1 suggests a unique mode of single peptide recognition by the shadow chromo domain dimer. EMBO J 2000; 19(7):1587-1597.

Brehm A, Tufteland KR, Aasland R, Becker PB. The many colours of chromodomains. Bioessays 2004; 26(2):133-140.

Brehm A, Miska EA, McCance DJ, Reid JL, Bannister AJ, Kouzarides T. Retinoblastoma protein recruits histone deacetylase to repress transcription. Nature 1998; 391(6667):597-601.

Bresnick EH, Johnson KD, Kim SI, Im H. Establishment and regulation of chromatin domains: mechanistic insights from studies of hemoglobin synthesis. Prog Nucleic Acid Res Mol Biol 2006; 81:435-471.

Brinkman AB, Pennings SW, Braliou GG, Rietveld LE, Stunnenberg HG. DNA methylation immediately adjacent to active histone marking does not silence transcription. Nucleic Acids Res 2007; 35(3):801-811.

Briggs SD, Bryk M, Strahl BD, Cheung WL, Davie JK, Dent SY et al. Histone H3 lysine 4 methylation is mediated by Set1 and required for cell growth and rDNA silencing in Saccharomyces cerevisiae. Genes Dev 2001; 15(24):3286-3295.

Briggs SD, Xiao T, Sun ZW, Caldwell JA, Shabanowitz J, Hunt DF et al. Gene silencing: trans-histone regulatory pathway in chromatin. Nature 2002; 418(6897):498.

Bruce K, Myers FA, Mantouvalou E, Lefevre P, Greaves I, Bonifer C et al. The replacement histone H2A.Z in a hyperacetylated form is a feature of active genes in the chicken. Nucleic Acids Res 2005; 33(17):5633-5639.

Burgess-Beusse B, Farrell C, Gaszner M, Litt M, Mutskov V, Recillas-Targa F et al. The insulation of genes from external enhancers and silencing chromatin. Proc Natl Acad Sci U S A 2002; 99 Suppl 4:16433-16437.

Burns LG, Peterson CL. The yeast SWI-SNF complex facilitates binding of a transcriptional activator to nucleosomal sites in vivo. Mol Cell Biol 1997; 17(8):4811-4819.

Buker SM, Iida T, Buhler M, Villen J, Gygi SP, Nakayama J et al. Two different Argonaute complexes are required for siRNA generation and heterochromatin assembly in fission yeast. Nat Struct Mol Biol 2007; 14(3):200-207.

Byrd K, Corces VG. Visualization of chromatin domains created by the gypsy insulator of Drosophila. J Cell Biol 2003; 162(4):565-574.

Cairns BR. The logic of chromatin architecture and remodelling at promoters. Nature 2009; 461(7261):193-198.

Capelson M, Corces VG. The ubiquitin ligase dTopors directs the nuclear organization of a chromatin insulator. Mol Cell 2005; 20(1):105-116.

Carrozza MJ, Li B, Florens L, Suganuma T, Swanson SK, Lee KK et al. Histone H3 methylation by Set2 directs deacetylation of coding regions by Rpd3S to suppress spurious intragenic transcription. Cell 2005; 123(4):581-592.

Carmen AA, Milne L, Grunstein M. Acetylation of the yeast histone H4 N terminus regulates its binding to heterochromatin protein SIR3. J Biol Chem 2002; 277(7):4778-4781.

Campos EI, Reinberg D. Histones: annotating chromatin. Annu Rev Genet 2009; 43:559-599.

Cao R, Tsukada Y, Zhang Y. Role of Bmi-1 and Ring1A in H2A ubiquitylation and Hox gene silencing. Mol Cell 2005; 20(6):845-854.

Cao R, Wang L, Wang H, Xia L, Erdjument-Bromage H, Tempst P et al. Role of histone H3 lysine 27 methylation in Polycomb-group silencing. Science 2002; 298(5595):1039-1043.

Casolari JM, Brown CR, Komili S, West J, Hieronymus H, Silver PA. Genome-wide localization of the nuclear transport machinery couples transcriptional status and nuclear organization. Cell 2004; 117(4):427-439.

Chandrasekharan MB, Huang F, Sun ZW. Ubiquitination of histone H2B regulates chromatin dynamics by enhancing nucleosome stability. Proc Natl Acad Sci U S A 2009; 106(39):16686-16691.

Chandy M, Gutierrez JL, Prochasson P, Workman JL. SWI/SNF displaces SAGA-acetylated nucleosomes. Eukaryot Cell 2006; 5(10):1738-1747.

Christensen J, Agger K, Cloos PA, Pasini D, Rose S, Sennels L et al. RBP2 belongs to a family of demethylases, specific for tri-and dimethylated lysine 4 on histone 3. Cell 2007; 128(6):1063-1076.

Chen D, Ma H, Hong H, Koh SS, Huang SM, Schurter BT et al. Regulation of transcription by a protein methyltransferase. Science 1999; 284(5423):2174-2177.

Chen YZ, Gu XF, Caen JP, Han ZC. Interleukin-3 is an autocrine growth factor of human megakaryoblasts, the DAMI and MEG-01 cells. Br J Haematol 1994; 88(3):481-487.

Chiu YH, Yu Q, Sandmeier JJ, Bi X. A targeted histone acetyltransferase can create a sizable region of hyperacetylated chromatin and counteract the propagation of transcriptionally silent chromatin. Genetics 2003; 165(1):115-125.

Chung JH, Whiteley M, Felsenfeld G. A 5' element of the chicken beta-globin domain serves as an insulator in human erythroid cells and protects against position effect in Drosophila. Cell 1993; 74(3):505-514.

Chung JH, Bell AC, Felsenfeld G. Characterization of the chicken beta-globin insulator. Proc Natl Acad Sci U S A 1997; 94(2):575-580.

Cho JH, Ha SJ, Kao LR, Megraw TL, Chae CB. A novel DNA-binding protein bound to the mitochondrial inner membrane restores the null mutation of mitochondrial histone Abf2p in Saccharomyces cerevisiae. Mol Cell Biol 1998; 18(10):5712-5723.

Clapier CR, Cairns BR. The biology of chromatin remodeling complexes. Annu Rev Biochem 2009; 78:273-304.

Cloos PA, Christensen J, Agger K, Maiolica A, Rappsilber J, Antal T et al. The putative oncogene GASC1 demethylates tri- and dimethylated lysine 9 on histone H3. Nature 2006; 442(7100):307-311.

Conerly ML, Teves SS, Diolaiti D, Ulrich M, Eisenman RN, Henikoff S. Changes in H2A.Z occupancy and DNA methylation during B-cell lymphomagenesis. Genome Res 2010; 20(10):1383-1390.

Cook JR, Lee JH, Yang ZH, Krause CD, Herth N, Hoffmann R et al. FBXO11/PRMT9, a new protein arginine methyltransferase, symmetrically dimethylates arginine residues. Biochem Biophys Res Commun 2006; 342(2):472-481.

Corpet F. Multiple sequence alignment with hierarchical clustering. Nucleic Acids Res 1988; 16(22):10881-10890.

Cowieson NP, Partridge JF, Allshire RC, McLaughlin PJ. Dimerisation of a chromo shadow domain and distinctions from the chromodomain as revealed by structural analysis. Curr Biol 2000; 10(9):517-525.

Cuthbert GL, Daujat S, Snowden AW, Erdjument-Bromage H, Hagiwara T, Yamada M et al. Histone deimination antagonizes arginine methylation. Cell 2004; 118(5):545-553.

Czermin B, Melfi R, McCabe D, Seitz V, Imhof A, Pirrotta V. Drosophila enhancer of Zeste/ESC complexes have a histone H3 methyltransferase activity that marks chromosomal Polycomb sites. Cell 2002; 111(2):185-196.

Czermin B, Schotta G, Hulsmann BB, Brehm A, Becker PB, Reuter G et al. Physical and functional association of SU(VAR)3-9 and HDAC1 in Drosophila. EMBO Rep 2001; 2(10):915-919.

Daniel JA, Torok MS, Sun ZW, Schieltz D, Allis CD, Yates JR, III et al. Deubiquitination of histone H2B by a yeast acetyltransferase complex regulates transcription. J Biol Chem 2004; 279(3):1867-1871.

Dannenberg JH, David G, Zhong S, van der TJ, Wong WH, Depinho RA. mSin3A corepressor regulates diverse transcriptional networks governing normal and neoplastic growth and survival. Genes Dev 2005; 19(13):1581-1595.

Das PM, Ramachandran K, vanWert J, Singal R. Chromatin immunoprecipitation assay. Biotechniques 2004; 37(6):961-969.

de lC, X, Lois S, Sanchez-Molina S, Martinez-Balbas MA. Do protein motifs read the histone code? Bioessays 2005; 27(2):164-175.

DeChiara TM, Robertson EJ, Efstratiadis A. Parental imprinting of the mouse insulin-like growth

factor II gene. Cell 1991; 64(4):849-859.

Deuring R, Fanti L, Armstrong JA, Sarte M, Papoulas O, Prestel M et al. The ISWI chromatin-remodeling protein is required for gene expression and the maintenance of higher order chromatin structure in vivo. Mol Cell 2000; 5(2):355-365.

Davey CA, Sargent DF, Luger K, Maeder AW, Richmond TJ. Solvent mediated interactions in the structure of the nucleosome core particle at 1.9 a resolution. J Mol Biol 2002; 319(5):1097-1113.

Deshpande G, Calhoun G, Schedl P. Drosophila argonaute-2 is required early in embryogenesis for the assembly of centric/centromeric heterochromatin, nuclear division, nuclear migration, and germ-cell formation. Genes Dev 2005; 19(14):1680-1685.

Dickson J, Gowher H, Strogantsev R, Gaszner M, Hair A, Felsenfeld G et al. VEZF1 elements mediate protection from DNA methylation. PLoS Genet 2010; 6(1):e1000804.

Djupedal I, Portoso M, Spahr H, Bonilla C, Gustafsson CM, Allshire RC et al. RNA Pol II subunit Rpb7 promotes centromeric transcription and RNAi-directed chromatin silencing. Genes Dev 2005; 19(19):2301-2306.

Donze D, Adams CR, Rine J, Kamakaka RT. The boundaries of the silenced HMR domain in Saccharomyces cerevisiae. Genes Dev 1999; 13(6):698-708.

Donze D, Kamakaka RT. RNA polymerase III and RNA polymerase II promoter complexes are heterochromatin barriers in Saccharomyces cerevisiae. EMBO J 2001; 20(3):520-531.

Donze D, Kamakaka RT. Braking the silence: how heterochromatic gene repression is stopped in its tracks. Bioessays 2002; 24(4):344-349.

Dover J, Schneider J, Tawiah-Boateng MA, Wood A, Dean K, Johnston M et al. Methylation of histone H3 by COMPASS requires ubiquitination of histone H2B by Rad6. J Biol Chem 2002; 277(32):28368-28371.

Dou Y, Milne TA, Ruthenburg AJ, Lee S, Lee JW, Verdine GL et al. Regulation of MLL1 H3K4 methyltransferase activity by its core components. Nat Struct Mol Biol 2006; 13(8):713-719.

Doyon Y, Selleck W, Lane WS, Tan S, Cote J. Structural and functional conservation of the NuA4 histone acetyltransferase complex from yeast to humans. Mol Cell Biol 2004; 24(5):1884-1896.

Dull T, Zufferey R, Kelly M, Mandel RJ, Nguyen M, Trono D et al. A third-generation lentivirus vector with a conditional packaging system. J Virol 1998; 72(11):8463-8471.

Eberharter A, Becker PB. Histone acetylation: a switch between repressive and permissive chromatin. Second in review series on chromatin dynamics. EMBO Rep 2002; 3(3):224-229.

Ellermeier C, Higuchi EC, Phadnis N, Holm L, Geelhood JL, Thon G et al. RNAi and heterochromatin repress centromeric meiotic recombination. Proc Natl Acad Sci U S A 2010; 107(19):8701-8705.

Emre NC, Ingvarsdottir K, Wyce A, Wood A, Krogan NJ, Henry KW et al. Maintenance of low histone ubiquitylation by Ubp10 correlates with telomere-proximal Sir2 association and gene silencing. Mol Cell 2005; 17(4):585-594.

Engel N, West AG, Felsenfeld G, Bartolomei MS. Antagonism between DNA hypermethylation and enhancer-blocking activity at the H19 DMD is uncovered by CpG mutations. Nat Genet 2004; 36(8):883-888.

Esnault G, Majocchi S, Martinet D, Besuchet-Schmutz N, Beckmann JS, Mermod N. Transcription factor CTF1 acts as a chromatin domain boundary that shields human telomeric genes from silencing. Mol Cell Biol 2009; 29(9):2409-2418.

Evert BO, Araujo J, Vieira-Saecker AM, de Vos RA, Harendza S, Klockgether T et al. Ataxin-3 represses transcription via chromatin binding, interaction with histone deacetylase 3, and histone deacetylation. J Neurosci 2006; 26(44):11474-11486.

Fagegaltier D, Bouge AL, Berry B, Poisot E, Sismeiro O, Coppee JY et al. The endogenous siRNA pathway is involved in heterochromatin formation in Drosophila. Proc Natl Acad Sci U S A 2009; 106(50):21258-21263.

Fan JY, Gordon F, Luger K, Hansen JC, Tremethick DJ. The essential histone variant H2A.Z regulates the equilibrium between different chromatin conformational states. Nat Struct Biol 2002; 9(3):172-176.

Felsenfeld G. Chromatin structure and the expression of globin-encoding genes. Gene 1993; 135(1-2):119-124.

Felsenfeld G, Groudine M. Controlling the double helix. Nature 2003; 421(6921):448-453.

Ferrari S, Simmen KC, Dusserre Y, Muller K, Fourel G, Gilson E et al. Chromatin domain boundaries delimited by a histone-binding protein in yeast. J Biol Chem 2004; 279(53):55520-55530.

Fischle W, Wang Y, Jacobs SA, Kim Y, Allis CD, Khorasanizadeh S. Molecular basis for the discrimination of repressive methyl-lysine marks in histone H3 by Polycomb and HP1 chromodomains. Genes Dev 2003; 17(15):1870-1881.

Flanagan JF, Mi LZ, Chruszcz M, Cymborowski M, Clines KL, Kim Y et al. Double chromodomains cooperate to recognize the methylated histone H3 tail. Nature 2005; 438(7071):1181-1185.

Fleming AB, Kao CF, Hillyer C, Pikaart M, Osley MA. H2B ubiquitylation plays a role in nucleosome dynamics during transcription elongation. Mol Cell 2008; 31(1):57-66.

Fordis CM, Anagnou NP, Dean A, Nienhuis AW, Schechter AN. A beta-globin gene, inactive in the K562 leukemic cell, functions normally in a heterologous expression system. Proc Natl Acad Sci U S A 1984; 81(14):4485-4489.

Frazar TF, Weisbein JL, Anderson SM, Cline AP, Garrett LJ, Felsenfeld G et al. Variegated expression from the murine band 3 (AE1) promoter in transgenic mice is associated with mRNA transcript initiation at upstream start sites and can be suppressed by the addition of the chicken beta-globin 5' HS4 insulator element. Mol Cell Biol 2003; 23(14):4753-4763.

Fu Y, Sinha M, Peterson CL, Weng Z. The insulator binding protein CTCF positions 20 nucleosomes around its binding sites across the human genome. PLoS Genet 2008; 4(7):e1000138.

Fukagawa T, Nogami M, Yoshikawa M, Ikeno M, Okazaki T, Takami Y et al. Dicer is essential for formation of the heterochromatin structure in vertebrate cells. Nat Cell Biol 2004; 6(8):784-791.

Fuks F. DNA methylation and histone modifications: teaming up to silence genes. Curr Opin Genet Dev 2005; 15(5):490-495.

Fuks F, Hurd PJ, Deplus R, Kouzarides T. The DNA methyltransferases associate with HP1 and the SUV39H1 histone methyltransferase. Nucleic Acids Res 2003; 31(9):2305-2312.

Gardner RG, Nelson ZW, Gottschling DE. Ubp10/Dot4p regulates the persistence of ubiquitinated histone H2B: distinct roles in telomeric silencing and general chromatin. Mol Cell Biol 2005; 25(14):6123-6139.

Gaszner M, Felsenfeld G. Insulators: exploiting transcriptional and epigenetic mechanisms. Nat Rev Genet 2006; 7(9):703-713.

Gaspar-Maia A, Alajem A, Polesso F, Sridharan R, Mason MJ, Heidersbach A et al. Chd1 regulates open chromatin and pluripotency of embryonic stem cells. Nature 2009; 460(7257):863-868.

Gaszner M, Felsenfeld G. Insulators: exploiting transcriptional and epigenetic mechanisms. Nat Rev Genet 2006; 7(9):703-713.

Gdula DA, Gerasimova TI, Corces VG. Genetic and molecular analysis of the gypsy chromatin insulator of Drosophila. Proc Natl Acad Sci U S A 1996; 93(18):9378-9383.

Gershenzon NI, Ioshikhes IP. Synergy of human Pol II core promoter elements revealed by statistical sequence analysis. Bioinformatics 2005; 21(8):1295-1300.

Gerasimova TI, Byrd K, Corces VG. A chromatin insulator determines the nuclear localization of DNA. Mol Cell 2000; 6(5):1025-1035.

Geyer PK, Corces VG. DNA position-specific repression of transcription by a Drosophila zinc finger protein. Genes Dev 1992; 6(10):1865-1873.

Ghosh D, Gerasimova TI, Corces VG. Interactions between the Su(Hw) and Mod(mdg4) proteins required for gypsy insulator function. EMBO J 2001; 20(10):2518-2527.

Giles KE, Ghirlando R, Felsenfeld G. Maintenance of a constitutive heterochromatin domain in vertebrates by a Dicer-dependent mechanism. Nat Cell Biol 2010; 12(1):94-99.

Girton JR, Johansen KM. Chromatin structure and the regulation of gene expression: the lessons of PEV in Drosophila. Adv Genet 2008; 61:1-43.

Goldmark JP, Fazzio TG, Estep PW, Church GM, Tsukiyama T. The Isw2 chromatin remodeling complex represses early meiotic genes upon recruitment by Ume6p. Cell 2000; 103(3):423-433.

Goldknopf IL, Busch H. Remarkable similarities of peptide fingerprints of histone 2A and nonhistone chromosomal protein A24. Biochem Biophys Res Commun 1975; 65(3):951-960.

Gowher H, Stuhlmann H, Felsenfeld G. Vezf1 regulates genomic DNA methylation through its effects on expression of DNA methyltransferase Dnmt3b. Genes Dev 2008; 22(15):2075-2084.

Grant PA, Duggan L, Cote J, Roberts SM, Browell JE, Candau R et al. Yeast Gcn5 functions in two multisubunit complexes to acetylate nucleosomal histones: characterization of an Ada complex and the SAGA (Spt/Ada) complex. Genes Dev 1997; 11(13):1640-1650.

Grewal SI, Elgin SC. Heterochromatin: new possibilities for the inheritance of structure. Curr Opin Genet Dev 2002; 12(2):178-187.

Grewal SI, Jia S. Heterochromatin revisited. Nat Rev Genet 2007; 8(1):35-46.

Griffiths AJ, Miller JH, Suzuki DT, Lewontin RC, Gelbart WM. An introduction to genetic analysis. 7th Ed. New York: W. H. Freeman; 2000.

Grunstein M. Histone acetylation in chromatin structure and transcription. Nature 1997; 389(6649):349-352.

Groudine M, Weintraub H. Activation of globin genes during chicken development. Cell 1981; 24(2):393-401.

Guenther MG, Levine SS, Boyer LA, Jaenisch R, Young RA. A chromatin landmark and transcription initiation at most promoters in human cells. Cell 2007; 130(1):77-88.

Guccione E, Bassi C, Casadio F, Martinato F, Cesaroni M, Schuchlautz H et al. Methylation of histone H3R2 by PRMT6 and H3K4 by an MLL complex are mutually exclusive. Nature 2007; 449(7164):933-937.

Guglielmi L, Truffinet V, Cogne M, Denizot Y. The beta-globin HS4 insulator confers copy-number dependent expression of IgH regulatory elements in stable B cell transfectants. Immunol Lett 2003; 89(2-3):119-123.

Hacke K, Falahati R, Flebbe-Rehwaldt L, Kasahara N, Gaensler KM. Suppression of HLA expression by lentivirus-mediated gene transfer of siRNA cassettes and in vivo chemoselection to enhance hematopoietic stem cell transplantation. Immunol Res 2009; 44(1-3):112-126.

Haldar D, Kamakaka RT. tRNA genes as chromatin barriers. Nat Struct Mol Biol 2006; 13(3):192-193.

Hall JA, Georgel PT. CHD proteins: a diverse family with strong ties. Biochem Cell Biol 2007; 85(4):463-476.

Hamiche A, Sandaltzopoulos R, Gdula DA, Wu C. ATP-dependent histone octamer sliding mediated by the chromatin remodeling complex NURF. Cell 1999; 97(7):833-842.

Han Q, Lu J, Duan J, Su D, Hou X, Li F et al. Gcn5- and Elp3-induced histone H3 acetylation regulates hsp70 gene transcription in yeast. Biochem J 2008; 409(3):779-788.

Hannon GJ. RNA interference. Nature 2002; 418(6894):244-251.

Hardy S, Jacques PE, Gevry N, Forest A, Fortin ME, Laflamme L et al. The euchromatic and heterochromatic landscapes are shaped by antagonizing effects of transcription on H2A.Z deposition. PLoS Genet 2009; 5(10):e1000687.

Hardy S, Robert F. Random deposition of histone variants: A cellular mistake or a novel regulatory mechanism? Epigenetics 2010; 5(5).

Hark AT, Schoenherr CJ, Katz DJ, Ingram RS, Levorse JM, Tilghman SM. CTCF mediates methylation-sensitive enhancer-blocking activity at the H19/Igf2 locus. Nature 2000; 405(6785):486-489.

Hassan AH, Prochasson P, Neely KE, Galasinski SC, Chandy M, Carrozza MJ et al. Function and selectivity of bromodomains in anchoring chromatin-modifying complexes to promoter nucleosomes. Cell 2002; 111(3):369-379.

Hassan AH, Awad S, Al Natour Z, Othman S, Mustafa F, Rizvi TA. Selective recognition of acetylated histones by bromodomains in transcriptional co-activators. Biochem J 2007; 402(1):125-133.

Heintzman ND, Hon GC, Hawkins RD, Kheradpour P, Stark A, Harp LF et al. Histone modifications at human enhancers reflect global cell-type-specific gene expression. Nature 2009; 459(7243):108-112.

Heintzman ND, Stuart RK, Hon G, Fu Y, Ching CW, Hawkins RD et al. Distinct and predictive chromatin signatures of transcriptional promoters and enhancers in the human genome. Nat Genet 2007; 39(3):311-318.

Henry KW, Wyce A, Lo WS, Duggan LJ, Emre NC, Kao CF et al. Transcriptional activation via sequential histone H2B ubiquitylation and deubiquitylation, mediated by SAGA-associated Ubp8. Genes Dev 2003; 17(21):2648-2663.

Hildmann C, Riester D, Schwienhorst A. Histone deacetylases--an important class of cellular regulators with a variety of functions. Appl Microbiol Biotechnol 2007; 75(3):487-497.

Hines KA, Cryderman DE, Flannery KM, Yang H, Vitalini MW, Hazelrigg T et al. Domains of heterochromatin protein 1 required for Drosophila melanogaster heterochromatin spreading. Genetics 2009; 182(4):967-977.

Hiragami-Hamada K, Xie SQ, Saveliev A, Uribe-Lewis S, Pombo A, Festenstein R. The molecular basis for stability of heterochromatin-mediated silencing in mammals. Epigenetics Chromatin 2009; 2(1):14.

Hirschhorn JN, Brown SA, Clark CD, Winston F. Evidence that SNF2/SWI2 and SNF5 activate transcription in yeast by altering chromatin structure. Genes Dev 1992; 6(12A):2288-2298.

Ho L, Crabtree GR. Chromatin remodelling during development. Nature 2010; 463(7280):474-484.

Hsu M, Richardson CA, Olivier E, Qiu C, Bouhassira EE, Lowrey CH et al. Complex developmental patterns of histone modifications associated with the human beta-globin switch in primary cells. Exp Hematol 2009; 37(7):799-806.

Hublitz P, Albert M, Peters AH. Mechanisms of transcriptional repression by histone lysine methylation. Int J Dev Biol 2009; 53(2-3):335-354.

Hutvagner G, Simard MJ. Argonaute proteins: key players in RNA silencing. Nat Rev Mol Cell Biol 2008; 9(1):22-32.

Huisinga KL, Brower-Toland B, Elgin SC. The contradictory definitions of heterochromatin: transcription and silencing. Chromosoma 2006; 115(2):110-122.

Hwang WW, Venkatasubrahmanyam S, Ianculescu AG, Tong A, Boone C, Madhani HD. A conserved RING finger protein required for histone H2B monoubiquitination and cell size control. Mol Cell 2003; 11(1):261-266.

Hyllus D, Stein C, Schnabel K, Schiltz E, Imhof A, Dou Y et al. PRMT6-mediated methylation of R2 in histone H3 antagonizes H3 K4 trimethylation. Genes Dev 2007; 21(24):3369-3380.

Holmgren C, Kanduri C, Dell G, Ward A, Mukhopadhya R, Kanduri M et al. CpG methylation regulates the Igf2/H19 insulator. Curr Biol 2001; 11(14):1128-1130.

Huang S, Litt M, Felsenfeld G. Methylation of histone H4 by arginine methyltransferase PRMT1 is essential in vivo for many subsequent histone modifications. Genes Dev 2005; 19(16):1885-1893.

Huang S, Li X, Yusufzai TM, Qiu Y, Felsenfeld G. USF1 recruits histone modification complexes and is critical for maintenance of a chromatin barrier. Mol Cell Biol 2007; 27(22):7991-8002.

Ikura T, Ogryzko VV, Grigoriev M, Groisman R, Wang J, Horikoshi M et al. Involvement of the TIP60 histone acetylase complex in DNA repair and apoptosis. Cell 2000; 102(4):463-473.

Irvine DV, Zaratiegui M, Tolia NH, Goto DB, Chitwood DH, Vaughn MW et al. Argonaute slicing is required for heterochromatic silencing and spreading. Science 2006; 313(5790):1134-1137.

Ishii K, Arib G, Lin C, Van Houwe G, Laemmli UK. Chromatin boundaries in budding yeast: the nuclear pore connection. Cell 2002; 109(5):551-562.

Ito T, Bulger M, Pazin MJ, Kobayashi R, Kadonaga JT. ACF, an ISWI-containing and ATP-utilizing chromatin assembly and remodeling factor. Cell 1997; 90(1):145-155.

Iwase S, Lan F, Bayliss P, Torre-Ubieta L, Huarte M, Qi HH et al. The X-linked mental retardation gene SMCX/JARID1C defines a family of histone H3 lysine 4 demethylases. Cell 2007; 128(6):1077-1088.

Jacobson RH, Ladurner AG, King DS, Tjian R. Structure and function of a human TAFII250 double bromodomain module. Science 2000; 288(5470):1422-1425.

Jason LJ, Moore SC, Lewis JD, Lindsey G, Ausio J. Histone ubiquitination: a tagging tail unfolds? Bioessays 2002; 24(2):166-174.

Jha S, Dutta A. RVB1/RVB2: running rings around molecular biology. Mol Cell 2009; 34(5):521-533.

Jin C, Felsenfeld G. Nucleosome stability mediated by histone variants H3.3 and H2A.Z. Genes Dev 2007; 21(12):1519-1529.

Jin J, Cai Y, Li B, Conaway RC, Workman JL, Conaway JW et al. In and out: histone variant exchange in chromatin. Trends Biochem Sci 2005; 30(12):680-687.

Jin C, Zang C, Wei G, Cui K, Peng W, Zhao K et al. H3.3/H2A.Z double variant-containing nucleosomes mark 'nucleosome-free regions' of active promoters and other regulatory regions. Nat Genet 2009; 41(8):941-945.

Jones PL, Veenstra GJ, Wade PA, Vermaak D, Kass SU, Landsberger N et al. Methylated DNA and MeCP2 recruit histone deacetylase to repress transcription. Nat Genet 1998; 19(2):187-191.

Joshi AA, Struhl K. Eaf3 chromodomain interaction with methylated H3-K36 links histone deacetylation to Pol II elongation. Mol Cell 2005; 20(6):971-978.

Joo HY, Zhai L, Yang C, Nie S, Erdjument-Bromage H, Tempst P et al. Regulation of cell cycle progression and gene expression by H2A deubiquitination. Nature 2007; 449(7165):1068-1072.

Kafri T, van Praag H, Gage FH, Verma IM. Lentiviral vectors: regulated gene expression. Mol Ther 2000; 1(6):516-521.

Kahana A, Gottschling DE. DOT4 links silencing and cell growth in Saccharomyces cerevisiae. Mol Cell Biol 1999; 19(10):6608-6620.

Kanduri C, Pant V, Loukinov D, Pugacheva E, Qi CF, Wolffe A et al. Functional association of CTCF with the insulator upstream of the H19 gene is parent of origin-specific and methylation-sensitive. Curr Biol 2000; 10(14):853-856.

Kanno T, Kanno Y, Siegel RM, Jang MK, Lenardo MJ, Ozato K. Selective recognition of acetylated histones by bromodomain proteins visualized in living cells. Mol Cell 2004; 13(1):33-43.

Kanellopoulou C, Muljo SA, Kung AL, Ganesan S, Drapkin R, Jenuwein T et al. Dicer-deficient mouse embryonic stem cells are defective in differentiation and centromeric silencing. Genes Dev 2005; 19(4):489-501.

Kao CF, Hillyer C, Tsukuda T, Henry K, Berger S, Osley MA. Rad6 plays a role in transcriptional activation through ubiquitylation of histone H2B. Genes Dev 2004;

18(2):184-195.

Kato H, Goto DB, Martienssen RA, Urano T, Furukawa K, Murakami Y. RNA polymerase II is required for RNAi-dependent heterochromatin assembly. Science 2005; 309(5733):467-469.

Kawamura Y, Saito K, Kin T, Ono Y, Asai K, Sunohara T et al. Drosophila endogenous small RNAs bind to Argonaute 2 in somatic cells. Nature 2008; 453(7196):793-797.

Kelley DE, Stokes DG, Perry RP. CHD1 interacts with SSRP1 and depends on both its chromodomain and its ATPase/helicase-like domain for proper association with chromatin. Chromosoma 1999; 108(1):10-25.

Keene MA, Elgin SC. Micrococcal nuclease as a probe of DNA sequence organization and chromatin structure. Cell 1981; 27(1 Pt 2):57-64.

Kellum R, Schedl P. A position-effect assay for boundaries of higher order chromosomal domains. Cell 1991; 64(5):941-950.

Kellum R, Schedl P. A group of scs elements function as domain boundaries in an enhancer-blocking assay. Mol Cell Biol 1992; 12(5):2424-2431.

Keogh MC, Kurdistani SK, Morris SA, Ahn SH, Podolny V, Collins SR et al. Cotranscriptional set2 methylation of histone H3 lysine 36 recruits a repressive Rpd3 complex. Cell 2005; 123(4):593-605.

Kim HS, Choi ES, Shin JA, Jang YK, Park SD. Regulation of Swi6/HP1-dependent heterochromatin assembly by cooperation of components of the mitogen-activated protein kinase pathway and a histone deacetylase Clr6. J Biol Chem 2004; 279(41):42850-42859.

Kim A, Dean A. A human globin enhancer causes both discrete and widespread alterations in chromatin structure. Mol Cell Biol 2003; 23(22):8099-8109.

Kim A, Kiefer CM, Dean A. Distinctive signatures of histone methylation in transcribed coding and noncoding human beta-globin sequences. Mol Cell Biol 2007; 27(4):1271-1279.

Kim J, Guermah M, McGinty RK, Lee JS, Tang Z, Milne TA et al. RAD6-Mediated transcription-coupled H2B ubiquitylation directly stimulates H3K4 methylation in human cells. Cell 2009; 137(3):459-471.

Kim J, Hake SB, Roeder RG. The human homolog of yeast BRE1 functions as a transcriptional coactivator through direct activator interactions. Mol Cell 2005; 20(5):759-770.

Klein E, Ben Bassat H, Neumann H, Ralph P, Zeuthen J, Polliack A et al. Properties of the K562 cell line, derived from a patient with chronic myeloid leukemia. Int J Cancer 1976; 18(4):421-431.

Klose RJ, Yan Q, Tothova Z, Yamane K, Erdjument-Bromage H, Tempst P et al. The retinoblastoma binding protein RBP2 is an H3K4 demethylase. Cell 2007; 128(5):889-900.

Klose RJ, Zhang Y. Regulation of histone methylation by demethylimination and demethylation. Nat Rev Mol Cell Biol 2007; 8(4):307-318.

Knemeyer JP, Marme N. Recent patents on self-quenching DNA probes. Recent Pat DNA Gene Seq 2007; 1(2):145-147.

Kobor MS, Venkatasubrahmanyam S, Meneghini MD, Gin JW, Jennings JL, Link AJ et al. A protein complex containing the conserved Swi2/Snf2-related ATPase Swr1p deposits histone variant H2A.Z into euchromatin. PLoS Biol 2004; 2(5):E131.

Konev AY, Tribus M, Park SY, Podhraski V, Lim CY, Emelyanov AV et al. CHD1 motor protein is required for deposition of histone variant H3.3 into chromatin in vivo. Science 2007; 317(5841):1087-1090.

Kouzarides T. Histone methylation in transcriptional control. Curr Opin Genet Dev 2002; 12(2):198-209.

Kouzarides T. SnapShot: Histone-modifying enzymes. Cell 2007; 131(4):822.

Kwon SH, Workman JL. The heterochromatin protein 1 (HP1) family: put away a bias toward HP1. Mol Cells 2008; 26(3):217-227.

Kukreti S, Kaur H, Kaushik M, Bansal A, Saxena S, Kaushik S et al. Structural polymorphism at LCR and its role in beta-globin gene regulation. Biochimie 2010; 92(9):1199-1206.

Kuzmichev A, Nishioka K, Erdjument-Bromage H, Tempst P, Reinberg D. Histone methyltransferase activity associated with a human multiprotein complex containing the Enhancer of Zeste protein. Genes Dev 2002; 16(22):2893-2905.

Lachner M, Jenuwein T. The many faces of histone lysine methylation. Curr Opin Cell Biol 2002; 14(3):286-298.

Lachner M, O'Carroll D, Rea S, Mechtler K, Jenuwein T. Methylation of histone H3 lysine 9 creates a binding site for HP1 proteins. Nature 2001; 410(6824):116-120.

Ladurner AG, Inouye C, Jain R, Tjian R. Bromodomains mediate an acetyl-histone encoded antisilencing function at heterochromatin boundaries. Mol Cell 2003; 11(2):365-376.

Lande-Diner L, Zhang J, Ben Porath I, Amariglio N, Keshet I, Hecht M et al. Role of DNA methylation in stable gene repression. J Biol Chem 2007; 282(16):12194-12200.

Landry J, Sutton A, Hesman T, Min J, Xu RM, Johnston M et al. Set2-catalyzed methylation of histone H3 represses basal expression of GAL4 in Saccharomyces cerevisiae. Mol Cell Biol 2003; 23(17):5972-5978.

Laribee RN, Krogan NJ, Xiao T, Shibata Y, Hughes TR, Greenblatt JF et al. BUR kinase selectively regulates H3 K4 trimethylation and H2B ubiquitylation through recruitment of the PAF elongation complex. Curr Biol 2005; 15(16):1487-1493.

Latham JA, Dent SY. Cross-regulation of histone modifications. Nat Struct Mol Biol 2007; 14(11):1017-1024.

Levine SS, King IF, Kingston RE. Division of labor in polycomb group repression. Trends Biochem Sci 2004; 29(9):478-485.

Lee DY, Teyssier C, Strahl BD, Stallcup MR. Role of protein methylation in regulation of transcription. Endocr Rev 2005; 26(2):147-170.

Lee HL, Archer TK. Prolonged glucocorticoid exposure dephosphorylates histone H1 and inactivates the MMTV promoter. EMBO J 1998; 17(5):1454-1466.

Lee J, Sayegh J, Daniel J, Clarke S, Bedford MT. PRMT8, a new membrane-bound tissue-specific member of the protein arginine methyltransferase family. J Biol Chem 2005; 280(38):32890-32896.

Lee JH, Skalnik DG. Wdr82 is a C-terminal domain-binding protein that recruits the Setd1A Histone H3-Lys4 methyltransferase complex to transcription start sites of transcribed human genes. Mol Cell Biol 2008; 28(2):609-618.

Lee JH, Cook JR, Yang ZH, Mirochnitchenko O, Gunderson SI, Felix AM et al. PRMT7, a new protein arginine methyltransferase that synthesizes symmetric dimethylarginine. J Biol Chem 2005; 280(5):3656-3664.

Lee JH, Tate CM, You JS, Skalnik DG. Identification and characterization of the human Set1B histone H3-Lys4 methyltransferase complex. J Biol Chem 2007; 282(18):13419-13428.

Lee JS, Shilatifard A. A site to remember: H3K36 methylation a mark for histone deacetylation. Mutat Res 2007; 618(1-2):130-134.

Lee JS, Shukla A, Schneider J, Swanson SK, Washburn MP, Florens L et al. Histone crosstalk between H2B monoubiquitination and H3 methylation mediated by COMPASS. Cell 2007; 131(6):1084-1096.

Lee JS, Smith E, Shilatifard A. The language of histone crosstalk. Cell 2010; 142(5):682-685.

Lee KK, Workman JL. Histone acetyltransferase complexes: one size doesn't fit all. Nat Rev Mol

Cell Biol 2007; 8(4):284-295.

Lee MG, Villa R, Trojer P, Norman J, Yan KP, Reinberg D et al. Demethylation of H3K27 regulates polycomb recruitment and H2A ubiquitination. Science 2007; 318(5849):447-450.

Lee MG, Wynder C, Cooch N, Shiekhattar R. An essential role for CoREST in nucleosomal histone 3 lysine 4 demethylation. Nature 2005; 437(7057):432-435.

Lee MG, Norman J, Shilatifard A, Shiekhattar R. Physical and functional association of a trimethyl H3K4 demethylase and Ring6a/MBLR, a polycomb-like protein. Cell 2007; 128(5):877-887.

Lee TF, Zhai J, Meyers BC. Conservation and divergence in eukaryotic DNA methylation. Proc Natl Acad Sci U S A 2010; 107(20):9027-9028.

Lee YH, Koh SS, Zhang X, Cheng X, Stallcup MR. Synergy among nuclear receptor coactivators: selective requirement for protein methyltransferase and acetyltransferase activities. Mol Cell Biol 2002; 22(11):3621-3632.

Lee CK, Shibata Y, Rao B, Strahl BD, Lieb JD. Evidence for nucleosome depletion at active regulatory regions genome-wide. Nat Genet 2004; 36(8):900-905.

Lehnertz B, Ueda Y, Derijck AA, Braunschweig U, Perez-Burgos L, Kubicek S et al. Suv39h-mediated histone H3 lysine 9 methylation directs DNA methylation to major satellite repeats at pericentric heterochromatin. Curr Biol 2003; 13(14):1192-1200.

Lewis CD, Clark SP, Felsenfeld G, Gould H. An erythrocyte-specific protein binds to the poly(dG) region of the chicken beta-globin gene promoter. Genes Dev 1988; 2(7):863-873.

Lewis PW, Elsaesser SJ, Noh KM, Stadler SC, Allis CD. Daxx is an H3.3-specific histone chaperone and cooperates with ATRX in replication-independent chromatin assembly at telomeres. Proc Natl Acad Sci U S A 2010; 107(32):14075-14080.

Li B, Gogol M, Carey M, Lee D, Seidel C, Workman JL. Combined action of PHD and chromo domains directs the Rpd3S HDAC to transcribed chromatin. Science 2007; 316(5827):1050-1054.

Li B, Pattenden SG, Lee D, Gutierrez J, Chen J, Seidel C et al. Preferential occupancy of histone variant H2AZ at inactive promoters influences local histone modifications and chromatin remodeling. Proc Natl Acad Sci U S A 2005; 102(51):18385-18390.

Li F, Huarte M, Zaratiegui M, Vaughn MW, Shi Y, Martienssen R et al. Lid2 is required for coordinating H3K4 and H3K9 methylation of heterochromatin and euchromatin. Cell 2008; 135(2):272-283.

Li H, Ilin S, Wang W, Duncan EM, Wysocka J, Allis CD et al. Molecular basis for site-specific read-out of histone H3K4me3 by the BPTF PHD finger of NURF. Nature 2006; 442(7098):91-95.

Li Q, Zhang M, Han H, Rohde A, Stamatoyannopoulos G. Evidence that DNase I hypersensitive site 5 of the human beta-globin locus control region functions as a chromosomal insulator in transgenic mice. Nucleic Acids Res 2002; 30(11):2484-2491.

Li X, Hu X, Patel B, Zhou Z, Liang S, Ybarra R et al. H4R3 methylation facilitates beta-globin transcription by regulating histone acetyltransferase binding and H3 acetylation. Blood 2010; 115(10):2028-2037.

Li XS, Trojer P, Matsumura T, Treisman JE, Tanese N. Mammalian SWI/SNF--a subunit BAF250/ARID1 is an E3 ubiquitin ligase that targets histone H2B. Mol Cell Biol 2010; 30(7):1673-1688.

Li Y, Reddy MA, Miao F, Shanmugam N, Yee JK, Hawkins D et al. Role of the histone H3 lysine 4 methyltransferase, SET7/9, in the regulation of NF-kappaB-dependent inflammatory genes. Relevance to diabetes and inflammation. J Biol Chem 2008; 283(39):26771-26781.

Liang G, Lin JC, Wei V, Yoo C, Cheng JC, Nguyen CT et al. Distinct localization of histone H3 acetylation and H3-K4 methylation to the transcription start sites in the human genome. Proc Natl Acad Sci U S A 2004; 101(19):7357-7362.

Link PA, Gangisetty O, James SR, Woloszynska-Read A, Tachibana M, Shinkai Y et al. Distinct roles for histone methyltransferases G9a and GLP in cancer germ-line antigen gene regulation in human cancer cells and murine embryonic stem cells. Mol Cancer Res 2009; 7(6):851-862.

Lippman Z, Martienssen R. The role of RNA interference in heterochromatic silencing. Nature 2004; 431(7006):364-370.

Litt MD, Simpson M, Gaszner M, Allis CD, Felsenfeld G. Correlation between histone lysine methylation and developmental changes at the chicken beta-globin locus. Science 2001a; 293(5539):2453-2455.

Litt MD, Simpson M, Recillas-Targa F, Prioleau MN, Felsenfeld G. Transitions in histone acetylation reveal boundaries of three separately regulated neighboring loci. EMBO J 2001b; 20(9):2224-2235.

Liu Y, Subrahmanyam R, Chakraborty T, Sen R, Desiderio S. A plant homeodomain in RAG-2 that binds Hypermethylated lysine 4 of histone H3 is necessary for efficient antigen-receptor-gene rearrangement. Immunity 2007; 27(4):561-571.

Livak KJ, Schmittgen TD. Analysis of relative gene expression data using real-time quantitative PCR and the 2(-Delta Delta C(T)) Method. Methods 2001; 25(4):402-408.

Lodish H, Berk A, Kaiser CA, Krieger M, Scott MP, Bretscher A et al. Molecular cell biology. 5th Ed. New York: W. H. Freeman & Company; 2004.

Lozzio CB, Lozzio BB. Human chronic myelogenous leukemia cell-line with positive Philadelphia chromosome. Blood 1975; 45(3):321-334.

Lu X, Simon MD, Chodaparambil JV, Hansen JC, Shokat KM, Luger K. The effect of H3K79 dimethylation and H4K20 trimethylation on nucleosome and chromatin structure. Nat Struct Mol Biol 2008; 15(10):1122-1124.

Lucio-Eterovic AK, Singh MM, Gardner JE, Veerappan CS, Rice JC, Carpenter PB. Role for the nuclear receptor-binding SET domain protein 1 (NSD1) methyltransferase in coordinating lysine 36 methylation at histone 3 with RNA polymerase II function. Proc Natl Acad Sci U S A 2010; 107(39):16952-16957.

Luk E, Vu ND, Patteson K, Mizuguchi G, Wu WH, Ranjan A et al. Chz1, a nuclear chaperone for histone H2AZ. Mol Cell 2007; 25(3):357-368.

Luger K, Mader AW, Richmond RK, Sargent DF, Richmond TJ. Crystal structure of the nucleosome core particle at 2.8 A resolution. Nature 1997; 389(6648):251-260.

Ma MK, Heath C, Hair A, West AG. Histone crosstalk directed by H2B ubiquitination is required for chromatin boundary integrity. PLoS Genet 2011; in press.

Mann RK, Grunstein M. Histone H3 N-terminal mutations allow hyperactivation of the yeast GAL1 gene in vivo. EMBO J 1992; 11(9):3297-3306.

Maston GA, Evans SK, Green MR. Transcriptional regulatory elements in the human genome. Annu Rev Genomics Hum Genet 2006; 7:29-59.

Mason MM, Lee E, Westphal H, Reitman M. Expression of the chicken beta-globin gene cluster in mice: correct developmental expression and distributed control. Mol Cell Biol 1995; 15(1):407-414.

Matthews AG, Kuo AJ, Ramon-Maiques S, Han S, Champagne KS, Ivanov D et al. RAG2 PHD finger couples histone H3 lysine 4 trimethylation with V(D)J recombination. Nature 2007; 450(7172):1106-1110.

Mavrich TN, Jiang C, Ioshikhes IP, Li X, Venters BJ, Zanton SJ et al. Nucleosome organization in the Drosophila genome. Nature 2008; 453(7193):358-362.

McGinty RK, Kim J, Chatterjee C, Roeder RG, Muir TW. Chemically ubiquitylated histone H2B stimulates hDot1L-mediated intranucleosomal methylation. Nature 2008; 453(7196):812-816.

Meersseman G, Pennings S, Bradbury EM. Mobile nucleosomes--a general behavior. EMBO J 1992; 11(8):2951-2959.

Meneghini MD, Wu M, Madhani HD. Conserved histone variant H2A.Z protects euchromatin from the ectopic spread of silent heterochromatin. Cell 2003; 112(5):725-736.

Miccio A, Wang Y, Hong W, Gregory GD, Wang H, Yu X et al. NuRD mediates activating and repressive functions of GATA-1 and FOG-1 during blood development. EMBO J 2010; 29(2):442-456.

Mikkelsen TS, Ku M, Jaffe DB, Issac B, Lieberman E, Giannoukos G et al. Genome-wide maps of chromatin state in pluripotent and lineage-committed cells. Nature 2007; 448(7153):553-560.

Millar CB, Xu F, Zhang K, Grunstein M. Acetylation of H2AZ Lys 14 is associated with genome-wide gene activity in yeast. Genes Dev 2006; 20(6):711-722.

Min J, Zhang Y, Xu RM. Structural basis for specific binding of Polycomb chromodomain to histone H3 methylated at Lys 27. Genes Dev 2003; 17(15):1823-1828.

Minsky N, Shema E, Field Y, Schuster M, Segal E, Oren M. Monoubiquitinated H2B is associated with the transcribed region of highly expressed genes in human cells. Nat Cell Biol 2008; 10(4):483-488.

Mittal V. Improving the efficiency of RNA interference in mammals. Nat Rev Genet 2004; 5(5):355-365.

Mizuguchi G, Shen X, Landry J, Wu WH, Sen S, Wu C. ATP-driven exchange of histone H2AZ variant catalyzed by SWR1 chromatin remodeling complex. Science 2004; 303(5656):343-348.

Mizuguchi G, Tsukiyama T, Wisniewski J, Wu C. Role of nucleosome remodeling factor NURF in transcriptional activation of chromatin. Mol Cell 1997; 1(1):141-150.

Mohrmann L, Verrijzer CP. Composition and functional specificity of SWI2/SNF2 class chromatin remodeling complexes. Biochim Biophys Acta 2005; 1681(2-3):59-73.

Morrison AJ, Highland J, Krogan NJ, Arbel-Eden A, Greenblatt JF, Haber JE et al. INO80 and gamma-H2AX interaction links ATP-dependent chromatin remodeling to DNA damage repair. Cell 2004; 119(6):767-775.

Morshead KB, Ciccone DN, Taverna SD, Allis CD, Oettinger MA. Antigen receptor loci poised for V(D)J rearrangement are broadly associated with BRG1 and flanked by peaks of histone H3 dimethylated at lysine 4. Proc Natl Acad Sci U S A 2003; 100(20):11577-11582.

Mosammaparast N, Shi Y. Reversal of histone methylation: biochemical and molecular mechanisms of histone demethylases. Annu Rev Biochem 2010; 79:155-179.

Motamedi MR, Verdel A, Colmenares SU, Gerber SA, Gygi SP, Moazed D. Two RNAi complexes, RITS and RDRC, physically interact and localize to noncoding centromeric RNAs. Cell 2004; 119(6):789-802.

Muller J, Hart CM, Francis NJ, Vargas ML, Sengupta A, Wild B et al. Histone methyltransferase activity of a Drosophila Polycomb group repressor complex. Cell 2002; 111(2):197-208.

Murchison EP, Partridge JF, Tam OH, Cheloufi S, Hannon GJ. Characterization of Dicer-deficient murine embryonic stem cells. Proc Natl Acad Sci U S A 2005; 102(34):12135-12140.

Mutskov V, Felsenfeld G. Silencing of transgene transcription precedes methylation of promoter DNA and histone H3 lysine 9. EMBO J 2004; 23(1):138-149.

Mutskov V, Gerber D, Angelov D, Ausio J, Workman J, Dimitrov S. Persistent interactions of core histone tails with nucleosomal DNA following acetylation and transcription factor binding. Mol Cell Biol 1998; 18(11):6293-6304.

Mutskov VJ, Farrell CM, Wade PA, Wolffe AP, Felsenfeld G. The barrier function of an insulator couples high histone acetylation levels with specific protection of promoter DNA from methylation. Genes Dev 2002; 16(12):1540-1554.

Nakayama J, Rice JC, Strahl BD, Allis CD, Grewal SI. Role of histone H3 lysine 9 methylation in epigenetic control of heterochromatin assembly. Science 2001; 292(5514):110-113.

Nakagawa T, Kajitani T, Togo S, Masuko N, Ohdan H, Hishikawa Y et al. Deubiquitylation of histone H2A activates transcriptional initiation via trans-histone cross-talk with H3K4 di- and trimethylation. Genes Dev 2008; 22(1):37-49.

Nan X, Ng HH, Johnson CA, Laherty CD, Turner BM, Eisenman RN et al. Transcriptional repression by the methyl-CpG-binding protein MeCP2 involves a histone deacetylase complex. Nature 1998; 393(6683):386-389.

Neely KE, Hassan AH, Brown CE, Howe L, Workman JL. Transcription activator interactions with multiple SWI/SNF subunits. Mol Cell Biol 2002; 22(6):1615-1625.

Newell-Price J, Clark AJ, King P. DNA methylation and silencing of gene expression. Trends Endocrinol Metab 2000; 11(4):142-148.

Nishioka K, Rice JC, Sarma K, Erdjument-Bromage H, Werner J, Wang Y et al. PR-Set7 is a nucleosome-specific methyltransferase that modifies lysine 20 of histone H4 and is associated with silent chromatin. Mol Cell 2002; 9(6):1201-1213.

Ng HH, Dole S, Struhl K. The Rtf1 component of the Paf1 transcriptional elongation complex is required for ubiquitination of histone H2B. J Biol Chem 2003; 278(36):33625-33628.

Ng HH, Xu RM, Zhang Y, Struhl K. Ubiquitination of histone H2B by Rad6 is required for efficient Dot1-mediated methylation of histone H3 lysine 79. J Biol Chem 2002; 277(38):34655-34657.

Noonan JP, McCallion AS. Genomics of long-range regulatory elements. Annu Rev Genomics Hum Genet 2010; 11:1-23.

Pal S, Sif S. Interplay between chromatin remodelers and protein arginine methyltransferases. J Cell Physiol 2007; 213(2):306-315.

Pan G, Tian S, Nie J, Yang C, Ruotti V, Wei H et al. Whole-genome analysis of histone H3 lysine 4 and lysine 27 methylation in human embryonic stem cells. Cell Stem Cell 2007; 1(3):299-312.

Papamichos-Chronakis M, Watanabe S, Rando OJ, Peterson CL. Global regulation of H2A.Z localization by the INO80 chromatin-remodeling enzyme is essential for genome integrity. Cell 2011; 144(2):200-213.

Papp B, Muller J. Histone trimethylation and the maintenance of transcriptional ON and OFF states by trxG and PcG proteins. Genes Dev 2006; 20(15):2041-2054.

Park JH, Cosgrove MS, Youngman E, Wolberger C, Boeke JD. A core nucleosome surface crucial for transcriptional silencing. Nat Genet 2002; 32(2):273-279.

Park YJ, Dyer PN, Tremethick DJ, Luger K. A new fluorescence resonance energy transfer approach demonstrates that the histone variant H2AZ stabilizes the histone octamer within the nucleosome. J Biol Chem 2004; 279(23):24274-24282.

Pavri R, Zhu B, Li G, Trojer P, Mandal S, Shilatifard A et al. Histone H2B monoubiquitination functions cooperatively with FACT to regulate elongation by RNA polymerase II. Cell 2006; 125(4):703-717.

Pelletier N, Gregoire S, Yang XJ. Analysis of protein lysine acetylation in vitro and in vivo. Curr Protoc Protein Sci 2008; Chapter 14:Unit.

Pena PV, Davrazou F, Shi X, Walter KL, Verkhusha VV, Gozani O et al. Molecular mechanism of histone H3K4me3 recognition by plant homeodomain of ING2. Nature 2006; 442(7098):100-103.

Peng JC, Karpen GH. Epigenetic regulation of heterochromatic DNA stability. Curr Opin Genet Dev 2008; 18(2):204-211.

Peters AH, Kubicek S, Mechtler K, O'Sullivan RJ, Derijck AA, Perez-Burgos L et al. Partitioning and plasticity of repressive histone methylation states in mammalian chromatin. Mol Cell 2003; 12(6):1577-1589.

Pikaart MJ, Recillas-Targa F, Felsenfeld G. Loss of transcriptional activity of a transgene is accompanied by DNA methylation and histone deacetylation and is prevented by insulators. Genes Dev 1998; 12(18):2852-2862.

Pinskaya M, Gourvennec S, Morillon A. H3 lysine 4 di- and tri-methylation deposited by cryptic transcription attenuates promoter activation. EMBO J 2009; 28(12):1697-1707.

Picketts DJ, Higgs DR, Bachoo S, Blake DJ, Quarrell OW, Gibbons RJ. ATRX encodes a novel member of the SNF2 family of proteins: mutations point to a common mechanism underlying the ATR-X syndrome. Hum Mol Genet 1996; 5(12):1899-1907.

Plath K, Mlynarczyk-Evans S, Nusinow DA, Panning B. Xist RNA and the mechanism of X chromosome inactivation. Annu Rev Genet 2002; 36:233-278.

Pray-Grant MG, Daniel JA, Schieltz D, Yates JR, III, Grant PA. Chd1 chromodomain links histone H3 methylation with. Nature 2005; 433(7024):434-438.

Prioleau MN, Nony P, Simpson M, Felsenfeld G. An insulator element and condensed chromatin region separate the chicken beta-globin locus from an independently regulated erythroid-specific folate receptor gene. EMBO J 1999; 18(14):4035-4048.

Prokhortchouk A, Hendrich B, Jorgensen H, Ruzov A, Wilm M, Georgiev G et al. The p120 catenin partner Kaiso is a DNA methylation-dependent transcriptional repressor. Genes Dev 2001; 15(13):1613-1618.

Prokhortchouk E, Hendrich B. Methyl-CpG binding proteins and cancer: are MeCpGs more important than MBDs? Oncogene 2002; 21(35):5394-5399.

Popovic R, Zeleznik L. MLL: how complex does it get? J Cell Biochem 2005; 95(2):234-242.

Pokholok DK, Harbison CT, Levine S, Cole M, Hannett NM, Lee TI et al. Genome-wide map of nucleosome acetylation and methylation in yeast. Cell 2005; 122(4):517-527.

Obrdlik A, Kukalev A, Louvet E, Farrants AK, Caputo L, Percipalle P. The histone acetyltransferase PCAF associates with actin and hnRNP U for RNA polymerase II transcription. Mol Cell Biol 2008; 28(20):6342-6357.

Ogbourne S, Antalis TM. Transcriptional control and the role of silencers in transcriptional regulation in eukaryotes. Biochem J 1998; 331 (Pt 1):1-14.

Ogawa H, Ishiguro K, Gaubatz S, Livingston DM, Nakatani Y. A complex with chromatin modifiers that occupies E2F- and Myc-responsive genes in G0 cells. Science 2002; 296(5570):1132-1136.

Ohlsson R, Bartkuhn M, Renkawitz R. CTCF shapes chromatin by multiple mechanisms: the impact of 20 years of CTCF research on understanding the workings of chromatin. Chromosoma 2010; 119(4):351-360.

Oki M, Valenzuela L, Chiba T, Ito T, Kamakaka RT. Barrier proteins remodel and modify chromatin to restrict silenced domains. Mol Cell Biol 2004; 24(5):1956-1967.

Oliveira RA, Coelho PA, Sunkel CE. The condensin I subunit Barren/CAP-H is essential for the structural integrity of centromeric heterochromatin during mitosis. Mol Cell Biol 2005; 25(20):8971-8984.

Ooi SK, Qiu C, Bernstein E, Li K, Jia D, Yang Z et al. DNMT3L connects unmethylated lysine 4 of histone H3 to de novo methylation of DNA. Nature 2007; 448(7154):714-717.

Orphanides G, Lagrange T, Reinberg D. The general transcription factors of RNA polymerase II. Genes Dev 1996; 10(21):2657-2683.

Orphanides G, Wu WH, Lane WS, Hampsey M, Reinberg D. The chromatin-specific transcription elongation factor FACT comprises human SPT16 and SSRP1 proteins. Nature 1999; 400(6741):284-288.

Osley MA. Regulation of histone H2A and H2B ubiquitylation. Brief Funct Genomic Proteomic 2006; 5(3):179-189.

Osley MA. The regulation of histone synthesis in the cell cycle. Annu Rev Biochem 1991; 60:827-861.

Raab JR, Kamakaka RT. Insulators and promoters: closer than we think. Nat Rev Genet 2010; 11(6):439-446.

Rada-Iglesias A, Wallerman O, Koch C, Ameur A, Enroth S, Clelland G et al. Binding sites for metabolic disease related transcription factors inferred at base pair resolution by chromatin immunoprecipitation and genomic microarrays. Hum Mol Genet 2005; 14(22):3435-3447.

Raisner RM, Hartley PD, Meneghini MD, Bao MZ, Liu CL, Schreiber SL et al. Histone variant H2A.Z marks the 5' ends of both active and inactive genes in euchromatin. Cell 2005; 123(2):233-248.

Rath AV, Schmahl GE, Niemeyer CM. Expression of transcription factors during sodium phenylacetate induced erythroid differentiation in K562 cells. Blood Cells Mol Dis 1997; 23(1):27-38.

Rea S, Eisenhaber F, O'Carroll D, Strahl BD, Sun ZW, Schmid M et al. Regulation of chromatin structure by site-specific histone H3 methyltransferases. Nature 2000; 406(6796):593-599.

Recillas-Targa F, Pikaart MJ, Burgess-Beusse B, Bell AC, Litt MD, West AG et al. Position-effect protection and enhancer blocking by the chicken beta-globin insulator are separable activities. Proc Natl Acad Sci U S A 2002; 99(10):6883-6888.

Recillas-Targa F, Valadez-Graham V, Farrell CM. Prospects and implications of using chromatin insulators in gene therapy and transgenesis. Bioessays 2004; 26(7):796-807.

Reitman M, Felsenfeld G. Developmental regulation of topoisomerase II sites and DNase I-hypersensitive sites in the chicken beta-globin locus. Mol Cell Biol 1990; 10(6):2774-2786.

Reuter G, Spierer P. Position effect variegation and chromatin proteins. Bioessays 1992; 14(9):605-612.

Richmond TJ, Davey CA. The structure of DNA in the nucleosome core. Nature 2003; 423(6936):145-150.

Rice JC, Briggs SD, Ueberheide B, Barber CM, Shabanowitz J, Hunt DF et al. Histone methyltransferases direct different degrees of methylation to define distinct chromatin domains. Mol Cell 2003; 12(6):1591-1598.

Rigaut G, Shevchenko A, Rutz B, Wilm M, Mann M, Séraphin. A generic protein purification method for protein complex characterization and proteome exploration. Nat Biotechnol 1999; 17:1030-1032.

Ring HZ, Vameghi-Meyers V, Wang W, Crabtree GR, Francke U. Five SWI/SNF-related, matrix-associated, actin-dependent regulator of chromatin (SMARC) genes are dispersed in the human genome. Genomics 1998; 51(1):140-143.

Robzyk K, Recht J, Osley MA. Rad6-dependent ubiquitination of histone H2B in yeast. Science 2000; 287(5452):501-504.

Ropero S, Esteller M. The role of histone deacetylases (HDACs) in human cancer. Mol Oncol 2007; 1(1):19-25.

Roseman RR, Pirrotta V, Geyer PK. The su(Hw) protein insulates expression of the Drosophila melanogaster white gene from chromosomal position-effects. EMBO J 1993; 12(2):435-442.

Rountree MR, Bachman KE, Baylin SB. DNMT1 binds HDAC2 and a new co-repressor, DMAP1, to form a complex at replication foci. Nat Genet 2000; 25(3):269-277.

Rudolph T, Yonezawa M, Lein S, Heidrich K, Kubicek S, Schafer C et al. Heterochromatin formation in Drosophila is initiated through active removal of H3K4 methylation by the LSD1 homolog SU(VAR)3-3. Mol Cell 2007; 26(1):103-115.

Ruhl DD, Jin J, Cai Y, Swanson S, Florens L, Washburn MP et al. Purification of a human SRCAP complex that remodels chromatin by incorporating the histone variant H2A.Z into nucleosomes. Biochemistry 2006; 45(17):5671-5677.

Ruthenburg AJ, Li H, Patel DJ, Allis CD. Multivalent engagement of chromatin modifications by linked binding modules. Nat Rev Mol Cell Biol 2007; 8(12):983-994.

Sadaie M, Iida T, Urano T, Nakayama J. A chromodomain protein, Chp1, is required for the establishment of heterochromatin in fission yeast. EMBO J 2004; 23(19):3825-3835.

Saha A, Wittmeyer J, Cairns BR. Chromatin remodelling: the industrial revolution of DNA around histones. Nat Rev Mol Cell Biol 2006; 7(6):437-447.

Saitoh N, Bell AC, Recillas-Targa F, West AG, Simpson M, Pikaart M et al. Structural and functional conservation at the boundaries of the chicken beta-globin domain. EMBO J 2000; 19(10):2315-2322.

Santos-Rosa H, Bannister AJ, Dehe PM, Geli V, Kouzarides T. Methylation of H3 lysine 4 at euchromatin promotes Sir3p association with heterochromatin. J Biol Chem 2004; 279(46):47506-47512.

Sanchez R, Zhou MM. The role of human bromodomains in chromatin biology and gene transcription. Curr Opin Drug Discov Devel 2009; 12(5):659-665.

Sanchez C, Sanchez I, Demmers JA, Rodriguez P, Strouboulis J, Vidal M. Proteomics analysis of Ring1B/Rnf2 interactors identifies a novel complex with the Fbxl10/Jhdm1B histone demethylase and the Bcl6 interacting corepressor. Mol Cell Proteomics 2007; 6(5):820-834.

Sapountzi V, Logan IR, Robson CN. Cellular functions of TIP60. Int J Biochem Cell Biol 2006; 38(9):1496-1509.

Sarcevic B, Mawson A, Baker RT, Sutherland RL. Regulation of the ubiquitin-conjugating enzyme hHR6A by CDK-mediated phosphorylation. EMBO J 2002; 21(8):2009-2018.

Schneider J, Wood A, Lee JS, Schuster R, Dueker J, Maguire C et al. Molecular regulation of histone H3 trimethylation by COMPASS and the regulation of gene expression. Mol Cell 2005; 19(6):849-856.

Schneider R, Bannister AJ, Myers FA, Thorne AW, Crane-Robinson C, Kouzarides T. Histone H3 lysine 4 methylation patterns in higher eukaryotic genes. Nat Cell Biol 2004; 6(1):73-77.

Schneider R, Bannister AJ, Weise C, Kouzarides T. Direct binding of INHAT to H3 tails disrupted by modifications. J Biol Chem 2004; 279(23):23859-23862.

Schmittgen TD, Livak KJ. Analyzing real-time PCR data by the comparative C(T) method. Nat Protoc 2008; 3(6):1101-1108.

Schotta G, Ebert A, Krauss V, Fischer A, Hoffmann J, Rea S et al. Central role of Drosophila SU(VAR)3-9 in histone H3-K9 methylation and heterochromatic gene silencing. EMBO J 2002; 21(5):1121-1131.

Schotta G, Lachner M, Sarma K, Ebert A, Sengupta R, Reuter G et al. A silencing pathway to induce H3-K9 and H4-K20 trimethylation at constitutive heterochromatin. Genes Dev 2004; 18(11):1251-1262.

Schultz J, Milpetz F, Bork P, Ponting CP. SMART, a simple modular architecture research tool: identification of signaling domains. Proc Natl Acad Sci U S A 1998; 95(11):5857-5864.

Schulze JM, Jackson J, Nakanishi S, Gardner JM, Hentrich T, Haug J et al. Linking cell cycle to histone modifications: SBF and H2B monoubiquitination machinery and cell-cycle regulation of H3K79 dimethylation. Mol Cell 2009; 35(5):626-641.

Scott KC, Merrett SL, Willard HF. A heterochromatin barrier partitions the fission yeast centromere into discrete chromatin domains. Curr Biol 2006; 16(2):119-129.

Schurter BT, Koh SS, Chen D, Bunick GJ, Harp JM, Hanson BL et al. Methylation of histone H3 by coactivator-associated arginine methyltransferase 1. Biochemistry 2001; 40(19):5747-5756.

Shahbazian MD, Zhang K, Grunstein M. Histone H2B ubiquitylation controls processive methylation but not monomethylation by Dot1 and Set1. Mol Cell 2005; 19(2):271-277.

Shema E, Tirosh I, Aylon Y, Huang J, Ye C, Moskovits N et al. The histone H2B-specific ubiquitin ligase RNF20/hBRE1 acts as a putative tumor suppressor through selective regulation of gene expression. Genes Dev 2008; 22(19):2664-2676.

Shen X, Yu L, Weir JW, Gorovsky MA. Linker histones are not essential and affect chromatin condensation in vivo. Cell 1995; 82(1):47-56.

Shi X, Hong T, Walter KL, Ewalt M, Michishita E, Hung T et al. ING2 PHD domain links histone H3 lysine 4 methylation to active gene repression. Nature 2006; 442(7098):96-99.

Shi Y, Lan F, Matson C, Mulligan P, Whetstine JR, Cole PA et al. Histone demethylation mediated by the nuclear amine oxidase homolog LSD1. Cell 2004; 119(7):941-953.

Shi YJ, Matson C, Lan F, Iwase S, Baba T, Shi Y. Regulation of LSD1 histone demethylase activity by its associated factors. Mol Cell 2005; 19(6):857-864.

Shia WJ, Li B, Workman JL. SAS-mediated acetylation of histone H4 Lys 16 is required for H2A.Z incorporation at subtelomeric regions in Saccharomyces cerevisiae. Genes Dev 2006; 20(18):2507-2512.

Shilatifard A. Molecular implementation and physiological roles for histone H3 lysine 4 (H3K4) methylation. Curr Opin Cell Biol 2008; 20(3):341-348.

Shin KJ, Wall EA, Zavzavadjian JR, Santat LA, Liu J, Hwang JI et al. A single lentiviral vector platform for microRNA-based conditional RNA interference and coordinated transgene expression. Proc Natl Acad Sci U S A 2006; 103(37):13759-13764.

Shin S, Janknecht R. Activation of androgen receptor by histone demethylases JMJD2A and JMJD2D. Biochem Biophys Res Commun 2007; 359(3):742-746.

Shin S, Janknecht R. Diversity within the JMJD2 histone demethylase family. Biochem Biophys Res Commun 2007; 353(4):973-977.

Shukla A, Chaurasia P, Bhaumik SR. Histone methylation and ubiquitination with their cross-talk and roles in gene expression and stability. Cell Mol Life Sci 2009; 66(8):1419-1433.

Smith ER, Lee MG, Winter B, Droz NM, Eissenberg JC, Shiekhattar R et al. Drosophila UTX is a histone H3 Lys27 demethylase that colocalizes with the elongating form of RNA polymerase II. Mol Cell Biol 2008; 28(3):1041-1046.

Smith KP, Byron M, Clemson CM, Lawrence JB. Ubiquitinated proteins including uH2A on the human and mouse inactive X chromosome: enrichment in gene rich bands. Chromosoma 2004; 113(6):324-335.

Simpson RT. Structure of chromatin containing extensively acetylated H3 and H4. Cell 1978; 13(4):691-699.

Sims JK, Houston SI, Magazinnik T, Rice JC. A trans-tail histone code defined by monomethylated H4 Lys-20 and H3 Lys-9 demarcates distinct regions of silent chromatin. J Biol Chem 2006; 281(18):12760-12766.

Slotkin RK, Martienssen R. Transposable elements and the epigenetic regulation of the genome. Nat Rev Genet 2007; 8(4):272-285.

Smallwood A, Esteve PO, Pradhan S, Carey M. Functional cooperation between HP1 and DNMT1 mediates gene silencing. Genes Dev 2007; 21(10):1169-1178.

Smith KP, Byron M, Clemson CM, Lawrence JB. Ubiquitinated proteins including uH2A on the human and mouse inactive X chromosome: enrichment in gene rich bands. Chromosoma 2004; 113(6):324-335.

Smith ST, Petruk S, Sedkov Y, Cho E, Tillib S, Canaani E et al. Modulation of heat shock gene expression by the TAC1 chromatin-modifying complex. Nat Cell Biol 2004; 6(2):162-167.

Song YH, Ahn SH. A Bre1-associated protein, large 1 (Lge1), promotes H2B ubiquitylation during the early stages of transcription elongation. J Biol Chem 2010; 285(4):2361-2367.

Southall SM, Wong PS, Odho Z, Roe SM, Wilson JR. Structural basis for the requirement of additional factors for MLL1 SET domain activity and recognition of epigenetic marks. Mol Cell 2009; 33(2):181-191.

Strahl BD, Grant PA, Briggs SD, Sun ZW, Bone JR, Caldwell JA et al. Set2 is a nucleosomal histone H3-selective methyltransferase that mediates transcriptional repression. Mol Cell Biol 2002; 22(5):1298-1306.

Stavropoulos P, Blobel G, Hoelz A. Crystal structure and mechanism of human lysine-specific demethylase-1. Nat Struct Mol Biol 2006; 13(7):626-632.

Stewart MD, Li J, Wong J. Relationship between histone H3 lysine 9 methylation, transcription repression, and heterochromatin protein 1 recruitment. Mol Cell Biol 2005; 25(7):2525-2538.

Steward MM, Lee JS, O'Donovan A, Wyatt M, Bernstein BE, Shilatifard A. Molecular regulation of H3K4 trimethylation by ASH2L, a shared subunit of MLL complexes. Nat Struct Mol Biol 2006; 13(9):852-854.

Strahl BD, Briggs SD, Brame CJ, Caldwell JA, Koh SS, Ma H et al. Methylation of histone H4 at arginine 3 occurs in vivo and is mediated by the nuclear receptor coactivator PRMT1. Curr Biol 2001; 11(12):996-1000.

Suto RK, Clarkson MJ, Tremethick DJ, Luger K. Crystal structure of a nucleosome core particle containing the variant histone H2A.Z. Nat Struct Biol 2000; 7(12):1121-1124.

Sugiyama T, Cam H, Verdel A, Moazed D, Grewal SI. RNA-dependent RNA polymerase is an essential component of a self-enforcing loop coupling heterochromatin assembly to siRNA production. Proc Natl Acad Sci U S A 2005; 102(1):152-157.

Sun ZW, Allis CD. Ubiquitination of histone H2B regulates H3 methylation and gene silencing in yeast. Nature 2002; 418(6893):104-108.

Szabo P, Tang SH, Rentsendorj A, Pfeifer GP, Mann JR. Maternal-specific footprints at putative CTCF sites in the H19 imprinting control region give evidence for insulator function. Curr Biol 2000; 10(10):607-610.

Szerlong H, Hinata K, Viswanathan R, Erdjument-Bromage H, Tempst P, Cairns BR. The HSA domain binds nuclear actin-related proteins to regulate chromatin-remodeling ATPases. Nat Struct Mol Biol 2008; 15(5):469-476.

Szerlong H, Saha A, Cairns BR. The nuclear actin-related proteins Arp7 and Arp9: a dimeric module that cooperates with architectural proteins for chromatin remodeling. EMBO J 2003; 22(12):3175-3187.

Tachibana M, Sugimoto K, Fukushima T, Shinkai Y. Set domain-containing protein, G9a, is a novel lysine-preferring mammalian histone methyltransferase with hyperactivity and specific selectivity to lysines 9 and 27 of histone H3. J Biol Chem 2001; 276(27):25309-25317.

Tachibana M, Ueda J, Fukuda M, Takeda N, Ohta T, Iwanari H et al. Histone methyltransferases G9a and GLP form heteromeric complexes and are both crucial for methylation of euchromatin at H3-K9. Genes Dev 2005; 19(7):815-826.

Takahashi YH, Lee JS, Swanson SK, Saraf A, Florens L, Washburn MP et al. Regulation of H3K4 trimethylation via Cps40 (Spp1) of COMPASS is monoubiquitination independent: implication for a Phe/Tyr switch by the catalytic domain of Set1. Mol Cell Biol 2009; 29(13):3478-3486.

Takai D, Gonzales FA, Tsai YC, Thayer MJ, Jones PA. Large scale mapping of methylcytosines in CTCF-binding sites in the human H19 promoter and aberrant hypomethylation in human bladder cancer. Hum Mol Genet 2001; 10(23):2619-2626.

Tanny JC, Erdjument-Bromage H, Tempst P, Allis CD. Ubiquitylation of histone H2B controls RNA polymerase II transcription elongation independently of histone H3 methylation. Genes Dev 2007; 21(7):835-847.

Tang J, Wu S, Liu H, Stratt R, Barak OG, Shiekhattar R et al. A novel transcription regulatory complex containing death domain-associated protein and the ATR-X syndrome protein. J Biol Chem 2004; 279(19):20369-20377.

Taverna SD, Li H, Ruthenburg AJ, Allis CD, Patel DJ. How chromatin-binding modules interpret histone modifications: lessons from professional pocket pickers. Nat Struct Mol Biol 2007; 14(11):1025-1040.

Thakar A, Parvin JD, Zlatanova J. BRCA1/BARD1 E3 ubiquitin ligase can modify histones H2A and H2B in the nucleosome particle. J Biomol Struct Dyn 2010; 27(4):399-406.

Thambirajah AA, Dryhurst D, Ishibashi T, Li A, Maffey AH, Ausio J. H2A.Z stabilizes chromatin in a way that is dependent on core histone acetylation. J Biol Chem 2006; 281(29):20036-20044.

Thatcher TH, Gorovsky MA. Phylogenetic analysis of the core histones H2A, H2B, H3, and H4. Nucleic Acids Res 1994; 22(2):174-179.

Thorne AW, Sautiere P, Briand G, Crane-Robinson C. The structure of ubiquitinated histone H2B. EMBO J 1987; 6(4):1005-1010.

Travers A. Chromatin modification by DNA tracking. Proc Natl Acad Sci U S A 1999; 96(24):13634-13637.

Tremethick DJ. Higher-order structures of chromatin: the elusive 30 nm fiber. Cell 2007; 128(4):651-654.

van Attikum H, Fritsch O, Hohn B, Gasser SM. Recruitment of the INO80 complex by H2A phosphorylation links ATP-dependent chromatin remodeling with DNA double-strand break repair. Cell 2004; 119(6):777-788.

van Welsem T, Frederiks F, Verzijlbergen KF, Faber AW, Nelson ZW, Egan DA et al. Synthetic lethal screens identify gene silencing processes in yeast and implicate the acetylated amino terminus of Sir3 in recognition of the nucleosome core. Mol Cell Biol 2008; 28(11):3861-3872.

Vermeulen M, Mulder KW, Denissov S, Pijnappel WW, van Schaik FM, Varier RA et al. Selective anchoring of TFIID to nucleosomes by trimethylation of histone H3 lysine 4. Cell 2007; 131(1):58-69.

Venkatasubrahmanyam S, Hwang WW, Meneghini MD, Tong AH, Madhani HD. Genome-wide, as opposed to local, antisilencing is mediated redundantly by the euchromatic factors Set1 and H2A.Z. Proc Natl Acad Sci U S A 2007; 104(42):16609-16614.

Verdel A, Jia S, Gerber S, Sugiyama T, Gygi S, Grewal SI et al. RNAi-mediated targeting of heterochromatin by the RITS complex. Science 2004; 303(5658):672-676.

Vire E, Brenner C, Deplus R, Blanchon L, Fraga M, Didelot C et al. The Polycomb group protein EZH2 directly controls DNA methylation. Nature 2006; 439(7078):871-874.

Vitaliano-Prunier A, Menant A, Hobeika M, Geli V, Gwizdek C, Dargemont C. Ubiquitylation of the COMPASS component Swd2 links H2B ubiquitylation to H3K4 trimethylation. Nat Cell Biol 2008; 10(11):1365-1371.

Volpe TA, Kidner C, Hall IM, Teng G, Grewal SI, Martienssen RA. Regulation of heterochromatic silencing and histone H3 lysine-9 methylation by RNAi. Science 2002; 297(5588):1833-1837.

Walhout AJ, Vidal M. Protein interaction maps for model organisms. Nat Rev Mol Cell Biol 2001; 2(1):55-62.

Wallrath LL. Unfolding the mysteries of heterochromatin. Curr Opin Genet Dev 1998; 8(2):147-153.

Wallace JA, Felsenfeld G. We gather together: insulators and genome organization. Curr Opin Genet Dev 2007; 17(5):400-407.

Wang H, Wang L, Erdjument-Bromage H, Vidal M, Tempst P, Jones RS et al. Role of histone H2A ubiquitination in Polycomb silencing. Nature 2004; 431(7010):873-878.

Wang H, Zhai L, Xu J, Joo HY, Jackson S, Erdjument-Bromage H et al. Histone H3 and H4 ubiquitylation by the CUL4-DDB-ROC1 ubiquitin ligase facilitates cellular response to DNA damage. Mol Cell 2006; 22(3):383-394.

Wang L, Brown JL, Cao R, Zhang Y, Kassis JA, Jones RS. Hierarchical recruitment of polycomb group silencing complexes. Mol Cell 2004; 14(5):637-646.

Wang Z, Zang C, Rosenfeld JA, Schones DE, Barski A, Cuddapah S et al. Combinatorial patterns of histone acetylations and methylations in the human genome. Nat Genet 2008; 40(7):897-903.

Wang Y, Wysocka J, Sayegh J, Lee YH, Perlin JR, Leonelli L et al. Human PAD4 regulates histone arginine methylation levels via demethylimination. Science 2004; 306(5694):279-283.

Wang GG, Cai L, Pasillas MP, Kamps MP. NUP98-NSD1 links H3K36 methylation to Hox-A gene activation and leukaemogenesis. Nat Cell Biol 2007; 9(7):804-812.

Weake VM, Lee KK, Guelman S, Lin CH, Seidel C, Abmayr SM et al. SAGA-mediated H2B deubiquitination controls the development of neuronal connectivity in the Drosophila visual system. EMBO J 2008; 27(2):394-405.

Weake VM, Workman JL. Histone ubiquitination: triggering gene activity. Mol Cell 2008; 29(6):653-663.

Weake VM, Workman JL. Inducible gene expression: diverse regulatory mechanisms. Nat Rev Genet 2010; 11(6):426-437.

Wendt KS, Yoshida K, Itoh T, Bando M, Koch B, Schirghuber E et al. Cohesin mediates transcriptional insulation by CCCTC-binding factor. Nature 2008; 451(7180):796-801.

Wery M, Shematorova E, Van Driessche B, Vandenhaute J, Thuriaux P, Van M, V. Members of the SAGA and Mediator complexes are partners of the transcription elongation factor TFIIS. EMBO J 2004; 23(21):4232-4242.

Weintraub H. Histone-H1-dependent chromatin superstructures and the suppression of gene activity. Cell 1984; 38(1):17-27.

West AG, Huang S, Gaszner M, Litt MD, Felsenfeld G. Recruitment of histone modifications by USF proteins at a vertebrate barrier element. Mol Cell 2004; 16(3):453-463.

West AG, Fraser P. Remote control of gene transcription. Hum Mol Genet 2005; 14 Spec No 1:R101-R111.

West MH, Bonner WM. Histone 2A, a heteromorphous family of eight protein species. Biochemistry 1980; 19(14):3238-3245.

West MH, Bonner WM. Histone 2B can be modified by the attachment of ubiquitin. Nucleic Acids Res 1980; 8(20):4671-4680.

Winkler GS, Kristjuhan A, Erdjument-Bromage H, Tempst P, Svejstrup JQ. Elongator is a histone H3 and H4 acetyltransferase important for normal histone acetylation levels in vivo. Proc Natl Acad Sci U S A 2002; 99(6):3517-3522.

Winston F, Allis CD. The bromodomain: a chromatin-targeting module? Nat Struct Biol 1999; 6(7):601-604.

Wittschieben BO, Otero G, de Bizemont T, Fellows J, Erdjument-Bromage H, Ohba R et al. A novel histone acetyltransferase is an integral subunit of elongating RNA polymerase II holoenzyme. Mol Cell 1999; 4(1):123-128.

Woelk T, Sigismund S, Penengo L, Polo S. The ubiquitination code: a signalling problem. Cell Div 2007; 2:11.

Wood A, Schneider J, Dover J, Johnston M, Shilatifard A. The Bur1/Bur2 complex is required for histone H2B monoubiquitination by Rad6/Bre1 and histone methylation by COMPASS. Mol Cell 2005; 20(4):589-599.

Wood A, Krogan NJ, Dover J, Schneider J, Heidt J, Boateng MA et al. Bre1, an E3 ubiquitin ligase required for recruitment and substrate selection of Rad6 at a promoter. Mol Cell 2003; 11(1):267-274.

Wood A, Schneider J, Dover J, Johnston M, Shilatifard A. The Paf1 complex is essential for histone monoubiquitination by the Rad6-Bre1 complex, which signals for histone methylation by COMPASS and Dot1p. J Biol Chem 2003; 278(37):34739-34742.

Woodcock CL, Ghosh RP. Chromatin higher-order structure and dynamics. Cold Spring Harb Perspect Biol 2010; 2(5):a000596.

Wu J, Huen MS, Lu LY, Ye L, Dou Y, Ljungman M et al. Histone ubiquitination associates with BRCA1-dependent DNA damage response. Mol Cell Biol 2009; 29(3):849-860.

Wu RS, Kohn KW, Bonner WM. Metabolism of ubiquitinated histones. J Biol Chem 1981; 256(11):5916-5920.

Wu M, Wang PF, Lee JS, Martin-Brown S, Florens L, Washburn M et al. Molecular regulation of H3K4 trimethylation by Wdr82, a component of human Set1/COMPASS. Mol Cell Biol 2008; 28(24):7337-7344.

Wu C. The 5' ends of Drosophila heat shock genes in chromatin are hypersensitive to DNase I. Nature 1980; 286(5776):854-860.

Wyce A, Xiao T, Whelan KA, Kosman C, Walter W, Eick D et al. H2B ubiquitylation acts as a barrier to Ctk1 nucleosomal recruitment prior to removal by Ubp8 within a SAGA-related complex. Mol Cell 2007; 27(2):275-288.

Wysocka J, Swigut T, Xiao H, Milne TA, Kwon SY, Landry J et al. A PHD finger of NURF couples histone H3 lysine 4 trimethylation with chromatin remodelling. Nature 2006; 442(7098):86-90.

Xiao T, Kao CF, Krogan NJ, Sun ZW, Greenblatt JF, Osley MA et al. Histone H2B ubiquitylation is associated with elongating RNA polymerase II. Mol Cell Biol 2005; 25(2):637-651.

Xu Q, Li M, Adams J, Cai HN. Nuclear location of a chromatin insulator in Drosophila melanogaster. J Cell Sci 2004; 117(Pt 7):1025-1032.

Xue Y, Canman JC, Lee CS, Nie Z, Yang D, Moreno GT et al. The human SWI/SNF-B chromatin-remodeling complex is related to yeast rsc and localizes at kinetochores of mitotic chromosomes. Proc Natl Acad Sci U S A 2000; 97(24):13015-13020.

Yamada T, Fischle W, Sugiyama T, Allis CD, Grewal SI. The nucleation and maintenance of heterochromatin by a histone deacetylase in fission yeast. Mol Cell 2005; 20(2):173-185.

Yao S, Osborne CS, Bharadwaj RR, Pasceri P, Sukonnik T, Pannell D et al. Retrovirus silencer blocking by the cHS4 insulator is CTCF independent. Nucleic Acids Res 2003; 31(18):5317-5323.

You A, Tong JK, Grozinger CM, Schreiber SL. CoREST is an integral component of the Co. Proc Natl Acad Sci U S A 2001; 98(4):1454-1458.

Yokoyama A, Wang Z, Wysocka J, Sanyal M, Aufiero DJ, Kitabayashi I et al. Leukemia proto-oncoprotein MLL forms a SET1-like histone methyltransferase complex with menin to regulate Hox gene expression. Mol Cell Biol 2004; 24(13):5639-5649.

Yoon HG, Chan DW, Reynolds AB, Qin J, Wong J. N-CoR mediates DNA methylation-dependent repression through a methyl CpG binding protein Kaiso. Mol Cell 2003; 12(3):723-734.

Yuan W, Xie J, Long C, Erdjument-Bromage H, Ding X, Zheng Y et al. Heterogeneous nuclear ribonucleoprotein L Is a subunit of human KMT3a/Set2 complex required for H3 Lys-36 trimethylation activity in vivo. J Biol Chem 2009; 284(23):15701-15707.

Yusufzai TM, Tagami H, Nakatani Y, Felsenfeld G. CTCF tethers an insulator to subnuclear sites, suggesting shared insulator mechanisms across species. Mol Cell 2004; 13(2):291-298.

Yusufzai TM, Felsenfeld G. The 5'-HS4 chicken beta-globin insulator is a CTCF-dependent nuclear matrix-associated element. Proc Natl Acad Sci U S A 2004; 101(23):8620-8624.

Zegerman P, Canas B, Pappin D, Kouzarides T. Histone H3 lysine 4 methylation disrupts binding of nucleosome remodeling and deacetylase (NuRD) repressor complex. J Biol Chem 2002; 277(14):11621-11624.

Zemach A, McDaniel IE, Silva P, Zilberman D. Genome-wide evolutionary analysis of eukaryotic DNA methylation. Science 2010; 328(5980):916-919.

Zeng PY, Vakoc CR, Chen ZC, Blobel GA, Berger SL. In vivo dual cross-linking for identification of indirect DNA-associated proteins by chromatin immunoprecipitation. Biotechniques 2006; 41(6):694, 696, 698.

Zhang D, Yoon HG, Wong J. JMJD2A is a novel N-CoR-interacting protein and is involved in repression of the human transcription factor achaete scute-like homologue 2 (ASCL2/Hash2). Mol Cell Biol 2005; 25(15):6404-6414.

Zhang F, Yu X. WAC, a Functional Partner of RNF20/40, Regulates Histone H2B Ubiquitination and Gene Transcription. Mol Cell 2011; 41(4):384-397.

Zhang H, Richardson DO, Roberts DN, Utley R, Erdjument-Bromage H, Tempst P et al. The Yaf9 component of the SWR1 and NuA4 complexes is required for proper gene expression, histone H4 acetylation, and Htz1 replacement near telomeres. Mol Cell Biol 2004; 24(21):9424-9436.

Zhang H, Roberts DN, Cairns BR. Genome-wide dynamics of Htz1, a histone H2A variant that poises repressed/basal promoters for activation through histone loss. Cell 2005; 123(2):219-231.

Zhang K, Dent SY. Histone modifying enzymes and cancer: going beyond histones. J Cell Biochem 2005; 96(6):1137-1148.

Zhang XY, Varthi M, Sykes SM, Phillips C, Warzecha C, Zhu W et al. The putative cancer stem cell marker USP22 is a subunit of the human SAGA complex required for activated transcription and cell-cycle progression. Mol Cell 2008; 29(1):102-111.

Zhang K, Mosch K, Fischle W, Grewal SI. Roles of the Clr4 methyltransferase complex in nucleation, spreading and maintenance of heterochromatin. Nat Struct Mol Biol 2008; 15(4):381-388.

Zhang Y, Ng HH, Erdjument-Bromage H, Tempst P, Bird A, Reinberg D. Analysis of the NuRD subunits reveals a histone deacetylase core complex and a connection with DNA methylation. Genes Dev 1999; 13(15):1924-1935.

Zhang Y, Reinberg D. Transcription regulation by histone methylation: interplay between different covalent modifications of the core histone tails. Genes Dev 2001; 15(18):2343-2360.

Zhao Y, Lang G, Ito S, Bonnet J, Metzger E, Sawatsubashi S et al. A TFTC/STAGA module mediates histone H2A and H2B deubiquitination, coactivates nuclear receptors, and counteracts heterochromatin silencing. Mol Cell 2008; 29(1):92-101.

Zhou VW, Goren A, Bernstein BE. Charting histone modifications and the functional organization of mammalian genomes. Nat Rev Genet 2010.

Zhou W, Wang X, Rosenfeld MG. Histone H2A ubiquitination in transcriptional regulation and DNA damage repair. Int J Biochem Cell Biol 2009; 41(1):12-15.

Zhu B, Zheng Y, Pham AD, Mandal SS, Erdjument-Bromage H, Tempst P et al. Monoubiquitination of human histone H2B: the factors involved and their roles in HOX gene regulation. Mol Cell 2005a; 20(4):601-611.

Zilberman D, Coleman-Derr D, Ballinger T, Henikoff S. Histone H2A.Z and DNA methylation are mutually antagonistic chromatin marks. Nature 2008; 456(7218):125-129.

Zlatanova J, Caiafa P. CTCF and its protein partners: divide and rule? J Cell Sci 2009; 122(Pt 9):1275-1284.